Carbon sequestration in ultramafic rocks from The Tablelands and White Hills, Newfoundland, Canada

by Benjamin Taylor

A Thesis submitted to the School of Graduate Studies in partial fulfillment of the requirements for the degree of

Master of Science, Department of Earth Science

Memorial University of Newfoundland

May 2023

St. John's Newfoundland and Labrador

Abstract

With the rising concentration of atmospheric CO_2 and a better understanding of its effect on global climate, there is increasing interest in developing methods of removing CO_2 from the atmosphere and its long-term storage. CO_2 mineralization is a naturally occurring process within igneous and ultramafic rocks that converts gaseous CO_2 into carbonate minerals. While a promising method, the many factors that affect CO_2 mineralization are not fully understood and require further investigation. This study focused on two ultramafic ophiolites located in Newfoundland, the Tablelands and the White Hills. In this study, field-based CO_2 sequestration experiments were conducted along with laboratory-based CO_2 sequestration experiments using rock samples from the two ophiolites. The field-based experiments recorded the CO_2 sequestration rates of naturally occurring ultra-basic springs with a pH of 11-12. The laboratory experiments varied parameters such as water chemistry, surface area, CO_2 supply, and sampling locations. This study found that the higher pH waters sequestered the most CO_2 and also had the greatest amount of carbonate mineral precipitation. Additionally, it was found that increasing CO_2 supply increased the amount of precipitated carbonate minerals in almost all experiments.

General Summary

Carbon dioxide mineralization is a naturally occurring process within calcium, magnesium, and iron rich rocks that converts carbon dioxide into solid minerals. Field and laboratory experiments were conducted using rock samples two locations in Newfoundland, the Tablelands and the White Hills, areas where iron and magnesium rich rocks from the ocean floor are now on land. The field-based experiments recorded the carbon dioxide removal rates of naturally occurring springs with a pH of 11-12. The laboratory experiments varied parameters such as water chemistry, pH, surface area, carbon dioxide supply, and rock sample locations. This study found that in the laboratory experiments the higher pH waters reduced carbon dioxide concentrations the most and also precipitated the largest volume of carbon-bearing minerals. Additionally, it was found that increasing carbon dioxide supply increased the amount of carbon-bearing minerals in almost all experiments.

Acknowledgments

I would first like to thank Dr. Penny Morrill for her support, guidance, and patience provided during the long, long road to the completion of this thesis.

Second, I would like to thank my committee members Steve Emberley and Dr. Mike Babechuk for their expertise and helpful suggestions throughout this project.

Thanks to Sherri, Wanda, Marcus, and Ines for all your help along the way with analyses, troubleshooting, and clean water.

Thanks to Susan for your work in the field, helping with basic rock identification, and for encouraging my love of science fiction.

I want to thank all the members of DELTAS during my time at MUN for their excellent feedback and help along the way, I would name all of you but I've been here so long I would have to add another page of acknowledgements.

Special thanks to Melissa for putting up with me while sharing an office and for being the person I turn to for academic commiseration. Sorry about your ankle.

Finally, I would like to thank my incredible fiancé and family – you have been an unending source of support over the almost five years of this thesis. I cannot put into words how important that has been to me, I love you all so much.

Table of Contents

List of Tables

List of Figures

List of Abbreviations

BIOC: Bay of Islands Ophiolite Complex

CCS: Carbon capture and storage

CDR: Carbon dioxide removal

CO_2 : Carbon dioxide

CREAIT: Core Research Equipment & Instrument Training Network

DI: Deionized

DIC: Dissolved inorganic carbon

ICP-OES: Inductively coupled plasma optical emission spectroscopy

ICP-MS: Inductively coupled plasma mass spectrometry

NDIR: Non-destructive infrared detector

SCR: White Hills Crushed Rock

SWR: White Hills Whole Rock

TCR: Tablelands Crushed Rock

TIC: Total inorganic carbon

TWR: Tablelands Whole Rock

List of Appendices

Chapter 1: Introduction

The concentration of carbon dioxide (CO_2) in the atmosphere has increased 40% from 1750 to 2011 and this increase is most likely due to anthropogenic influences (Costa et al., 2021). With the rising concentration of atmospheric CO_2, there has been increasing global interest regarding the impacts of CO_2 on climate change. These impacts have been linked to changes in many aspects of global climate such as average global temperature, radiation budgets, the hydrological cycle, extreme weather events, and climate variability (Costa et al., 2021). As more research takes place and these impacts are better understood, it is becoming clear that finding solutions to reduce or mitigate these impacts is of increasing importance. There are already multiple methods being proposed and/or being tested with almost all the methods falling under the umbrella of carbon dioxide removal (CDR), also known as carbon capture and storage (CCS) or carbon sequestration (Bui et al., 2018)

Carbon sequestration methods are designed to remediate increasing atmospheric CO_2 concentrations by removing CO_2 from the atmosphere and storing it in a reservoir. The process of removing CO_2 from the atmosphere is an essential part of many modelling scenarios with the goal of slowing or reversing the effects of climate change. Without this removal, many scenarios still show increasing atmospheric CO_2 concentrations over the upcoming decades (Costa et al., 2021). One part of the carbon sequestration process is the conversion and storage of the CO_2 that has been removed from the atmosphere. Each sequestration strategy has a different method for the conversion of gaseous CO_2 into a form where it can then be stored in various reservoirs. All these methods can be broadly divided into three categories: biological, geochemical, and chemical. Some of these methods such as direct-air capture use technological methods to remove CO_2 from the atmosphere (Boot-Handford et al., 2014). However, most of the methods in the

three categories look to modify or accelerate naturally occurring processes that can take decades to centuries to remove CO_2 from the atmosphere under normal conditions. Some of these processes include reforestation, biomass burial, modifying ocean conditions, and carbon mineralization. Another important consideration of carbon sequestration methods is the choice of storage location, as different storage and capture methods will require different reservoirs. For example, if the sequestration method is using direct-air capture then a possible storage solution would be to inject the CO_2 into depleted oil reservoirs deep under the surface. This type of reservoir is attractive as is utilizes existing technology and infrastructure, but variations in permeability and porosity across the reservoirs can pose challenges for long term storage (Asghari & Al-Dliwe, 2005). The stability of where the carbon is stored is an important factor in determining effective methods of carbon sequestration. Some reservoirs are considered short-term (e.g. reforestation) but could potentially be at risk from the effects of climate change (Zhou et al., 2008). Other reservoirs (e.g. geological formations and mineral phases) are considered long-term or potentially permanent solutions and are at minimal risk of re-releasing CO_2 into the atmosphere (Gislason & Oelkers, 2014).

One method that results in long-term, stable storage is the conversion of atmospheric CO_2 into carbonate mineral phases, also known as carbon or CO_2 mineralization. CO_2 mineralization is a naturally occurring process and has been the subject of many studies around the world (Kelemen et al., 2020; Snæbjörnsdóttir et al., 2020). Many of these studies focus on the serpentinization process, and how it can enhance or accelerate CO_2 mineralization. Serpentinization is the hydrothermal alteration of ultramafic rocks, such as peridotite (composed mostly of olivine and pyroxene), as a result of reactions with fluids such as seawater or meteoric water and produces serpentine minerals, iron and magnesium hydroxides, and basic to ultra-basic

waters (Eq. 1; Barnes and O'Neil (1969). The basic waters (pH 8-9) are a result of surface water and/or shallow groundwater interacting with ultramafic rocks in an open system and in contact with the atmosphere. The basic waters are enriched in Mg^{2+} and HCO_3^- and are often referred to as Type I waters (Eq.2). The ultra-basic water, or Type II water, is characterized by pH 11-12 and are enriched in Ca^{2+} and OH^- as a result of Type I waters penetrating ultramafic rock at depth and becoming disconnected from atmospheric CO_2 supply (Eq. 3, Paukert et al. (2012). Ongoing precipitation of Mg^{2+} into mineral phases such as serpentine, magnesite, brucite, and results in the above mentioned characteristics (Barnes et al., 1967). When these waters return to the surface and reconnect with an atmospheric CO_2 supply or mix with another water source, they can precipitate carbonate minerals such as calcite and magnesite (Eq. 4*; (Barnes et al., 1967; Kelemen & Matter, 2008). *Generalized formula.

Eq. 1 $2Mg_2SiO_4 + 3H_2O \rightarrow Mg_3Si_2O_5(OH)_4 + Mg(OH)_2$

Olivine *Serpentine* *Brucite*

Eq. 2 $Mg_2SiO_4 + 4CO_2 + 2H_2O \rightarrow 2Mg^{2+} + 4HCO_3^- + SiO_2$

Olivine

Eq. 3 $4Mg_2SiO_4 + CaMgSi_2O_6 + 7H_2O \rightarrow 3Mg_3Si_2O_5(OH)_4 + Ca^{2+} + 2OH^-$

Olivine *Pyroxene* *Serpentine*

Eq. 4 $Mg_2SiO_4 + CaMgSi_2O_6 + 2CO_2 + 2H_2O \rightarrow Mg_3Si_2O_5(OH)_4 + CaCO_3 + MgCO_3$

Olivine *Pyroxene* *Serpentine* *Calcite* *Magnesite*

To fully understand the mineralization process, it must be examined for potential rate-limiting steps, and to determine possible methods to increase the reaction rate of this step. Two possible rate-limiting steps are the dissolution of host rock and the precipitation of carbonate minerals. This study will focus on the effects of pH, CO_2 supply, and surface area on these two potential rate-limiting steps.

The rate of incongruent dissolution in silicate minerals, such as olivine and pyroxene, is increased under acidic conditions (Park & Fan, 2004; Schott et al., 2009). This incongruent dissolution can provide the calcium and magnesium necessary for the precipitation of carbonate minerals such as calcite or magnesite. Under basic to ultra-basic conditions, the dominant species of dissolved inorganic carbon (DIC) in water is CO_3^{2-}, which is another important component in the precipitation of carbonate minerals (Clark & Fritz, 2013; Park & Fan, 2004). Basic to ultra-basic conditions are also the favored conditions for carbonate mineral precipitation. This contrast in favorable conditions, acidic conditions for dissolution and basic to ultra-basic for precipitation, demonstrates why studies such as this are important to further our understanding of how multiple factors influence the overall rate of CO_2 mineralization.

Another method for increasing the amount of carbonation is to increase the availability of CO_2 to react with the ultramafic rock. Dissolving CO_2 into water which is then injected into a target rock formation not only increases the supply of CO_2 but also causes the water to increase in density and sink deeper into the formation, resulting in an increased extent of carbonation (Matter et al., 2016; Snæbjörnsdóttir et al., 2014).

Ensuring that enough surface area is available for reactions to take place is another important factor in the mineralization process (Kelemen & Matter, 2008; van Noort et al., 2017). The serpentinization and carbonation reactions can potentially cause micro-fractures leading to

increased surface area and increased reaction area (van Noort et al., 2017). It is also possible that the reactions lack the force necessary to fracture the rock, as shown in some laboratory and modelling scenarios, and they may instead lead to reduced fluid interactions with the host rock (Rudge et al., 2010; van Noort et al., 2017).

The rate of incongruent dissolution may also be affected by the mineralogy of the host rock (Lacinska et al., 2017; Schott et al., 2009). Certain minerals will tend to dissolve more rapidly than others in given conditions, which may help determine the optimal host rock mineralogy. An increase in the amount of silica polymerization, or average Si-O-Si bonds in a crystal structure, will reduce dissolution rate (Schott et al., 2009). For example: forsterite, an un-polymerized orthosilicate, will dissolve more rapidly than phyllosilicates such as serpentine group minerals (Schott et al., 2009). An increase in existing, easily dissolved minerals such as brucite may also help in the overall dissolution process; as these minerals dissolve, they can open previously blocked fractures, allowing fluid to propagate deeper into the host rock (Lacinska et al., 2017).

As previously mentioned, host rock mineralogy can play an important role in the efficiency of carbon mineralization. There have been two lithologies identified as the most promising for carbon mineralization: mafic (e.g., basalt) and ultramafic rocks (e.g., peridotite). These two rock types are composed of minerals that, when incongruently dissolved or weathered, will provide the necessary reactants for carbon mineralization. One of the main differences between mafic and ultramafic rocks is the weight percent of minerals bearing the necessary reactants, calcium (Ca) and magnesium (Mg). Mafic rocks such as basalt and gabbro contain between 9-13% Ca- and between 6-10% Mg-oxides by weight, whereas ultramafic rocks such as dunite and harzburgite contain between 0-8% Ca- and 28-50% Mg-oxides by weight

(Lackner et al., 1995). This means that ultramafic rocks will be able to provide much more of the necessary reactants when dissolved compared to mafic rocks. Studies have also demonstrated that carbonation reaction rates in ultramafic rocks are much faster than in mafic rocks and can proceed at lower temperatures (Kelemen et al., 2011). Ultramafic rocks are not commonly found at the earth's surface, but they are found across the globe in oceanic crust beneath the ocean and also in areas where oceanic crust has been obducted onto a continental margin such as the case with ophiolite sequences.

Ophiolites have an abundance of materials necessary to facilitate CO_2 mineralization, to the point where Kelemen and Matter (2008) calculated that for an addition of 1 wt% of CO_2 to the Samail ophiolite in Oman, it could be possible to store 25% of the Earth's atmospheric CO_2. This estimate is for an ideal modeled scenario where all silicate magnesium ions in the ophiolite are converted to carbonate, but it shows the storage potential of ultramafic rocks. Lacinska et al. (2017) calculated that serpentine has the ability to sequester 30 kg of CO_2 per ton of host rock resulting in about 2-3% carbonation of the host rock. Carbonate is commonly found around ultra-basic springs in serpentinized continental ophiolites and the presence of which suggests that the mineralization reaction can proceed at near surface conditions (Barnes et al., 1967; Kelemen & Matter, 2008; Morrill et al., 2013; Szponar et al., 2013).

Newfoundland has multiple ophiolites, many of which have been extensively studied with the best studied being those related to the Taconic Orogeny (middle Ordovician) and located on the west coast of the island. This study will focus on two ophiolites emplaced during the Taconic Orogeny: the Tablelands, part of the Bay of Islands Complex (BOIC), located in the Humber Arm Allochthon and the White Hills Ophiolite located in the Hare Bay Allochthon. The two allochthons are lithologically very similar to each other with both consisting of almost

complete ophiolite sequences (ultramafic material overlying metamorphic aureoles) (Williams & Smyth, 1973).

The Tablelands is an ultramafic massif consisting of gabbro and peridotite (harzburgite varying to dunite), which has been altered to serpentine in many locations. Another feature of the Tablelands is the series of ultra-basic springs that have been located in some valleys and along the flanks of the massif. A number of these springs are actively precipitating carbonate, which is evidenced by the carbonate rims surrounding the springs. Other locations show evidence of springs, but only remain as carbonate swathes.

The White Hills Ophiolite is an ophiolite located on the tip of the northern peninsula of Newfoundland, extending 130 km along the eastern coast and up to 32 km inland. The formation of interest for this study within the ophiolite sequence is the White Hills Peridotite that consists of serpentinized harzburgite, dunite, and lherzolite (Williams & Smyth, 1973). No ultra-basic springs have been discovered at the White Hills Ophiolite.

The objectives of this study are:

1. To examine which environmental and geological factors have the greatest effect on CO_2 mineralization at sites of continental serpentinization
2. To examine the Tablelands and White Hills continental ophiolites for CO_2 mineralization potential.
3. To conduct carbon sequestration field studies at existing sites of ultra-basic springs in the Tablelands
4. To search for new ultra-basic springs in the Tablelands and White Hills Ophiolites

Chapter 2: Methods

2.1 Field sample collection and in-situ measurements

Rock samples were collected from the Tablelands and White Hills ophiolites (Fig. 1). When possible, samples were chosen to best represent the mineralogy at each location, highlight any features of importance, and be of sufficient mass to provide enough material for laboratory experiments. Laboratory experiments required approximately 4 kg of crushed rock from each field location. Rock samples collected for laboratory experiments in the Tablelands were fine-grained dunite. The samples were weathered light green to brown on the exterior surface, and dark green to black on the interior. There were also small fractures on the interior of the samples that were filled mostly with serpentine, but also minor amounts of carbonate. Samples collected from the White Hills were fine to coarse grained harzburgites with large olivine and pyroxene crystals. There is evidence of more extensive serpentinization on the interior of the samples when compared to the samples from the Tablelands, with small veins of serpentine and minor carbonates surrounding the larger olivine and pyroxene crystals.

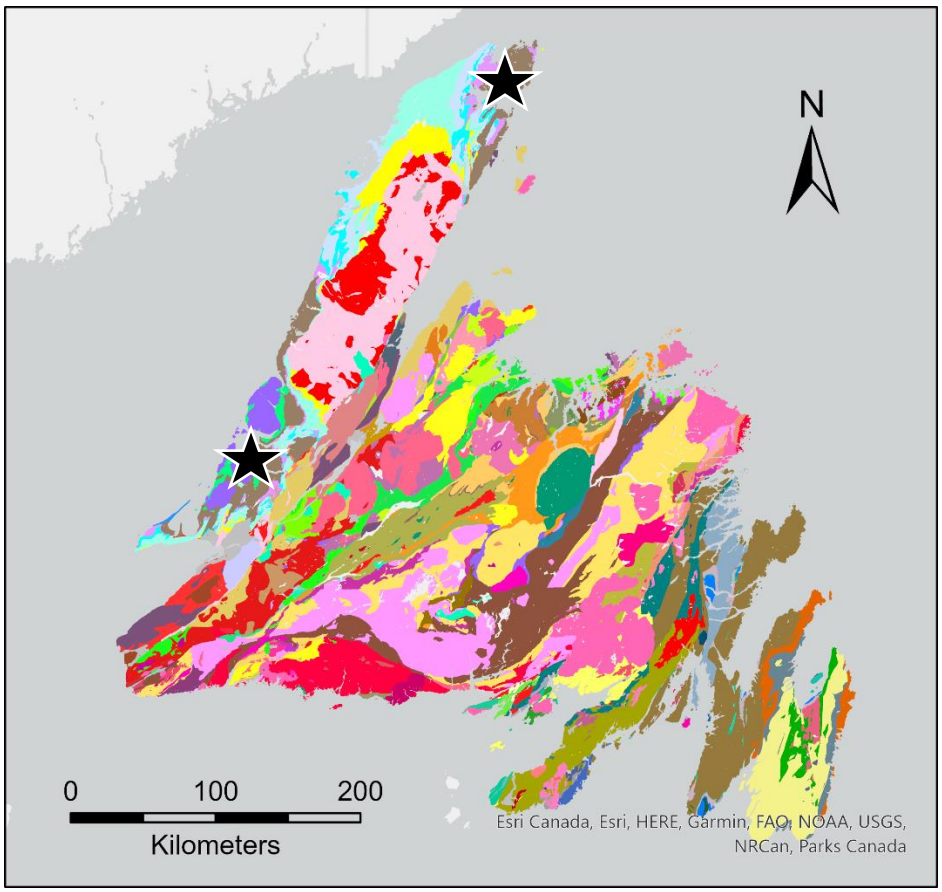

Fig. 1. Generalized regional geology map of Newfoundland showing the location of The Tablelands and the White Hills ophiolites, indicated by the black stars. The Tablelands is located on the west coast of the island and the White Hills is located on the tip of the northern peninsula. Data from NL Geoscience Atlas (https://gis.geosurv.gov.nl.ca/).

CO_2 flux was measured in the field using a LI-COR 8100A Single Chamber Survey System with a CO_2 analyzer. The LI-COR system was deployed at sampling locations for a minimum of one hour and up to a maximum of six hours. The LI-COR was controlled through a wireless connection to an iPad allowing for remote operation and monitoring. The LI-COR measured CO_2 concentrations every second of the observation except for the first minute of operation. During this time, the chamber was purged for 30 seconds (known as pre-purge) and data recording was delayed by 30 seconds (this delay is known as the deadband) to avoid errors

from pressure fluctuations of the closing sampling chamber. The sample chamber was mounted on a PVC soil collar to ensure a tight seal and to prevent gas leaks during the observation. The other end of the soil collar formed a tight seal over and around the area of interest (spring, rock, vegetation). In areas where uneven terrain made forming an air-tight seal difficult, modeling clay was used to complete the seal.

To better understand the overall CO_2 flux at each field location in the Tablelands, the LI-COR was deployed at multiple areas of interest. These sites included: ultra-basic springs (WHC2 and WHC500), local vegetation, a small bog, and ultramafic rock and ultramafic gravel that might impact the net flux of each field location (Fig. 2).

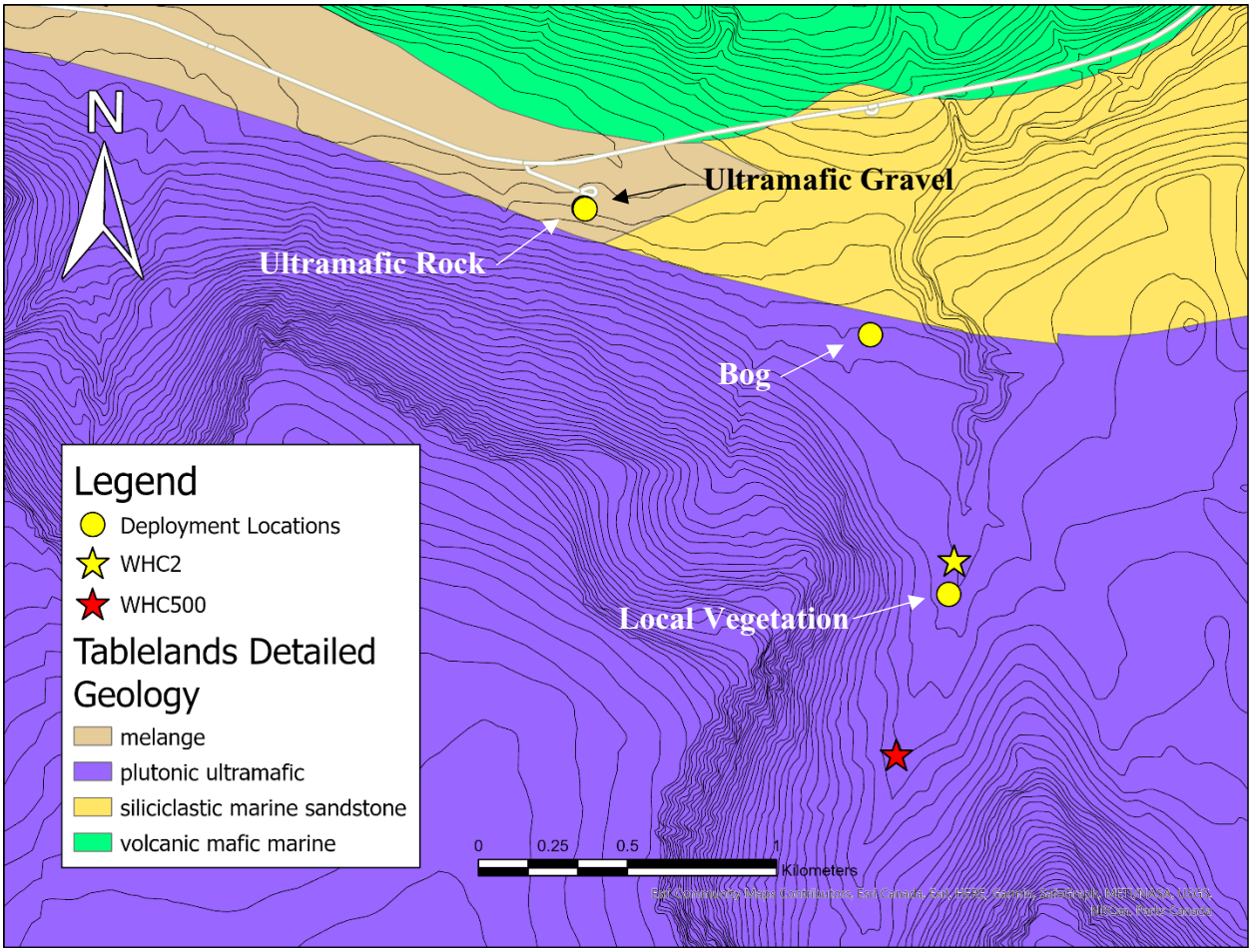

Fig. 2. Map showing ultra-basic spring locations of WHC2 and WHC500 and LICOR deployment locations in the Tablelands. Data from NL Geoscience Atlas (https://gis.geosurv.gov.nl.ca/).

The LI-COR was not deployed in the White Hills as no ultra-basic springs were discovered. It is possible that there are ultra-basic springs in the White Hills, but access into the interior of the ophiolite proved too difficult in both field seasons. Rock samples collected for laboratory experiments were collected at the location indicated in Figure 3. Also indicated in Figure 3 are the areas that were searched while attempting to located ultra-basic springs.

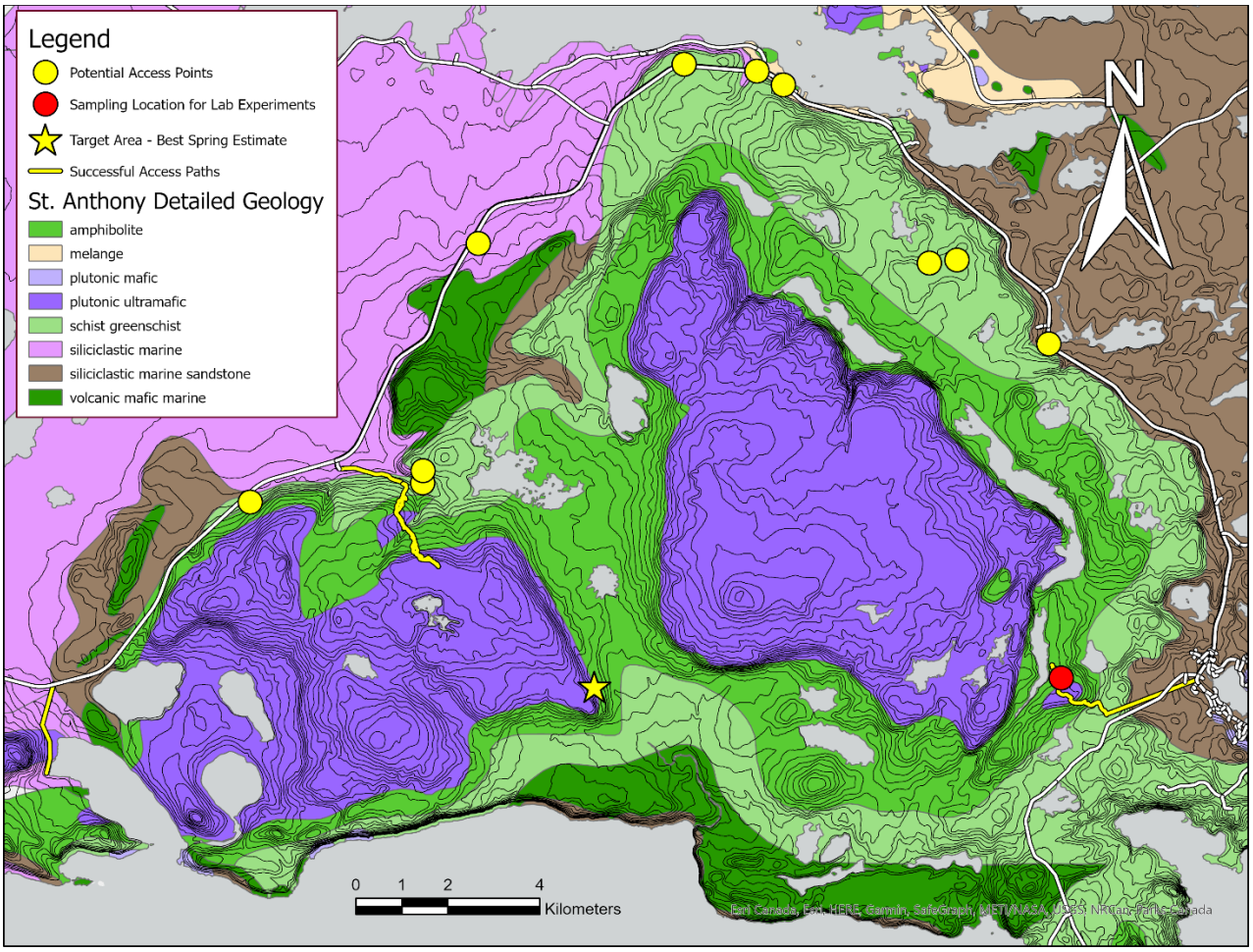

Fig. 3. Map of White Hills Ophiolite showing potential access points, sampling locations, target areas, and successful access paths. Data from NL Geoscience Atlas (https://gis.geosurv.gov.nl.ca/).

2.2 Laboratory experiments

In the laboratory, experiments were focused on determining the ideal conditions for carbon mineralization to take place. Thirty-five different experiments were conducted. Each experiment was replicated in triplicate. The experimental parameters that were varied included: CO_2 supply (atmospheric or elevated), surface area (no rock, crushed rock, or whole rock) and water type (deionized (DI) water, CaOH, CaOH-high, or MgOH). CO_2 supply was varied by using either ambient CO_2 concentrations or dissolving 2.67 g of $NaHCO_3$ into 1 L of water. Rock samples from the Tablelands and White Hills were cut into 5 cm cubes or crushed and sieved through a 7 mm mesh and used the material that passed through the sieve. Experiments with rock used 125 cm^3 of crushed rock or one of the 5 cm rock cubes (Fig 2).

Fig. 4. Tablelands (left) and White Hills (right) rock cubes used for sequestration experiments.

The water types used were the following: deionized water, 0.1 g/L CaOH, 1.0 g/L CaOH (referred to as CaOH-high), or 0.1 g/L MgOH. All experiments used 600 mL of one of the four water types and included either no rock, 125 cm^3 of crushed rock, or one 5 cm^3 rock cube. All the Tablelands experiments, except for CaOH plus crushed rock and CaOH plus whole rock, were 5 hours in length. All the White Hills experiments plus the CaOH plus crushed rock and

CaOH plus whole rock were 4 hours in length. The LI-COR 8100A Single Chamber Survey System was used to measure atmospheric chamber CO_2 concentrations and mounted on a PVC collar fixed to a glass plate and sealed to prevent gas escape (Fig. 5). A glass bowl filled with water and rock was placed within the collar and the chamber was placed on top of the collar (Fig. 6).

Fig. 5. The LI-COR 8100A Single Chamber Survey System (left) and attached CO_2 analyzer (right).

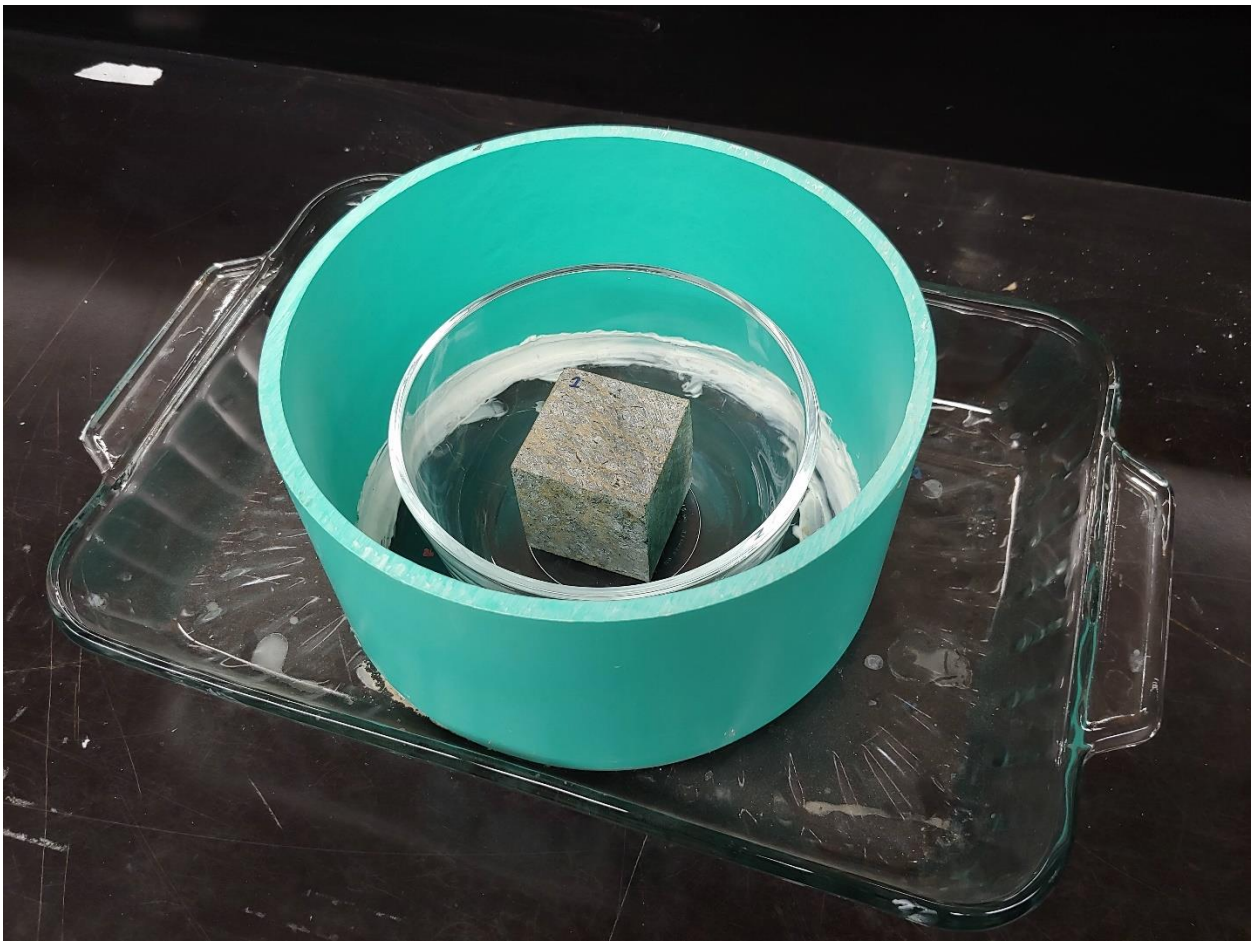

Fig 6. PVC collar attached to glass plate containing the glass bowl and a White Hills rock cube used in laboratory experiments.

2.3 Analytical methods

2.3.1 Fluid elemental analysis

Dissolved element concentrations for the Tablelands experiments were measured at Memorial University of Newfoundland in a Core Research Equipment and Instrument Training (CREAIT) Network laboratory using a PE ELAN DRC II quadrupole inductively coupled plasma mass spectrometer (ICP-MS) with a Cetac ASX-520 autosampler for sample introduction. Analyses were conducted in standard mode, using multi-element standard solutions (covering full mass range) for external calibration and Sc, Re, Rh, and Th for internal standards

to correct for drift and matrix effects, following the method of Friel et al. (1990). Method detection limits and quality assurance and quality controls were monitored through the multiple analyses of certified reference materials (e.g. USGS T-143), method preparation duplicates and 0.2 M HNO_3 containing only the internal standard.

Conversely, analysis for dissolved element concentrations for the White Hills experiments were measured on a Perkin Elmer Optima 5300 DV inductively coupled plasma - optical emission spectrometer (ICP-OES) equipped with an Cetac ASX-520 autosampler. ICP-OES was used instead of ICP-MS as it better equipped and adjusted for the high concentrations of calcium and magnesium used in the laboratory experiments. Yttrium was used as an internal standard and co-aspirated with a concentration of 10mg/L. All calibration solutions were prepared from 10000 mg/L single element standard solutions (SCP Science). The following elements and optical emission lines were measured: Fe (238.204, 239.562, 259.939), Ni (231.604, 221.648), Al (308.215, 394.401), Mg (285.213, 279.077), Ca (317.933, 315.887, 393.366), Na (589.592), Zn (206.200, 213.857, 202.548), Mn (257.610, 259.372, 260.568, 294.920), Si (212.412, 288.158, 251.611) and Y (internal standard) (371.029, 324.227, 360.073). Concentrations were calculated for each line individually and an average was reported as the result, unless one of the lines was affected by an interference or in cases where an element was present in low concentration. Only the more sensitive lines were used for low concentration samples, e.g. for Ca concentrations below 5mg/L only line 393.366 was used whereas for Ca concentrations above 25mg/L lines 317.933 and 315.887 were used due to saturation of line 393.366. The stability and blank of the instrument were checked by analyzing standard solutions and a blank solution after every 12 samples. Furthermore, the instrument was rinsed with 2% HNO_3 for 30 s between measurements.

2.3.2 CO_2 concentrations

CO_2 concentrations were measured using a LI-COR 8100A Single Chamber Survey System with a CO_2 infrared gas analyzer. The LI-COR system settings were the same for both laboratory experiments and for field deployments. The LI-COR was factory calibrated using CO_2 and H_2O gas standards and determined to have less than 1% error (Pronost et al. (2012) lists 1.5% precision and 0-3000 ppm) for both gases. Before the first experiment the instrument was zeroed using soda lime and drierite to set a zero concentration for CO_2 and H_2O, respectively.

2.3.3 Conductivity and pH

Conductivity and pH measurements for Tablelands experiments were recorded using an OAKTON pH/CON 10 Series field probe. The probe was calibrated daily using pH 4.01, 7.00, and 10.01 calibration solutions. A pH 12.01 solution used as a check standard for high pH solutions. Conductivity calibration was done using 100 µS/cm, 1413 µS/cm, and 12.9 mS/cm calibration solutions. Conductivity and pH from the White Hills experiments were measured using a Orion Star A325 pH/Conductivity Portable Multiparameter Meter with attached Orion Conductivity Cell and Orion ROSS Ultra pH/ATC Triode. The Orion probe was used in place of the OAKTON probe due to the OAKTON probe ceasing to calibrate properly and providing incorrect pH readings. The Orion pH and conductivity probes were calibrated at the beginning of each week using pH 4.00, 7.00, 10.00 and 12.64 calibration solutions, and 100 µS/cm, 1413 µS/cm, and 12.9 mS/cm conductivity calibration solutions. The calibration was checked daily with standard solutions of similar pH and conductivity to the experiments being conducted. If a drift was observed, then the probe was recalibrated before proceeding to the experiments.

2.3.4 Total inorganic carbon

Total inorganic carbon (TIC) concentration analysis was performed using a modified OI Analytical Aurora model 1030 wet TOC analyser, with a model 1051 autosampler at the Ján Veizer Stable Isotope Laboratory at the University of Ottawa. Three external standards were prepared in solution no more than three days before the beginning of analysis. An aliquot of each sample was acidified with 5% H_3PO_4 to convert dissolved TIC to gaseous CO_2. The concentration of CO_2 was measured using a non-destructive infrared detector (NDIR). The analytical precision (2 sigma) of the analyses was +/- 0.5 ppm C.

2.3.5 CO_2 flux calculation

Gas flux between gaseous and liquid phases was measured by recording gas concentrations using the LI-8100A. Using the measured data from the sequestration experiments, flux (mol/m^2·min) was calculated from the initial and final concentrations using Equation 9.

Eq. 9

$$\text{Flux} = \frac{V(P_2 - P_1)}{RTA(t_2 - t_1)}$$

Where V is the volume of the chamber (m^3); P_1 and P_2 are partial pressures of gas measured at two different time points (Pa); R is the ideal gas constant 8.314462 (m^3·Pa/K·mol); T is the air temperature (K); A is the surface area of the liquid (m^2); and t_1 and t_2 are the times the samples were taken (min). This equation assumed that there was a linear relationship between gas concentrations and time (Podgrajsek et al., 2014). The time interval used for the flux calculation was between 0 and 30 minutes, where the concentration change with time was closest to a linear relationship and most closely resembled an open system. This linearity was confirmed by

checking the correlation coefficient of the line of best fit. The R^2 values were always better than 0.90 except for experiments with rock.

2.3.6 Statistical analysis

Using two-tailed unpaired t-tests, p-values were calculated to determine if flux, pH, conductivity, and TIC results were significantly different between experiments. A probability value (p-value) > 0.05 indicated that there was <95% confidence that the data were significant, therefore the experimental parameters being compared were not significantly different from each other. A p-value < 0.05 indicated that there was >95% confidence that the data were significant, therefore the experimental parameters being compared were significantly different from each other.

Chapter 3: Tablelands results

3.1 CO_2 sequestration field experiments

To better understand natural CO_2 sequestration rates and to provide a comparison for laboratory sequestration experiments, the LI-8100A was deployed over two previously discovered ultra-basic springs in the Tablelands. These ultra-basic springs, WHC2 and WHC500, both sequestered CO_2 during the field experiments (Fig. 7 and Fig. 8, respectively).

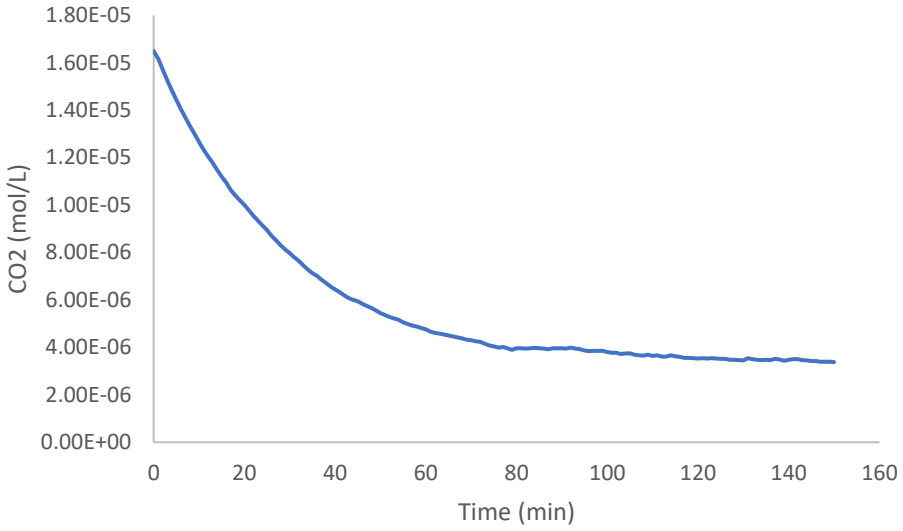

Fig. 7. Change in CO_2 concentration over time, recorded during deployment of the LI-8100A over the ultra-basic spring WHC2 (Tablelands, June 26, 2019).

During the WHC2 field experiment, CO_2 concentration in the LI-8100A chamber decreased from 1.7×10^{-5} mol/L to 3.4×10^{-6} mol/L, a total decrease in CO_2 concentration of -1.3×10^{-5} mol/L in 150 minutes. The WHC500 field experiment measured a decrease in CO_2 concentration from 1.7×10^{-5} mol/L to 1.2×10^{-5} mol/L, resulting in a total decrease in CO_2

concentration of -4.6 × 10^{-6} mol/L in 80 minutes.

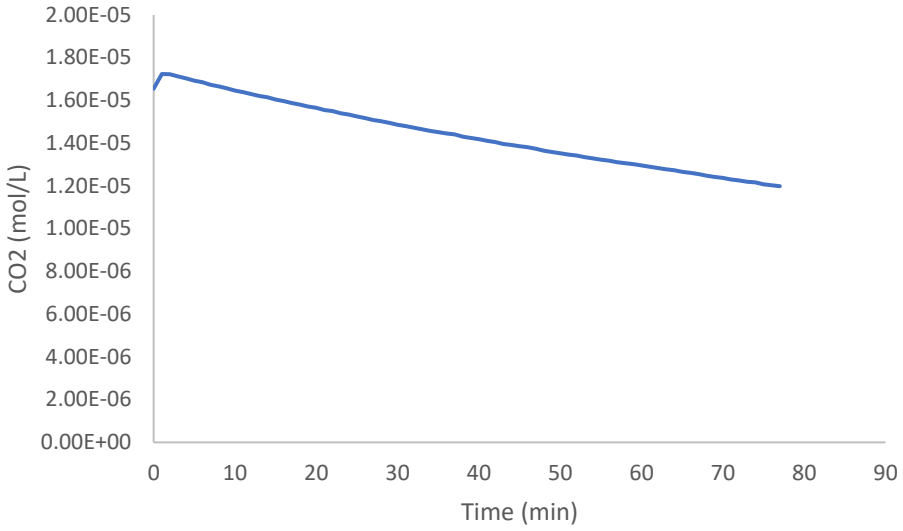

Fig. 8. Change in CO_2 concentration over time, recorded during deployment of the LI-8100A over the ultra-basic spring WHC500 (Tablelands, June 24, 2019).

In addition to deploying the LI-8100A over known ultra-basic springs, it was also deployed over dry ultramafic rock (Fig. 9), local vegetation (Fig. 10), loose ultramafic gravel (Fig. 11), and a small bog located near the ultra-basic springs (Fig. 12). Over the course of each of these experiments there was an increase in CO_2 concentration in the chamber. The field experiments over dry ultramafic rock and loose ultramafic gravel had an increase in CO_2 concentration of 2.2 × 10^{-7} mol/L over 60 minutes and 3.0 × 10^{-6} mol/L over 45 minutes, respectively. Note the change in scale for Figure 9. The field experiment deployed over the small bog resulted in a CO_2 concentration increase of 4.2 × 10^{-6} mol/L over 105 minutes and the field experiment over local vegetation resulted in a CO_2 concentration increase of 2.4 × 10^{-5} mol/L over 120 minutes. To compare experiment locations the change in CO_2 concentration over the

first 45 minutes (the length of the shortest experiment) is reported in Figure 13.

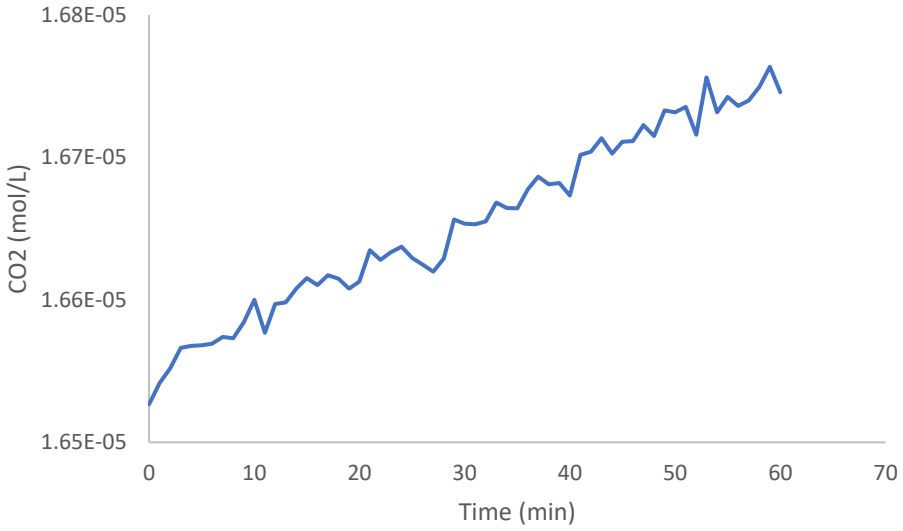

Fig. 9. Change in CO_2 concentration over time, recorded during deployment of the LI-8100A over dry ultramafic rock (Tablelands, June 25, 2019).

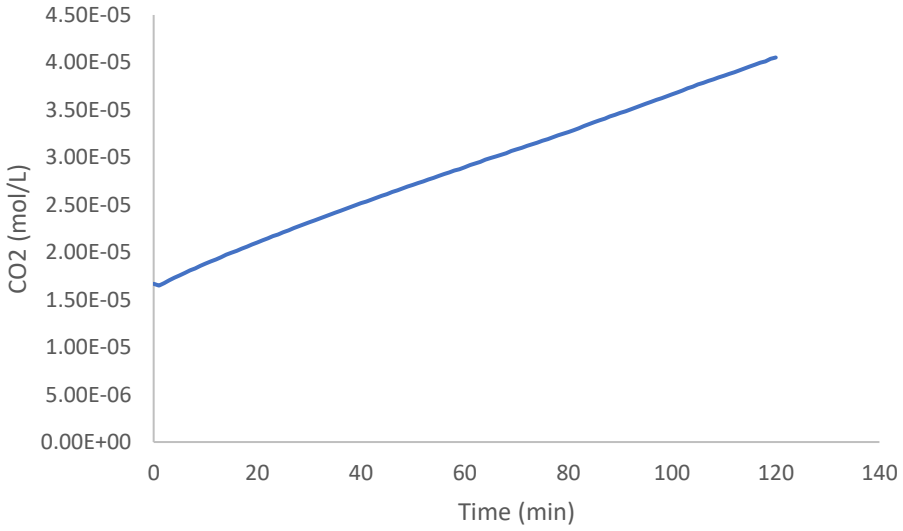

Fig. 10. Change in CO_2 concentration over time, recorded during deployment of the LI-8100A over local vegetation (Tablelands, June 25, 2019).

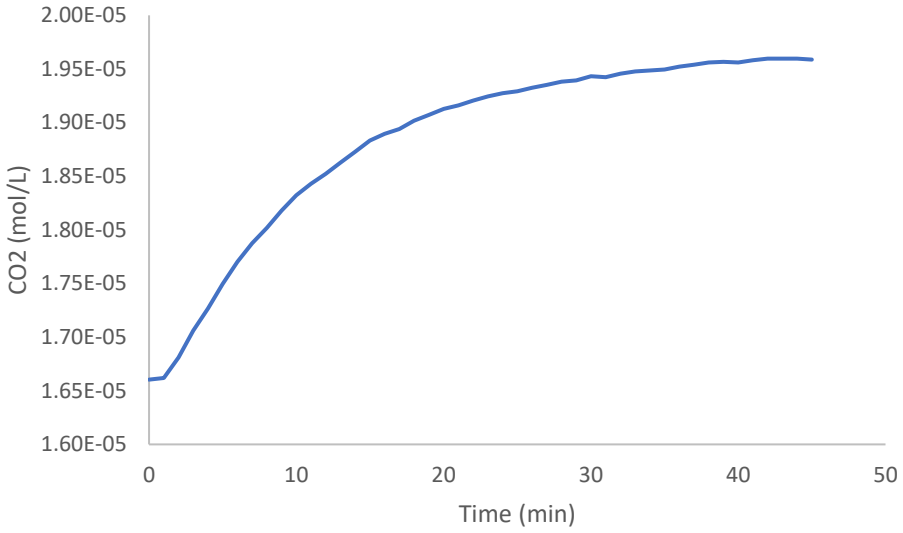

Fig. 11. Change in CO_2 concentration over time, recorded during deployment of the LI-8100A over dry ultramafic gravel (Tablelands, June 25, 2019).

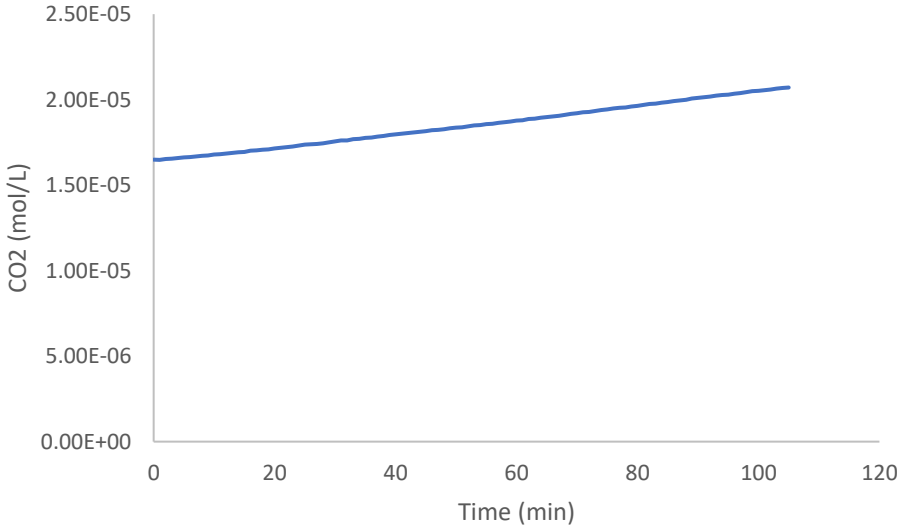

Fig. 12. Change in CO_2 concentration over time, recorded during deployment of the LI-8100A over a small bog (Tablelands, June 23, 2019).

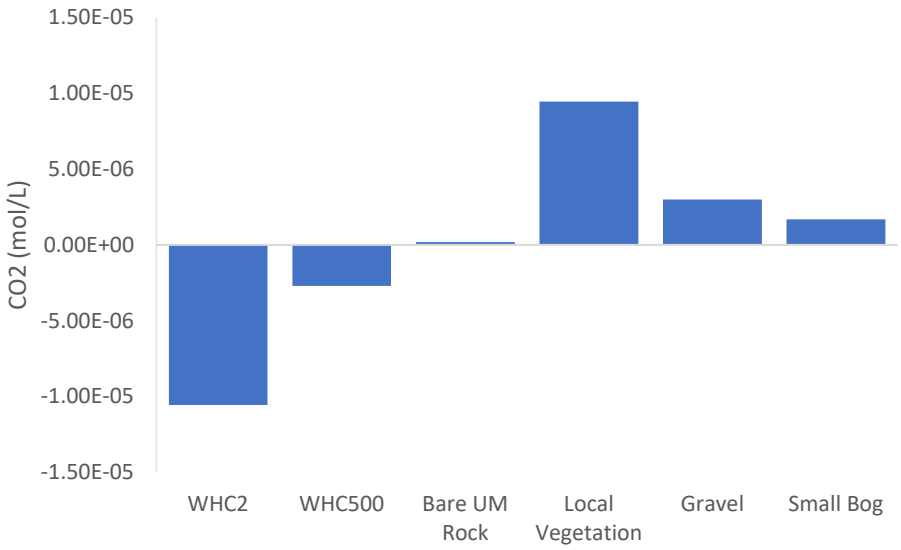

Fig. 13. Change in CO_2 concentration at each location over the first 45 minutes of each measurement (Tablelands, 2019).

Over the first 45 minutes only two locations recorded a decrease in CO_2 concentrations: WHC2 with a change of -1.1×10^{-5} mol/L, and WHC500 with a change of -2.7×10^{-6} mol/L (Fig. 10). The other four locations all had increases in CO_2 concentration: local vegetation with the largest change of 9.4×10^{-6} mol/L, gravel with a change of 3.0×10^{-6} mol/L, small bog with a change of 1.7×10^{-6} mol/L, and bare ultramafic rock with the smallest increase of 1.8×10^{-7} mol/L.

3.2 Five-hour CO_2 sequestration experiments with atmospheric CO_2 concentrations and Tablelands rocks

3.2.1 Total CO_2 sequestered over 5 hours

CO_2 concentrations decreased with time in all the atmospheric CO_2 sequestration experiments, except for experiments using deionized (DI) water only (Fig. 14A, DI). These DI water experiments provided a baseline for comparison for other experiments using other water types and with rock additions. The DI-water plus crushed rock experiments had an average

decrease of $-1.1 \times 10^{-5} \pm 9.3 \times 10^{-7}$ mol CO_2 removed from the headspace over the course of the five hour experiment while the DI water only experiments had an average decrease of $-2.5 \times 10^{-6} \pm 8.6 \times 10^{-7}$ mol CO_2 over the course of the five hour experiment. The DI water plus Tablelands whole rock (TWR) experiments were conducted twice, in triplicate, with two different rock cubes cut from the same rock sample to test experimental reproducibility (Fig. 14A, DI + TWR1 and DI + TWR2). This reproducibility check was only done for DI water experiment and not repeated for the experiments at higher pH. These two sets of experiments resulted in an average decrease of $-3.6 \times 10^{-6} \pm 9.1 \times 10^{-7}$ mol CO_2 for experiments using cube 1, and an average change of $-1.7 \times 10^{-6} \pm 2.6 \times 10^{-6}$ mol CO_2 for experiments using cube 2 over the course of the five hour experiments. There was a significant difference in the change in CO_2 concentration between the DI-water only experiments and the DI-water plus whole rock cube 1 experiments (p-value 0.23). However, the addition of crushed rock was significantly different than DI-water only (p-value 0.01). There were no significant differences in the change of CO_2 concentration between experiments with crushed rock and whole rock (p-value 0.06).

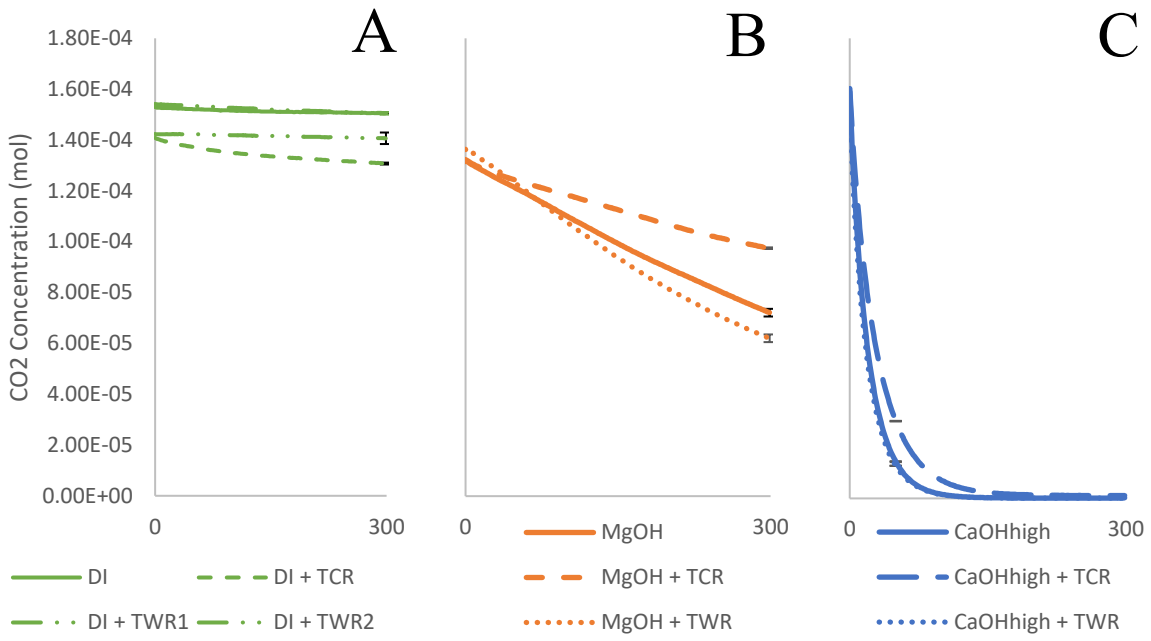

Fig. 14. Average CO_2 concentrations measured during the DI water (A), MgOH water (B), and CaOH-high water (C) experiments run with atmospheric CO_2 concentrations, where TCR represents experiments run with Tablelands crushed rock and TWR represents experiments run with Tablelands whole rock. Values are averages of triplicate experiments with error bars on the last plotted point representing standard deviation of the averages.

The experiments with MgOH water and no rock had an average CO_2 concentration decrease of $-5.9 \times 10^{-5} \pm 1.0 \times 10^{-5}$ mol CO_2 over the course of the five-hour experiments (Fig. 14B). Crushed rock plus MgOH water experiments resulted in an average decrease in CO_2 concentration of $-3.5 \times 10^{-5} \pm 4.0 \times 10^{-6}$ mol. The MgOH with whole rock experiments resulted in an average decrease of $-7.4 \times 10^{-5} \pm 1.2 \times 10^{-5}$ mol CO_2. For MgOH water experiments, the addition of either crushed rock or whole rock cubes had no significant effect (p-values of 0.07 and 0.79, respectively) on the amount of CO_2 sequestered compared to MgOH water only experiments. There were also no significant differences between crushed rock or whole rock experiments (p-value 0.15).

CaOH-high experiments sequestered the most CO_2 compared to the other experiments performed with ambient CO_2 (Fig. 14C). All of the experiments sequestered CO_2 rapidly at the beginning of the experiments but slowed over the course of the experiments as CO_2 concentrations in the chamber decreased. The CaOH-high water experiments had an average decrease in CO_2 concentration of $-1.4 \times 10^{-4} \pm 1.0 \times 10^{-5}$ mol over the five-hour experiments. The CaOH-high water and crushed rock experiments resulted in an average decrease in CO_2 concentration of $-1.4 \times 10^{-4} \pm 5.4 \times 10^{-6}$ mol during the five-hour experiments. The CaOH-high water and whole rock experiments had a decrease of $-1.4 \times 10^{-4} \pm 5.2 \times 10^{-6}$ mol CO_2 over the course of the five hour experiments. The CaOH-high water only experiments were not significantly different than the experiments with added crushed rock (p-value 0.87) or whole rock cubes (p-value 0.46). There were no significant differences between crushed rock and whole rock experiments (p-value 0.21).

3.2.2 *CO_2 flux*

The average CO_2 gas flux was calculated for the first 30 minutes of each experiment (Fig. 15). This time segment was selected because it was where the concentration change with time was closest to a linear relationship, an assumption that must be made to apply Equation 1. During this part of the experiment the conditions inside the chamber represented when the experimental set-up most closely resembled an open system. Linearity in the concentration versus time data was confirmed by checking the correlation coefficient of the linear line of best fit. The R^2 values were always better than 0.90 except for experiments with rock.

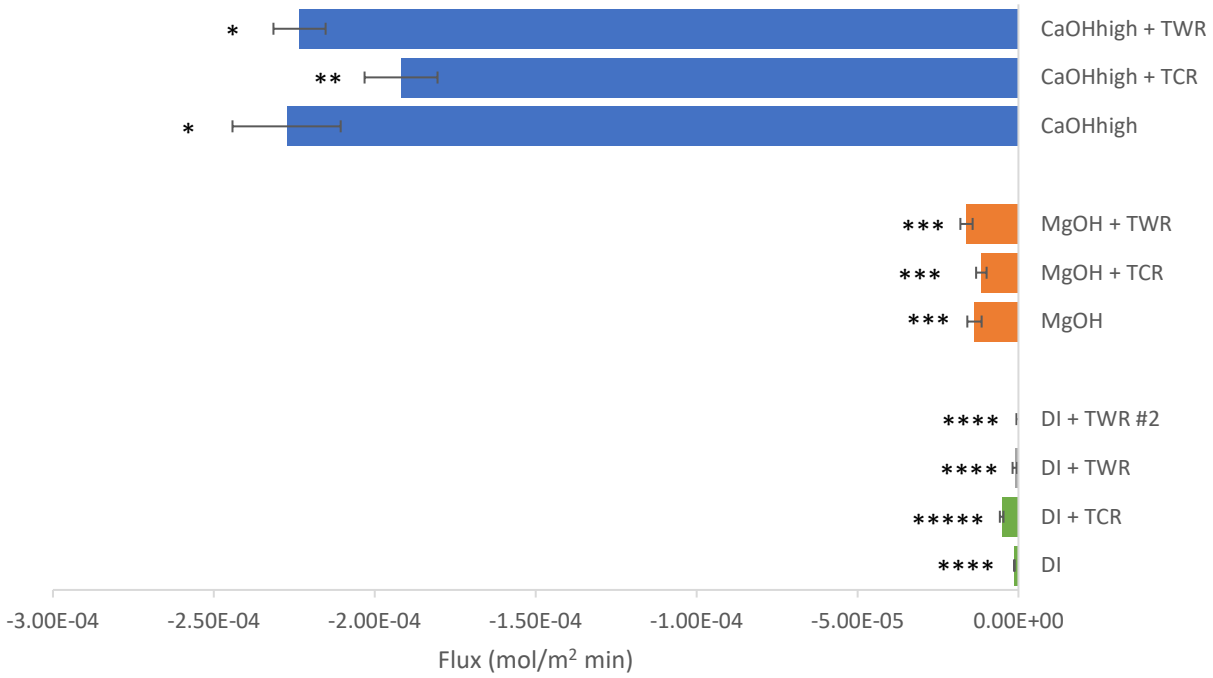

Fig. 15. Average flux values (mol/m^2·min) from triplicate experiments, calculated from the first 30 minutes of each experiment. Error bars are standard deviation of the average flux values from triplicate experiments. Experiments showing no significant difference compared to each other are indicated with matching asterisks.

The DI water plus crushed rock experiments had an average flux of $-5.2 \times 10^{-6} \pm 5.6 \times 10^{-7}$ mol/m^2·min. There was a significant difference in CO_2 flux between the DI water only experiments and the DI water plus crushed rock experiments (p-value 0.01). There was also a significant difference when comparing the DI water plus crushed rock experiments to the first and second DI water plus whole rock experiments (p-value <0.01 for both whole rock experiments). As expected, there was no significant difference between the first and second DI plus whole rock experiments when compared to each other (p-value 0.13). MgOH water experiments had CO_2 fluxes ranging from MgOH water plus crushed experiments with an average flux of $-1.2 \times 10^{-5} \pm 1.6 \times 10^{-6}$ mol/m^2·min to MgOH water plus whole rock experiments

with an average CO_2 flux of $-1.6 \times 10^{-5} \pm 1.9 \times 10^{-6}$ mol/m^2·min. There was no significant difference in CO_2 flux between any of the MgOH experiments. CaOH-high experiments sequestered the most CO_2 of all the sequestration experiments during the five hour experiments. The CaOH-high water only experiments had an average flux of $-2.3 \times 10^{-4} \pm 1.7 \times 10^{-5}$ mol/m^2·min. The CaOH-high water plus crushed rock experiments resulted in an average flux of $-1.9 \times 10^{-4} \pm 1.1 \times 10^{-5}$ mol/m^2·min while the CaOH-high water plus whole rock experiments had an average flux of $-2.2 \times 10^{-4} \pm 8.1 \times 10^{-6}$ mol/m^2·min. There was a significant difference in CO_2 flux between CaOH-high water only experiments and CaOH-high water plus crushed rock experiments (p-value 0.05). There was also a significant difference in CO_2 flux between CaOH-high water plus crushed rock and CaOH-high water plus whole rock experiments (p-value 0.02). There was no significant difference between CaOH-high water only experiments and whole rock experiments (p-value 0.73).

3.2.3 Change in pH

All experiments where the mean change in pH value was greater than the standard deviation resulted in average decreases in pH (more acidic conditions) over the course of the five-hour experiments (Fig. 16). The DI water plus crushed rock experiments resulted in the largest decrease had an average pH change of -3.1 ± 0.5 while the DI water plus whole rock cube #2 experiments resulted in an average pH change of -0.8 ± 0.5. There was a significant difference between the DI water plus crushed rock experiments and the DI-water plus whole rock cube #2 experiments (p-value <0.01). The MgOH water only experiments resulted in slightly more acidic conditions and had an average pH change of -0.1 ± 0.04 over the course of the five-hour experiments. MgOH water with crushed rock experiments resulted in more acidic conditions and an average pH change of -0.4 ± 0.1 during the five-hour experiments. There was a

significant difference in pH between the MgOH water only experiments and the MgOH water plus crushed rock experiments (p-value 0.04).

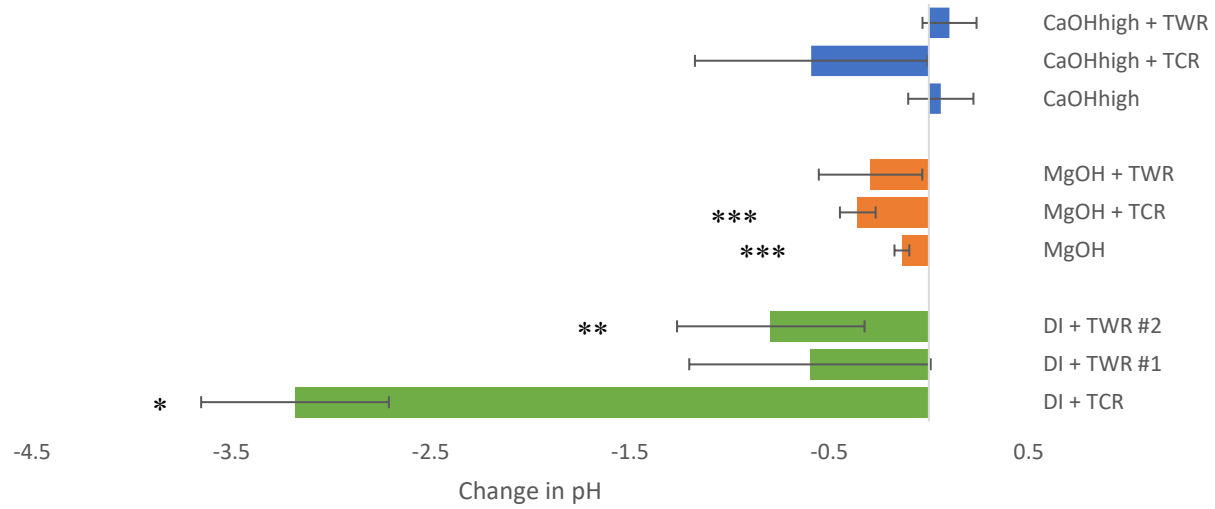

Fig. 16. The average change in pH of triplicate CO_2 sequestration experiments starting with atmospheric CO_2 experiments. Error bars are the standard deviation of the average of triplicate experiments. Experiments showing no significant difference compared to each other are indicated with matching asterisks. Statistics were not run on mean values when standard deviation was greater than the mean value.

3.2.4 Change in aqueous total inorganic carbon

DI water with crushed rock experiments had an average increase of $1.9 \times 10^{-4} \pm 3.9 \times 10^{-5}$ mol/L of C over the course of the five-hour experiments (Fig. 17). The experiments using cube #1 and DI water had an average increase of $2.4 \times 10^{-5} \pm 1.3 \times 10^{-5}$ mol/L of C. The DI water and cube #2 experiments had an average increase of $1.9 \times 10^{-5} \pm 6.8 \times 10^{-6}$ mol/L of C. The DI water plus crushed rock experiments were significantly different in the average change of TIC concentration when compared to both the DI water plus whole rock experiments (p-values of 0.01 for both cube #1 and #2). There was no significant difference in the average change of TIC

concentration when comparing the two DI plus whole rock experiments to each other (p-value 0.59).

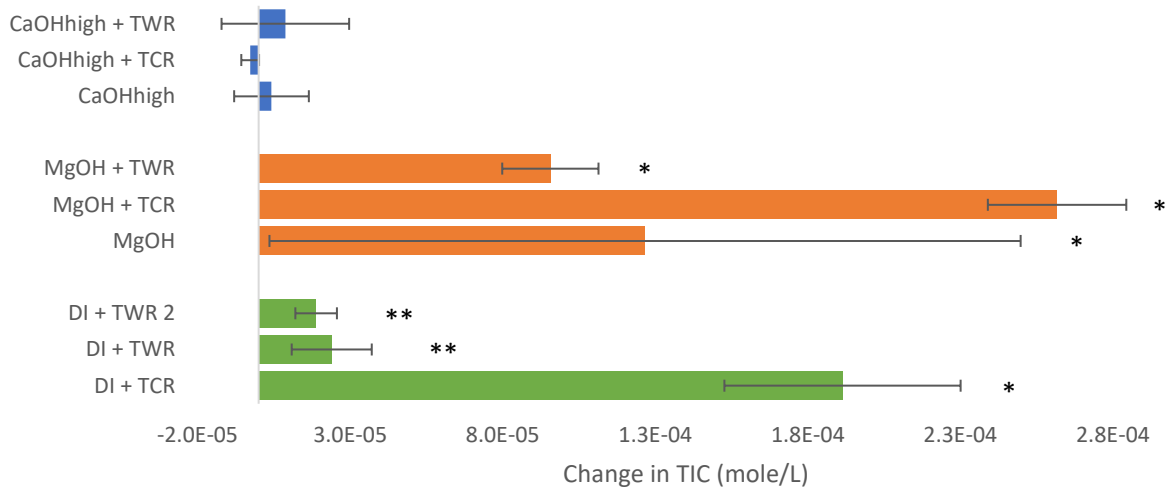

Fig. 17. The average change in TIC (mol/L) of triplicate CO_2 sequestration experiments starting with atmospheric CO_2 concentrations. Values are the average change in concentration between initial and final TIC concentrations. Error bars are the standard deviations of the triplicate experiments. Statistics were not run on mean values when standard deviation was greater than the mean value.

The MgOH water experiments with no rock had an average increase in mol/L of C of $5.6 \times 10^{-5} \pm 1.7 \times 10^{-5}$ over the course of the five-hour experiments (Fig. 17). MgOH water and crushed rock experiments had an average increase of $2.6 \times 10^{-4} \pm 2.3 \times 10^{-5}$ mol/L of C. The experiments with MgOH water and whole rock had an average increase of $9.6 \times 10^{-5} \pm 1.6 \times 10^{-5}$ mol/L of C. There was no significant difference in the average change of TIC concentration when comparing the MgOH water only experiments to either the MgOH water plus crushed rock experiments (p-value 0.19) or the MgOH water plus whole rock experiments (p-value 0.71). There is a significant difference when comparing the average change in TIC concentration of the

MgOH water plus crushed rock experiments to the MgOH water plus whole rock experiments (p-value <0.01).

3.2.5 Change in conductivity

CaOH-high experiments were the only experiments to show decreases in conductivity over the course of the five-hour experiments with CaOH plus crushed rock experiments having the greatest average decrease in conductivity of $-1.1 \times 10^{0} \pm 2.2 \times 10^{-1}$ mS/cm (Fig. 18). The CaOH-high water only experiments and CaOH-high water plus whole rock experiments were the next largest decreases with average decreases of $-1.6 \times 10^{-1} \pm 8.4 \times 10^{-2}$ mS/cm and $-2.4 \times 10^{-1} \pm 1.9 \times 10^{-1}$ mS/cm, respectively. DI water plus crushed rock was the only experiment to show an increase in conductivity with an average increase of $4.6 \times 10^{-2} \pm 7.2 \times 10^{-3}$ mS/cm. There was a significant difference in conductivity between CaOH-high water only experiments and CaOH-high water plus crushed rock experiments (p-value 0.01) as well as between CaOH-high water plus crushed rock and CaOH-high water plus whole rock (p-value 0.01).

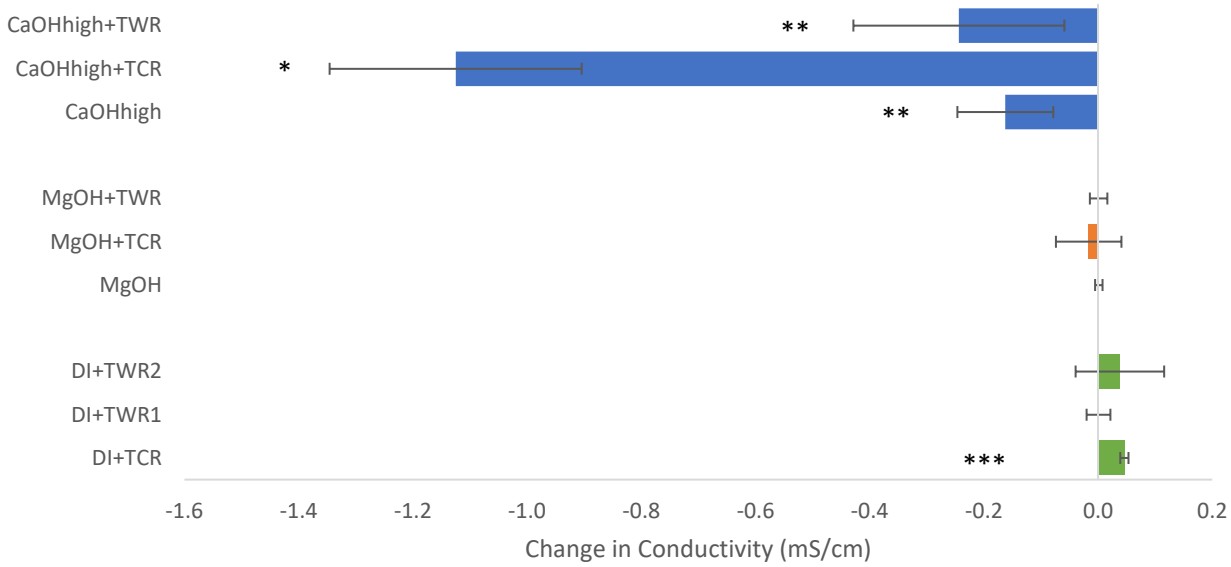

Fig. 18. Average change in conductivity (mS/cm) of triplicate CO_2 sequestration starting with atmospheric CO_2 concentrations. Values are the average change in concentration between initial and final conductivity measurements. Error bars are the standard deviations of the average of the triplicate experiments. Experiments showing no significant difference compared to each other are indicated with matching asterisks. Statistics were not run on mean values when standard deviation was greater than the mean value.

3.2.6 Change in dissolved elemental concentrations

CaOH-high experiments resulted in the largest average decreases with the largest being CaOH-high water only experiments with an average decrease in Ca concentration of $-6.4 \times 10^{-3} \pm 5.5 \times 10^{-3}$ mol/L to CaOH-high water plus whole rock with an average decrease of $-1.1 \times 10^{-3} \pm 7.6 \times 10^{-4}$ mol/L of Ca. There was no significant differences between any of the CaOH-high experiments. The DI water plus whole rock cube #2 experiments resulted in an average Ca increase of $5.8 \times 10^{-6} \pm 1.4 \times 10^{-6}$ mol/L over the course of the five-hour experiments (Fig. 19). MgOH plus crushed rock were the only MgOH experiments to have an average change above the instrument detection limit with an average increase of $2.5 \times 10^{-5} \pm 2.2 \times 10^{-5}$ mol/L of Ca. Ca concentrations in the MgOH water only and MgOH water plus whole rock experiments were both below instrument detection limit.

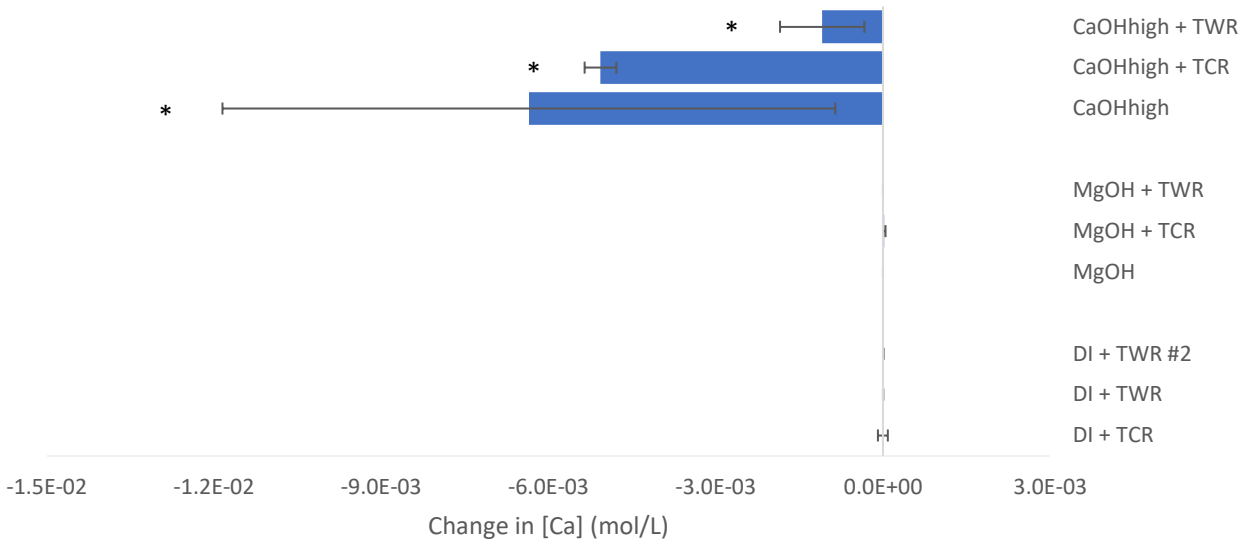

Fig. 19. Average change in Ca concentration in mol/L of triplicate CO_2 sequestration experiments starting with atmospheric CO_2 concentrations. Values are the average change in concentration between initial and final measurements. Error bars are the standard deviations of the average of the triplicate experiments. Statistics were not run on mean values when standard deviation was greater than the mean value.

All MgOH water sequestration experiments resulted in an average increase in Mg concentrations (Fig. 20). MgOH experiments ranged between MgOH water only experiments with an average increase in Mg concentration of $1.2 \times 10^{-4} \pm 1.9 \times 10^{-5}$ mol/L to MgOH water plus crushed rock experiments, which resulted in an average increase of $1.9 \times 10^{-4} \pm 7.4 \times 10^{-5}$ mol/L. The DI water experiments also all resulted in average increases in Mg concentration with the DI water plus crushed rock experiments having the largest average increase of $1.9 \times 10^{-4} \pm 1.0 \times 10^{-5}$ mol/L and with DI water plus whole rock cube #2 experiments resulting in an average change of Mg of $1.4 \times 10^{-5} \pm 2.8 \times 10^{-6}$ mol/L. All of the CaOH-high water experiments resulted in values where the standard deviation was greater than the average change in Mg concentration.

There was no significant difference between any of the MgOH experiments. There was also no significant difference between any of the DI water experiments.

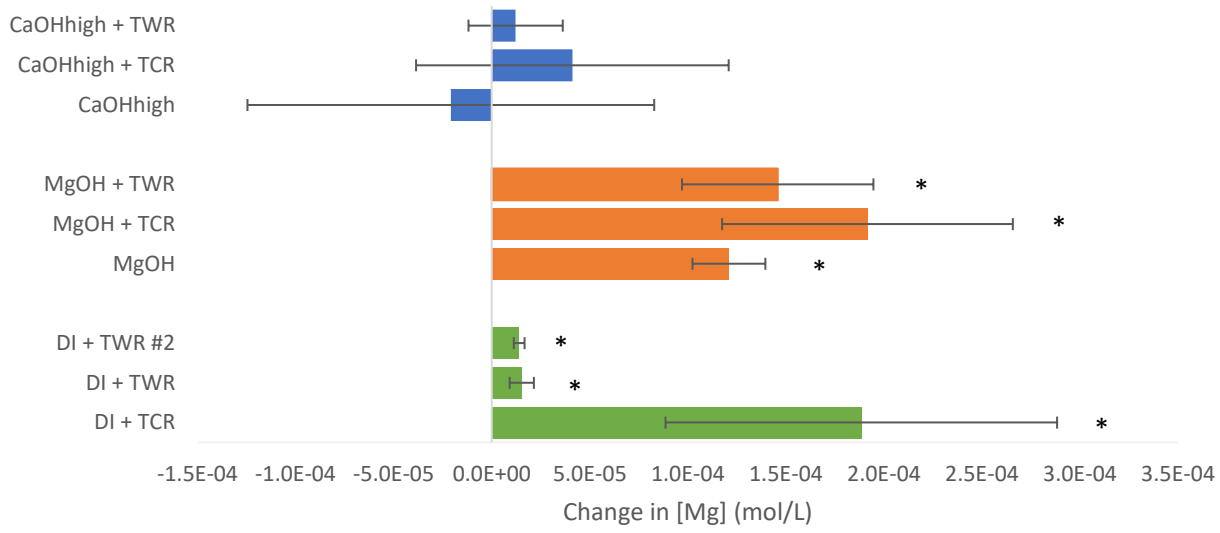

Fig. 20. Average change in Mg concentration in mol/L of triplicate CO_2 sequestration experiments starting with atmospheric CO_2 concentrations. Values are the average change in concentration between initial and final measurements. Error bars are the standard deviations of the average of the triplicate experiments. Statistics were not run on mean values when standard deviation was greater than the mean value.

Average Si concentration increased over the course of all of the five-hour sequestration experiments with the exception of CaOH-high water plus crushed rock and CaOH-high water only experiments (Fig. 21). The largest average increases were during the DI water plus crushed rock experiments with an average increase in Si concentration of $1.4 \times 10^{-5} \pm 6.5 \times 10^{-6}$ mol/L and the MgOH water plus crushed rock experiments which had an average increase of $9.7 \times 10^{-6} \pm 1.9 \times 10^{-6}$ mol/L. There was no significant difference between any of the DI water

experiments. However, there was a significant difference between the MgOH water only and MgOH water plus crushed rock experiments (p-value 0.02) and also between MgOH water plus crushed rock and MgOH water plus whole rock experiments (p-value 0.02). There was no significant difference between MgOH water only experiments and MgOH water plus whole rock experiments (p-value 0.06).

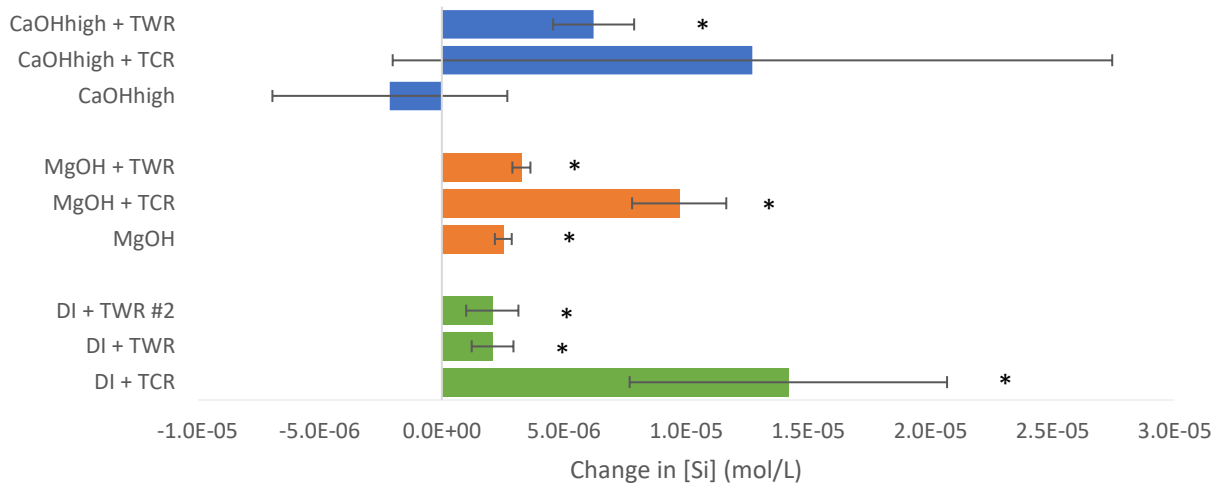

Fig. 21. Average change in Si concentration in mol/L of triplicate CO_2 sequestration experiments starting with atmospheric CO_2 concentrations. Values are the average change in concentration between initial and final measurements. Error bars are the standard deviations of the average of the triplicate experiments. Statistics were not run on mean values when standard deviation was greater than the mean value.

3.3 Four hour CO_2 Sequestration experiments with atmospheric CO_2 concentrations and Tablelands rocks

3.3.1 Total CO_2 sequestered over four-hour experiments

Both CaOH water plus crushed rock and CaOH water plus whole rock experiments sequestered CO_2 over the course of the four-hour experiments. The CaOH water plus crushed

rock experiments resulted in an average decrease in CO_2 concentration of $-1.1 \times 10^{-4} \pm 4.5 \times 10^{-6}$ mol C, while CaOH water plus whole rock resulted in an average decrease of $-1.1 \times 10^{-4} \pm 6.4 \times 10^{-5}$ mol C. There was no significant difference between the two experiments (p-value 0.95).

3.3.2 CO_2 flux

Over the first 30 minutes of the experiments, all CaOH water experiments resulted in negative fluxes (Fig. 22). There were no significant differences between any of the experiments: CaOH water plus crushed rock versus CaOH plus whole rock experiments (p-value 0.42), CaOH water plus crushed rock versus. CaOH water only experiments (p-value 0.44), and CaOH water only vs. CaOH water plus whole rock experiments (p-value 0.44).

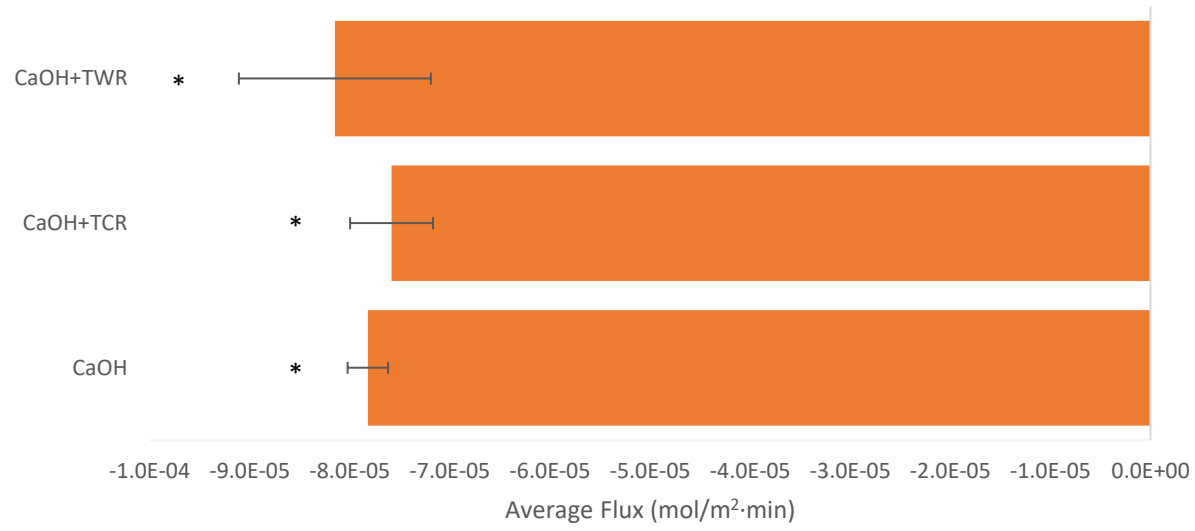

Fig. 22. Average flux values (mol/m^2·min) from triplicate CO_2 sequestration experiments, calculated from the first 30 minutes of each experiment. Error bars are the standard deviations of the average of the triplicate experiments. Experiments showing no significant differences compared to each other are indicated with matching asterisks.

3.3.3 Change in pH

CaOH water only and both CaOH water plus crushed rock and CaOH water plus whole rock experiments resulted in average decreases in pH over the course of the experiments (Fig. 23). There were no significant differences between the three experiments (p-value 0.65).

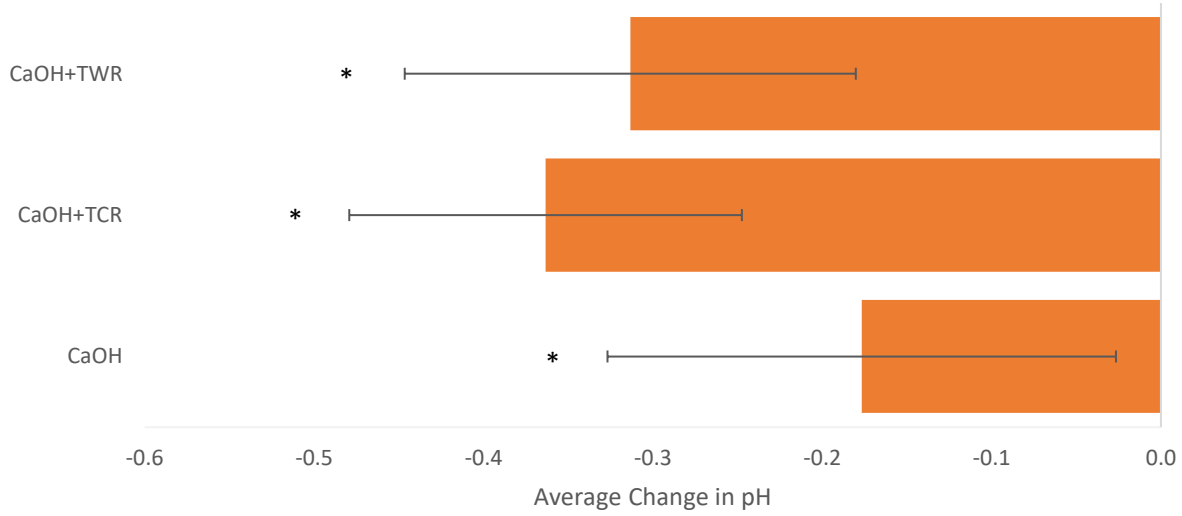

Fig. 23 Average change in pH from triplicate CO_2 sequestration experiments. Error bars are the standard deviations of the average of the triplicate experiments. Experiments showing no significant differences compared to each other are indicated with matching asterisks.

3.3.4 Change in total inorganic carbon

Over the course of the four-hour experiments CaOH water only, CaOH water plus crushed rock, and CaOH water plus whole rock experiments resulted in average decreases in TIC (Fig. 24). There was a significant difference between CaOH water only and CaOH water plus crushed rock experiments (p-value 0.01). There were no significant differences between the CaOH water plus crushed rock and CaOH water plus whole rock experiments (p-value 0.52) and also between CaOH water only and CaOH water plus whole rock experiments (p-value 0.09).

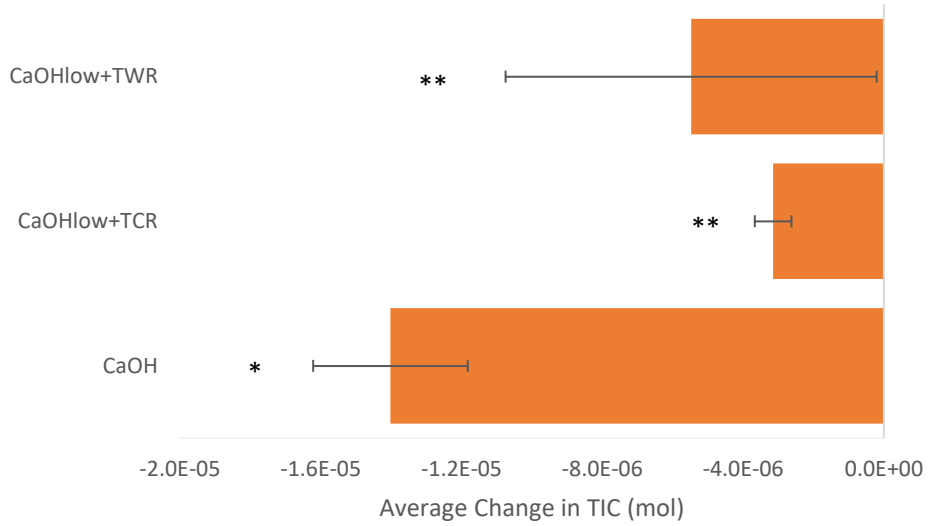

Fig. 24 Average change in total inorganic carbon (in mol C) from triplicate CO_2 sequestration experiments. Error bars are the standard deviation of the average of the triplicate experiments. Experiments showing no significant differences compared to each other are indicated with matching asterisks.

3.3.5 Change in conductivity

All three sets of experiments resulted in an average decrease in conductivity over the course of the four-hour experiments (Fig. 25). There was a significant difference in the conductivity change between the CaOH water only and CaOH water plus crushed rock experiments (p-value <0.01). There was no significant difference between the CaOH water plus crushed rock and CaOH water plus whole rock experiments (p-value 0.13) and there was also no difference between the CaOH water only and CaOH water plus whole rock experiments (p-value 0.23).

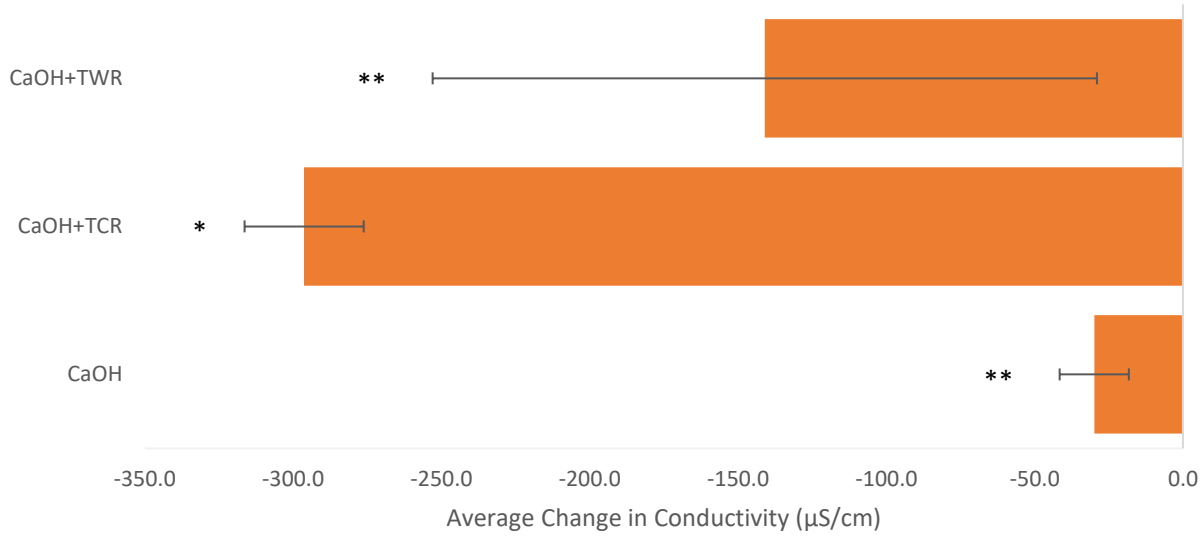

Fig. 25 Average change in conductivity (in µS/cm) from triplicate CO_2 sequestration experiments. Error bars are the standard deviations of the average of the triplicate experiments. Experiments showing no significant differences compared to each other are indicated with matching asterisks.

3.3.6 Change in dissolved element concentrations

Both of the CaOH water experiments resulted in an average decrease in Ca concentrations over the course of the four hour experiments (Fig. 26). There was a significant difference between the two experiments (p-value <0.01).

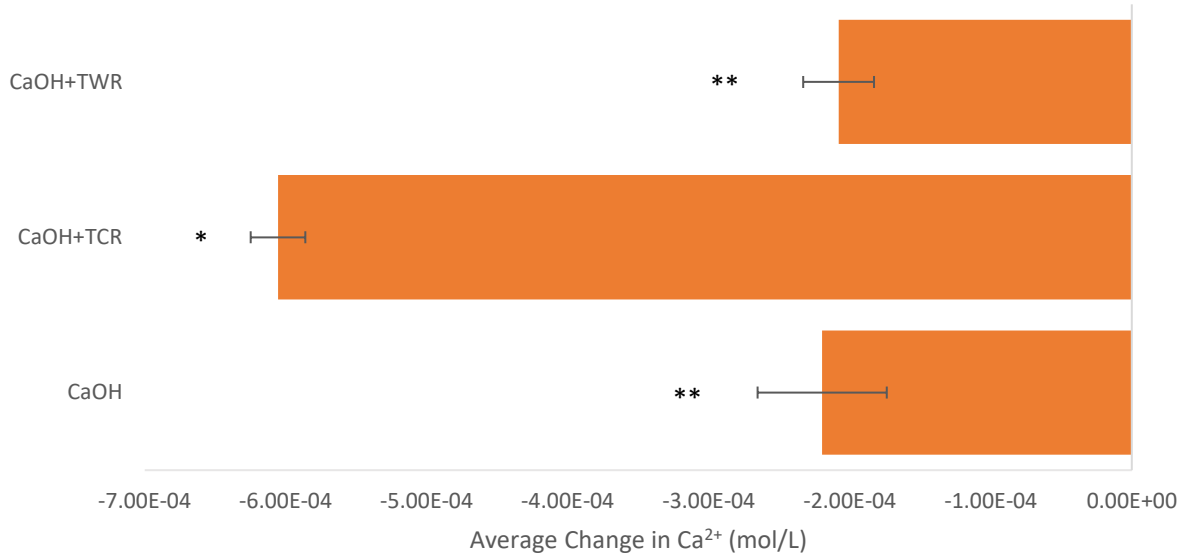

Fig. 26 Average change in Ca (in mol/L) from triplicate CO_2 sequestration experiments. Error bars are the standard deviations of the average of the triplicate experiments. Experiments showing no significant differences compared to each other are indicated with matching asterisks.

CaOH water plus crushed rock resulted in an average increase in Mg over the course of the four hour experiments (Fig. 27). Statistics were not run to compare the three sets of experiments as the crushed rock experiments were the only experiments to have an average greater than the standard deviation.

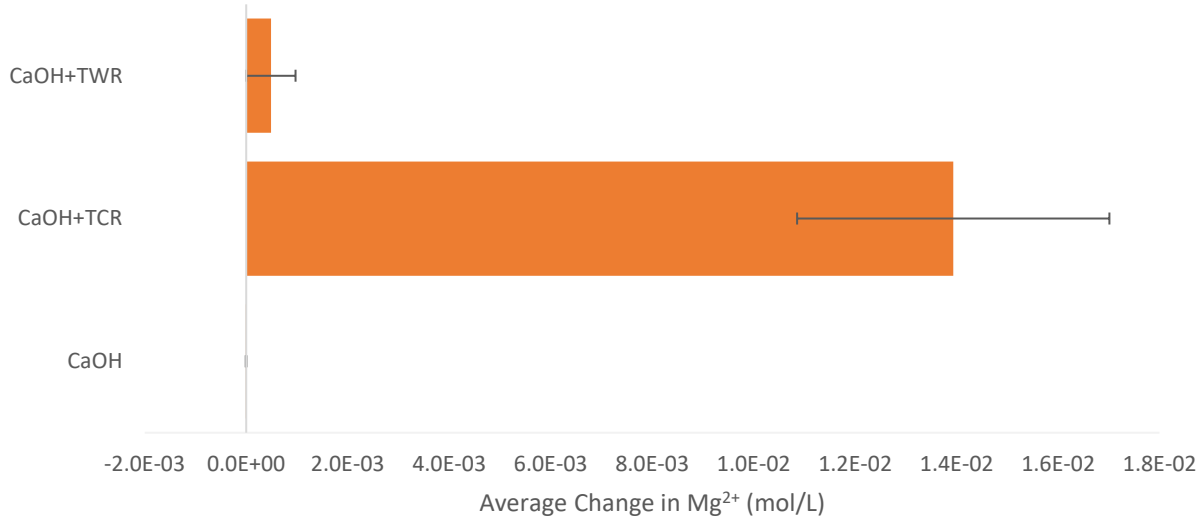

Fig. 27 Average change in Mg (in mol/L) from triplicate CO_2 sequestration experiments. Error bars are the standard deviations of the average of the triplicate experiments. Experiments showing no significant differences compared to each other are indicated with matching asterisks.

Both CaOH water experiments resulted in average increases in Si over the course of the four-hour experiments with CaOH water plus crushed rock having the largest increase (Fig. 28). There was a significant difference between the two experiments (p-value <0.01).

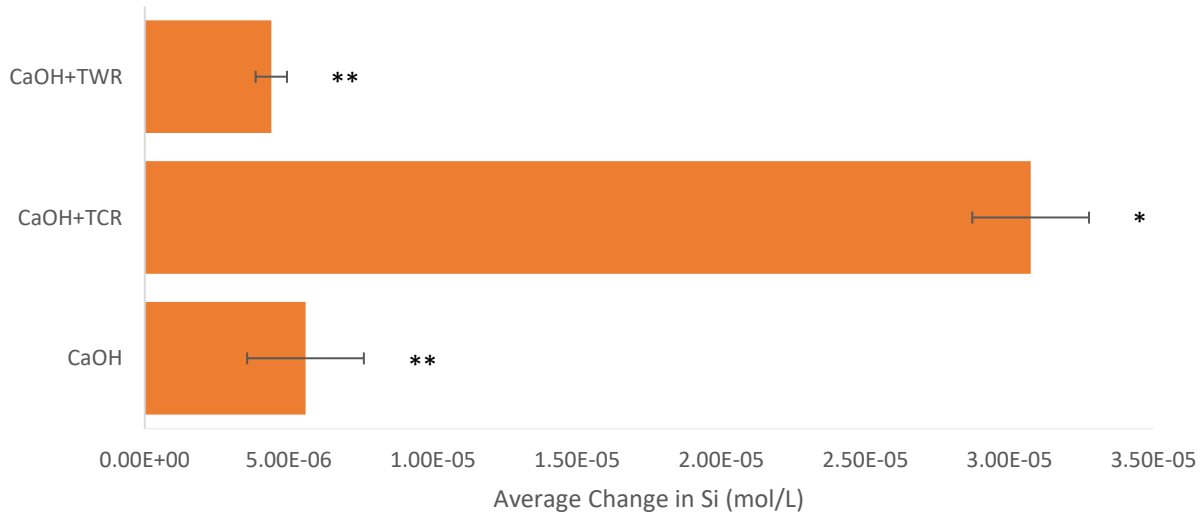

Fig. 28 Average change in Si (in mol/L) from triplicate CO_2 sequestration experiments. Error bars are the standard deviations of the average of the triplicate experiments. Experiments showing no significant differences compared to each other are indicated with matching asterisks.

3.4 CO_2 sequestration experiments with elevated CO_2 concentrations and Tablelands rocks

3.4.1 Total CO_2 sequestered over 5 hour experiments

All of the elevated CO_2 experiments resulted in an increase of CO_2 over the course of the five hour experiments with the exception of the CaOH-high water experiments (Fig. 29A). The DI water only experiment resulted in an average increase of $2.9 \times 10^{-5} \pm 1.1 \times 10^{-6}$ mol CO_2 over the course of the five hours. DI water plus crushed experiments resulted in an average increase of $2.7 \times 10^{-5} \pm 4.7 \times 10^{-6}$ mol CO_2 while the DI water plus whole rock experiments resulted in an increase in CO_2 concentration of $3.2 \times 10^{-5} \pm 1.3 \times 10^{-6}$ mol. There was no significant difference between any of the elevated CO_2 DI water experiments.

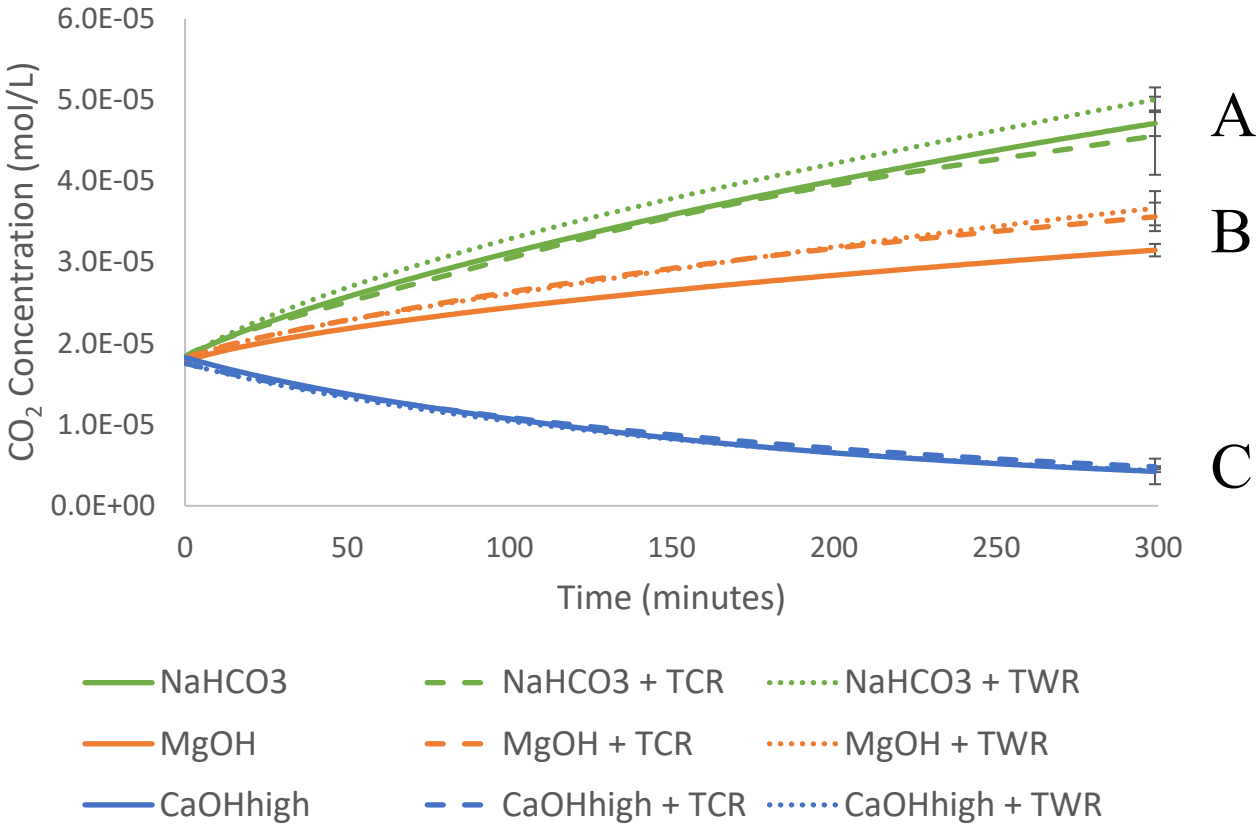

Fig. 29. Average CO_2 concentrations measured during the DI water (A), MgOH water (B), and CaOH-high water (C) experiments run with elevated CO_2 concentrations, where TCR represents experiments run with Tablelands crushed rock and TWR represents experiments run with Tablelands whole rock. Values are averages of triplicate experiments with error bars on the last plotted point representing average standard deviation.

All of the MgOH experiments removed more CO_2 from the survey chamber than the DI water experiments (Fig 29B) over the course of the five-hour experiments. The MgOH water only experiments with increased CO_2 concentration had an average increase of CO_2 of $1.4 \times 10^{-5} \pm 1.1 \times 10^{-6}$ mol. The MgOH water with crushed rock experiment resulted in an average increase of $1.7 \times 10^{-5} \pm 2.5 \times 10^{-6}$ mol CO_2. The MgOH water plus whole rock experiments resulted in an

average increased CO_2 concentration of $1.9 \times 10^{-5} \pm 2.0 \times 10^{-6}$ mole. There was no significant difference between any of the elevated CO_2 MgOH experiments.

Experiments with CaOH-high water removed the most CO_2 from the headspace over the course of the five hour experiments (Fig. 29C). The CaOH-high water only experiment resulted in an average decrease of $-1.4 \times 10^{-5} \pm 7.9 \times 10^{-7}$ mol CO_2 while the CaOH-high water plus crushed rock experiments resulted in an average decrease in total CO_2 of $-1.3 \times 10^{-5} \pm 1.9 \times 10^{-7}$ mol. The CaOH-high water plus whole rock experiments had an average decrease of $-1.3 \times 10^{-5} \pm 3.3 \times 10^{-7}$ mol CO_2. There was a significant difference between the elevated CO_2 CaOH-high water only and the elevated CO_2 CaOH-high water plus crushed rock experiments (p-value 0.02) and also between the elevated CO_2 CaOH-high water plus crushed rock and elevated CO_2 CaOH-high water plus whole rock experiments (p-value <0.01).

3.4.2 CO_2 flux

All of the elevated CO_2 DI water experiments had a positive CO_2 flux (Fig. 30). These experiments ranged between DI water plus crushed rock experiments with an average positive flux of $7.0 \times 10^{-5} \pm 6.0 \times 10^{-6}$ mol/m^2·min to the DI water plus whole rock experiments which resulted in an average positive a flux of $9.5 \times 10^{-5} \pm 5.2 \times 10^{-7}$ mol/m^2·min. There was no significant difference between elevated CO_2 DI water only experiments when compared to either elevated CO_2 DI water plus crushed rock experiments (p-value 0.14) or elevated CO_2 DI water plus whole rock experiments (p-value 0.08). There was a significant difference when comparing elevated CO_2 DI water plus crushed rock and elevated CO_2 DI water plus whole rock

experiments (p-value 0.02).

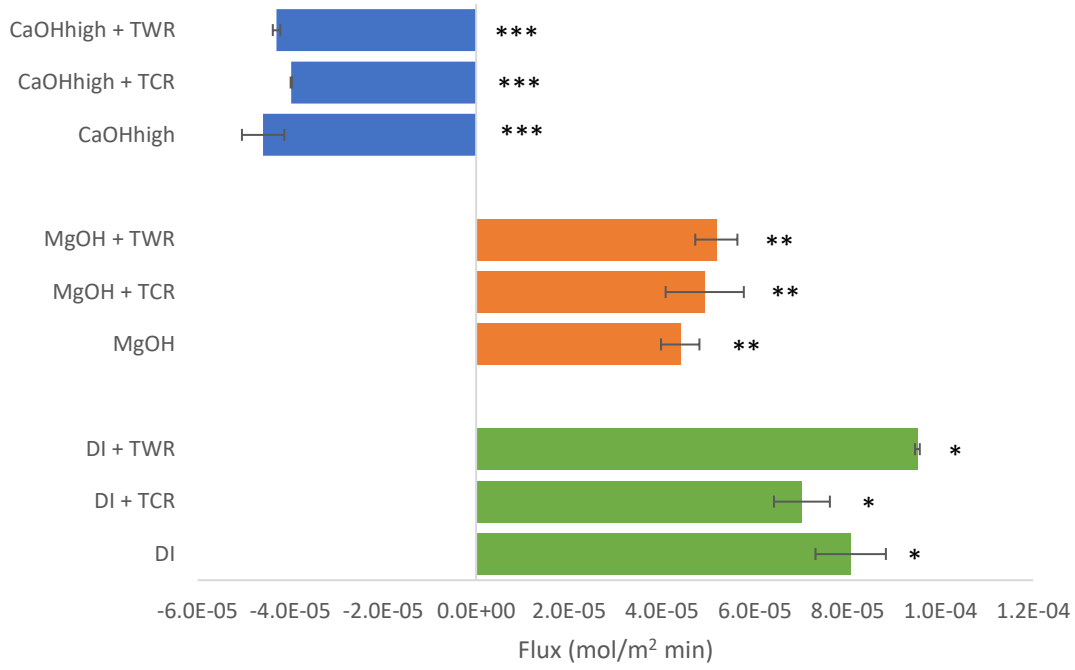

Fig. 30. Average flux values (mol/m^2·min) from triplicate experiments, calculated from the first 30 minutes of each experiment. Error bars are standard deviations of the average flux values from triplicate experiments. Experiments showing no significant difference compared to each other are indicated with matching asterisks.

All of the MgOH experiments had a positive CO_2 flux (Fig. 30). The MgOH water experiments ranged from MgOH water only experiments with an average positive flux of $4.4 \times 10^{-5} \pm 4.1 \times 10^{-6}$ mol/m^2·min to MgOH water plus whole rock experiments which resulted in an average positive flux of $5.2 \times 10^{-5} \pm 4.5 \times 10^{-6}$ mol/m^2·min. There was no significant difference between any of the elevated CO_2 MgOH experiments.

All of the CaOH-high experiments had a negative CO_2 flux, opposite to the other experiments (Fig. 30). The CaOH-high water experiments ranged between CaOH-high water only experiments which had an average negative flux of $-4.6 \times 10^{-5} \pm 4.6 \times 10^{-6}$ mol/m^2·min to

the CaOH-high water plus crushed rock experiments with an average negative CO_2 flux of -4.0 $\times 10^{-5} \pm 1.5 \times 10^{-7}$ mol/m^2·min. There was no significant difference between elevated CO_2 CaOH-high water only experiments and elevated CO_2 CaOH-high water plus crushed rock experiments (p-value 0.15). There was also no significant difference between elevated CO_2 CaOH-high water only experiments and elevated CO_2 CaOH-high water plus crushed rock experiments (p-value 0.39). However, there was a significant difference between elevated CO_2 CaOH-high water plus crushed rock and elevated CO_2 CaOH-high water plus whole rock experiments (p-value 0.02).

3.4.3 Change in pH

There were only two experiments where the average change in pH was greater than the standard deviation over the course of the five hour experiments (Fig. 31). MgOH water only experiments had an average increase in pH of 0.05 ± 0.04 and CaOH-high water only experiments resulted in an average increase in pH of 0.07 ± 0.05, the only CaOH-high experiments to show an average increase. There was no significant difference between the two experiments.

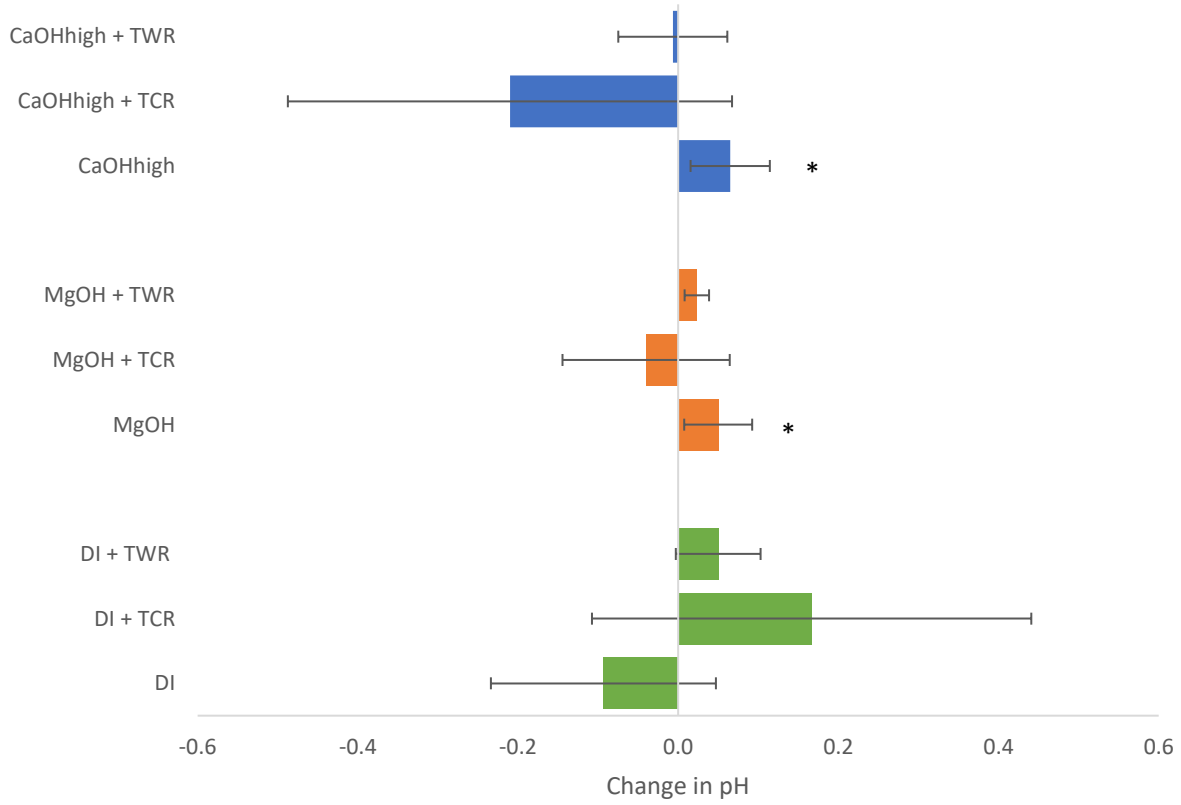

Fig. 31. The average change in pH of triplicate CO_2 sequestration experiments starting with elevated CO_2. Error bars are the average standard deviations of the average. Experiments showing no significant difference compared to each other are indicated with matching asterisks. Statistics were not run on mean values when standard deviation was greater than the mean value.

3.4.4 Change in aqueous total inorganic carbon

All the experiments where the average change in TIC was greater than the standard deviation resulted in decreases in TIC with the exception of CaOH-high water plus crushed rock which resulted in an average increase in TIC (Fig. 32). CaOH-high water only experiments resulted in an average decrease in TIC of $-1.2 \times 10^{-3} \pm 8.8 \times 10^{-4}$ mol/L of C. CaOH-high water plus crushed rock experiments had an average increase of $2.0 \times 10^{-3} \pm 2.6 \times 10^{-4}$ mol/L of C, while CaOH-high water plus whole rock experiments had an average decrease of $-2.2 \times 10^{-3} \pm$

2.9×10^{-4} mol/L of C. There was a significant difference between the elevated CO_2 CaOH-high water only experiments and the elevated CO_2 CaOH-high water plus crushed rock experiments (p-value 0.02). There was also a significant difference between the elevated CO_2 CaOH-high water plus crushed rock experiments and the elevated CO_2 CaOH-high water plus whole rock experiments (p-value <0.01). There was no significant difference between the elevated CO_2 CaOH-high water only experiments and the elevated CO_2 CaOH-high water plus whole rock experiments. MgOH plus crushed rock experiments were the only MgOH experiments to result in values where the average value was greater than the standard deviation and showed an average decrease of mol of C/L of $-8.4 \times 10^{-4} \pm 6.1 \times 10^{-4}$. Whole rock plus DI water experiments resulted in an average change of $-9.8 \times 10^{-4} \pm 5.8 \times 10^{-4}$ mol/L of C.

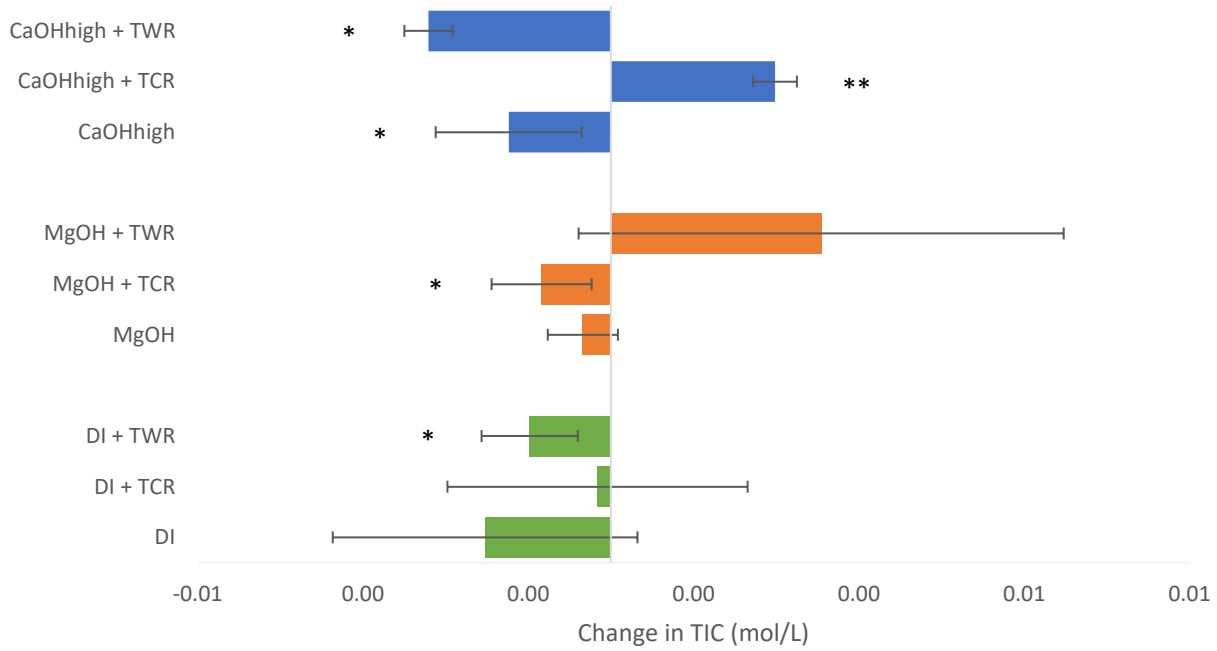

Fig. 32. The average change in TIC (mol/L of C) of triplicate CO_2 sequestration experiments starting with elevated CO_2 concentrations. Values are the average change in concentration between initial and final

TIC concentrations. Error bars are standard deviations of the triplicate experiments. Statistics were not run on mean values when standard deviation was greater than the mean value.

3.4.5 Change in conductivity

DI water plus crushed rock experiments were the only DI water experiments to result in values where the mean was greater than the standard deviation with an average increase in conductivity of $4.3 \times 10^{-2} \pm 1.3 \times 10^{-2}$ mS/cm (Fig. 33). MgOH water only experiments resulted in an average increase of $3.7 \times 10^{-2} \pm 2.9 \times 10^{-2}$ mS/cm while MgOH water plus whole rock experiments resulted in an average increase of $3.9 \times 10^{-2} \pm 3.4 \times 10^{-2}$ mS/cm. There was no significant difference between any of the elevated CO_2 MgOH water experiments. All three CaOH-high water experiments resulted in values where the standard deviation was greater than the average change.

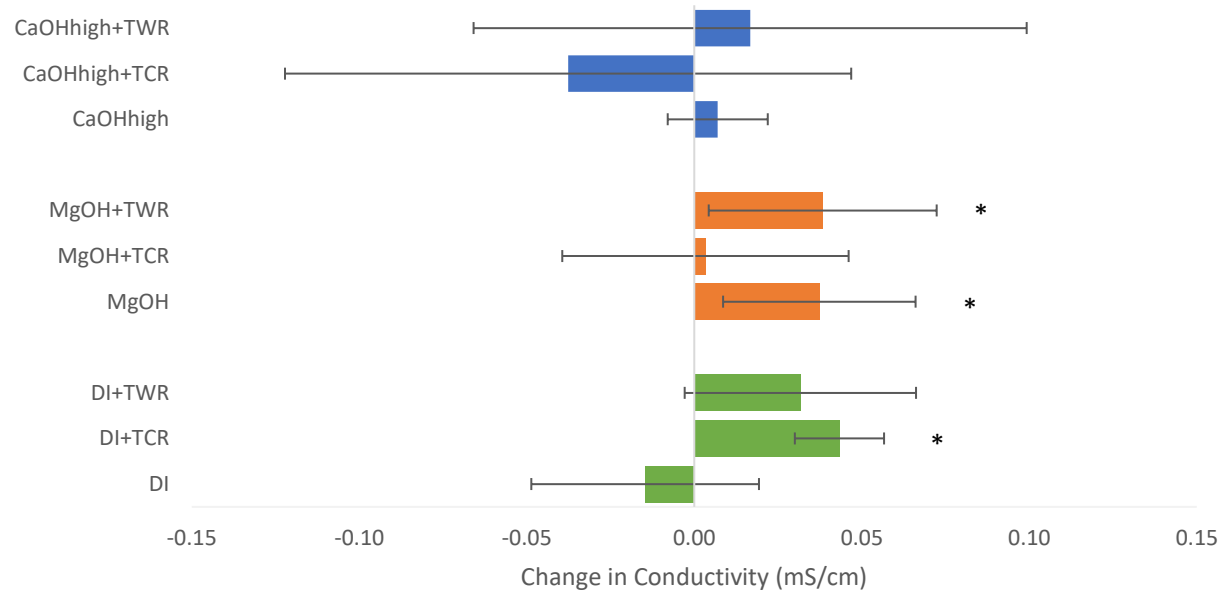

Fig. 33. Average change in conductivity (mS/cm) of triplicate CO_2 sequestration starting with elevated CO_2 concentrations. Values are the average change in concentration between initial and final conductivity measurements. Error bars are the standard deviations of the average of the triplicate experiments.

Experiments showing no significant difference compared to each other are indicated with matching asterisks. Statistics were not run on mean values when standard deviation was greater than the mean value.

3.4.6 Change in dissolved element concentrations

The only sequestration experiments to result in values where the standard deviation was larger than the average Ca concentration change was MgOH water plus crushed rock with an average concentration increase of $7.7 \times 10^{-6} \pm 2.9 \times 10^{-6}$ mol/L, CaOH-high water plus whole rock with an average decrease of $-2.7 \times 10^{-6} \pm 2.1 \times 10^{-6}$ mol/L, and MgOH water plus whole rock with and average increase of $2.7 \times 10^{-6} \pm 1.8 \times 10^{-6}$ (Fig. 34). Two experiments resulted in values below detection limits, DI water plus whole rock and DI water plus crushed rock, and the remaining experiments had results where the standard deviation was greater than the average change in Ca concentration. There was a significant difference in the change in Ca concentration between the MgOH water only experiments and MgOH water plus crushed rock experiments (p-value 0.03).

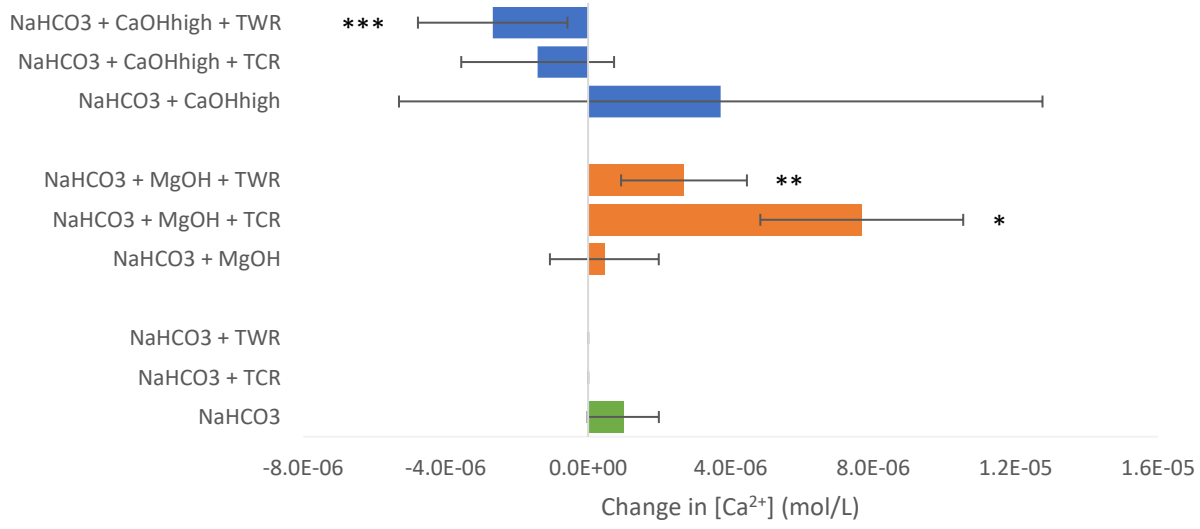

Fig. 34. Average change in Ca concentration in mol/L of triplicate CO_2 sequestration experiments starting with elevated CO_2 concentrations. Values are the average change in concentration between initial and final measurements. Error bars are the standard deviations of the average of the triplicate experiments. Statistics were not run on mean values when standard deviation was greater than the mean value.

All sequestration experiments showed an average increase in Mg concentration over the course of the five-hour experiments (Fig. 35). MgOH experiments had the largest average changes of all experiments with MgOH water only experiments resulting in an average increase of $5.1 \times 10^{-4} \pm 2.0 \times 10^{-4}$ mol/L, MgOH water plus crushed rock experiments having an average increase of $3.1 \times 10^{-4} \pm 6.4 \times 10^{-5}$ mol/L, and MgOH plus whole rock experiments resulted in an average Mg concentration increase of $5.5 \times 10^{-4} \pm 2.6 \times 10^{-4}$ mol/L. CaOH-high water plus crushed rock was the largest average increase among CaOH-high experiments with an average increase of $1.3 \times 10^{-4} \pm 2.0 \times 10^{-5}$ mol/L. The crushed rock experiments also resulted in the largest average Mg concentration increase for the DI water experiments with an average increase of $2.9 \times 10^{-4} \pm 7.5 \times 10^{-5}$ mol/L. There was a significant difference in the change in Mg concentrations between all the elevated CO_2 DI-water plus crushed rock experiments and the elevated CO_2 DI-water plus whole rock experiments (p-value 0.03). There was no significant difference in the change in Mg concentrations between any of the MgOH water experiments. Compared to the elevated CO_2 CaOH-high water plus crushed rock experiments there was a significant difference between elevated CO_2 CaOH-high water only experiments (p-value 0.01) and elevated CO_2 CaOH-high water plus whole rock experiments (p-value 0.01).

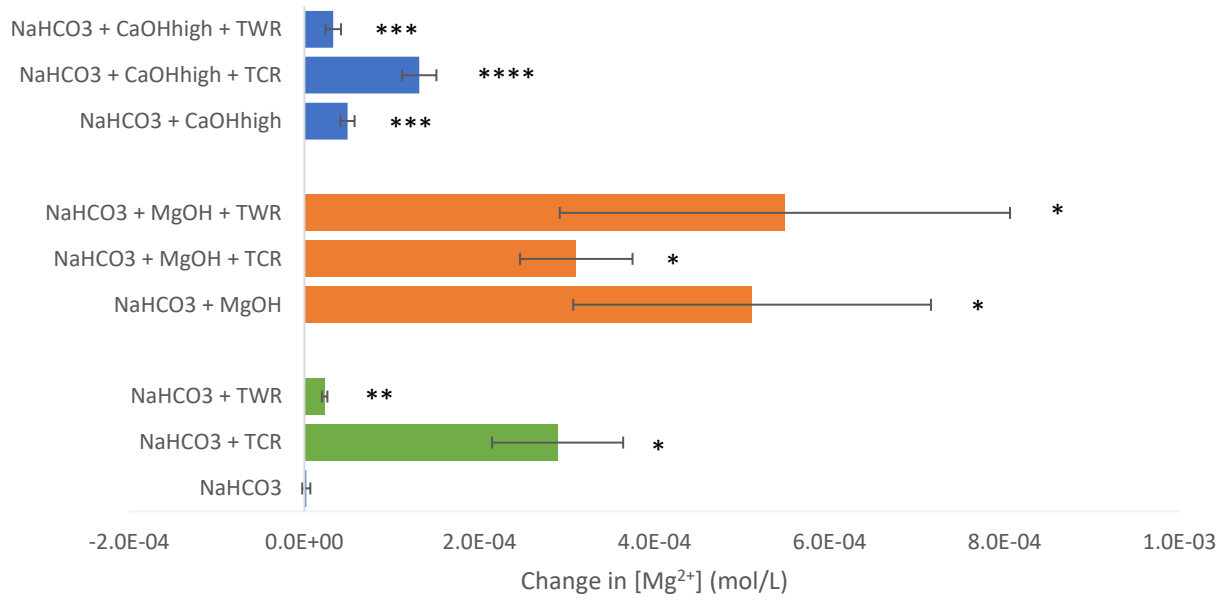

Fig. 35. Average change in Mg concentration in mol/L of triplicate CO_2 sequestration experiments starting with elevated CO_2 concentrations. Values are the average change in concentration between initial and final measurements. Error bars are the standard deviations of the average of the triplicate experiments. Statistics were not run on mean values when standard deviation was greater than the mean value.

All sequestration experiments showed an average increase in Si concentration over the course of the five hour experiments with experiments using crushed rock having the largest average increases (Fig. 36). These experiments had average concentration increases of $6.6 \times 10^{-5} \pm 3.2 \times 10^{-5}$ mol/L, $6.0 \times 10^{-5} \pm 2.7 \times 10^{-5}$ mol/L, and $5.6 \times 10^{-5} \pm 1.0 \times 10^{-6}$ mol/L for DI-water plus crushed rock, MgOH water plus crushed rock, and CaOH-high water plus crushed rock, respectively. There were no significant differences between any of the elevated CO_2 DI-water experiments. There was a significant difference when comparing elevated CO_2 MgOH water only experiments and elevated CO_2 MgOH water plus whole rock experiments (p-value 0.05).

Finally, there were also significant differences between elevated CO_2 CaOH-high water plus crushed rock and elevated CO_2 CaOH-high water plus whole rock experiments (p-value 0.01).

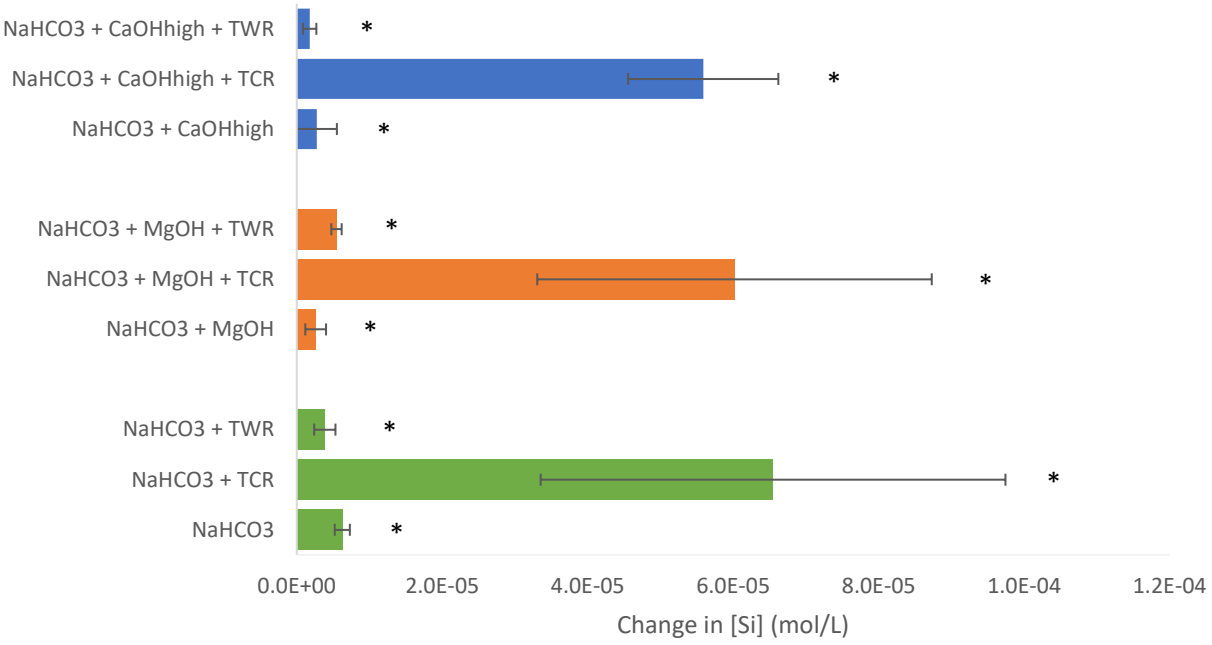

Fig. 36. Average change in Si concentration in mol/L of triplicate CO_2 sequestration experiments starting with elevated CO_2 concentrations. Values are the average change in concentration between initial and final measurements. Error bars are the standard deviations of the average of the triplicate experiments. Statistics were not run on mean values when standard deviation was greater than the mean value.

Chapter 4: White Hills Results

4.1 CO_2 Sequestration Experiments with atmospheric CO_2 concentrations and White Hills peridotite

4.1.1 Total CO_2 sequestered over four hour experiments

All CO_2 sequestration experiments using rocks from White Hills decreased the CO_2 concentration in the LI-8100A chamber over the course of the four-hour experiments (Fig. 37). The largest average decreases in CO_2 concentration were recorded during the CaOH water experiments with the high concentration CaOH-high water only experiments having the largest

average decrease of $-1.4 \times 10^{-4} \pm 2.8 \times 10^{-6}$ mol/L. The remaining CaOH water experiments resulted in average decreases of $-1.1 \times 10^{-4} \pm 9.0 \times 10^{-7}$ mol/L for CaOH water only experiments, $-1.1 \times 10^{-4} \pm 1.3 \times 10^{-5}$ mol/L for CaOH plus whole rock experiments, and $-1.1 \times 10^{-4} \pm 4.1 \times 10^{-6}$ mol/L for CaOH plus crushed rock experiments. MgOH water plus crushed rock experiments resulted in average decreases in CO_2 concentration of $-3.6 \times 10^{-5} \pm 3.9 \times 10^{-6}$ mol/L while MgOH water plus whole rock resulted in an average decrease of $-2.7 \times 10^{-5} \pm 2.2 \times 10^{-5}$ mol/L. The experiment with the smallest average decrease was the DI water plus whole rock experiment with an average decrease of $-1.9 \times 10^{-6} \pm 1.5 \times 10^{-6}$ mol/L. DI water plus crushed rock had an average decrease of $-2.4 \times 10^{-5} \pm 2.2 \times 10^{-6}$ mol/L. When comparing the total amount of CO_2 removed from the chamber, there was a significant difference between DI water plus crushed rock and DI water plus whole rock experiments (p-value <0.01). There was also a significant difference in total change of CO_2 when CaOH high concentration experiments were compared to both CaOH low concentration experiments (p-value <0.01) and to CaOH low concentration plus crushed rock experiments (p-value <0.01). There were no significant differences in total CO_2 concentration change between any of the other experiments.

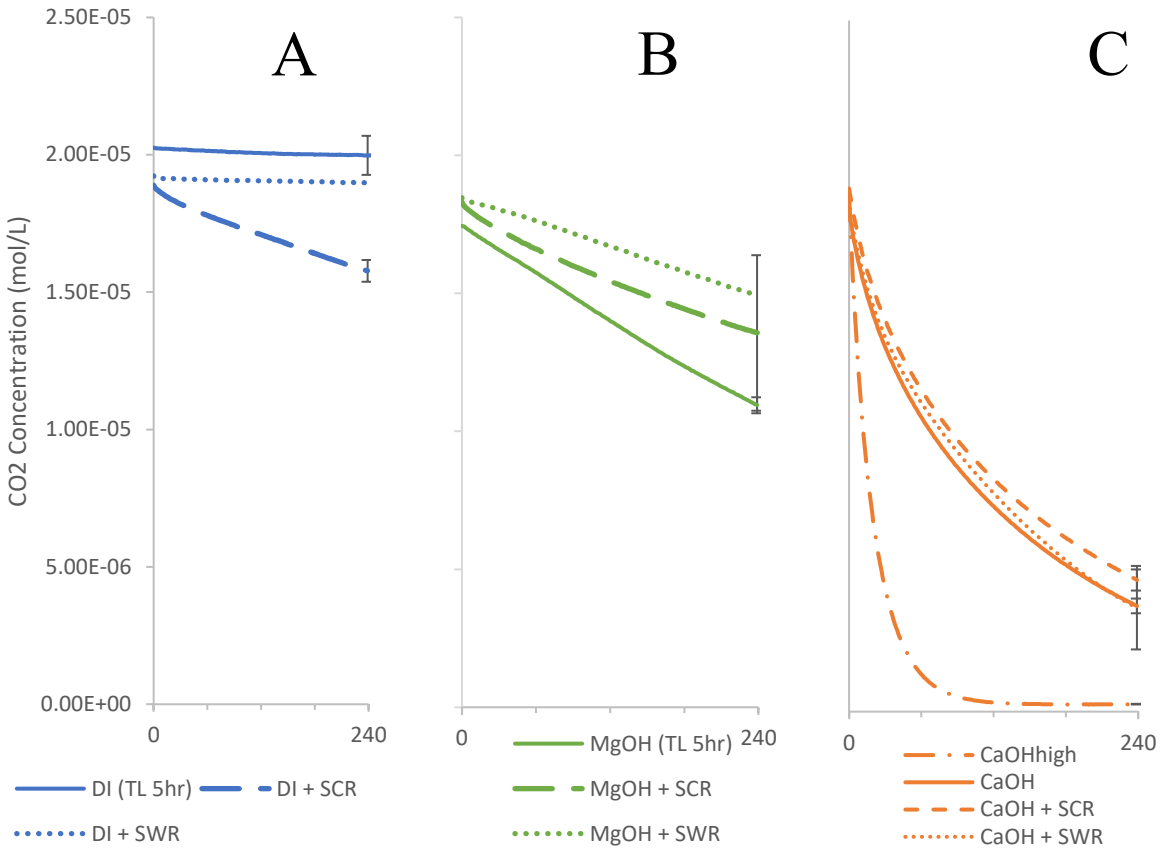

Fig. 37. Average CO_2 concentrations measured during the DI water (A), MgOH water and rock (B), and CaOH water (C) experiments run with atmospheric CO2 concentrations, where SCR represents experiments run with White Hills crushed rock and SWR represents experiments run with White Hills whole rock. Values are averages of triplicate experiments with errors bars on the last plotted point representing the standard deviation of the averages.

4.1.2 CO_2 flux

All of the atmospheric CO_2 sequestration experiments recorded a negative flux over the first 30 minutes of the experiments (Fig. 38). The CaOH water experiments had the greatest negative flux and ranged from CaOH-high water only experiments having the greatest negative flux of $-2.2 \times 10^{-4} \pm 8.3 \times 10^{-7}$ mol/m^2·min to CaOH water plus crushed rock with an average flux of $-7.5 \times 10^{-5} \pm 1.7 \times 10^{-7}$ mol/m^2·min. For the DI water experiments, the experiments with

crushed rock had greater fluxes than the experiments without. MgOH water plus crushed rock had a negative flux of $-1.6 \times 10^{-5} \pm 2.7 \times 10^{-7}$ mol/m^2·min and DI water plus crushed rock had a negative flux of $-1.1 \times 10^{-5} \pm 4.2 \times 10^{-7}$ mol/m^2·min. There was a significant difference in CO_2 flux between the CaOH high concentration experiments and the other three CaOH experiments: CaOH water only (p-value <0.01), CaOH water plus crushed rock (p-value <0.01), and CaOH water plus whole rock (p-value <0.01). There was no significant difference between all of the CaOH water experiments. There was also no significant difference in CO_2 flux between the MgOH water experiments. There was a significant difference in CO_2 flux between the DI water plus crushed rock experiments when compared to the DI water plus whole rock (p-value <0.01) and also to DI water only experiments (p-value 0.01).

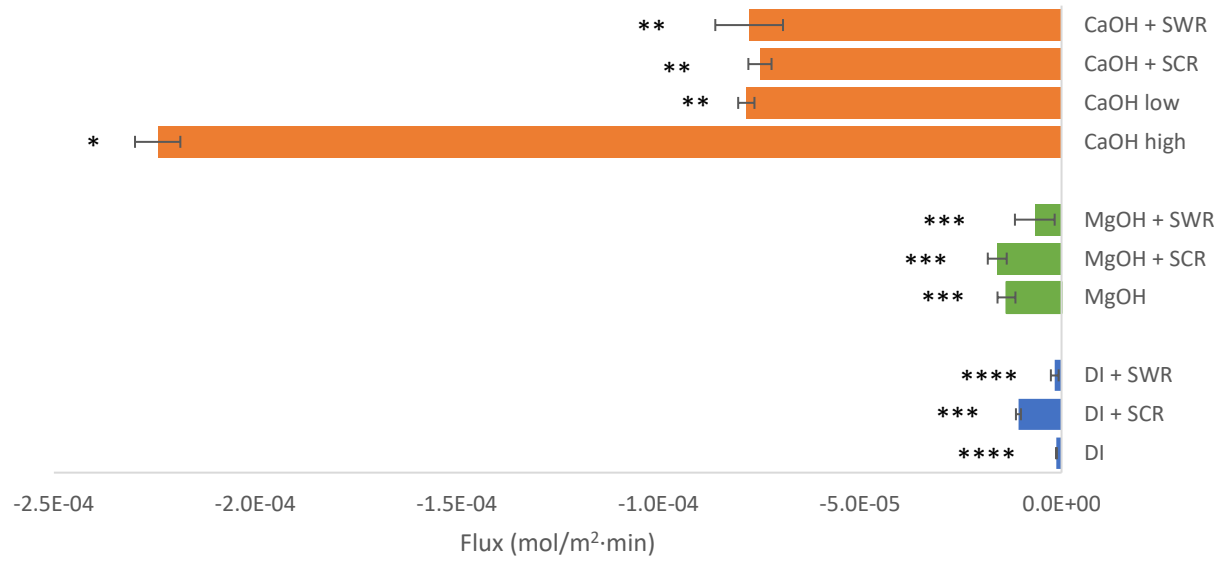

Fig. 38. Average flux values (mol/m^2·min) from triplicate experiments, calculated from the first 30 minutes of each experiment. Error bars are standard deviation calculated from the average flux values from triplicate experiments. Experiments showing no significant difference compared to each other are indicated with matching asterisks.

4.1.3 Change in pH

There were two sets of sequestration experiments that showed an average increase in pH over the course of the four hour experiments, DI water plus crushed rock with an average change of 2.85 ± 0.62 and MgOH water plus whole rock with an average change of 0.30 ± 0.05 (Fig. 39). Three sets of experiments resulted in average decreases in pH: CaOH water only experiments with -0.18 ± 0.15, CaOH water plus crushed rock with -0.23 ± 0.05, and CaOH water plus whole rock with an average change of -0.10 ± 0.03. The remaining experiments resulted in values where the standard deviation was greater than the average values. There was a significant difference in the average pH change between low concentration CaOH-high water plus crushed rock experiments and low concentration CaOH-high water plus whole rock experiments (p-value 0.03). There was no significant difference in average pH change between any of the other experiments.

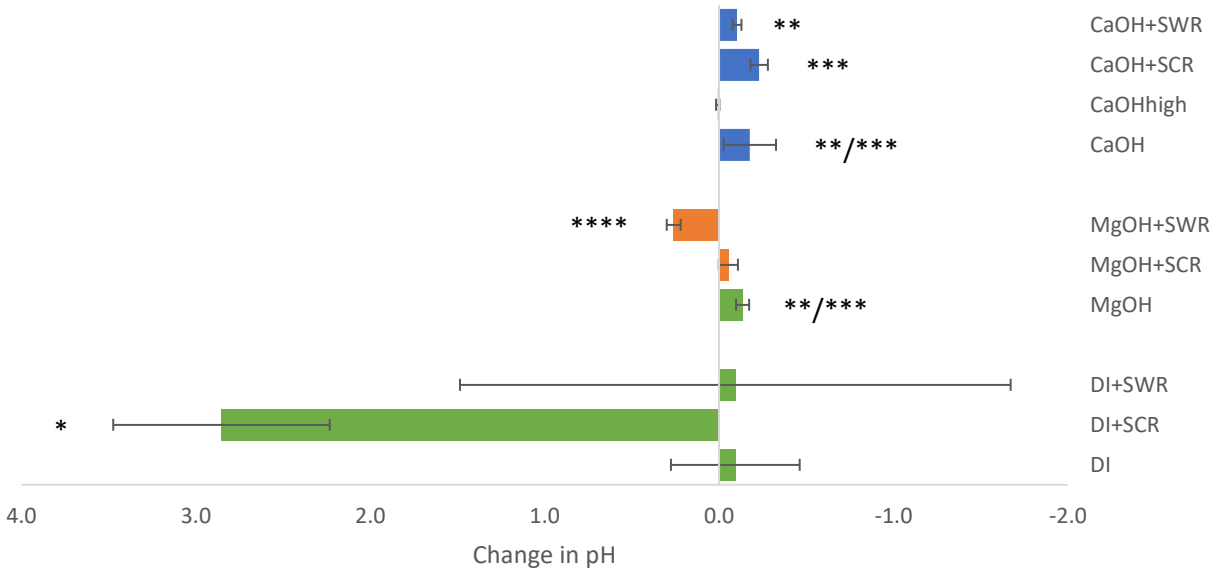

Fig. 39. Average change in pH for atmospheric CO_2 experiments from triplicate experiments. Error bars are the standard deviation of the average from triplicate experiments. Experiments showing no significant

difference compared to each other are indicated with matching asterisks. Statistics were not run on mean values when standard deviation was greater than the mean value.

4.1.4 Change in aqueous total inorganic carbon

CaOH water experiments showed an average decrease in TIC over the course of the four hour experiments while MgOH water and DI water experiments resulted in average increases (Fig. 40). The CaOH experiments ranged from an average decrease of $-1.4 \times 10^{-5} \pm 2.2 \times 10^{-6}$ mol C for CaOH water only experiments to $-1.9 \times 10^{-5} \pm 9.7 \times 10^{-6}$ mol C for CaOH plus whole rock experiments. The experiments that resulted in average increases in TIC ranged from $1.9 \times 10^{-4} \pm 3.2 \times 10^{-5}$ mol C for DI water plus crushed rock to $5.0 \times 10^{-5} \pm 2.2 \times 10^{-5}$ mol C for MgOH water plus whole rock. There was a significant difference in the change in TIC between the MgOH water experiments (p-value 0.01). There were no significant differences between any of the other experiments.

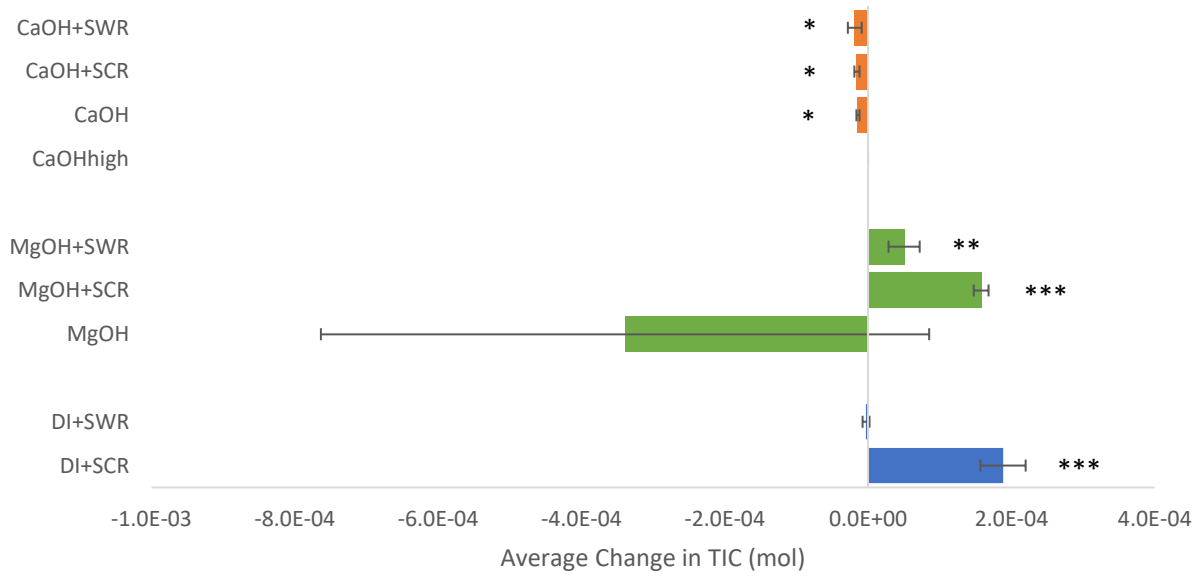

Fig. 40. Average change in TIC for atmospheric CO_2 experiments from triplicate experiments. Error bars are the standard deviation of the average from triplicate experiments. Experiments showing no significant

difference compared to each other are indicated with matching asterisks. Statistics were not run on mean values when standard deviation was greater than the mean value.

4.1.5 Change in conductivity

All of the CaOH water experiments showed a decrease in average conductivity over the course of the four-hour experiments (Fig. 41). This ranged from $-2.5 \times 10^{-1} \pm 1.4 \times 10^{-2}$ mS/cm for the CaOH water plus crushed rock experiments to the CaOH water only experiments with an average decrease of $-3.0 \times 10^{-2} \pm 1.2 \times 10^{-2}$ mS/cm. Of the remaining experiments, the only ones to result in an average increase in conductivity were MgOH water plus crushed rock, MgOH water plus whole rock, and DI water plus crushed rock experiments. The remaining experiments resulted in values where the standard deviation was larger than the average values. There was no significant difference in conductivity change in the MgOH experiments. There was a significant difference in average conductivity change when high concentration CaOH-high water experiments were compared to low concentration CaOH-high water only experiments (p-value <0.01) and low concentration CaOH-high water plus crushed rock experiments (p-value <0.01). Low concentration CaOH-high water only experiments resulted in significantly different average conductivity changes when compared to both low concentration CaOH-high water plus crushed rock experiments (p-value <0.01) and also to low concentration CaOH-high water plus whole rock experiments (p-value 0.03). There was also a significant difference in average conductivity change between low concentration CaOH-high water plus crushed rock and low concentration CaOH-high water plus whole rock experiments (p-value <0.01).

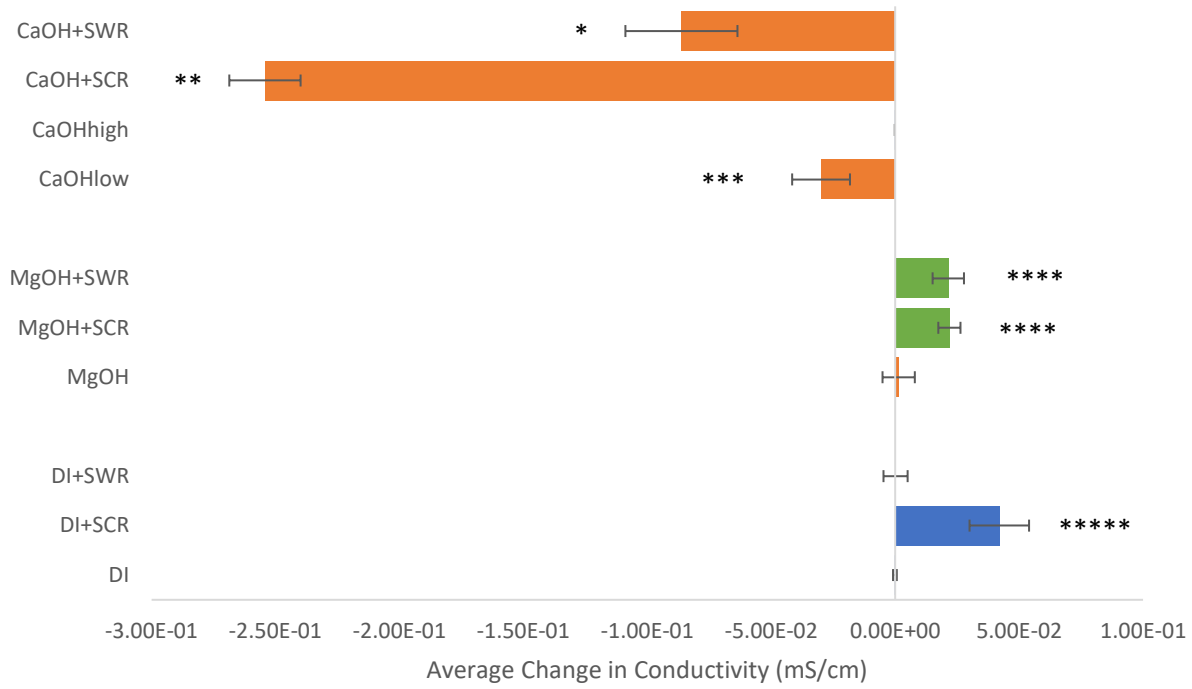

Fig. 41. Average change in conductivity (mS/cm) for atmospheric CO_2 experiments from triplicate experiments. Error bars are the standard deviation of the average from triplicate experiments. Experiments showing no significant difference compared to each other are indicated with matching asterisks. Statistics were not run on mean values when standard deviation was greater than the mean value.

4.1.6 Change in dissolved element concentrations

All CaOH water experiments except for CaOH-high water only resulted in an average decrease in Ca concentration over the course of the four hour experiments (Fig. 42). The largest average decrease in the CaOH-high water experiments was low concentration CaOH-high water plus crushed rock experiments with an average change of $-4.5 \times 10^{-4} \pm 2.5 \times 10^{-4}$ mol/L. MgOH experiments showed opposite results in the two experiments with the MgOH water plus crushed rock experiments having an average Ca concentration increase of $2.2 \times 10^{-5} \pm 3.4 \times 10^{-6}$ mol/L while MgOH water plus whole rock experiments had an average decrease of $-1.8 \times 10^{-5} \pm 2.3 \times$

10^{-6} mol/L. DI water plus crushed rock experiments had an average concentration increase of 2.9 × 10^{-5} ± 8.5 × 10^{-6} mol/L. There was no significant difference in the average Ca concentration change besides between the two sets of MgOH experiments (0.00).

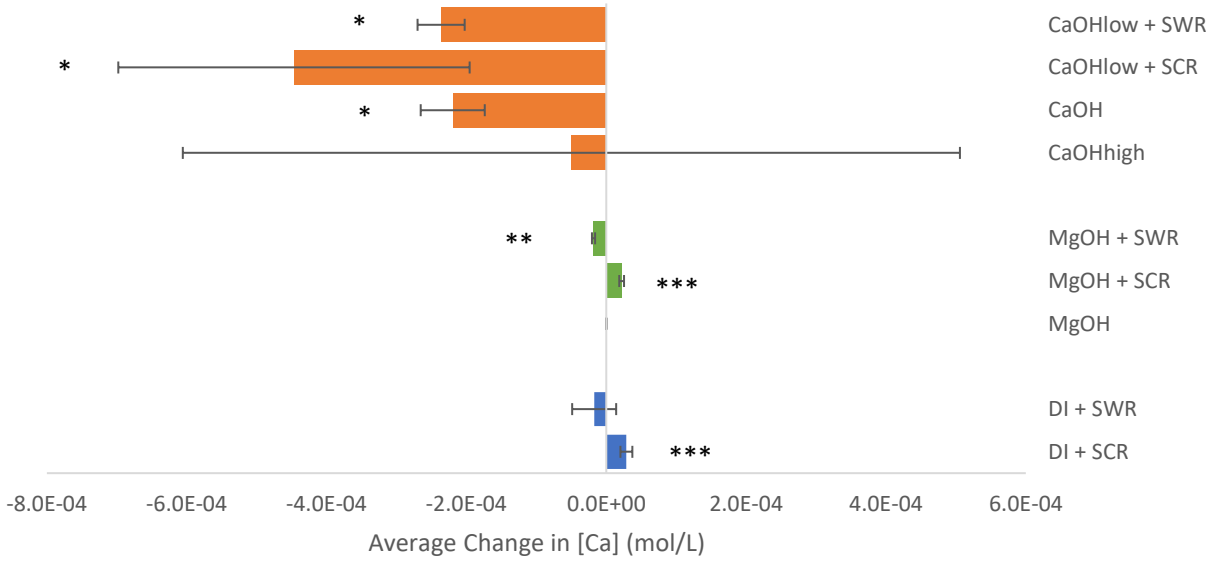

Fig. 42 Average change in Ca concentration in mol/L of triplicate CO_2 sequestration experiments starting with elevated CO_2 concentrations. Values are the average change in concentration between initial and final measurements. Error bars are the standard deviation of the average of the triplicate experiments. Statistics were not run on mean values when standard deviation was greater than the mean value.

Each set of experiments with average results greater than standard deviation resulted in an average increase in Mg concentration over the course of the four-hour experiments (Fig. 43). DI water plus crushed rock experiments resulted in the largest average change of 1.0 × 10^{-4} ± 3.4 × 10^{-5} mol/L while DI water plus whole rock experiments resulted in the smallest average change of 3.3 × 10^{-6} ± 2.7 × 10^{-6} mol/L. There was a significant difference in the average change in Mg concentration between DI water plus crushed rock and DI water plus whole rock experiments (p-value 0.04). There were no other significant differences between any other sets of experiments.

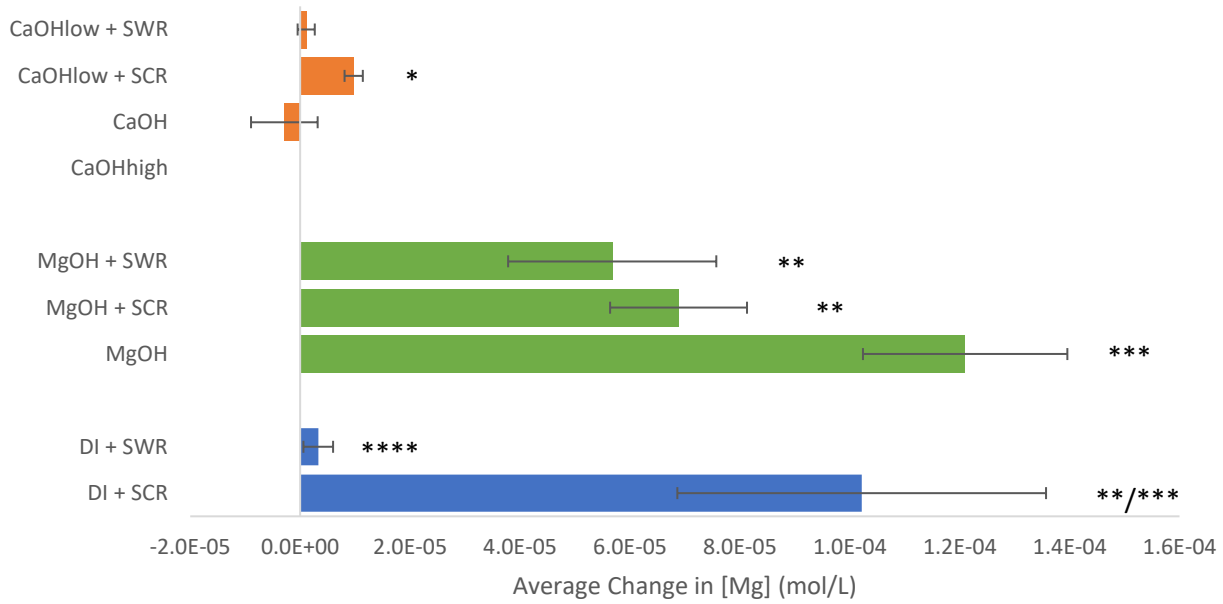

Fig. 43 Average change in Mg concentration in mol/L of triplicate CO_2 sequestration experiments starting with elevated CO_2 concentrations. Values are the average change in concentration between initial and final measurements. Error bars are the standard deviation of the average of the triplicate experiments. Statistics were not run on mean values when standard deviation was greater than the mean value.

All sequestration experiments resulted in an average increase in Si concentration over the course of the four hour experiments (Fig. 44). With all water types, the addition of crushed rock resulted in the largest average increases in Si concentration. DI water plus crushed rock resulted an average increase of $4.3 \times 10^{-5} \pm 1.4 \times 10^{-5}$ mol/L, CaOH water plus crushed rock resulted in $4.8 \times 10^{-5} \pm 8.2 \times 10^{-8}$ mol/L, and MgOH water plus crushed rock resulted in an average change of $3.2 \times 10^{-5} \pm 7.0 \times 10^{-6}$ mol/L. There was a significant difference in the average Si concentration change between DI water plus crushed rock and DI water plus whole rock experiments (p-value 0.04) and also between MgOH water plus crushed rock and MgOH water plus whole rock (p-value 0.02). There was also a significant difference in average Si concentration change when CaOH water plus crushed rock experiments were compared to the

other CaOH water experiments: CaOH-high water only (p-value <0.01), CaOH water only (p-value <0.01), and CaOH water plus whole rock (0.00).

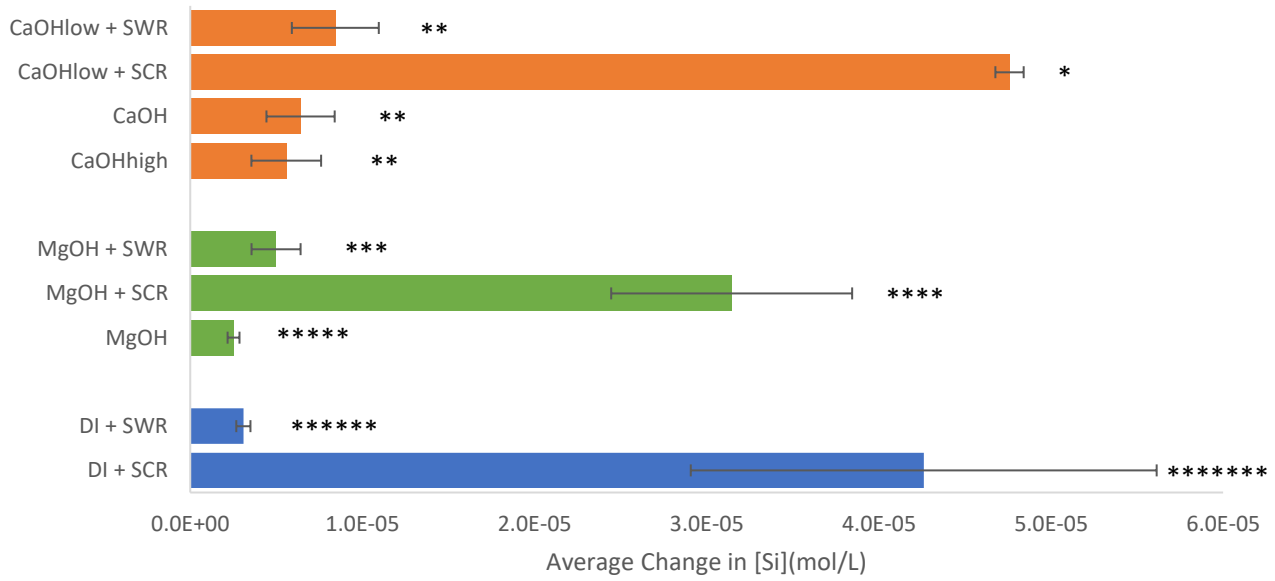

Fig. 44 Average change in Si concentration in mol/L of triplicate CO_2 sequestration experiments starting with elevated CO_2 concentrations. Values are the average change in concentration between initial and final measurements. Error bars are the standard deviation of the average of the triplicate experiments.

4.2 CO_2 sequestration experiments with elevated CO_2 concentrations and White Hills rocks

4.2.1 Total CO_2 sequestered over four hour experiments

All elevated CO_2 concentration sequestration experiments showed an average increase in chamber CO_2 concentrations over the course of the four hour experiments (Fig. 45). The DI water plus crushed rock experiments resulted in an average total increase in CO_2 concentration of $1.2 \times 10^{-4} \pm 1.2 \times 10^{-5}$ mol CO_2 while DI water plus whole rock resulted in an average change of $1.6 \times 10^{-4} \pm 2.6 \times 10^{-5}$ mol CO_2. MgOH experiments resulted in average changes of $9.2 \times 10^{-5} \pm 6.0 \times 10^{-6}$ mol CO_2 and $8.5 \times 10^{-5} \pm 3.6 \times 10^{-6}$ mol CO_2 for MgOH water plus crushed rock and MgOH water plus whole rock, respectively. The lowest average increase in total CO_2

concentration was CaOH water plus crushed rock experiments with an average increase of $7.9 \times 10^{-5} \pm 7.2 \times 10^{-6}$ mol CO_2 over the course of the experiments. CaOH water plus whole rock resulted in an average increase of $1.1 \times 10^{-4} \pm 2.1 \times 10^{-5}$ mol CO_2. There was no significant difference in average CO_2 concentration change between any of the experiments.

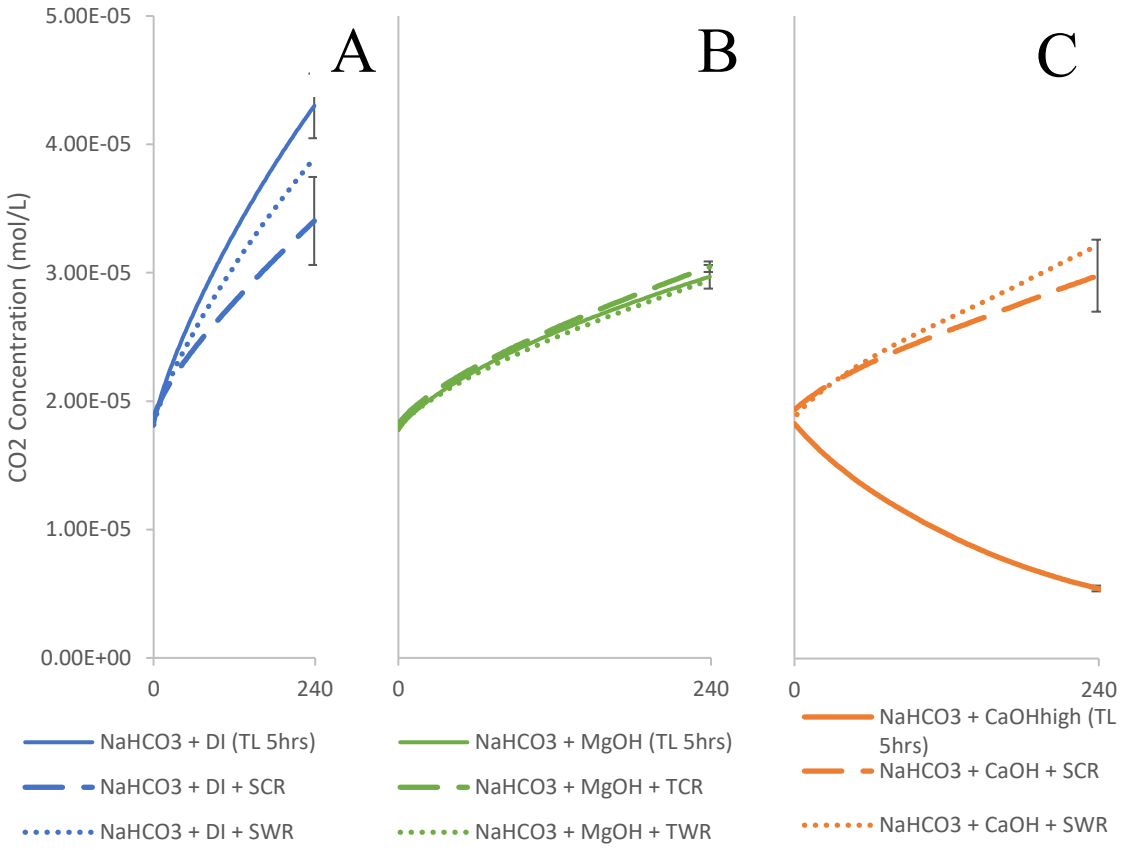

Fig. 45. Average CO_2 concentrations measuring during the DI water plus rock (A), MgOH water plus rock (B), and CaOH-high water plus rock (C) experiments run with elevated CO_2 concentrations where SCR represents White Hills crushed rock and SWR represents White Hills whole rock. Values are average of triplicate experiments with error bars on the last plotted point representing the standard deviation of the averages.

4.2.2 CO_2 flux

All of the elevated CO_2 experiments resulted in a positive flux over the first 30 minutes of the experiments except for elevated CO_2 high concentration CaOH water only experiments (Fig. 46). The greatest flux was an average increase of $6.6 \times 10^{-5} \pm 3.9 \times 10^{-6}$ mol/m^2·min from the DI water plus whole rock experiments. In contrast, the smallest increase was the CaOH water plus crushed rock experiments with an average increase of $3.3 \times 10^{-5} \pm 9.3 \times 10^{-7}$ mol/m^2·min. There was a significant difference in average CO_2 flux between DI-water plus crushed rock and DI-water plus whole rock experiments (p-value <0.01).

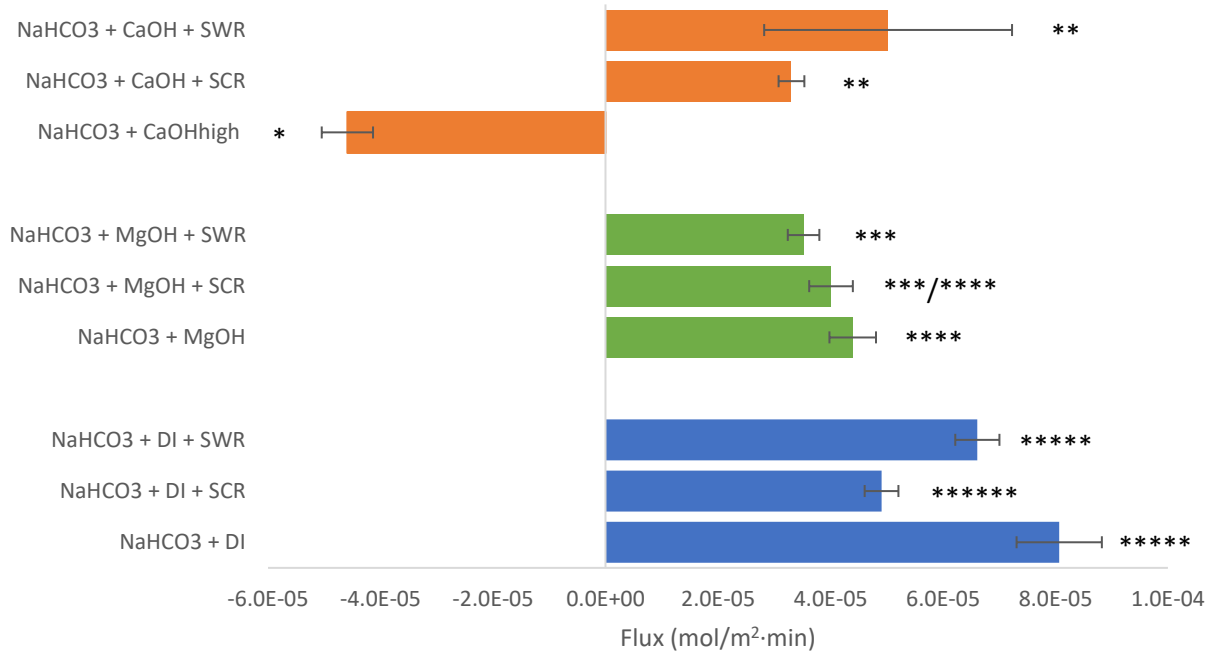

Fig. 46. Average flux values (mol/m^2·min) from triplicate experiments, calculated from the first 30 minutes of each experiment. Error bars represent the standard deviation of the averages from triplicate experiments. Experiments showing no significant difference compared to each other are indicated with matching asterisks.

4.2.3 Change in pH

All elevated CO_2 sequestration experiments with a mean value greater than the standard deviation resulted in an average increase in pH over the course of the four-hour experiments (Fig. 47). The MgOH water experiments average change in pH ranged from 0.25 ± 0.14 for MgOH water plus whole rock, to 0.05 ± 0.04 for MgOH water only experiments. DI water plus crushed rock experiments resulted in an average pH change of 0.25 ± 0.04 and were the only DI water experiments where the average change was greater than the standard deviation. There was no significant difference in the average pH change between any of the experiments.

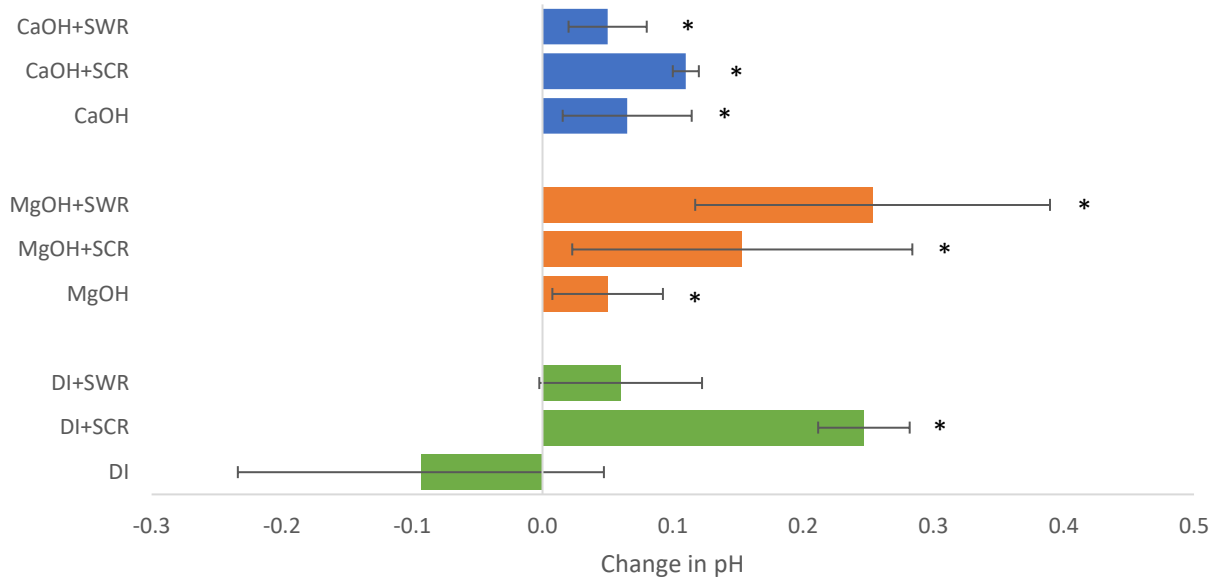

Fig. 47. Average change in pH for elevated CO_2 experiments from triplicate experiments. Error bars represent the standard deviation of the averages from triplicate experiments. Experiments showing no significant difference compared to each other are indicated with matching asterisks. Statistics were not run on mean values when standard deviation was greater than the mean value.

4.2.4 Change in aqueous total inorganic carbon

All experiments with mean values greater than the standard deviation resulted in average decreases in TIC over the course of the experiments (Fig. 48). The average decreases ranged from $-3.0 \times 10^{-4} \pm 2.9 \times 10^{-5}$ mol C for DI water plus crushed rock experiments to MgOH water plus crushed rock with an average decrease of $-4.9 \times 10^{-4} \pm 1.8 \times 10^{-5}$ mol C. There were no significant differences between any of the experiments.

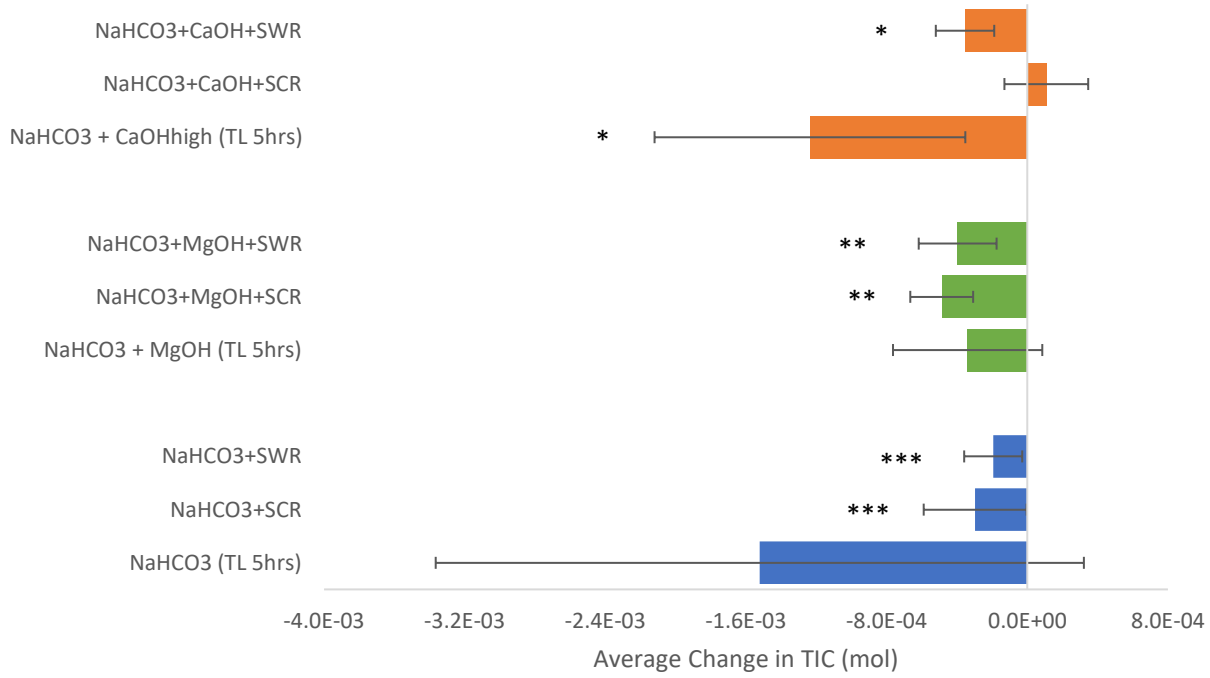

Fig. 48. Average change in TIC for elevated CO_2 experiments from triplicate experiments. Error bars represent the standard deviation of the averages from triplicate experiments. Experiments showing no significant difference compared to each other are indicated with matching asterisks. Statistics were not run on mean values when standard deviation was greater than the mean value.

4.2.5 Change in conductivity

Each elevated CO_2 sequestration experiment resulted in an average conductivity increase over the course of the four-hour experiments, with the exception of the experiments that resulted in average values that were smaller than the standard deviation (Fig. 49). The CaOH-high water plus crushed rock experiments resulted in an average conductivity increase of $3.0 \times 10^{-2} \pm 1.0 \times 10^{-2}$ mS/cm while the MgOH experiments resulted in an average change of $3.6 \times 10^{-2} \pm 1.4 \times 10^{-2}$ mS/cm for MgOH water plus crushed rock and $5.3 \times 10^{-2} \pm 9.3 \times 10^{-3}$ mS for MgOH water plus whole rock. There was no significant difference in the average conductivity change between any of the experiments.

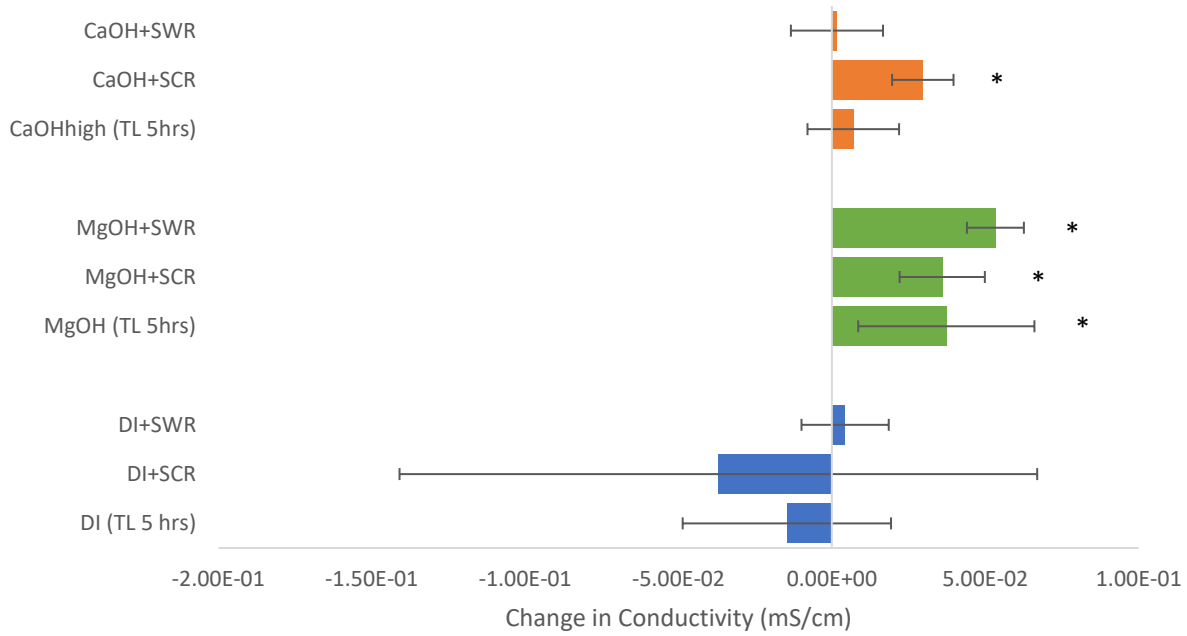

Fig. 49. Average change in conductivity (mS/cm) for elevated CO_2 experiments from triplicate experiments. Error bars represent the standard deviation of the averages from triplicate experiments. Experiments showing no significant difference compared to each other are indicated with matching

asterisks. Statistics were not run on mean values when standard deviation was greater than the mean value.

4.2.6 Change in dissolved element concentrations

All of the elevated CO_2 sequestration experiments where the mean was greater than the standard deviation resulted in an average increase in Ca concentration with the exception of CaOH-high water plus whole rock with an average decrease of $-1.4 \times 10^{-5} \pm 9.5 \times 10^{-6}$ mol/L (Fig. 50). The average increases in concentration ranged from $1.8 \times 10^{-5} \pm 1.5 \times 10^{-6}$ mol/L MgOH water plus crushed rock experiments to MgOH water plus whole rock experiments with an average change of $2.3 \times 10^{-6} \pm 1.1 \times 10^{-6}$ mol/L. There was a significant difference in the average Ca concentration change between MgOH water plus crushed rock and MgOH water plus whole rock experiments (p-value <0.01).

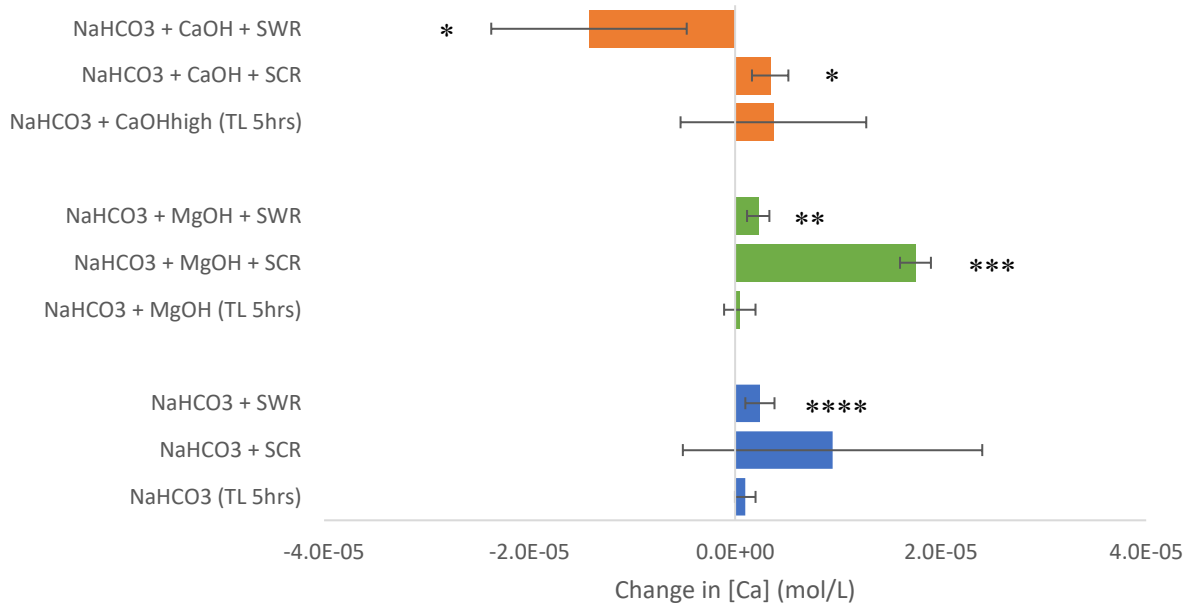

Fig. 50 Average change in Ca concentration in mol/L of triplicate CO_2 sequestration experiments starting with elevated CO_2 concentrations. Values are the average change in concentration between initial and

final measurements. Error bars represent the standard deviation of the averages from triplicate experiments. Statistics were not run on mean values when standard deviation was greater than the mean value.

The elevated CO_2 sequestration experiments all resulted in average Mg concentration increases over the course of the four hour experiments (Fig. 51). There were two distinct groups of experiments, one with a larger average change and another with a much smaller average change. The group with the larger average concentration change ranged from MgOH water plus whole rock with $2.1 \times 10^{-4} \pm 9.3 \times 10^{-5}$ mol/L to CaOH water plus crushed rock with an average change of $1.6 \times 10^{-4} \pm 4.0 \times 10^{-5}$ mol/L. The smaller average concentration change group includes CaOH water plus whole rock with $8.0 \times 10^{-6} \pm 5.0 \times 10^{-6}$ mol/L and DI water plus whole rock with an average change of $9.5 \times 10^{-6} \pm 6.5 \times 10^{-6}$ mol/L. There was a significant difference in average Mg concentration change between the two DI water experiments (p-value <0.01) and also between the two CaOH water experiments (p-value 0.02).

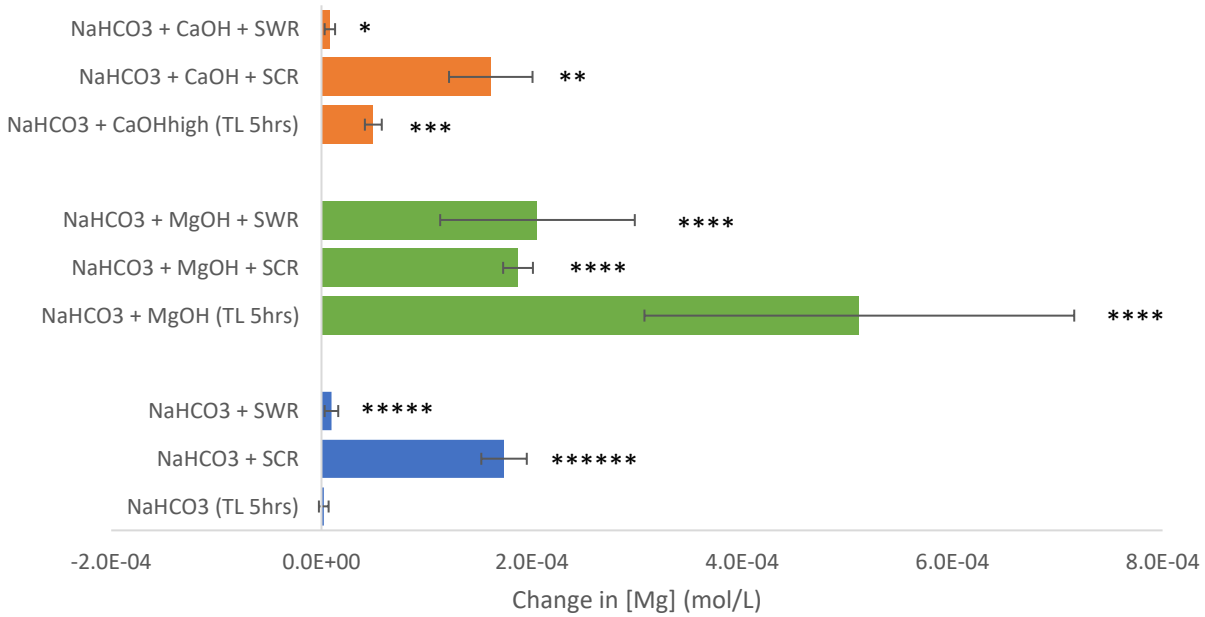

Fig. 51 Average change in Mg concentration in mol/L of triplicate CO_2 sequestration experiments starting with elevated CO_2 concentrations. Values are the average change in concentration between initial and final measurements. Error bars represent the standard deviation of the averages from triplicate experiments. Statistics were not run on mean values when standard deviation was greater than the mean value.

The elevated CO_2 sequestration experiments with crushed rock resulted in the largest average Si concentration increases over the course of the four-hour experiments (Fig. 52). These experiments ranged in average concentration change from $5.1 \times 10^{-5} \pm 4.3 \times 10^{-6}$ mol/L for MgOH water plus crushed rock to $4.0 \times 10^{-5} \pm 4.9 \times 10^{-6}$ mol/L for DI water plus crushed rock experiments. DI water plus whole rock experiments resulted in an average concentration change of $1.9 \times 10^{-6} \pm 1.8 \times 10^{-6}$ mol/L. The remaining experiments resulted in changes below instrument detection limit or average values smaller than the standard deviation. There was a significant difference between the DI water plus crushed rock experiments and the DI water and whole rock experiments (p-value <0.01).

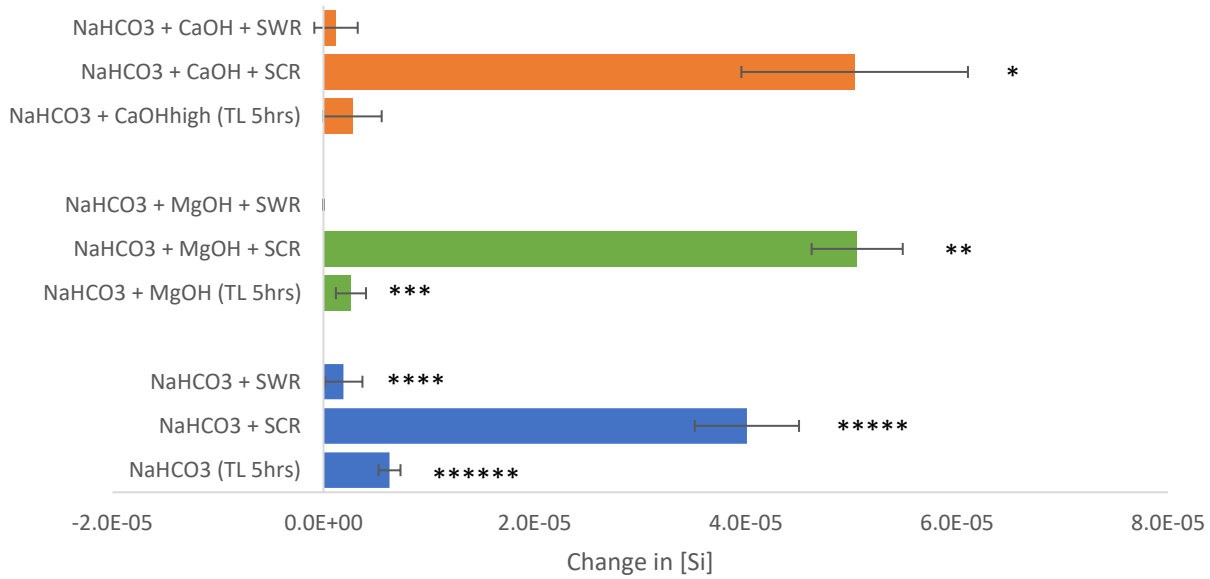

Fig. 52 Average change in Si concentration in mol/L of triplicate CO_2 sequestration experiments starting with elevated CO_2 concentrations. Values are the average change in concentration between initial and final measurements. Error bars represent the standard deviation of the averages from triplicate experiments. Statistics were not run on mean values when standard deviation was greater than the mean value.

Chapter 5: Discussion

5.1.1 Dissolution and precipitation

For carbon mineralization to happen there are two important steps that must occur: incongruent dissolution of existing ultramafic rock and precipitation of carbonate minerals. Dissolution provides the calcium and magnesium for inclusion in carbonate minerals and widens fractures for other water-rock reactions to take place. Precipitation of carbonate minerals is the mechanism by which carbon is stored in a solid form. These two steps can be considered in balance and depending on the geochemical conditions the balance may shift between dissolution or precipitation. For each of the laboratory experiments, each of the analyses was able to help determine whether the results indicated dissolution of ultramafic rock or carbonates, or carbonate precipitation (Table 1).

Table 1: Indicators of precipitation and dissolution. Down and up arrows indicate a decrease or increase in that measurement. For example: a decrease in pH would be an indication of dissolution.

	Dissolution	Precipitation
pH	↑	↓
Conductivity	↓	↑
TIC	↓	↑
Ion concentrations	↓	↑
CO_2 flux	↓	↑

As ultramafic minerals dissolve, OH^- ions are produced, and as a result the pH increases (Equation 3). Therefore, an increase in pH indicates dissolution. Conversely, a decrease in pH could indicated carbonate precipitation if the inorganic speciation of carbon reactions (Equations 5-7) is shifted to the right. Conductivity will increase as the concentration of dissolved ions

increases. The dissolution of ultramafic rock increases the concentration of dissolved ions and therefore increase the conductivity of the fluid. Conversely, the precipitation of carbonate minerals removes cations such as Ca^{2+} and Mg^{2+}, as well as carbonate ions from solution, which can decrease the conductivity of the fluid. As TIC concentration in the experimental water decreases, this is interpreted as precipitation of solid carbonate minerals at higher pH, or the exsolution of CO_2 at lower pH. An increase in TIC is potentially indicative of dissolution of pre-existing carbonate minerals in the rocks used in the experiments. Increases in elements such as calcium, magnesium, and silicon are indicators of dissolution of ultramafic rocks. Decreases in calcium and magnesium are attributed to their inclusion in the precipitation of carbonate minerals. A positive CO_2 flux is an indicator of carbonate dissolution and is only found in experiments with elevated CO_2 concentrations. This increase is interpreted to be the exsolution of excess CO_2 from the aqueous phase into the gaseous phase.

This increase is found in all elevated CO_2 experiments except for the high concentration CaOH water experiments which were the only elevated experiments to result in a decrease in CO_2 concentrations and negative CO_2 fluxes (Fig. 29C).

5.1.2 Source of ions during laboratory experiments

Experimental waters were analyzed for Ca, Mg, and Si for use as an indicator of dissolution of ultramafic silicate minerals and/or precipitation of carbonate minerals during the experiments. For many of the experiments the results of these analyses were as hypothysized, but for some experiments the results raise some questions as to the source of the ions.

In almost all experiments the greatest increase in Si concentrations were from experiments that used crushed rock, indicating that the increased surface area of the crushed rock allowed for faster dissolution rates. Experiments using the whole rock cubes resulted in the next

greatest concentration increases, but for many of the experiments there was no significant difference between the whole rock experiments and water only experiments. This reinforces the idea that increasing surface area also increases the rate of dissolution. This does raise questions regarding water only experiments showing increasing Si concentrations when there was no source of silicon. In the laboratory experiments the only source of Si should be from the dissolution of ultramafic silicate rocks. One potential source of Si could be the dissolution of the glass bowl used for the experiments from the elevated pH of the experimental waters. Another potential source of Si could be remnants of previous experiments (e.g. very fine-grained particles or some kind of silica precipitation) that was not completely removed during the acid bath procedure between experiments.

In the elevated CO_2 Ca^{2+}-rich water only experiments, there was an increase in Mg^{2+} (Fig. 32). Without added ultramafic rock, there should be no source of magnesium in these experiments.

The largest increases in Mg^{2+} were from the Mg-rich water only experiments (figures 41 and 49). This was unexpected as it was hypothesized that as the crushed and solid rock are dissolved there should be a larger increase in Mg^{2+}. The water only experiments should have no increase in Mg^{2+} over the course of the experiments as the amount of Mg^{2+} should remain the same as the amount of MgOH added to the DI water to create the waters for the experiment. One potential reason for the increase in magnesium is continued dissolution of MgOH powder that was added to DI water to make the experimental waters. Another potential reason for the high amounts of Mg^{2+} in the water only experiments compared to the experiments with added rock is that the experiments with added rock are precipitating Mg-carbonate and have reduced the amount of Mg^{2+}.

5.1.3 Solid carbon precipitation

As the experimental chamber is a closed system the total amount of carbon in the experiment should not change over the course of the experiment. However, carbon may change phase during the experiment. Carbon is located in the gaseous phase as carbon dioxide, in the aqueous phase as bicarbonate and carbonate ions, and as carbonate minerals in the solid phase. Between the gaseous phases and the aqueous phase carbon is exchanged across the air-water interface. Gaseous carbon dioxide can dissolve into water and depending on the pH of the water will be dissociated into either carbonic acid (neutral pH), bicarbonate ions (basic pH), or carbonate ions (ultra-basic pH). The reverse reaction is also possible if the experiment waters are saturated with CO_2, which will result in the exsolution of CO_2 out of the water and into the headspace of the chamber. In ultra-basic conditions, such as the CaOH experiments, the carbonate ions will be consumed during the precipitation of carbonate minerals such as calcite or magnesite. To determine which experiments could be precipitating carbonate minerals a carbon balance equation was created (Eq. 5). This equation assumes that the total amount of carbon in the chamber does not change and that there is no solid carbon at the beginning of the experiments. Total initial carbon and total final carbon can also be written as the sum of carbon in the gaseous, aqueous, and solid phases (Eq. 6). To solve for the amount of solid carbon precipitated in the experiment the equation can be rearranged into Eq. 7.

(5) $\text{Total Carbon}_{(\text{Initial})} = \text{Total Carbon}_{(\text{Final})}$

(6) $C_{(IG)} + C_{(IAq)} + C_{(IS)} = C_{(FG)} + C_{(FAq)} + C_{(FS)}$

(7) $C_{(IG)} + C_{(IAq)} + C_{(IS)} - C_{(FG)} - C_{(FAq)} = C_{(FS)}$

The variables in the above equations are: $C_{(IG)}$ is the initial concentration of carbon in the gas phase (as CO_2), $C_{(IAq)}$ is the initial concentration of carbon in the aqueous phase (as TIC), $C_{(IS)}$ is the initial concentration of carbon in the solid phase (assumed to be zero), $C_{(FG)}$ is the final concentration of carbon in the gas phase (as CO_2), $C_{(FAq)}$ is the final concentration of carbon in the aqueous phase (as TIC), and $C_{(FS)}$ is the final concentration of carbon in the solid phase (as precipitated carbonate minerals). The results of the calculated precipitated solid carbon are in Fig. 53, experiments with a calculated decrease are in blue, a calculated increase in green, and experiments with standard deviations larger than the calculated value were not added. Experiments with a calculated increase in solid carbon indicate conditions favorable to the precipitation of carbonate minerals. Experiments with a calculated decrease in solid carbon indicate conditions favorable to the dissolution of carbonate rock. Some estimates resulted in propagated errors larger than the average calculated value such that carbonate formation or dissolution was smaller than uncertainty. Out of the 34 experiments, 18 resulted in increases in solid carbon, 7 resulted in decreases, and 9 resulted in standard deviations larger than the calculated value. The 7 experiments which resulted in decreases in solid carbon were all experiments that had either crushed or whole rock. It is possible that the rock used in the experiments did contain solid carbonate, which was dissolved during the experiments and would increase the amount of dissolved carbon measured and result in a negative amount of solid carbon.

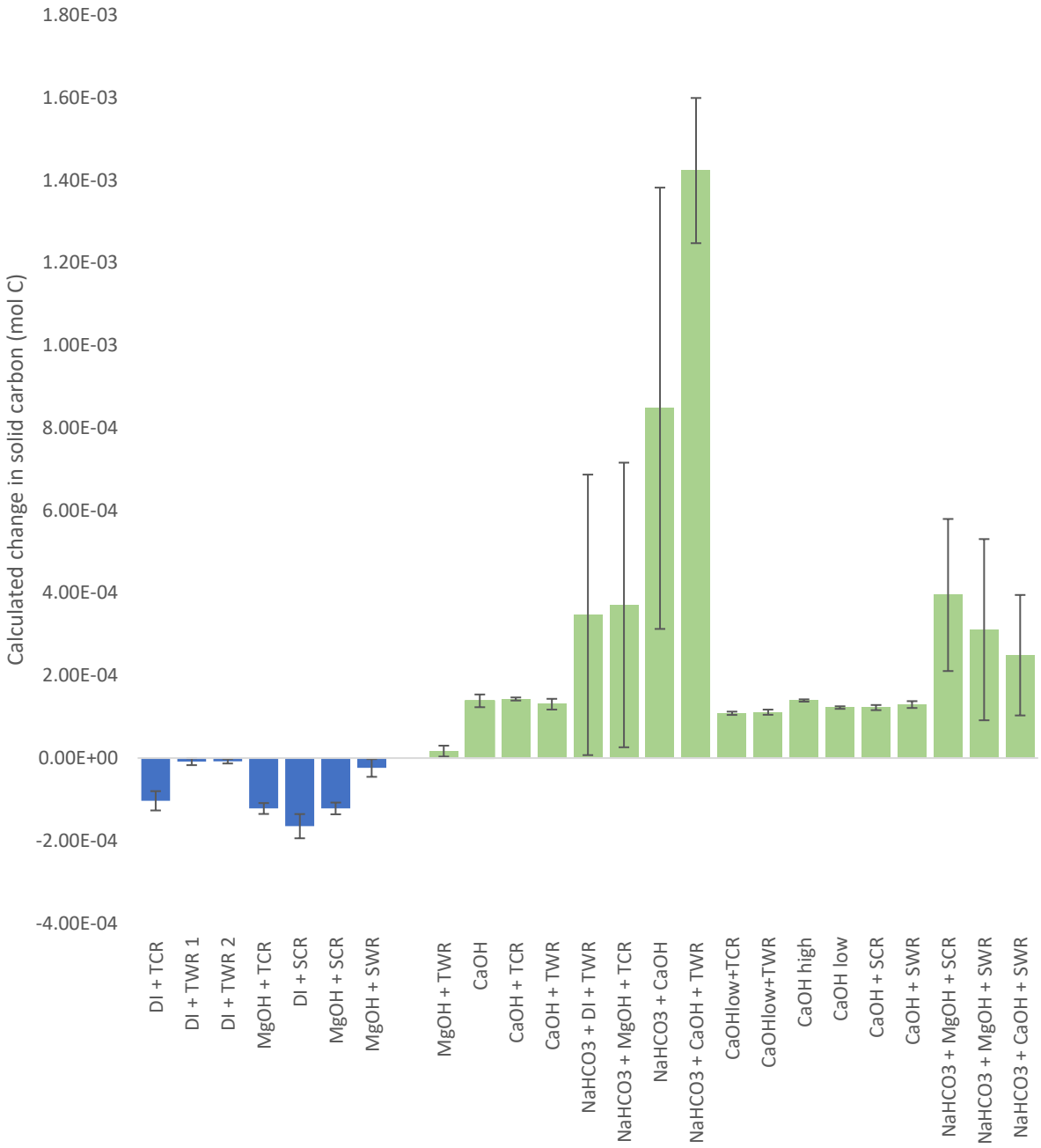

Fig. 53. Calculated changes in solid carbon (see equations 5-7) over the course of laboratory experiments. Values in blue are experiments with a calculated decrease in solid carbon, values in green are calculated increases in solid carbon. Values are results of triplicate experiments and error bars are propagated errors from the change in CO_2 concentration and the change in total inorganic carbon.

When examining the calculated changes in solid carbon there are some trends that become apparent. One of these trends is that out of the 18 experiments with calculated increases, 10 of those are CaOH water based experiments suggesting that the higher pH of these experiments may result in favorable conditions for precipitation of carbonate minerals. It is also interesting that no CaOH water based experiments resulted in decreases in solid carbon, this grouping only includes experiments with deionized or MgOH water based experiments. This decrease in solid carbon indicates dissolution and could be a result of the lower pH of these experiments.

There are also some experiments which demonstrate the effect of increasing CO_2 concentration on the precipitation of solid carbon. The experiments which best demonstrate this are the MgOH water plus White Hills crushed rock experiments (MgOH + SCR, Fig. 51) and elevated CO_2 MgOH water plus White Hills crushed rock experiments ($NaHCO_3$ + MgOH + SCR, Fig. 51). The atmospheric concentration experiments (MgOH+ SCR) resulted in a negative amount of solid carbon, indicating conditions favorable for dissolution, but when CO_2 is added to the experiment ($NaHCO_3$ + MgOH + SCR), there is now a calculated increase in solid carbon which indicated precipitation. This is the ideal situation for carbon mineralization potential: creating conditions that will have the necessary reactants (dissolution) so that when CO_2 is added to the system for long term storage, carbon mineralization will occur (precipitation).

5.1.4 Experimental groupings

CO_2 flux and changes in aqueous geochemistry were used to group experiments based on whether there were indicators for mineral dissolution, carbon mineralization, and CO_2 exsolution (Fig. 54). It was possible for experiments to fall into multiple groups which resulted in seven possible groups or intersections between groups: carbon mineralization only, mineral dissolution

only, CO_2 exsolution only, A (carbon mineralization + mineral dissolution), B (all groups), C (carbon mineralization + CO_2 exsolution), and D (carbon mineralization + CO_2 exsolution). For engineered in-situ carbon mineralization to occur, mineral dissolution is needed to provide cations, therefore the ideal conditions would be experiments in groups A or B. Group A has indicators of both dissolution and mineralization, while group B also has indicators of CO_2 exsolution. This exsolution of CO_2 indicates the fluid is oversaturated with respect to CO_2, a necessary ingredient for carbon mineralization. There were 11 experiments in Group A and 4 experiments in Group B for a total of 15 experiments in the ideal groups. Group A was only CaOH water (high and low) experiments and group B consisted of basic and ultra-basic pH plus rock experiments. The only experiments in the mineral dissolution group were atmospheric concentration DI water and Mg-rich water experiments.

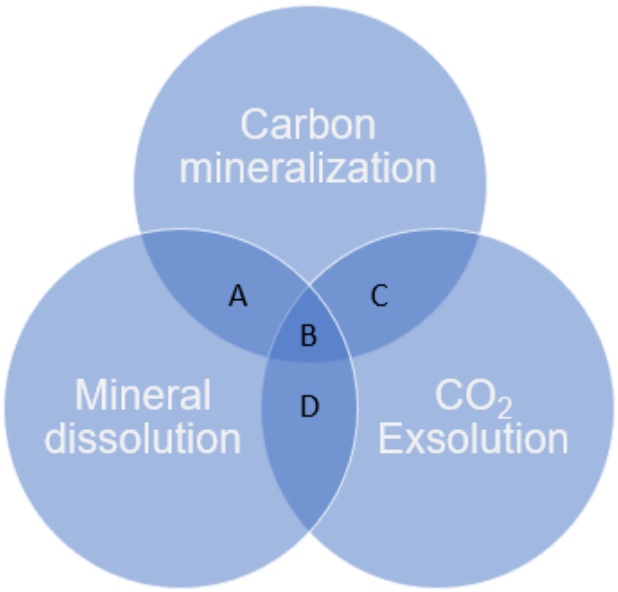

A: Only CaOH experiments

B: High pH, elevated CO_2 plus rock experiments

C: No experiments

D: All other elevated CO_2 experiments

Fig. 54. Experimental groupings and intersections from the results of carbon sequestration experiments as listed in Table/Appendices Y. The experiments in each area are as described as experimental groupings and number of experiments in brackets followed by each experiment found in that grouping: **A: (11)** CaOH, CaOH+TCR, CaOH+TWR, $NaHCO_3$+CaOH, $NaHCO_3$+CaOH+TWR, CaOHlow+TCR, CaOHlow+TWR, CaOHhigh, CaOHlow, CaOH+SCR, CaOH+SWR, **B: (4)** $NaHCO_3$+MgOH+TCR, $NaHCO_3$+MgOH+SCR, $NaHCO_3$+MgOH+SWR, $NaHCO_3$+CaOH+SWR, **C: (0), D: (8)** $NaHCO_3$+DI, $NaHCO_3$+DI+TCR, $NaHCO_3$+DI+TWR, $NaHCO_3$+MgOH, $NaHCO_3$+MgOH+TWR, $NaHCO_3$+DI+SCR, $NaHCO_3$+DI+SWR, $NaHCO_3$+CaOH+SCR, **Carbon mineralization only: (0), Mineral dissolution only: (10)** DI+TCR, DI+TWR1, DI+TWR2, MgOH, MgOH+TCR, MgOH+TWR, DI+SCR, DI+SWR, MgOH+SCR, MgOH+SWR, **CO2 Exsolution only: (0).**

5.1.5 Comparing laboratory results and field measurements

Two ultra-basic springs in the Tablelands, WHC2 and WHC500, demonstrated active atmospheric CO_2 sequestration. The WHC2 spring had the greatest decrease in CO_2 concentration and followed a decreasing, negative exponential trend. The WHC500 spring had a more linear decrease in CO_2 concentration. The difference in decreases in CO2 could be the result of differences in bedrock and water surface area exposures between the two spring locations. At WHC2 the analyzer was placed over a large pool of spring water, such that bottom of the chamber covered an aqueous ultra-basic surface area of 314 cm^2. At WHC500 the analyzer was placed over bare rock which contained three 5 cm diameter drilled holes that were discharging high pH water. This meant that the bottom of the analyzer chamber was mostly exposed to rock with a lesser amount of water. In addition to WHC2 and WHC500, the analyzer was also deployed over bare ultramafic rock, gravel, local vegetation, and a small bog. During these deployments small increases in CO_2 concentration were observed over time, which was expected in all locations except for over the local vegetation. In that location, it was expected to

have a decrease in CO_2 concentration from plants using the CO_2 for photosynthesis. It is possible that because of the size of the chamber restricting the deployment to small plants that there was not enough vegetation to decrease the CO_2 concentration. It was also possible that the area selected for local vegetation was also the site of a small boggy area, which can release CO_2 from the breakdown of organic material as demonstrated by the deployment over the boggy area (Fig. 9).

The fluxes recorded at the ultra-basic spring WHC2 in this thesis (Fig. 4) are similar to previous studies of the spring: -1.1×10^{-5} mol/m^2·min and -2.6×10^{-4} mol/m^2·min (Cumming, 2018), and $-1.9 \times 10^{-5} \pm 1.0 \times 10^{-8}$ mol/m^2·min (Morrisey and Morrill, 2017). It has been suggested that the difference in fluxes could be due to seasonal variation (Cumming, 2018). It is also possible that the difference in methods between studies could result in these variations as well. Cumming (2018) also used the LI-8100A to measure CO_2 flux over the ultra-basic spring, while Morrisey and Morrill (2017) developed a gas sampling method using a gas port attached to a sealed container suspended in the spring.

The calculated fluxes over the first 30 minutes for the field locations were -5.6×10^{-5} mol/m^2·min for WHC2 and -1.5×10^{-5} mol/m^2·min for WHC500. The flux recorded at WHC2 was the most similar to the low concentration CaOH laboratory experiments, approximately 1.5 times less, and the flux recorded WHC500 was approximately 3 times less (Figure 55).

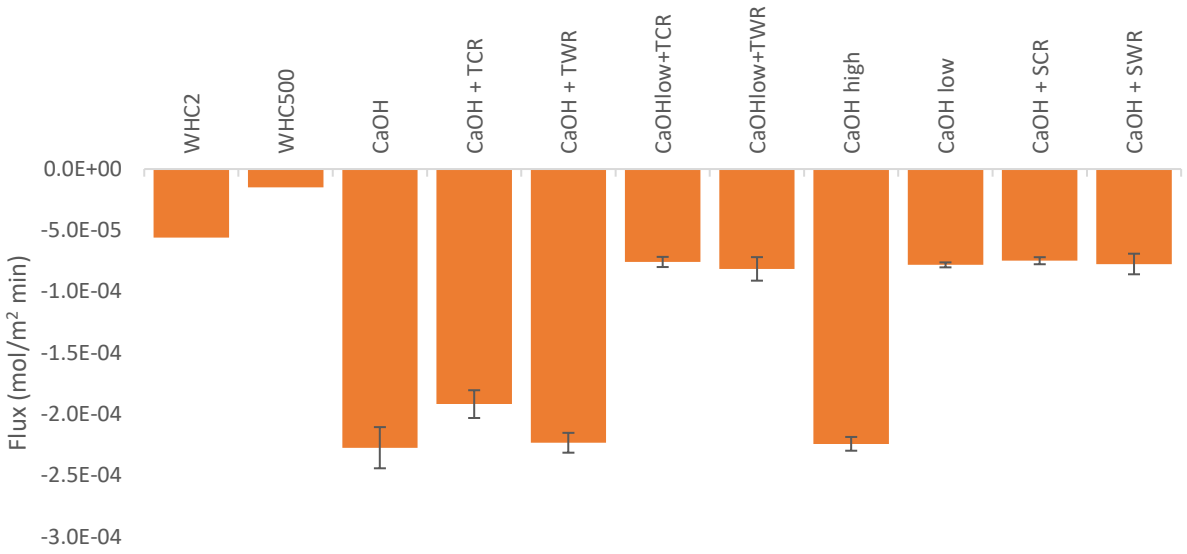

Fig. 55. Average flux values (mol/m2·min) from field data and triplicate laboratory experiments, calculated from the first 30 minutes of each deployment and experiment. Error bars are standard deviation of the average flux values from triplicate experiments. There are no error bars on field data (WHC2 and WHC500) as these experiments were only run once.

Szponar et al. (2013) examined the aqueous chemistry of WHC2 in three locations, designated WHC2a, WHC2b, and WHC2c (Table 2). When compared to CaOH water experiments from both the Tablelands and White Hills, the laboratory experiments are most similar to the chemistry of WHC2c for pH, Ca^{2+} concentration, and TIC but are most similar to WHC2a for Mg^{2+} concentration (Table 2).

Table 2: Water chemistry comparison between WHC2 (from Szponar et al. 2013) and laboratory experiments (this study).

	Szponar et al. 2013*			Lab Experiments				
	WHC2 a	**WHC2 b**	**WHC2 c**	**CaOH**	**CaOH + TCR**	**CaOH + TWR**	**CaOH + SCR**	**CaOH +SWR**
pH	12.3	12.3	11.8	11.39	11.30	11.30	11.31	11.55
Mg^{2+} (mg/L)	0.61	1.12	7.57	0.07	0.69	0.12	0.31	0.09
Ca^{2+} (mg/L)	59.17	63.84	22.71	37.93	25.97	33.70	26.07	38.60
TIC (mg/L)	1.1	4.45	14.9	0.11	0.20	0.19	0.19	0.15

*Data from Szponar et al. were single measurements while data from laboratory experiments are the average of triplicate values.

5.1.6 Tablelands versus White Hills

To compare the two study locations, the Tablelands, and the White Hills, four experiments plus one baseline experiment were conducted in triplicate to determine if there was a difference in sequestration potential of the rocks sampled from these the two locations. These experiments all used CaOH water and used either crushed or whole rock from either the Tablelands or the White Hills. The baseline experiment was conducted with low concentration CaOH water and no rock. All five of the experiments resulted in an average negative flux, and there was no significant difference in flux values between the experiments (Fig. 56)

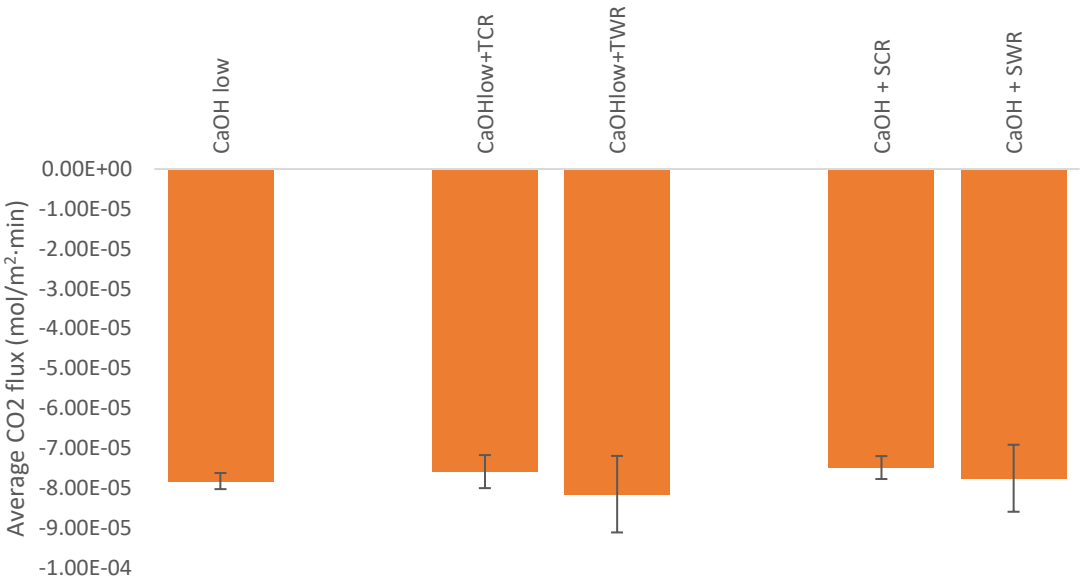

Fig. 56. Comparison of average flux values between Tablelands versus White Hills triplicate experiments. Error bars represent the standard deviation of the averages from triplicate experiments.

The baseline water only experiments and the White Hills experiments resulted in small average increases in conductivity while the two Tablelands experiments resulted in much larger average decreases, with CaOH + TCR having the largest decrease. The increase in conductivity indicates that the White Hills experiments have conditions more favorable to dissolution while the decrease in conductivity indicates that the Tablelands experiments have conditions more favorable to precipitation (Fig. 57).

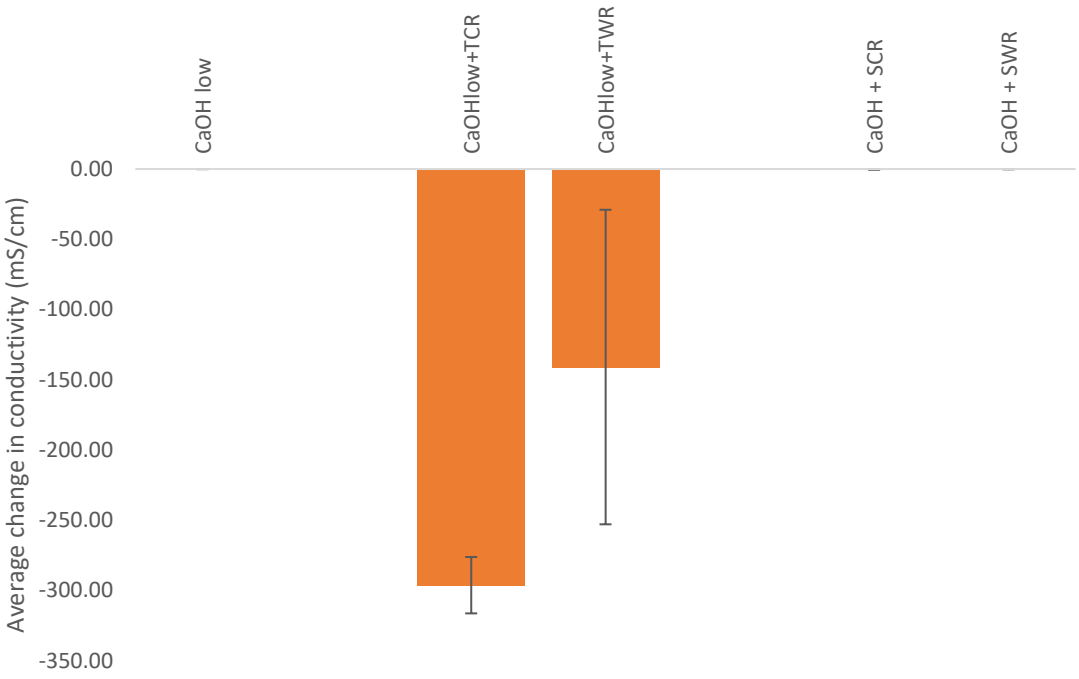

Fig. 57. Comparison of average change in conductivity values between Tablelands versus White Hills triplicate experiments. Error bars represent the standard deviation of the averages from triplicate experiments.

Each of the experiments resulted in an average pH decrease and there was no significant difference in the change in pH between any of the experiments (Fig. 58). While there was no significant difference between the experiments from each location, the decrease in pH indicates experimental conditions favor precipitation.

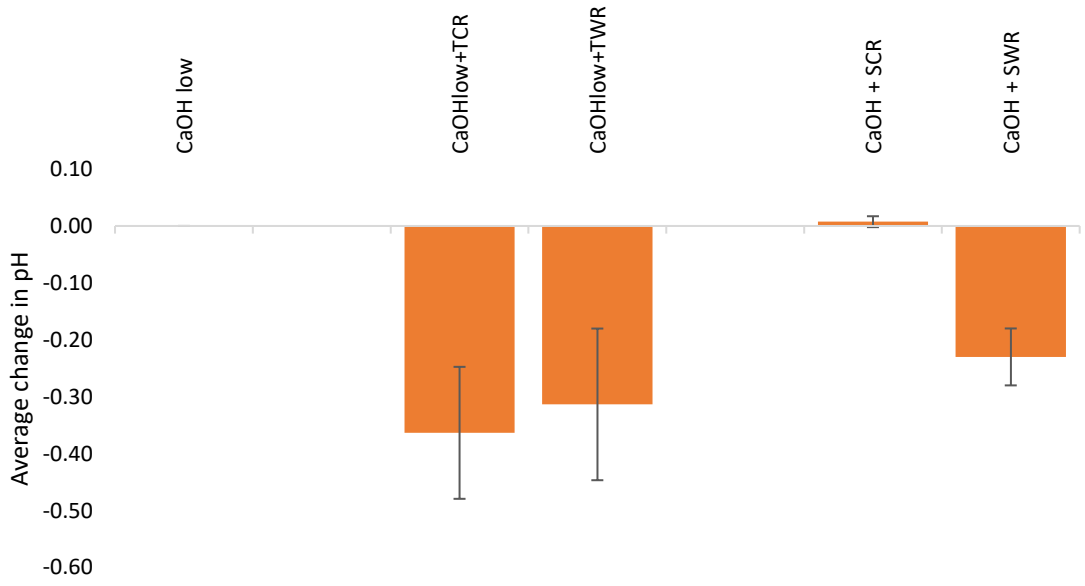

Fig. 58. Comparison of average change in pH values between Tablelands versus White Hills triplicate experiments. Error bars represent the standard deviation of the averages from triplicate experiments.

All of the experiments resulted in an average decrease in TIC concentrations, which is an indication of precipitation (Fig. 59). There was a significant difference between the Tablelands and White Hills crushed rock experiments (p-value 0.03) with the White Hills experiments having the larger decrease in TIC concentration.

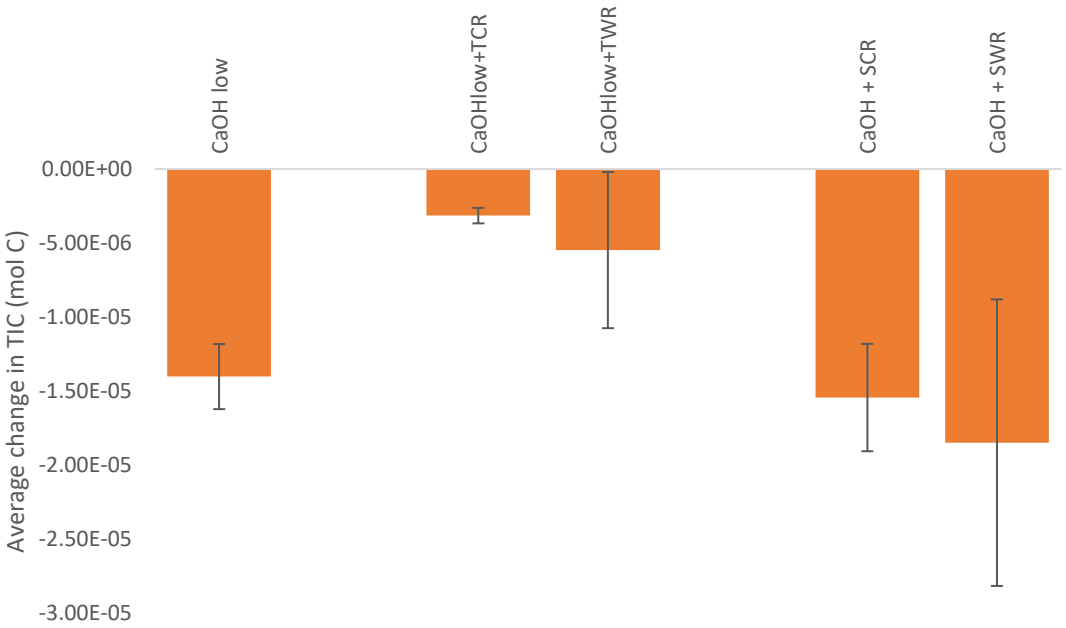

Fig. 59. Comparison of average change in TIC between Tablelands versus White Hills triplicate experiments. Error bars represent the standard deviation of the averages from triplicate experiments.

Out of the five experiments, CaOH water plus Tablelands crushed rock experiments showed the greatest average changes in elemental concentrations (Figures 60, 61, and 62). These experiments had the largest decrease in Ca concentrations, and largest increase in Mg and Si concentrations. The second largest changes in concentration were in the other Tablelands experiments, CaOH water plus Tablelands whole rock. Both of the Tablelands experiments resulted in changes that were 3-4 orders of magnitude larger than the White Hills experiments. The large decrease in Ca concentrations indicates that the Tablelands experiments have conditions more suitable to precipitation and the large increases in Mg and Si concentrations indicate that they also have conditions more suitable for dissolution.

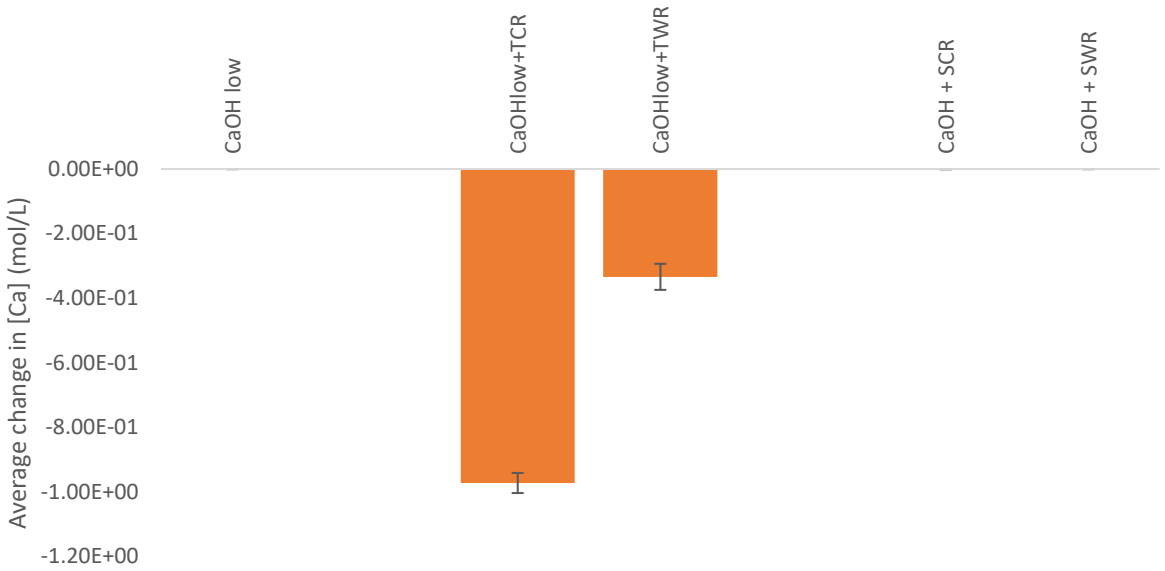

Fig. 60. Comparison of the average change in Ca concentration between Tablelands and White Hills triplicate experiments. Error bars represent the standard deviation of the averages from triplicate experiments.

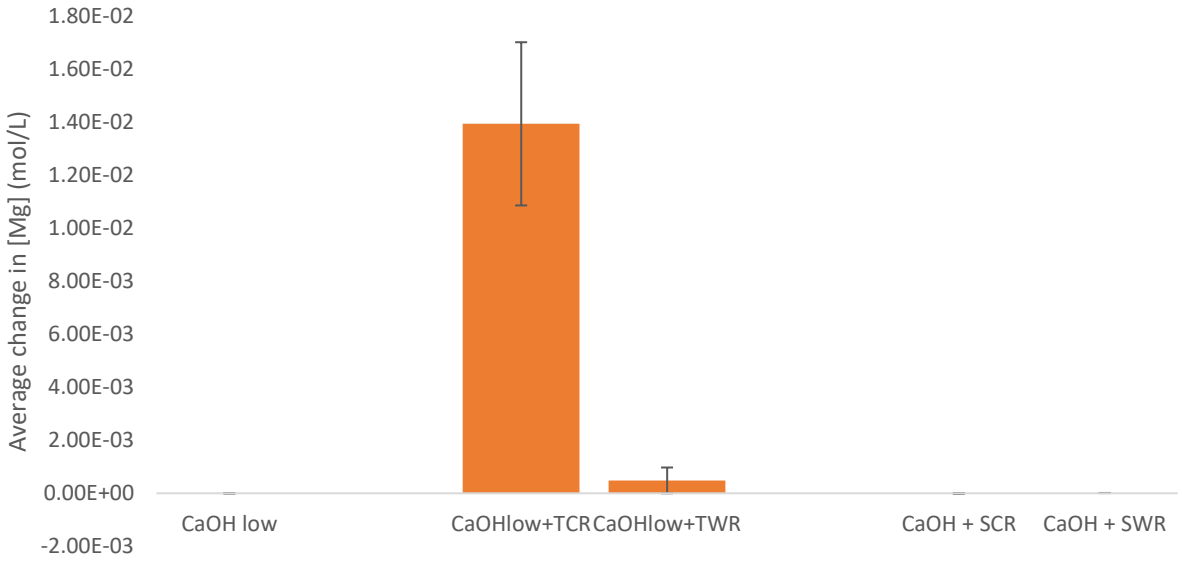

Fig. 61. Comparison of the average change in Mg concentration between Tablelands and White Hills triplicate experiments. Error bars represent the standard deviation of the averages from triplicate experiments.

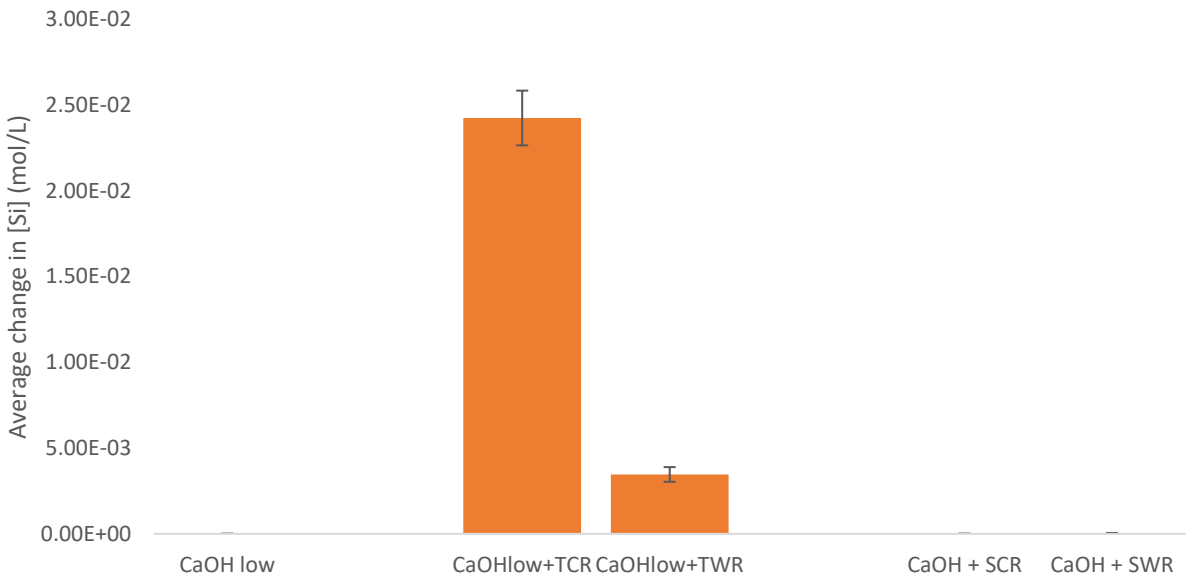

Fig. 62. Comparison of the average change in Si concentration between Tablelands and White Hills triplicate experiments. Error bars represent the standard deviation of the averages from triplicate experiments.

All five experiments showed an average calculated increase in solid carbon over the course of the experiments (Fig. 63). When compared to the baseline CaOH water only experiments, the only experiments that were significantly different were the CaOH plus Tablelands crushed rock experiments (p-value 0.01). However, when the crushed rock experiments were compared to each other, there was a significant difference between them (p-value 0.04). This was the same for whole rock experiments (p-value 0.04), and in both cases the experiments using White Hills rock were the experiments that had the larger average change in solid carbon. This indicates that the experiments from the White Hills might have slightly more favorable conditions for precipitation (11-15% difference) than experiments from the Tablelands.

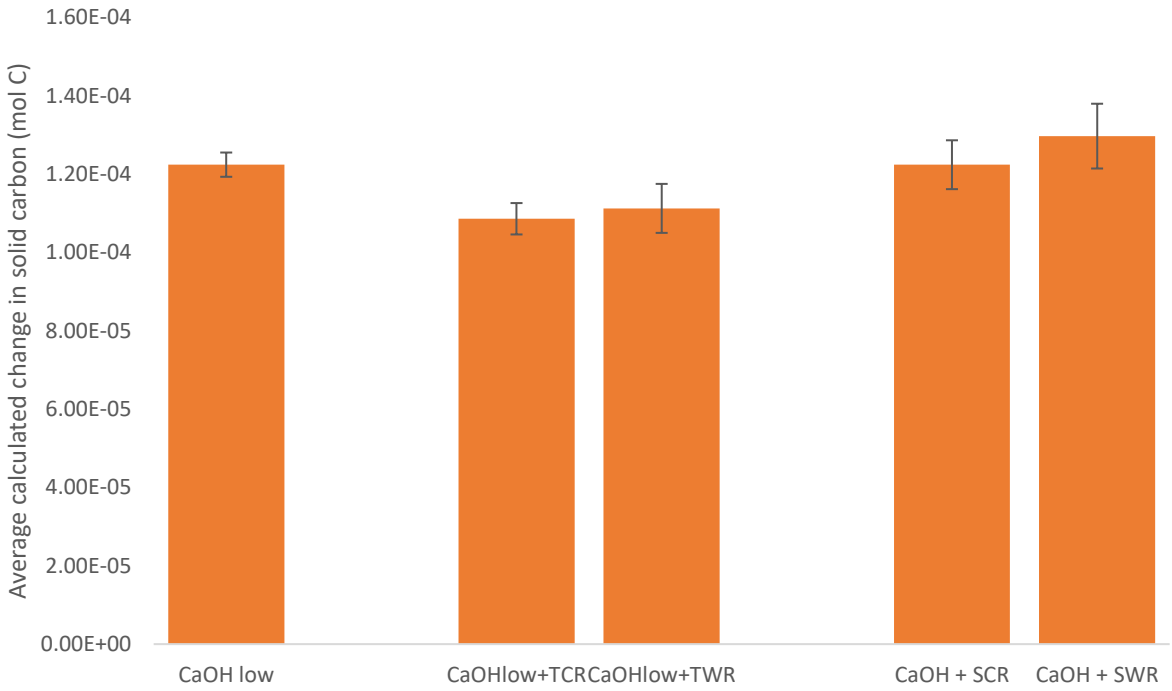

Fig. 63. Comparison of the average calculated changes in solid carbon between the Tablelands and the White Hills. Values are results of triplicate experiments and error bars are propagated errors from the change in CO_2 concentration and the change in total inorganic carbon.

When comparing both locations by examining the indicators from the various analyses recorded during each experiment, the experiments using Tablelands rock have conditions favorable for both dissolution and precipitation while the experiments using White Hills rock have conditions favorable for precipitation with less evidence of dissolution. The Tablelands experiments clearly demonstrated more extensive dissolution through the increases in aqueous Mg and Si concentrations, while the decreases in conductivity, Ca and TIC concentrations, and pH indicated precipitation. The experiments also had a calculated increase in solid carbon and negative flux, two more indicators of precipitation. The White Hills experiments resulted in a negative flux, larger decreases in TIC concentrations and also larger increases in calculated solid carbon, indicating that the White Hills experiments had conditions more suited to precipitation.

The mineralogy of the rock used for laboratory experiments will also have an effect on the results of the experiments. Since the dunite from the Tablelands showed a lesser extent of serpentinization, it is possible that the increased evidence of dissolution is due to more "fresh" rock available for reaction. The greater extent of the serpentinization of the harzburgite from the White Hills may limit dissolution, but the indicators for precipitation are evidence that carbon mineralization is still possible.

As previously mentioned, for carbon mineralization to occur there are two important steps: dissolution and precipitation. Whereas the White Hills experiments resulted in multiple indicators for precipitation that were similar to the Tablelands experiments, the additional multiple indicators of dissolution demonstrates that the Tablelands would be the location of choice for carbon mineralization in Newfoundland.

5.1.7 Future work

To better understand the processes involved in carbon mineralization, more work is needed. This study focused on measuring the changes from varying water type and surface area on carbon mineralization potential. Research has suggested that pressure and temperature may also play an important role in increasing the rate of carbon mineralization. Unfortunately, the instruments used in this study were unable to operate at the higher temperatures and pressures proposed by other studies. Future experiments should use instruments capable of withstanding these higher temperatures and pressures so their effects can be better understood. This study was also limited to a closed system for the experiments, a new method to allow for a simulation of an open or flow-through system should be developed for future studies.

Determining the amount of solid carbonate precipitated during laboratory experiments is an important method for evaluating the carbon mineralization potential of different experiment

parameters and also sampling locations. Additionally, differentiating between the precipitation of Ca-carbonate and Mg-carbonate would also be beneficial to understanding the balance between dissolution and precipitation.

One shortcoming of the carbon balance equations used in this study is the assumption that the amount of solid carbonate at the beginning of the experiments is equal to zero. Unfortunately, the equations demonstrated that this assumption was not perfect with the negative values for solid carbonate, which were interpreted as an indicator of dissolution. A method for measuring the amount of carbonate at the beginning of the experiments is necessary to improve this equation.

To help find more ultra-basic springs, more field work should be completed to search areas that have been identified as potential spring sites. These field seasons should have access to all terrain vehicles or plan to overnight in the field to allow for a more complete survey of the potential spring locations.

Chapter 6: Conclusions

This study found that of the parameters investigated (pH, surface area, CO_2 supply, and sample location), pH had the largest effect on CO_2 sequestration rates. Type II simulated waters (ultra-basic, pH 11-12) sequestered the most CO_2, sequestered CO_2 the fastest, and also had the largest calculated increase in precipitated carbon. Increasing CO_2 supply resulted in an increase in calculated precipitated carbonate minerals in almost all experiments. Of the two study locations the Tablelands appears to be the slightly more favorable location when similar experiments are compared. Although more work is needed to fully understand the CO_2 mineralization processes, these results help to affirm that CO_2 mineralization in exposed continental ultramafic rocks represents a promising potential long-term CO_2 storage solution.

Chapter 7: References cited

Asghari, K., & Al-Dliwe, A. (2005). - Optimization of carbon dioxide sequestration and improved oil recovery in oil reservoirs. In E. S. Rubin, D. W. Keith, C. F. Gilboy, M. Wilson, T. Morris, J. Gale, & K. Thambimuthu (Eds.), *Greenhouse Gas Control Technologies 7* (pp. 381-389). Elsevier Science Ltd. https://doi.org/https://doi.org/10.1016/B978-008044704-9/50039-2

Barnes, I., LaMarche Jr, V. C., & Himmelberg, G. (1967). Geochemical evidence of present-day serpentinization. *Science, 156*(3776), 830-832.

Barnes, I., & O'Neil, J. R. (1969). The relationship between fluids in some fresh alpine-type ultramafics and possible modern serpentinization, western United States. *Geological Society of America Bulletin, 80*(10), 1947-1960.

Boot-Handford, M. E., Abanades, J. C., Anthony, E. J., Blunt, M. J., Brandani, S., Mac Dowell, N., Fernández, J. R., Ferrari, M. C., Gross, R., Hallett, J. P., Haszeldine, R. S., Heptonstall, P., Lyngfelt, A., Makuch, Z., Mangano, E., Porter, R. T. J., Pourkashanian, M., Rochelle, G. T., Shah, N., Yao, J. G., & Fennell, P. S. (2014). Carbon capture and storage update [Review]. *Energy and Environmental Science, 7*(1), 130-189. https://doi.org/10.1039/c3ee42350f

Bui, M., Adjiman, C. S., Bardow, A., Anthony, E. J., Boston, A., Brown, S., Fennell, P. S., Fuss, S., Galindo, A., Hackett, L. A., Hallett, J. P., Herzog, H. J., Jackson, G., Kemper, J., Krevor, S., Maitland, G. C., Matuszewski, M., Metcalfe, I. S., Petit, C., Puxty, G., Reimer, J., Reiner, D. M., Rubin, E. S., Scott, S. A., Shah, N., Smit, B., Trusler, J. P. M., Webley, P., Wilcox, J., & Mac Dowell, N. (2018). Carbon capture and storage (CCS): The way forward [Review]. *Energy and Environmental Science, 11*(5), 1062-1176. https://doi.org/10.1039/c7ee02342a

Clark, I. D., & Fritz, P. (2013). *Environmental isotopes in hydrogeology*. CRC press.

Costa, M. H., Cotrim da Cunha, L., Cox, P. M., Eliseev, A. V., Hensen, S., Ishii, M., Jaccard, S., Koven, C., Lohila, A., & Patra, P. K. (2021). Global Carbon and other Biogeochemical Cycles and Feedbacks. In. IPCC.

Friel, J. K., Skinner, C. S., Jackson, S. E., & Longerich, H. P. (1990). Analysis of biological reference materials, prepared by microwave dissolution, using inductively coupled plasma mass spectrometry. *Analyst, 115*(3), 269-273.

Gislason, S. R., & Oelkers, E. H. (2014). Carbon Storage in Basalt. *Science, 344*(6182), 373-374. https://doi.org/doi:10.1126/science.1250828

Kelemen, P. B., & Matter, J. (2008). In situ carbonation of peridotite for CO2 storage. *Proceedings of the National Academy of Sciences, 105*(45), 17295-17300.

Kelemen, P. B., Matter, J., Streit, E. E., Rudge, J. F., Curry, W. B., & Blusztajn, J. (2011). Rates and Mechanisms of Mineral Carbonation in Peridotite: Natural Processes and Recipes for Enhanced, in situ CO2Capture and Storage. *Annual Review of Earth and Planetary Sciences, 39*(1), 545-576. https://doi.org/10.1146/annurev-earth-092010-152509

Kelemen, P. B., McQueen, N., Wilcox, J., Renforth, P., Dipple, G., & Vankeuren, A. P. (2020). Engineered carbon mineralization in ultramafic rocks for CO2 removal from air: Review and new insights. *Chemical Geology, 550*. https://doi.org/10.1016/j.chemgeo.2020.119628

Lacinska, A. M., Styles, M. T., Bateman, K., Hall, M., & Brown, P. D. (2017). An Experimental Study of the Carbonation of Serpentinite and Partially Serpentinised Peridotites. *Frontiers in Earth Science, 5*. https://doi.org/10.3389/feart.2017.00037

Lackner, K. S., Wendt, C. H., Butt, D. P., Joyce Jr, E. L., & Sharp, D. H. (1995). Carbon dioxide disposal in carbonate minerals. *Energy, 20*(11), 1153-1170.

Matter, J. M., Stute, M., Snæbjörnsdottir, S. Ó., Oelkers, E. H., Gislason, S. R., Aradottir, E. S., Sigfusson, B., Gunnarsson, I., Sigurdardottir, H., & Gunnlaugsson, E. (2016). Rapid carbon mineralization for permanent disposal of anthropogenic carbon dioxide emissions. *Science, 352*(6291), 1312-1314.

Morrill, P. L., Kuenen, J. G., Johnson, O. J., Suzuki, S., Rietze, A., Sessions, A. L., Fogel, M. L., & Nealson, K. H. (2013). Geochemistry and geobiology of a present-day serpentinization site in California: The Cedars. *Geochimica et Cosmochimica Acta, 109*, 222-240. https://doi.org/10.1016/j.gca.2013.01.043

Park, A.-H. A., & Fan, L.-S. (2004). CO2 mineral sequestration: physically activated dissolution of serpentine and pH swing process. *Chemical Engineering Science, 59*(22-23), 5241-5247. https://doi.org/10.1016/j.ces.2004.09.008

Paukert, A. N., Matter, J. M., Kelemen, P. B., Shock, E. L., & Havig, J. R. (2012). Reaction path modeling of enhanced in situ CO2 mineralization for carbon sequestration in the peridotite of the Samail Ophiolite, Sultanate of Oman. *Chemical Geology, 330*, 86-100.

Podgrajsek, E., Sahlée, E., Bastviken, D., Holst, J., Lindroth, A., Tranvik, L., & Rutgersson, A. (2014). Comparison of floating chamber and eddy covariance measurements of lake greenhouse gas fluxes. *Biogeosciences, 11*(15), 4225-4233.

Pronost, J., Beaudoin, G., Lemieux, J.-M., Hébert, R., Constantin, M., Marcouiller, S., Klein, M., Duchesne, J., Molson, J. W., & Larachi, F. (2012). CO2-depleted warm air venting from chrysotile milling waste (Thetford Mines, Canada): Evidence for in-situ carbon capture from the atmosphere. *Geology, 40*(3), 275-278.

Rudge, J. F., Kelemen, P. B., & Spiegelman, M. (2010). A simple model of reaction-induced cracking applied to serpentinization and carbonation of peridotite. *Earth and Planetary Science Letters, 291*(1-4), 215-227. https://doi.org/10.1016/j.epsl.2010.01.016

Schott, J., Pokrovsky, O. S., & Oelkers, E. H. (2009). The Link Between Mineral Dissolution/Precipitation Kinetics and Solution Chemistry. *Reviews in Mineralogy and Geochemistry, 70*(1), 207-258. https://doi.org/10.2138/rmg.2009.70.6

Snæbjörnsdóttir, S. Ó., Sigfússon, B., Marieni, C., Goldberg, D., Gislason, S. R., & Oelkers, E. H. (2020). Carbon dioxide storage through mineral carbonation [Review]. *Nature Reviews Earth and Environment, 1*(2), 90-102. https://doi.org/10.1038/s43017-019-0011-8

Snæbjörnsdóttir, S. Ó., Wiese, F., Fridriksson, T., Ármansson, H., Einarsson, G. M., & Gislason, S. R. (2014). CO2 storage potential of basaltic rocks in Iceland and the oceanic ridges. *Energy Procedia, 63*, 4585-4600. https://doi.org/10.1016/j.egypro.2014.11.491

Szponar, N., Brazelton, W. J., Schrenk, M. O., Bower, D. M., Steele, A., & Morrill, P. L. (2013). Geochemistry of a continental site of serpentinization, the Tablelands Ophiolite, Gros Morne National Park: A Mars analogue. *Icarus, 224*(2), 286-296. https://doi.org/10.1016/j.icarus.2012.07.004

van Noort, R., Wolterbeek, T., Drury, M., Kandianis, M., & Spiers, C. (2017). The Force of Crystallization and Fracture Propagation during In-Situ Carbonation of Peridotite. *Minerals, 7*(10). https://doi.org/10.3390/min7100190

Williams, H., & Smyth, W. (1973). Metamorphic aureoles beneath ophiolite suites and alpine peridotites; tectonic implications with west Newfoundland examples. *American Journal of Science, 273*(7), 594-621.

Zhou, C., Wei, X., Zhou, G., Yan, J., Wang, X., Wang, C., Liu, H., Tang, X., & Zhang, Q. (2008, 2008/03/20/). Impacts of a large-scale reforestation program on carbon storage dynamics in Guangdong, China. *Forest Ecology and Management, 255*(3), 847-854. https://doi.org/https://doi.org/10.1016/j.foreco.2007.09.081

Chapter 8: Appendices

Appendix A: CO_2 concentrations from field deployments in the Tablelands

Table A1: CO_2 concentrations from field deployments over ultra-basic springs in the Tablelands.

time (min)	WHC2	WHC500
0	1.65E-05	1.66E-05
1	1.62E-05	1.72E-05
2	1.57E-05	1.72E-05
3	1.53E-05	1.71E-05
4	1.48E-05	1.70E-05
5	1.44E-05	1.69E-05
6	1.40E-05	1.69E-05
7	1.37E-05	1.67E-05
8	1.33E-05	1.67E-05
9	1.30E-05	1.66E-05
10	1.27E-05	1.65E-05
11	1.23E-05	1.64E-05
12	1.20E-05	1.63E-05
13	1.18E-05	1.62E-05
14	1.15E-05	1.62E-05
15	1.12E-05	1.60E-05
16	1.09E-05	1.60E-05
17	1.06E-05	1.59E-05
18	1.04E-05	1.58E-05
19	1.02E-05	1.57E-05
20	1.00E-05	1.57E-05
21	9.78E-06	1.55E-05
22	9.55E-06	1.55E-05
23	9.35E-06	1.54E-05
24	9.12E-06	1.53E-05
25	8.93E-06	1.52E-05
26	8.70E-06	1.52E-05
27	8.50E-06	1.51E-05
28	8.30E-06	1.50E-05
29	8.14E-06	1.50E-05
30	7.97E-06	1.49E-05
31	7.79E-06	1.48E-05
32	7.64E-06	1.47E-05
33	7.45E-06	1.46E-05
34	7.28E-06	1.46E-05
35	7.14E-06	1.45E-05

36	7.01E-06	1.45E-05
37	6.85E-06	1.44E-05
38	6.71E-06	1.43E-05
39	6.56E-06	1.43E-05
40	6.44E-06	1.42E-05
41	6.33E-06	1.41E-05
42	6.19E-06	1.41E-05
43	6.08E-06	1.40E-05
44	6.00E-06	1.39E-05
45	5.94E-06	1.39E-05
46	5.84E-06	1.38E-05
47	5.75E-06	1.37E-05
48	5.66E-06	1.37E-05
49	5.55E-06	1.36E-05
50	5.45E-06	1.35E-05
51	5.36E-06	1.35E-05
52	5.29E-06	1.34E-05
53	5.22E-06	1.33E-05
54	5.16E-06	1.33E-05
55	5.06E-06	1.32E-05
56	4.98E-06	1.32E-05
57	4.93E-06	1.31E-05
58	4.88E-06	1.31E-05
59	4.81E-06	1.30E-05
60	4.75E-06	1.30E-05
61	4.66E-06	1.29E-05
62	4.61E-06	1.28E-05
63	4.59E-06	1.28E-05
64	4.54E-06	1.27E-05
65	4.50E-06	1.27E-05
66	4.46E-06	1.26E-05
67	4.42E-06	1.25E-05
68	4.38E-06	1.25E-05
69	4.32E-06	1.24E-05
70	4.30E-06	1.24E-05
71	4.25E-06	1.23E-05
72	4.24E-06	1.23E-05
73	4.16E-06	1.22E-05
74	4.09E-06	1.22E-05
75	4.04E-06	1.21E-05
76	3.98E-06	1.20E-05
77	4.01E-06	1.20E-05
78	3.96E-06	
79	3.89E-06	

80	3.96E-06
81	3.96E-06
82	3.95E-06
83	3.96E-06
84	3.98E-06
85	3.96E-06
86	3.94E-06
87	3.93E-06
88	3.96E-06
89	3.96E-06
90	3.97E-06
91	3.95E-06
92	3.99E-06
93	3.95E-06
94	3.92E-06
95	3.87E-06
96	3.85E-06
97	3.85E-06
98	3.86E-06
99	3.86E-06
100	3.79E-06
101	3.77E-06
102	3.77E-06
103	3.72E-06
104	3.75E-06
105	3.74E-06
106	3.69E-06
107	3.66E-06
108	3.65E-06
109	3.70E-06
110	3.63E-06
111	3.66E-06
112	3.61E-06
113	3.61E-06
114	3.66E-06
115	3.63E-06
116	3.59E-06
117	3.56E-06
118	3.55E-06
119	3.54E-06
120	3.54E-06
121	3.54E-06
122	3.53E-06
123	3.54E-06

124	3.53E-06
125	3.52E-06
126	3.52E-06
127	3.48E-06
128	3.48E-06
129	3.46E-06
130	3.45E-06
131	3.55E-06
132	3.50E-06
133	3.48E-06
134	3.46E-06
135	3.47E-06
136	3.47E-06
137	3.51E-06
138	3.48E-06
139	3.43E-06
140	3.47E-06
141	3.50E-06
142	3.50E-06
143	3.46E-06
144	3.45E-06
145	3.43E-06
146	3.42E-06
147	3.39E-06
148	3.40E-06
149	3.39E-06
150	3.38E-06

Table A2: CO_2 concentrations from field deployments over solid ultramafic rock, local vegetation, ultramafic gravel, and a small bog in the Tablelands.

time (min)	Rock	Vegetation	Gravel	Bog
0	1.65E-05	1.67E-05	1.66E-05	1.65E-05
1	1.65E-05	1.65E-05	1.66E-05	1.65E-05
2	1.66E-05	1.67E-05	1.68E-05	1.65E-05
3	1.66E-05	1.71E-05	1.71E-05	1.66E-05
4	1.66E-05	1.73E-05	1.73E-05	1.66E-05
5	1.66E-05	1.76E-05	1.75E-05	1.66E-05
6	1.66E-05	1.78E-05	1.77E-05	1.66E-05
7	1.66E-05	1.81E-05	1.79E-05	1.67E-05
8	1.66E-05	1.83E-05	1.80E-05	1.67E-05
9	1.66E-05	1.86E-05	1.82E-05	1.67E-05
10	1.66E-05	1.88E-05	1.83E-05	1.68E-05
11	1.66E-05	1.90E-05	1.84E-05	1.68E-05
12	1.66E-05	1.92E-05	1.85E-05	1.69E-05
13	1.66E-05	1.95E-05	1.86E-05	1.69E-05
14	1.66E-05	1.97E-05	1.87E-05	1.69E-05
15	1.66E-05	1.99E-05	1.88E-05	1.70E-05
16	1.66E-05	2.02E-05	1.89E-05	1.70E-05
17	1.66E-05	2.04E-05	1.89E-05	1.70E-05
18	1.66E-05	2.06E-05	1.90E-05	1.71E-05
19	1.66E-05	2.08E-05	1.91E-05	1.71E-05
20	1.66E-05	2.10E-05	1.91E-05	1.72E-05
21	1.66E-05	2.13E-05	1.92E-05	1.72E-05
22	1.66E-05	2.15E-05	1.92E-05	1.72E-05
23	1.66E-05	2.17E-05	1.92E-05	1.73E-05
24	1.66E-05	2.19E-05	1.93E-05	1.73E-05
25	1.66E-05	2.21E-05	1.93E-05	1.74E-05
26	1.66E-05	2.23E-05	1.93E-05	1.74E-05
27	1.66E-05	2.25E-05	1.94E-05	1.74E-05
28	1.66E-05	2.27E-05	1.94E-05	1.75E-05
29	1.67E-05	2.29E-05	1.94E-05	1.75E-05
30	1.67E-05	2.32E-05	1.94E-05	1.76E-05
31	1.67E-05	2.34E-05	1.94E-05	1.76E-05
32	1.67E-05	2.35E-05	1.95E-05	1.76E-05
33	1.67E-05	2.37E-05	1.95E-05	1.77E-05
34	1.67E-05	2.40E-05	1.95E-05	1.77E-05
35	1.67E-05	2.42E-05	1.95E-05	1.78E-05
36	1.67E-05	2.44E-05	1.95E-05	1.78E-05
37	1.67E-05	2.46E-05	1.95E-05	1.78E-05

38	1.67E-05	2.48E-05	1.96E-05	1.79E-05
39	1.67E-05	2.50E-05	1.96E-05	1.79E-05
40	1.67E-05	2.52E-05	1.96E-05	1.80E-05
41	1.67E-05	2.53E-05	1.96E-05	1.80E-05
42	1.67E-05	2.55E-05	1.96E-05	1.81E-05
43	1.67E-05	2.58E-05	1.96E-05	1.81E-05
44	1.67E-05	2.59E-05	1.96E-05	1.81E-05
45	1.67E-05	2.61E-05	1.96E-05	1.82E-05
46	1.67E-05	2.64E-05		1.82E-05
47	1.67E-05	2.65E-05		1.82E-05
48	1.67E-05	2.67E-05		1.83E-05
49	1.67E-05	2.69E-05		1.83E-05
50	1.67E-05	2.71E-05		1.84E-05
51	1.67E-05	2.73E-05		1.84E-05
52	1.67E-05	2.75E-05		1.84E-05
53	1.68E-05	2.77E-05		1.85E-05
54	1.67E-05	2.78E-05		1.85E-05
55	1.67E-05	2.80E-05		1.86E-05
56	1.67E-05	2.82E-05		1.86E-05
57	1.67E-05	2.84E-05		1.86E-05
58	1.67E-05	2.86E-05		1.87E-05
59	1.68E-05	2.88E-05		1.87E-05
60	1.67E-05	2.90E-05		1.88E-05
61		2.92E-05		1.88E-05
62		2.93E-05		1.89E-05
63		2.95E-05		1.89E-05
64		2.98E-05		1.90E-05
65		2.99E-05		1.90E-05
66		3.01E-05		1.90E-05
67		3.03E-05		1.91E-05
68		3.04E-05		1.91E-05
69		3.07E-05		1.92E-05
70		3.08E-05		1.92E-05
71		3.10E-05		1.93E-05
72		3.12E-05		1.93E-05
73		3.14E-05		1.93E-05
74		3.16E-05		1.94E-05
75		3.18E-05		1.94E-05
76		3.19E-05		1.95E-05
77		3.21E-05		1.95E-05
78		3.23E-05		1.96E-05
79		3.25E-05		1.96E-05
80		3.27E-05		1.96E-05
81		3.29E-05		1.97E-05

82	3.31E-05	1.97E-05
83	3.33E-05	1.98E-05
84	3.35E-05	1.98E-05
85	3.37E-05	1.99E-05
86	3.39E-05	1.99E-05
87	3.41E-05	2.00E-05
88	3.43E-05	2.00E-05
89	3.45E-05	2.01E-05
90	3.47E-05	2.01E-05
91	3.48E-05	2.01E-05
92	3.51E-05	2.02E-05
93	3.53E-05	2.02E-05
94	3.54E-05	2.03E-05
95	3.57E-05	2.03E-05
96	3.58E-05	2.03E-05
97	3.61E-05	2.04E-05
98	3.62E-05	2.04E-05
99	3.64E-05	2.05E-05
100	3.66E-05	2.05E-05
101	3.68E-05	2.05E-05
102	3.70E-05	2.06E-05
103	3.73E-05	2.06E-05
104	3.75E-05	2.07E-05
105	3.77E-05	2.07E-05
106	3.78E-05	
107	3.80E-05	
108	3.82E-05	
109	3.84E-05	
110	3.86E-05	
111	3.88E-05	
112	3.90E-05	
113	3.92E-05	
114	3.94E-05	
115	3.96E-05	
116	3.98E-05	
117	4.00E-05	
118	4.01E-05	
119	4.04E-05	
120	4.05E-05	

Appendix B: CO_2 concentrations from laboratory sequestration experiments

Table B1: Average CO_2 concentration of five-hour Tablelands experiments with DI water.

Time (min)	DI	DI + TCR	DI + TWR1	DI + TWR2
0	2.03E-05	1.87E-05	2.04E-05	1.89E-05
1	2.02E-05	1.86E-05	2.04E-05	1.88E-05
2	2.02E-05	1.86E-05	2.04E-05	1.88E-05
3	2.02E-05	1.86E-05	2.04E-05	1.88E-05
4	2.02E-05	1.86E-05	2.04E-05	1.89E-05
5	2.02E-05	1.86E-05	2.04E-05	1.88E-05
6	2.02E-05	1.86E-05	2.04E-05	1.88E-05
7	2.02E-05	1.85E-05	2.04E-05	1.88E-05
8	2.02E-05	1.85E-05	2.04E-05	1.88E-05
9	2.02E-05	1.85E-05	2.04E-05	1.88E-05
10	2.02E-05	1.85E-05	2.04E-05	1.88E-05
11	2.02E-05	1.85E-05	2.04E-05	1.88E-05
12	2.02E-05	1.85E-05	2.04E-05	1.88E-05
13	2.02E-05	1.85E-05	2.04E-05	1.89E-05
14	2.02E-05	1.85E-05	2.04E-05	1.88E-05
15	2.02E-05	1.85E-05	2.04E-05	1.89E-05
16	2.02E-05	1.84E-05	2.04E-05	1.89E-05
17	2.02E-05	1.84E-05	2.04E-05	1.89E-05
18	2.02E-05	1.84E-05	2.04E-05	1.88E-05
19	2.02E-05	1.84E-05	2.04E-05	1.89E-05
20	2.02E-05	1.84E-05	2.04E-05	1.89E-05
21	2.02E-05	1.84E-05	2.04E-05	1.89E-05
22	2.02E-05	1.84E-05	2.04E-05	1.89E-05
23	2.02E-05	1.84E-05	2.04E-05	1.88E-05
24	2.02E-05	1.84E-05	2.04E-05	1.89E-05
25	2.02E-05	1.84E-05	2.04E-05	1.89E-05
26	2.02E-05	1.84E-05	2.04E-05	1.88E-05
27	2.02E-05	1.84E-05	2.04E-05	1.89E-05
28	2.02E-05	1.83E-05	2.04E-05	1.88E-05
29	2.02E-05	1.83E-05	2.04E-05	1.89E-05
30	2.02E-05	1.83E-05	2.04E-05	1.88E-05
31	2.02E-05	1.83E-05	2.04E-05	1.89E-05
32	2.02E-05	1.83E-05	2.04E-05	1.89E-05
33	2.02E-05	1.83E-05	2.04E-05	1.88E-05
34	2.02E-05	1.83E-05	2.04E-05	1.89E-05
35	2.02E-05	1.83E-05	2.04E-05	1.88E-05
36	2.02E-05	1.83E-05	2.04E-05	1.88E-05

37	2.02E-05	1.83E-05	2.03E-05	1.89E-05
38	2.02E-05	1.83E-05	2.04E-05	1.88E-05
39	2.02E-05	1.83E-05	2.04E-05	1.89E-05
40	2.02E-05	1.82E-05	2.03E-05	1.89E-05
41	2.02E-05	1.82E-05	2.03E-05	1.88E-05
42	2.02E-05	1.82E-05	2.03E-05	1.89E-05
43	2.02E-05	1.82E-05	2.03E-05	1.88E-05
44	2.02E-05	1.82E-05	2.03E-05	1.89E-05
45	2.02E-05	1.82E-05	2.03E-05	1.88E-05
46	2.02E-05	1.82E-05	2.03E-05	1.88E-05
47	2.02E-05	1.82E-05	2.03E-05	1.88E-05
48	2.02E-05	1.82E-05	2.03E-05	1.88E-05
49	2.02E-05	1.82E-05	2.03E-05	1.88E-05
50	2.02E-05	1.82E-05	2.03E-05	1.88E-05
51	2.02E-05	1.82E-05	2.03E-05	1.88E-05
52	2.02E-05	1.82E-05	2.03E-05	1.88E-05
53	2.01E-05	1.81E-05	2.03E-05	1.88E-05
54	2.02E-05	1.81E-05	2.03E-05	1.88E-05
55	2.02E-05	1.81E-05	2.03E-05	1.88E-05
56	2.02E-05	1.81E-05	2.03E-05	1.88E-05
57	2.02E-05	1.81E-05	2.03E-05	1.88E-05
58	2.01E-05	1.81E-05	2.03E-05	1.88E-05
59	2.01E-05	1.81E-05	2.03E-05	1.88E-05
60	2.01E-05	1.81E-05	2.03E-05	1.88E-05
61	2.01E-05	1.81E-05	2.03E-05	1.88E-05
62	2.01E-05	1.81E-05	2.03E-05	1.88E-05
63	2.01E-05	1.81E-05	2.03E-05	1.88E-05
64	2.01E-05	1.81E-05	2.03E-05	1.88E-05
65	2.01E-05	1.81E-05	2.03E-05	1.88E-05
66	2.01E-05	1.81E-05	2.03E-05	1.88E-05
67	2.01E-05	1.81E-05	2.03E-05	1.88E-05
68	2.01E-05	1.80E-05	2.03E-05	1.88E-05
69	2.01E-05	1.80E-05	2.03E-05	1.88E-05
70	2.01E-05	1.80E-05	2.03E-05	1.88E-05
71	2.01E-05	1.80E-05	2.03E-05	1.88E-05
72	2.01E-05	1.80E-05	2.03E-05	1.88E-05
73	2.01E-05	1.80E-05	2.03E-05	1.88E-05
74	2.01E-05	1.80E-05	2.03E-05	1.88E-05
75	2.01E-05	1.80E-05	2.03E-05	1.88E-05
76	2.01E-05	1.80E-05	2.03E-05	1.88E-05
77	2.01E-05	1.80E-05	2.03E-05	1.88E-05
78	2.01E-05	1.80E-05	2.03E-05	1.88E-05
79	2.01E-05	1.80E-05	2.03E-05	1.88E-05
80	2.01E-05	1.80E-05	2.03E-05	1.88E-05

81	2.01E-05	1.80E-05	2.03E-05	1.88E-05
82	2.01E-05	1.80E-05	2.03E-05	1.88E-05
83	2.01E-05	1.80E-05	2.03E-05	1.88E-05
84	2.01E-05	1.80E-05	2.03E-05	1.88E-05
85	2.01E-05	1.79E-05	2.03E-05	1.88E-05
86	2.01E-05	1.79E-05	2.03E-05	1.88E-05
87	2.01E-05	1.79E-05	2.03E-05	1.88E-05
88	2.01E-05	1.79E-05	2.02E-05	1.88E-05
89	2.01E-05	1.79E-05	2.02E-05	1.88E-05
90	2.01E-05	1.79E-05	2.03E-05	1.88E-05
91	2.01E-05	1.79E-05	2.02E-05	1.88E-05
92	2.01E-05	1.79E-05	2.02E-05	1.88E-05
93	2.01E-05	1.79E-05	2.02E-05	1.88E-05
94	2.01E-05	1.79E-05	2.02E-05	1.88E-05
95	2.01E-05	1.79E-05	2.02E-05	1.88E-05
96	2.01E-05	1.79E-05	2.02E-05	1.88E-05
97	2.01E-05	1.79E-05	2.02E-05	1.88E-05
98	2.01E-05	1.79E-05	2.02E-05	1.88E-05
99	2.01E-05	1.79E-05	2.02E-05	1.88E-05
100	2.01E-05	1.79E-05	2.02E-05	1.88E-05
101	2.01E-05	1.79E-05	2.02E-05	1.88E-05
102	2.01E-05	1.79E-05	2.02E-05	1.88E-05
103	2.01E-05	1.79E-05	2.02E-05	1.88E-05
104	2.01E-05	1.79E-05	2.02E-05	1.88E-05
105	2.01E-05	1.79E-05	2.02E-05	1.88E-05
106	2.01E-05	1.79E-05	2.02E-05	1.88E-05
107	2.01E-05	1.79E-05	2.02E-05	1.88E-05
108	2.01E-05	1.78E-05	2.02E-05	1.88E-05
109	2.01E-05	1.78E-05	2.02E-05	1.88E-05
110	2.01E-05	1.78E-05	2.02E-05	1.88E-05
111	2.01E-05	1.78E-05	2.02E-05	1.88E-05
112	2.01E-05	1.78E-05	2.02E-05	1.88E-05
113	2.01E-05	1.78E-05	2.02E-05	1.88E-05
114	2.01E-05	1.78E-05	2.02E-05	1.88E-05
115	2.01E-05	1.78E-05	2.02E-05	1.88E-05
116	2.01E-05	1.78E-05	2.02E-05	1.88E-05
117	2.01E-05	1.78E-05	2.02E-05	1.88E-05
118	2.01E-05	1.78E-05	2.02E-05	1.88E-05
119	2.01E-05	1.78E-05	2.02E-05	1.88E-05
120	2.01E-05	1.78E-05	2.02E-05	1.88E-05
121	2.01E-05	1.78E-05	2.02E-05	1.88E-05
122	2.01E-05	1.78E-05	2.02E-05	1.88E-05
123	2.00E-05	1.78E-05	2.02E-05	1.88E-05
124	2.01E-05	1.78E-05	2.02E-05	1.88E-05

125	2.01E-05	1.78E-05	2.02E-05	1.88E-05
126	2.00E-05	1.78E-05	2.02E-05	1.88E-05
127	2.01E-05	1.78E-05	2.02E-05	1.88E-05
128	2.00E-05	1.78E-05	2.02E-05	1.88E-05
129	2.01E-05	1.78E-05	2.02E-05	1.88E-05
130	2.00E-05	1.78E-05	2.02E-05	1.88E-05
131	2.00E-05	1.78E-05	2.02E-05	1.88E-05
132	2.00E-05	1.78E-05	2.02E-05	1.88E-05
133	2.00E-05	1.78E-05	2.02E-05	1.88E-05
134	2.00E-05	1.78E-05	2.02E-05	1.88E-05
135	2.00E-05	1.77E-05	2.02E-05	1.88E-05
136	2.00E-05	1.77E-05	2.02E-05	1.88E-05
137	2.00E-05	1.77E-05	2.02E-05	1.88E-05
138	2.00E-05	1.77E-05	2.02E-05	1.88E-05
139	2.00E-05	1.77E-05	2.02E-05	1.88E-05
140	2.00E-05	1.77E-05	2.02E-05	1.88E-05
141	2.00E-05	1.77E-05	2.02E-05	1.88E-05
142	2.00E-05	1.77E-05	2.02E-05	1.88E-05
143	2.00E-05	1.77E-05	2.02E-05	1.88E-05
144	2.00E-05	1.77E-05	2.02E-05	1.88E-05
145	2.00E-05	1.77E-05	2.02E-05	1.87E-05
146	2.00E-05	1.77E-05	2.01E-05	1.88E-05
147	2.00E-05	1.77E-05	2.02E-05	1.88E-05
148	2.00E-05	1.77E-05	2.01E-05	1.88E-05
149	2.00E-05	1.77E-05	2.01E-05	1.88E-05
150	2.00E-05	1.77E-05	2.01E-05	1.88E-05
151	2.00E-05	1.77E-05	2.01E-05	1.87E-05
152	2.00E-05	1.77E-05	2.01E-05	1.88E-05
153	2.00E-05	1.77E-05	2.01E-05	1.88E-05
154	2.00E-05	1.77E-05	2.01E-05	1.88E-05
155	2.00E-05	1.77E-05	2.01E-05	1.88E-05
156	2.00E-05	1.77E-05	2.01E-05	1.88E-05
157	2.00E-05	1.77E-05	2.01E-05	1.88E-05
158	2.00E-05	1.77E-05	2.01E-05	1.87E-05
159	2.00E-05	1.77E-05	2.01E-05	1.87E-05
160	2.00E-05	1.77E-05	2.01E-05	1.88E-05
161	2.00E-05	1.77E-05	2.01E-05	1.87E-05
162	2.00E-05	1.77E-05	2.01E-05	1.87E-05
163	2.00E-05	1.77E-05	2.01E-05	1.87E-05
164	2.00E-05	1.77E-05	2.01E-05	1.87E-05
165	2.00E-05	1.76E-05	2.01E-05	1.87E-05
166	2.00E-05	1.76E-05	2.01E-05	1.87E-05
167	2.00E-05	1.76E-05	2.01E-05	1.87E-05
168	2.00E-05	1.76E-05	2.01E-05	1.87E-05

169	2.00E-05	1.76E-05	2.01E-05	1.87E-05
170	2.00E-05	1.76E-05	2.01E-05	1.87E-05
171	2.00E-05	1.76E-05	2.01E-05	1.87E-05
172	2.00E-05	1.76E-05	2.01E-05	1.87E-05
173	2.00E-05	1.76E-05	2.01E-05	1.87E-05
174	2.00E-05	1.76E-05	2.01E-05	1.87E-05
175	2.00E-05	1.76E-05	2.01E-05	1.87E-05
176	2.00E-05	1.76E-05	2.01E-05	1.87E-05
177	2.00E-05	1.76E-05	2.01E-05	1.87E-05
178	2.00E-05	1.76E-05	2.01E-05	1.87E-05
179	2.00E-05	1.76E-05	2.01E-05	1.87E-05
180	2.00E-05	1.76E-05	2.01E-05	1.87E-05
181	2.00E-05	1.76E-05	2.01E-05	1.87E-05
182	2.00E-05	1.76E-05	2.01E-05	1.87E-05
183	2.00E-05	1.76E-05	2.01E-05	1.87E-05
184	2.00E-05	1.76E-05	2.01E-05	1.87E-05
185	2.00E-05	1.76E-05	2.01E-05	1.87E-05
186	2.00E-05	1.76E-05	2.01E-05	1.87E-05
187	2.00E-05	1.76E-05	2.01E-05	1.87E-05
188	2.00E-05	1.76E-05	2.01E-05	1.87E-05
189	2.00E-05	1.76E-05	2.01E-05	1.87E-05
190	2.00E-05	1.76E-05	2.01E-05	1.87E-05
191	2.00E-05	1.76E-05	2.01E-05	1.87E-05
192	2.00E-05	1.76E-05	2.01E-05	1.87E-05
193	2.00E-05	1.76E-05	2.01E-05	1.87E-05
194	2.00E-05	1.76E-05	2.01E-05	1.87E-05
195	2.00E-05	1.76E-05	2.01E-05	1.87E-05
196	2.00E-05	1.76E-05	2.01E-05	1.87E-05
197	2.00E-05	1.76E-05	2.01E-05	1.87E-05
198	2.00E-05	1.76E-05	2.01E-05	1.87E-05
199	2.00E-05	1.76E-05	2.01E-05	1.87E-05
200	2.00E-05	1.76E-05	2.01E-05	1.87E-05
201	2.00E-05	1.75E-05	2.01E-05	1.87E-05
202	2.00E-05	1.76E-05	2.01E-05	1.87E-05
203	2.00E-05	1.76E-05	2.01E-05	1.87E-05
204	2.00E-05	1.75E-05	2.01E-05	1.87E-05
205	2.00E-05	1.75E-05	2.01E-05	1.87E-05
206	2.00E-05	1.75E-05	2.01E-05	1.87E-05
207	2.00E-05	1.75E-05	2.01E-05	1.87E-05
208	2.00E-05	1.75E-05	2.01E-05	1.87E-05
209	2.00E-05	1.75E-05	2.01E-05	1.87E-05
210	2.00E-05	1.75E-05	2.01E-05	1.87E-05
211	2.00E-05	1.75E-05	2.01E-05	1.87E-05
212	2.00E-05	1.75E-05	2.00E-05	1.87E-05

213	2.00E-05	1.75E-05	2.01E-05	1.87E-05
214	2.00E-05	1.75E-05	2.01E-05	1.87E-05
215	2.00E-05	1.75E-05	2.01E-05	1.87E-05
216	2.00E-05	1.75E-05	2.01E-05	1.87E-05
217	2.00E-05	1.75E-05	2.00E-05	1.87E-05
218	2.00E-05	1.75E-05	2.00E-05	1.87E-05
219	2.00E-05	1.75E-05	2.00E-05	1.87E-05
220	2.00E-05	1.75E-05	2.00E-05	1.87E-05
221	2.00E-05	1.75E-05	2.00E-05	1.87E-05
222	2.00E-05	1.75E-05	2.00E-05	1.87E-05
223	2.00E-05	1.75E-05	2.00E-05	1.87E-05
224	2.00E-05	1.75E-05	2.00E-05	1.87E-05
225	2.00E-05	1.75E-05	2.00E-05	1.87E-05
226	2.00E-05	1.75E-05	2.00E-05	1.87E-05
227	2.00E-05	1.75E-05	2.00E-05	1.87E-05
228	2.00E-05	1.75E-05	2.00E-05	1.87E-05
229	2.00E-05	1.75E-05	2.00E-05	1.87E-05
230	2.00E-05	1.75E-05	2.00E-05	1.87E-05
231	2.00E-05	1.75E-05	2.00E-05	1.87E-05
232	2.00E-05	1.75E-05	2.00E-05	1.87E-05
233	2.00E-05	1.75E-05	2.00E-05	1.87E-05
234	2.00E-05	1.75E-05	2.00E-05	1.87E-05
235	2.00E-05	1.75E-05	2.00E-05	1.87E-05
236	2.00E-05	1.75E-05	2.00E-05	1.87E-05
237	2.00E-05	1.75E-05	2.00E-05	1.87E-05
238	2.00E-05	1.75E-05	2.00E-05	1.87E-05
239	2.00E-05	1.75E-05	2.00E-05	1.87E-05
240	2.00E-05	1.75E-05	2.00E-05	1.87E-05
241	2.00E-05	1.75E-05	2.00E-05	1.87E-05
242	2.00E-05	1.75E-05	2.00E-05	1.87E-05
243	2.00E-05	1.74E-05	2.00E-05	1.87E-05
244	2.00E-05	1.75E-05	2.00E-05	1.87E-05
245	2.00E-05	1.74E-05	2.00E-05	1.87E-05
246	2.00E-05	1.74E-05	2.00E-05	1.87E-05
247	2.00E-05	1.74E-05	2.00E-05	1.87E-05
248	2.00E-05	1.74E-05	2.00E-05	1.87E-05
249	2.00E-05	1.74E-05	2.00E-05	1.87E-05
250	2.00E-05	1.74E-05	2.00E-05	1.87E-05
251	2.00E-05	1.74E-05	2.00E-05	1.87E-05
252	2.00E-05	1.74E-05	2.00E-05	1.87E-05
253	2.00E-05	1.74E-05	2.00E-05	1.87E-05
254	2.00E-05	1.74E-05	2.00E-05	1.87E-05
255	2.00E-05	1.74E-05	2.00E-05	1.87E-05
256	2.00E-05	1.74E-05	2.00E-05	1.87E-05

257	2.00E-05	1.74E-05	2.00E-05	1.87E-05
258	2.00E-05	1.74E-05	2.00E-05	1.87E-05
259	2.00E-05	1.74E-05	2.00E-05	1.87E-05
260	2.00E-05	1.74E-05	2.00E-05	1.87E-05
261	2.00E-05	1.74E-05	2.00E-05	1.87E-05
262	2.00E-05	1.74E-05	2.00E-05	1.87E-05
263	2.00E-05	1.74E-05	2.00E-05	1.87E-05
264	2.00E-05	1.74E-05	2.00E-05	1.87E-05
265	2.00E-05	1.74E-05	2.00E-05	1.87E-05
266	2.00E-05	1.74E-05	2.00E-05	1.87E-05
267	2.00E-05	1.74E-05	2.00E-05	1.87E-05
268	2.00E-05	1.74E-05	2.00E-05	1.87E-05
269	2.00E-05	1.74E-05	2.00E-05	1.87E-05
270	2.00E-05	1.74E-05	2.00E-05	1.87E-05
271	2.00E-05	1.74E-05	2.00E-05	1.87E-05
272	2.00E-05	1.74E-05	2.00E-05	1.87E-05
273	2.00E-05	1.74E-05	2.00E-05	1.87E-05
274	1.99E-05	1.74E-05	2.00E-05	1.87E-05
275	2.00E-05	1.74E-05	2.00E-05	1.87E-05
276	2.00E-05	1.74E-05	2.00E-05	1.87E-05
277	2.00E-05	1.74E-05	2.00E-05	1.87E-05
278	2.00E-05	1.74E-05	2.00E-05	1.87E-05
279	2.00E-05	1.74E-05	2.00E-05	1.87E-05
280	2.00E-05	1.74E-05	2.00E-05	1.87E-05
281	2.00E-05	1.74E-05	2.00E-05	1.87E-05
282	2.00E-05	1.74E-05	2.00E-05	1.87E-05
283	2.00E-05	1.74E-05	2.00E-05	1.86E-05
284	2.00E-05	1.74E-05	2.00E-05	1.87E-05
285	1.99E-05	1.74E-05	2.00E-05	1.87E-05
286	1.99E-05	1.74E-05	2.00E-05	1.86E-05
287	1.99E-05	1.73E-05	2.00E-05	1.86E-05
288	2.00E-05	1.73E-05	2.00E-05	1.86E-05
289	2.00E-05	1.74E-05	2.00E-05	1.87E-05
290	1.99E-05	1.73E-05	2.00E-05	1.86E-05
291	1.99E-05	1.73E-05	2.00E-05	1.87E-05
292	1.99E-05	1.73E-05	2.00E-05	1.86E-05
293	1.99E-05	1.73E-05	2.00E-05	1.86E-05
294	1.99E-05	1.73E-05	2.00E-05	1.86E-05
295	1.99E-05	1.73E-05	2.00E-05	1.86E-05
296	1.99E-05	1.73E-05	2.00E-05	1.86E-05
297	1.99E-05	1.73E-05	2.00E-05	1.86E-05
298	1.99E-05	1.73E-05	1.99E-05	1.86E-05
299	1.99E-05	1.73E-05	1.99E-05	1.86E-05

Table B2: Average CO_2 concentration of five-hour Tablelands experiments with Mg-rich water.

Time (min)	MgOH	MgOH + TCR	MgOH + TWR
0	1.74E-05	1.75E-05	1.81E-05
1	1.74E-05	1.75E-05	1.80E-05
2	1.74E-05	1.75E-05	1.80E-05
3	1.74E-05	1.74E-05	1.79E-05
4	1.73E-05	1.74E-05	1.79E-05
5	1.73E-05	1.74E-05	1.80E-05
6	1.73E-05	1.73E-05	1.79E-05
7	1.73E-05	1.73E-05	1.79E-05
8	1.72E-05	1.73E-05	1.78E-05
9	1.72E-05	1.73E-05	1.78E-05
10	1.71E-05	1.72E-05	1.78E-05
11	1.71E-05	1.72E-05	1.77E-05
12	1.71E-05	1.72E-05	1.77E-05
13	1.71E-05	1.72E-05	1.76E-05
14	1.70E-05	1.71E-05	1.76E-05
15	1.70E-05	1.71E-05	1.76E-05
16	1.70E-05	1.71E-05	1.75E-05
17	1.69E-05	1.71E-05	1.75E-05
18	1.69E-05	1.70E-05	1.75E-05
19	1.69E-05	1.70E-05	1.74E-05
20	1.69E-05	1.70E-05	1.74E-05
21	1.68E-05	1.70E-05	1.74E-05
22	1.68E-05	1.69E-05	1.73E-05
23	1.68E-05	1.69E-05	1.73E-05
24	1.67E-05	1.69E-05	1.73E-05
25	1.67E-05	1.69E-05	1.72E-05
26	1.67E-05	1.69E-05	1.72E-05
27	1.67E-05	1.69E-05	1.71E-05
28	1.66E-05	1.68E-05	1.71E-05
29	1.66E-05	1.68E-05	1.71E-05
30	1.66E-05	1.68E-05	1.70E-05
31	1.65E-05	1.68E-05	1.70E-05
32	1.65E-05	1.68E-05	1.70E-05
33	1.65E-05	1.67E-05	1.69E-05
34	1.65E-05	1.67E-05	1.69E-05
35	1.64E-05	1.67E-05	1.68E-05
36	1.64E-05	1.67E-05	1.68E-05
37	1.64E-05	1.67E-05	1.68E-05
38	1.64E-05	1.66E-05	1.67E-05

39	1.63E-05	1.66E-05	1.67E-05
40	1.63E-05	1.66E-05	1.67E-05
41	1.63E-05	1.66E-05	1.66E-05
42	1.62E-05	1.66E-05	1.66E-05
43	1.62E-05	1.66E-05	1.65E-05
44	1.62E-05	1.66E-05	1.65E-05
45	1.62E-05	1.65E-05	1.65E-05
46	1.61E-05	1.65E-05	1.64E-05
47	1.61E-05	1.65E-05	1.64E-05
48	1.61E-05	1.65E-05	1.63E-05
49	1.60E-05	1.65E-05	1.63E-05
50	1.60E-05	1.65E-05	1.63E-05
51	1.60E-05	1.64E-05	1.62E-05
52	1.60E-05	1.64E-05	1.62E-05
53	1.59E-05	1.64E-05	1.61E-05
54	1.59E-05	1.64E-05	1.61E-05
55	1.59E-05	1.64E-05	1.61E-05
56	1.59E-05	1.64E-05	1.60E-05
57	1.58E-05	1.63E-05	1.60E-05
58	1.58E-05	1.63E-05	1.59E-05
59	1.58E-05	1.63E-05	1.59E-05
60	1.57E-05	1.63E-05	1.59E-05
61	1.57E-05	1.63E-05	1.58E-05
62	1.57E-05	1.63E-05	1.58E-05
63	1.57E-05	1.62E-05	1.57E-05
64	1.56E-05	1.62E-05	1.57E-05
65	1.56E-05	1.62E-05	1.57E-05
66	1.56E-05	1.62E-05	1.56E-05
67	1.55E-05	1.62E-05	1.56E-05
68	1.55E-05	1.62E-05	1.55E-05
69	1.55E-05	1.62E-05	1.55E-05
70	1.55E-05	1.61E-05	1.54E-05
71	1.54E-05	1.61E-05	1.54E-05
72	1.54E-05	1.61E-05	1.54E-05
73	1.54E-05	1.61E-05	1.53E-05
74	1.53E-05	1.61E-05	1.53E-05
75	1.53E-05	1.61E-05	1.52E-05
76	1.53E-05	1.60E-05	1.52E-05
77	1.53E-05	1.60E-05	1.52E-05
78	1.52E-05	1.60E-05	1.51E-05
79	1.52E-05	1.60E-05	1.51E-05
80	1.52E-05	1.60E-05	1.50E-05
81	1.51E-05	1.60E-05	1.50E-05
82	1.51E-05	1.60E-05	1.50E-05

83	1.51E-05	1.59E-05	1.49E-05
84	1.51E-05	1.59E-05	1.49E-05
85	1.50E-05	1.59E-05	1.49E-05
86	1.50E-05	1.59E-05	1.48E-05
87	1.50E-05	1.59E-05	1.48E-05
88	1.49E-05	1.59E-05	1.47E-05
89	1.49E-05	1.58E-05	1.47E-05
90	1.49E-05	1.58E-05	1.46E-05
91	1.48E-05	1.58E-05	1.46E-05
92	1.48E-05	1.58E-05	1.46E-05
93	1.48E-05	1.58E-05	1.45E-05
94	1.48E-05	1.58E-05	1.45E-05
95	1.47E-05	1.58E-05	1.45E-05
96	1.47E-05	1.57E-05	1.44E-05
97	1.47E-05	1.57E-05	1.44E-05
98	1.46E-05	1.57E-05	1.43E-05
99	1.46E-05	1.57E-05	1.43E-05
100	1.46E-05	1.57E-05	1.43E-05
101	1.46E-05	1.57E-05	1.42E-05
102	1.45E-05	1.57E-05	1.42E-05
103	1.45E-05	1.56E-05	1.41E-05
104	1.45E-05	1.56E-05	1.41E-05
105	1.44E-05	1.56E-05	1.41E-05
106	1.44E-05	1.56E-05	1.40E-05
107	1.44E-05	1.56E-05	1.40E-05
108	1.43E-05	1.56E-05	1.40E-05
109	1.43E-05	1.55E-05	1.39E-05
110	1.43E-05	1.55E-05	1.39E-05
111	1.43E-05	1.55E-05	1.38E-05
112	1.42E-05	1.55E-05	1.38E-05
113	1.42E-05	1.55E-05	1.38E-05
114	1.42E-05	1.55E-05	1.37E-05
115	1.41E-05	1.55E-05	1.37E-05
116	1.41E-05	1.54E-05	1.37E-05
117	1.41E-05	1.54E-05	1.36E-05
118	1.41E-05	1.54E-05	1.36E-05
119	1.40E-05	1.54E-05	1.35E-05
120	1.40E-05	1.54E-05	1.35E-05
121	1.40E-05	1.54E-05	1.35E-05
122	1.39E-05	1.53E-05	1.34E-05
123	1.39E-05	1.53E-05	1.34E-05
124	1.39E-05	1.53E-05	1.33E-05
125	1.39E-05	1.53E-05	1.33E-05
126	1.38E-05	1.53E-05	1.33E-05

127	1.38E-05	1.53E-05	1.32E-05
128	1.38E-05	1.53E-05	1.32E-05
129	1.37E-05	1.52E-05	1.32E-05
130	1.37E-05	1.52E-05	1.31E-05
131	1.37E-05	1.52E-05	1.31E-05
132	1.37E-05	1.52E-05	1.31E-05
133	1.36E-05	1.52E-05	1.30E-05
134	1.36E-05	1.52E-05	1.30E-05
135	1.36E-05	1.52E-05	1.29E-05
136	1.35E-05	1.51E-05	1.29E-05
137	1.35E-05	1.51E-05	1.29E-05
138	1.35E-05	1.51E-05	1.28E-05
139	1.35E-05	1.51E-05	1.28E-05
140	1.34E-05	1.51E-05	1.28E-05
141	1.34E-05	1.51E-05	1.27E-05
142	1.34E-05	1.50E-05	1.27E-05
143	1.33E-05	1.50E-05	1.27E-05
144	1.33E-05	1.50E-05	1.26E-05
145	1.33E-05	1.50E-05	1.26E-05
146	1.33E-05	1.50E-05	1.26E-05
147	1.32E-05	1.50E-05	1.25E-05
148	1.32E-05	1.49E-05	1.25E-05
149	1.32E-05	1.49E-05	1.24E-05
150	1.32E-05	1.49E-05	1.24E-05
151	1.31E-05	1.49E-05	1.24E-05
152	1.31E-05	1.49E-05	1.23E-05
153	1.31E-05	1.49E-05	1.23E-05
154	1.30E-05	1.49E-05	1.23E-05
155	1.30E-05	1.48E-05	1.22E-05
156	1.30E-05	1.48E-05	1.22E-05
157	1.30E-05	1.48E-05	1.22E-05
158	1.29E-05	1.48E-05	1.21E-05
159	1.29E-05	1.48E-05	1.21E-05
160	1.29E-05	1.48E-05	1.21E-05
161	1.29E-05	1.47E-05	1.20E-05
162	1.28E-05	1.47E-05	1.20E-05
163	1.28E-05	1.47E-05	1.20E-05
164	1.28E-05	1.47E-05	1.19E-05
165	1.27E-05	1.47E-05	1.19E-05
166	1.27E-05	1.47E-05	1.19E-05
167	1.27E-05	1.46E-05	1.18E-05
168	1.27E-05	1.46E-05	1.18E-05
169	1.26E-05	1.46E-05	1.18E-05
170	1.26E-05	1.46E-05	1.17E-05

171	1.26E-05	1.46E-05	1.17E-05
172	1.26E-05	1.46E-05	1.17E-05
173	1.25E-05	1.46E-05	1.16E-05
174	1.25E-05	1.45E-05	1.16E-05
175	1.25E-05	1.45E-05	1.16E-05
176	1.25E-05	1.45E-05	1.15E-05
177	1.24E-05	1.45E-05	1.15E-05
178	1.24E-05	1.45E-05	1.15E-05
179	1.24E-05	1.45E-05	1.14E-05
180	1.24E-05	1.44E-05	1.14E-05
181	1.23E-05	1.44E-05	1.14E-05
182	1.23E-05	1.44E-05	1.13E-05
183	1.23E-05	1.44E-05	1.13E-05
184	1.23E-05	1.44E-05	1.13E-05
185	1.22E-05	1.44E-05	1.12E-05
186	1.22E-05	1.43E-05	1.12E-05
187	1.22E-05	1.43E-05	1.12E-05
188	1.22E-05	1.43E-05	1.11E-05
189	1.21E-05	1.43E-05	1.11E-05
190	1.21E-05	1.43E-05	1.11E-05
191	1.21E-05	1.43E-05	1.11E-05
192	1.21E-05	1.43E-05	1.10E-05
193	1.20E-05	1.42E-05	1.10E-05
194	1.20E-05	1.42E-05	1.10E-05
195	1.20E-05	1.42E-05	1.09E-05
196	1.20E-05	1.42E-05	1.09E-05
197	1.19E-05	1.42E-05	1.09E-05
198	1.19E-05	1.42E-05	1.08E-05
199	1.19E-05	1.42E-05	1.08E-05
200	1.19E-05	1.41E-05	1.08E-05
201	1.18E-05	1.41E-05	1.07E-05
202	1.18E-05	1.41E-05	1.07E-05
203	1.18E-05	1.41E-05	1.07E-05
204	1.18E-05	1.41E-05	1.07E-05
205	1.17E-05	1.41E-05	1.06E-05
206	1.17E-05	1.40E-05	1.06E-05
207	1.17E-05	1.40E-05	1.06E-05
208	1.17E-05	1.40E-05	1.05E-05
209	1.16E-05	1.40E-05	1.05E-05
210	1.16E-05	1.40E-05	1.05E-05
211	1.16E-05	1.40E-05	1.05E-05
212	1.16E-05	1.40E-05	1.04E-05
213	1.16E-05	1.39E-05	1.04E-05
214	1.15E-05	1.39E-05	1.04E-05

215	1.15E-05	1.39E-05	1.03E-05
216	1.15E-05	1.39E-05	1.03E-05
217	1.15E-05	1.39E-05	1.03E-05
218	1.14E-05	1.39E-05	1.03E-05
219	1.14E-05	1.38E-05	1.02E-05
220	1.14E-05	1.38E-05	1.02E-05
221	1.14E-05	1.38E-05	1.02E-05
222	1.13E-05	1.38E-05	1.01E-05
223	1.13E-05	1.38E-05	1.01E-05
224	1.13E-05	1.38E-05	1.01E-05
225	1.13E-05	1.38E-05	1.01E-05
226	1.13E-05	1.38E-05	1.00E-05
227	1.12E-05	1.37E-05	1.00E-05
228	1.12E-05	1.37E-05	9.98E-06
229	1.12E-05	1.37E-05	9.95E-06
230	1.12E-05	1.37E-05	9.92E-06
231	1.11E-05	1.37E-05	9.89E-06
232	1.11E-05	1.37E-05	9.87E-06
233	1.11E-05	1.37E-05	9.83E-06
234	1.11E-05	1.36E-05	9.81E-06
235	1.10E-05	1.36E-05	9.79E-06
236	1.10E-05	1.36E-05	9.75E-06
237	1.10E-05	1.36E-05	9.73E-06
238	1.10E-05	1.36E-05	9.70E-06
239	1.09E-05	1.36E-05	9.67E-06
240	1.09E-05	1.36E-05	9.65E-06
241	1.09E-05	1.36E-05	9.62E-06
242	1.09E-05	1.35E-05	9.60E-06
243	1.09E-05	1.35E-05	9.56E-06
244	1.08E-05	1.35E-05	9.54E-06
245	1.08E-05	1.35E-05	9.52E-06
246	1.08E-05	1.35E-05	9.49E-06
247	1.08E-05	1.35E-05	9.47E-06
248	1.07E-05	1.35E-05	9.44E-06
249	1.07E-05	1.35E-05	9.41E-06
250	1.07E-05	1.34E-05	9.39E-06
251	1.06E-05	1.34E-05	9.36E-06
252	1.06E-05	1.34E-05	9.34E-06
253	1.06E-05	1.34E-05	9.30E-06
254	1.06E-05	1.34E-05	9.29E-06
255	1.06E-05	1.34E-05	9.26E-06
256	1.05E-05	1.34E-05	9.23E-06
257	1.05E-05	1.34E-05	9.20E-06
258	1.05E-05	1.34E-05	9.18E-06

259	1.05E-05	1.33E-05	9.16E-06
260	1.04E-05	1.33E-05	9.14E-06
261	1.04E-05	1.33E-05	9.11E-06
262	1.04E-05	1.33E-05	9.08E-06
263	1.04E-05	1.33E-05	9.06E-06
264	1.03E-05	1.33E-05	9.03E-06
265	1.03E-05	1.33E-05	9.01E-06
266	1.03E-05	1.33E-05	8.99E-06
267	1.03E-05	1.33E-05	8.96E-06
268	1.03E-05	1.32E-05	8.93E-06
269	1.02E-05	1.32E-05	8.91E-06
270	1.02E-05	1.32E-05	8.89E-06
271	1.02E-05	1.32E-05	8.86E-06
272	1.02E-05	1.32E-05	8.84E-06
273	1.01E-05	1.32E-05	8.81E-06
274	1.01E-05	1.32E-05	8.79E-06
275	1.01E-05	1.32E-05	8.76E-06
276	1.01E-05	1.32E-05	8.74E-06
277	1.00E-05	1.32E-05	8.72E-06
278	1.00E-05	1.31E-05	8.69E-06
279	1.00E-05	1.31E-05	8.67E-06
280	9.98E-06	1.31E-05	8.65E-06
281	9.96E-06	1.31E-05	8.62E-06
282	9.94E-06	1.31E-05	8.60E-06
283	9.91E-06	1.31E-05	8.58E-06
284	9.89E-06	1.31E-05	8.55E-06
285	9.87E-06	1.31E-05	8.53E-06
286	9.84E-06	1.30E-05	8.51E-06
287	9.83E-06	1.30E-05	8.49E-06
288	9.81E-06	1.30E-05	8.46E-06
289	9.78E-06	1.30E-05	8.45E-06
290	9.76E-06	1.30E-05	8.41E-06
291	9.73E-06	1.30E-05	8.39E-06
292	9.71E-06	1.30E-05	8.38E-06
293	9.70E-06	1.30E-05	8.35E-06
294	9.66E-06	1.30E-05	8.33E-06
295	9.65E-06	1.30E-05	8.31E-06
296	9.62E-06	1.29E-05	8.29E-06
297	9.60E-06	1.29E-05	8.26E-06
298	9.58E-06	1.29E-05	8.24E-06
299	9.56E-06	1.29E-05	8.22E-06

Table B3: Average CO_2 concentration of five-hour Tablelands experiments with Ca-rich water.

Time (min)	CaOHhigh	CaOHhigh + TCR	CaOHhigh + TWR
0	1.87E-05	1.89E-05	1.80E-05
1	1.77E-05	1.81E-05	1.69E-05
2	1.67E-05	1.74E-05	1.59E-05
3	1.59E-05	1.67E-05	1.50E-05
4	1.50E-05	1.61E-05	1.42E-05
5	1.43E-05	1.55E-05	1.34E-05
6	1.35E-05	1.49E-05	1.26E-05
7	1.28E-05	1.44E-05	1.19E-05
8	1.22E-05	1.39E-05	1.13E-05
9	1.16E-05	1.34E-05	1.07E-05
10	1.10E-05	1.29E-05	1.01E-05
11	1.05E-05	1.24E-05	9.61E-06
12	9.97E-06	1.20E-05	9.11E-06
13	9.47E-06	1.16E-05	8.65E-06
14	9.02E-06	1.12E-05	8.20E-06
15	8.58E-06	1.08E-05	7.80E-06
16	8.17E-06	1.05E-05	7.42E-06
17	7.78E-06	1.01E-05	7.05E-06
18	7.42E-06	9.80E-06	6.71E-06
19	7.07E-06	9.48E-06	6.38E-06
20	6.73E-06	9.17E-06	6.07E-06
21	6.42E-06	8.88E-06	5.78E-06
22	6.12E-06	8.59E-06	5.50E-06
23	5.85E-06	8.31E-06	5.24E-06
24	5.57E-06	8.05E-06	4.99E-06
25	5.32E-06	7.79E-06	4.76E-06
26	5.08E-06	7.53E-06	4.53E-06
27	4.85E-06	7.30E-06	4.33E-06
28	4.62E-06	7.07E-06	4.13E-06
29	4.42E-06	6.85E-06	3.93E-06
30	4.22E-06	6.64E-06	3.75E-06
31	4.02E-06	6.43E-06	3.58E-06
32	3.85E-06	6.23E-06	3.42E-06
33	3.67E-06	6.04E-06	3.26E-06
34	3.51E-06	5.85E-06	3.12E-06
35	3.35E-06	5.67E-06	2.97E-06
36	3.20E-06	5.50E-06	2.84E-06
37	3.06E-06	5.32E-06	2.70E-06
38	2.92E-06	5.16E-06	2.59E-06
39	2.79E-06	5.00E-06	2.46E-06

40	2.67E-06	4.84E-06	2.35E-06
41	2.54E-06	4.70E-06	2.25E-06
42	2.44E-06	4.56E-06	2.16E-06
43	2.33E-06	4.42E-06	2.05E-06
44	2.22E-06	4.29E-06	1.96E-06
45	2.12E-06	4.15E-06	1.88E-06
46	2.03E-06	4.03E-06	1.79E-06
47	1.94E-06	3.90E-06	1.71E-06
48	1.85E-06	3.79E-06	1.64E-06
49	1.78E-06	3.67E-06	1.57E-06
50	1.70E-06	3.56E-06	1.50E-06
51	1.62E-06	3.45E-06	1.43E-06
52	1.55E-06	3.35E-06	1.37E-06
53	1.48E-06	3.25E-06	1.31E-06
54	1.42E-06	3.16E-06	1.25E-06
55	1.35E-06	3.06E-06	1.19E-06
56	1.29E-06	2.97E-06	1.14E-06
57	1.23E-06	2.88E-06	1.09E-06
58	1.18E-06	2.80E-06	1.05E-06
59	1.13E-06	2.71E-06	9.99E-07
60	1.08E-06	2.63E-06	9.58E-07
61	1.03E-06	2.56E-06	9.14E-07
62	9.93E-07	2.48E-06	8.77E-07
63	9.41E-07	2.40E-06	8.36E-07
64	9.09E-07	2.33E-06	7.99E-07
65	8.64E-07	2.26E-06	7.69E-07
66	8.29E-07	2.19E-06	7.35E-07
67	7.91E-07	2.13E-06	7.01E-07
68	7.55E-07	2.07E-06	6.70E-07
69	7.25E-07	2.01E-06	6.45E-07
70	6.94E-07	1.95E-06	6.18E-07
71	6.61E-07	1.90E-06	5.90E-07
72	6.33E-07	1.84E-06	5.65E-07
73	6.08E-07	1.78E-06	5.45E-07
74	5.79E-07	1.73E-06	5.17E-07
75	5.56E-07	1.68E-06	4.94E-07
76	5.28E-07	1.63E-06	4.71E-07
77	5.01E-07	1.59E-06	4.53E-07
78	4.85E-07	1.54E-06	4.36E-07
79	4.67E-07	1.50E-06	4.14E-07
80	4.45E-07	1.46E-06	3.98E-07
81	4.20E-07	1.41E-06	3.81E-07
82	4.06E-07	1.38E-06	3.66E-07
83	3.89E-07	1.33E-06	3.51E-07

84	3.70E-07	1.29E-06	3.37E-07
85	3.57E-07	1.26E-06	3.26E-07
86	3.37E-07	1.22E-06	3.11E-07
87	3.30E-07	1.19E-06	2.94E-07
88	3.15E-07	1.16E-06	2.87E-07
89	2.99E-07	1.12E-06	2.74E-07
90	2.91E-07	1.10E-06	2.62E-07
91	2.73E-07	1.06E-06	2.53E-07
92	2.61E-07	1.04E-06	2.40E-07
93	2.50E-07	1.01E-06	2.31E-07
94	2.41E-07	9.76E-07	2.24E-07
95	2.33E-07	9.52E-07	2.11E-07
96	2.20E-07	9.23E-07	2.03E-07
97	2.15E-07	9.04E-07	1.96E-07
98	2.06E-07	8.82E-07	1.85E-07
99	1.97E-07	8.55E-07	1.82E-07
100	1.85E-07	8.31E-07	1.75E-07
101	1.83E-07	8.06E-07	1.67E-07
102	1.72E-07	7.90E-07	1.57E-07
103	1.68E-07	7.74E-07	1.54E-07
104	1.63E-07	7.41E-07	1.44E-07
105	1.50E-07	7.25E-07	1.38E-07
106	1.44E-07	7.08E-07	1.36E-07
107	1.42E-07	6.89E-07	1.31E-07
108	1.37E-07	6.72E-07	1.25E-07
109	1.34E-07	6.54E-07	1.21E-07
110	1.29E-07	6.37E-07	1.18E-07
111	1.22E-07	6.22E-07	1.12E-07
112	1.15E-07	6.10E-07	1.07E-07
113	1.11E-07	5.92E-07	9.90E-08
114	1.06E-07	5.82E-07	9.39E-08
115	1.01E-07	5.62E-07	9.48E-08
116	9.99E-08	5.51E-07	8.68E-08
117	9.70E-08	5.36E-07	8.85E-08
118	8.85E-08	5.22E-07	8.76E-08
119	9.08E-08	5.11E-07	8.12E-08
120	8.90E-08	4.98E-07	7.41E-08
121	8.31E-08	4.90E-07	7.70E-08
122	7.83E-08	4.77E-07	7.66E-08
123	7.47E-08	4.71E-07	7.51E-08
124	7.15E-08	4.55E-07	6.98E-08
125	7.04E-08	4.47E-07	6.47E-08
126	7.20E-08	4.37E-07	6.40E-08
127	6.56E-08	4.30E-07	6.28E-08

128	6.29E-08	4.18E-07	6.02E-08
129	6.24E-08	4.09E-07	5.82E-08
130	5.67E-08	4.00E-07	5.53E-08
131	6.06E-08	3.94E-07	5.34E-08
132	5.45E-08	3.82E-07	5.49E-08
133	5.41E-08	3.74E-07	5.36E-08
134	5.59E-08	3.69E-07	4.62E-08
135	4.44E-08	3.63E-07	4.90E-08
136	4.80E-08	3.56E-07	4.51E-08
137	4.25E-08	3.44E-07	4.44E-08
138	4.83E-08	3.38E-07	4.36E-08
139	4.71E-08	3.29E-07	4.33E-08
140	4.33E-08	3.25E-07	4.35E-08
141	4.15E-08	3.15E-07	4.53E-08
142	4.02E-08	3.12E-07	3.71E-08
143	4.11E-08	3.13E-07	3.66E-08
144	3.89E-08	2.98E-07	4.24E-08
145	4.32E-08	2.97E-07	3.86E-08
146	2.88E-08	2.87E-07	3.67E-08
147	3.15E-08	2.87E-07	3.44E-08
148	3.41E-08	2.82E-07	3.34E-08
149	2.87E-08	2.82E-07	3.49E-08
150	3.66E-08	2.73E-07	2.82E-08
151	3.04E-08	2.68E-07	3.15E-08
152	3.35E-08	2.60E-07	3.26E-08
153	3.08E-08	2.59E-07	3.78E-08
154	2.83E-08	2.55E-07	3.00E-08
155	2.80E-08	2.54E-07	3.01E-08
156	2.59E-08	2.48E-07	2.80E-08
157	2.65E-08	2.47E-07	2.79E-08
158	2.43E-08	2.41E-07	2.90E-08
159	2.68E-08	2.36E-07	3.13E-08
160	2.68E-08	2.36E-07	2.66E-08
161	2.53E-08	2.28E-07	2.79E-08
162	2.58E-08	2.22E-07	2.54E-08
163	2.50E-08	2.21E-07	2.64E-08
164	2.26E-08	2.17E-07	2.69E-08
165	1.93E-08	2.19E-07	2.77E-08
166	2.32E-08	2.17E-07	2.26E-08
167	2.19E-08	2.07E-07	2.55E-08
168	2.31E-08	2.11E-07	1.90E-08
169	2.21E-08	2.07E-07	2.39E-08
170	2.32E-08	2.03E-07	2.19E-08
171	1.63E-08	2.00E-07	1.78E-08

172	2.07E-08	1.98E-07	2.61E-08
173	1.41E-08	1.99E-07	1.88E-08
174	1.85E-08	1.97E-07	2.48E-08
175	1.78E-08	1.93E-07	1.53E-08
176	1.81E-08	1.95E-07	1.79E-08
177	1.67E-08	1.88E-07	2.07E-08
178	2.00E-08	1.87E-07	2.00E-08
179	1.64E-08	1.85E-07	1.24E-08
180	1.48E-08	1.85E-07	1.95E-08
181	1.46E-08	1.82E-07	2.00E-08
182	1.53E-08	1.81E-07	1.81E-08
183	2.08E-08	1.79E-07	2.00E-08
184	2.08E-08	1.78E-07	1.88E-08
185	1.82E-08	1.79E-07	1.63E-08
186	1.27E-08	1.80E-07	1.95E-08
187	2.10E-08	1.72E-07	1.89E-08
188	1.37E-08	1.70E-07	1.85E-08
189	1.23E-08	1.71E-07	1.38E-08
190	1.46E-08	1.73E-07	1.73E-08
191	1.63E-08	1.64E-07	1.64E-08
192	1.57E-08	1.70E-07	1.63E-08
193	1.19E-08	1.70E-07	1.74E-08
194	1.34E-08	1.67E-07	1.67E-08
195	1.68E-08	1.67E-07	1.81E-08
196	1.37E-08	1.63E-07	1.66E-08
197	1.41E-08	1.63E-07	1.81E-08
198	1.39E-08	1.60E-07	1.63E-08
199	1.16E-08	1.60E-07	1.45E-08
200	1.35E-08	1.56E-07	1.74E-08
201	1.46E-08	1.50E-07	1.68E-08
202	1.60E-08	1.53E-07	1.84E-08
203	1.64E-08	1.57E-07	1.79E-08
204	1.73E-08	1.57E-07	1.77E-08
205	1.33E-08	1.52E-07	1.52E-08
206	1.46E-08	1.56E-07	1.41E-08
207	1.52E-08	1.52E-07	1.75E-08
208	1.28E-08	1.48E-07	1.19E-08
209	1.35E-08	1.52E-07	1.13E-08
210	1.33E-08	1.53E-07	1.77E-08
211	1.78E-08	1.46E-07	1.42E-08
212	1.42E-08	1.49E-07	1.24E-08
213	1.57E-08	1.53E-07	1.33E-08
214	1.21E-08	1.47E-07	1.33E-08
215	1.59E-08	1.47E-07	1.28E-08

216	1.27E-08	1.48E-07	1.30E-08
217	1.79E-08	1.43E-07	1.50E-08
218	1.66E-08	1.49E-07	1.35E-08
219	1.74E-08	1.44E-07	1.37E-08
220	1.44E-08	1.43E-07	1.15E-08
221	1.75E-08	1.41E-07	2.15E-08
222	1.88E-08	1.43E-07	1.27E-08
223	1.37E-08	1.38E-07	1.26E-08
224	1.55E-08	1.42E-07	1.63E-08
225	1.44E-08	1.39E-07	1.19E-08
226	1.41E-08	1.45E-07	1.19E-08
227	1.06E-08	1.42E-07	1.55E-08
228	1.45E-08	1.38E-07	1.23E-08
229	1.35E-08	1.36E-07	1.46E-08
230	1.41E-08	1.42E-07	1.20E-08
231	1.56E-08	1.39E-07	1.39E-08
232	1.04E-08	1.43E-07	1.26E-08
233	2.02E-08	1.37E-07	1.53E-08
234	1.75E-08	1.38E-07	1.21E-08
235	1.31E-08	1.34E-07	1.12E-08
236	1.34E-08	1.36E-07	1.09E-08
237	1.56E-08	1.38E-07	1.37E-08
238	1.50E-08	1.32E-07	1.64E-08
239	1.16E-08	1.35E-07	1.50E-08
240	1.42E-08	1.36E-07	1.27E-08
241	1.52E-08	1.37E-07	1.19E-08
242	1.42E-08	1.37E-07	1.44E-08
243	1.21E-08	1.35E-07	1.17E-08
244	1.45E-08	1.36E-07	1.95E-08
245	1.60E-08	1.36E-07	1.70E-08
246	1.38E-08	1.29E-07	1.30E-08
247	1.33E-08	1.36E-07	8.42E-09
248	1.85E-08	1.36E-07	1.15E-08
249	1.30E-08	1.37E-07	1.39E-08
250	1.04E-08	1.42E-07	9.66E-09
251	1.42E-08	1.35E-07	1.66E-08
252	1.37E-08	1.36E-07	1.56E-08
253	1.82E-08	1.37E-07	1.12E-08
254	1.31E-08	1.31E-07	1.37E-08
255	1.16E-08	1.29E-07	1.52E-08
256	1.74E-08	1.32E-07	1.59E-08
257	1.81E-08	1.36E-07	1.45E-08
258	1.38E-08	1.33E-07	1.79E-08
259	1.74E-08	1.34E-07	1.49E-08

260	1.44E-08	1.29E-07	1.79E-08
261	1.50E-08	1.37E-07	1.17E-08
262	1.59E-08	1.31E-07	1.66E-08
263	1.21E-08	1.31E-07	1.45E-08
264	1.68E-08	1.36E-07	1.44E-08
265	1.56E-08	1.34E-07	1.41E-08
266	1.85E-08	1.33E-07	1.74E-08
267	1.50E-08	1.31E-07	1.70E-08
268	1.39E-08	1.33E-07	1.52E-08
269	1.19E-08	1.32E-07	1.78E-08
270	1.96E-08	1.27E-07	1.68E-08
271	1.39E-08	1.29E-07	1.42E-08
272	8.97E-09	1.32E-07	1.77E-08
273	1.13E-08	1.29E-07	1.64E-08
274	1.67E-08	1.30E-07	1.44E-08
275	1.45E-08	1.33E-07	1.55E-08
276	1.27E-08	1.33E-07	1.46E-08
277	1.49E-08	1.31E-07	1.95E-08
278	1.81E-08	1.33E-07	1.53E-08
279	1.63E-08	1.29E-07	1.50E-08
280	1.30E-08	1.29E-07	1.39E-08
281	1.46E-08	1.31E-07	1.35E-08
282	1.53E-08	1.35E-07	1.67E-08
283	1.73E-08	1.31E-07	1.82E-08
284	1.09E-08	1.29E-07	1.85E-08
285	1.71E-08	1.30E-07	1.44E-08
286	1.17E-08	1.31E-07	1.48E-08
287	1.56E-08	1.31E-07	1.86E-08
288	1.41E-08	1.29E-07	1.85E-08
289	1.92E-08	1.32E-07	1.75E-08
290	1.60E-08	1.26E-07	1.89E-08
291	2.11E-08	1.34E-07	1.45E-08
292	1.85E-08	1.32E-07	2.24E-08
293	2.03E-08	1.32E-07	1.92E-08
294	2.53E-08	1.30E-07	1.63E-08
295	1.88E-08	1.29E-07	1.61E-08
296	1.89E-08	1.28E-07	2.07E-08
297	1.89E-08	1.30E-07	1.42E-08
298	2.50E-08	1.33E-07	1.70E-08
299	2.19E-08	1.35E-07	1.60E-08

Table B4: Average CO_2 concentration of five-hour Tablelands experiments with elevated CO_2 concentration and DI water.

Time (min)	$NaHCO_3$	$NaHCO_3$ + TCR	$NaHCO_3$ + TWR
0	1.81E-05	1.84E-05	1.79E-05
1	1.84E-05	1.86E-05	1.83E-05
2	1.86E-05	1.89E-05	1.86E-05
3	1.89E-05	1.91E-05	1.89E-05
4	1.91E-05	1.92E-05	1.91E-05
5	1.93E-05	1.94E-05	1.94E-05
6	1.95E-05	1.96E-05	1.96E-05
7	1.97E-05	1.98E-05	1.98E-05
8	1.99E-05	1.99E-05	2.01E-05
9	2.00E-05	2.01E-05	2.03E-05
10	2.02E-05	2.03E-05	2.05E-05
11	2.04E-05	2.04E-05	2.07E-05
12	2.06E-05	2.05E-05	2.09E-05
13	2.07E-05	2.07E-05	2.11E-05
14	2.09E-05	2.08E-05	2.13E-05
15	2.10E-05	2.10E-05	2.15E-05
16	2.12E-05	2.11E-05	2.16E-05
17	2.14E-05	2.12E-05	2.18E-05
18	2.15E-05	2.14E-05	2.20E-05
19	2.17E-05	2.15E-05	2.22E-05
20	2.18E-05	2.16E-05	2.24E-05
21	2.20E-05	2.18E-05	2.25E-05
22	2.21E-05	2.19E-05	2.27E-05
23	2.22E-05	2.20E-05	2.28E-05
24	2.24E-05	2.22E-05	2.30E-05
25	2.25E-05	2.23E-05	2.32E-05
26	2.27E-05	2.24E-05	2.34E-05
27	2.28E-05	2.25E-05	2.35E-05
28	2.30E-05	2.26E-05	2.37E-05
29	2.31E-05	2.27E-05	2.38E-05
30	2.32E-05	2.29E-05	2.40E-05
31	2.34E-05	2.30E-05	2.41E-05
32	2.35E-05	2.31E-05	2.43E-05
33	2.36E-05	2.32E-05	2.45E-05
34	2.38E-05	2.33E-05	2.46E-05
35	2.39E-05	2.34E-05	2.48E-05
36	2.40E-05	2.36E-05	2.49E-05
37	2.41E-05	2.37E-05	2.51E-05

38	2.43E-05	2.38E-05	2.52E-05
39	2.44E-05	2.39E-05	2.54E-05
40	2.45E-05	2.40E-05	2.55E-05
41	2.47E-05	2.41E-05	2.57E-05
42	2.48E-05	2.42E-05	2.58E-05
43	2.49E-05	2.43E-05	2.59E-05
44	2.50E-05	2.45E-05	2.61E-05
45	2.51E-05	2.46E-05	2.62E-05
46	2.53E-05	2.47E-05	2.63E-05
47	2.54E-05	2.48E-05	2.65E-05
48	2.55E-05	2.49E-05	2.66E-05
49	2.56E-05	2.50E-05	2.68E-05
50	2.58E-05	2.51E-05	2.69E-05
51	2.59E-05	2.52E-05	2.70E-05
52	2.60E-05	2.53E-05	2.72E-05
53	2.61E-05	2.54E-05	2.73E-05
54	2.62E-05	2.55E-05	2.74E-05
55	2.63E-05	2.57E-05	2.76E-05
56	2.65E-05	2.58E-05	2.77E-05
57	2.66E-05	2.59E-05	2.78E-05
58	2.67E-05	2.60E-05	2.80E-05
59	2.68E-05	2.61E-05	2.81E-05
60	2.69E-05	2.62E-05	2.82E-05
61	2.70E-05	2.63E-05	2.83E-05
62	2.71E-05	2.64E-05	2.85E-05
63	2.73E-05	2.65E-05	2.86E-05
64	2.74E-05	2.66E-05	2.87E-05
65	2.75E-05	2.67E-05	2.88E-05
66	2.76E-05	2.68E-05	2.90E-05
67	2.77E-05	2.69E-05	2.91E-05
68	2.78E-05	2.70E-05	2.92E-05
69	2.79E-05	2.72E-05	2.93E-05
70	2.80E-05	2.73E-05	2.94E-05
71	2.81E-05	2.74E-05	2.96E-05
72	2.82E-05	2.75E-05	2.97E-05
73	2.84E-05	2.76E-05	2.98E-05
74	2.85E-05	2.77E-05	2.99E-05
75	2.86E-05	2.78E-05	3.01E-05
76	2.87E-05	2.79E-05	3.02E-05
77	2.88E-05	2.80E-05	3.03E-05
78	2.89E-05	2.81E-05	3.04E-05
79	2.90E-05	2.82E-05	3.05E-05
80	2.91E-05	2.83E-05	3.06E-05
81	2.92E-05	2.84E-05	3.08E-05

82	2.93E-05	2.86E-05	3.09E-05
83	2.94E-05	2.87E-05	3.10E-05
84	2.96E-05	2.88E-05	3.11E-05
85	2.97E-05	2.89E-05	3.12E-05
86	2.97E-05	2.90E-05	3.13E-05
87	2.99E-05	2.91E-05	3.15E-05
88	3.00E-05	2.92E-05	3.16E-05
89	3.01E-05	2.93E-05	3.17E-05
90	3.02E-05	2.94E-05	3.18E-05
91	3.03E-05	2.95E-05	3.19E-05
92	3.04E-05	2.96E-05	3.20E-05
93	3.05E-05	2.98E-05	3.21E-05
94	3.06E-05	2.99E-05	3.22E-05
95	3.07E-05	3.00E-05	3.23E-05
96	3.08E-05	3.01E-05	3.24E-05
97	3.09E-05	3.02E-05	3.26E-05
98	3.10E-05	3.03E-05	3.27E-05
99	3.11E-05	3.04E-05	3.28E-05
100	3.12E-05	3.05E-05	3.29E-05
101	3.13E-05	3.06E-05	3.30E-05
102	3.14E-05	3.07E-05	3.31E-05
103	3.15E-05	3.08E-05	3.32E-05
104	3.16E-05	3.09E-05	3.33E-05
105	3.17E-05	3.10E-05	3.34E-05
106	3.18E-05	3.12E-05	3.35E-05
107	3.19E-05	3.13E-05	3.36E-05
108	3.20E-05	3.14E-05	3.37E-05
109	3.21E-05	3.15E-05	3.38E-05
110	3.22E-05	3.16E-05	3.39E-05
111	3.23E-05	3.17E-05	3.41E-05
112	3.24E-05	3.18E-05	3.42E-05
113	3.25E-05	3.19E-05	3.43E-05
114	3.26E-05	3.20E-05	3.44E-05
115	3.27E-05	3.21E-05	3.45E-05
116	3.28E-05	3.22E-05	3.46E-05
117	3.28E-05	3.23E-05	3.47E-05
118	3.29E-05	3.24E-05	3.48E-05
119	3.30E-05	3.25E-05	3.49E-05
120	3.31E-05	3.27E-05	3.50E-05
121	3.32E-05	3.28E-05	3.51E-05
122	3.33E-05	3.29E-05	3.52E-05
123	3.34E-05	3.30E-05	3.53E-05
124	3.35E-05	3.31E-05	3.54E-05
125	3.36E-05	3.32E-05	3.55E-05

126	3.37E-05	3.33E-05	3.56E-05
127	3.38E-05	3.34E-05	3.57E-05
128	3.39E-05	3.35E-05	3.58E-05
129	3.40E-05	3.36E-05	3.59E-05
130	3.41E-05	3.37E-05	3.60E-05
131	3.41E-05	3.38E-05	3.61E-05
132	3.42E-05	3.39E-05	3.61E-05
133	3.43E-05	3.40E-05	3.63E-05
134	3.44E-05	3.41E-05	3.63E-05
135	3.45E-05	3.42E-05	3.64E-05
136	3.46E-05	3.43E-05	3.65E-05
137	3.47E-05	3.44E-05	3.66E-05
138	3.48E-05	3.45E-05	3.67E-05
139	3.49E-05	3.46E-05	3.68E-05
140	3.50E-05	3.47E-05	3.69E-05
141	3.51E-05	3.47E-05	3.70E-05
142	3.52E-05	3.48E-05	3.71E-05
143	3.52E-05	3.49E-05	3.72E-05
144	3.53E-05	3.50E-05	3.73E-05
145	3.54E-05	3.51E-05	3.74E-05
146	3.55E-05	3.52E-05	3.75E-05
147	3.56E-05	3.53E-05	3.76E-05
148	3.57E-05	3.54E-05	3.77E-05
149	3.58E-05	3.55E-05	3.78E-05
150	3.59E-05	3.56E-05	3.78E-05
151	3.59E-05	3.57E-05	3.79E-05
152	3.60E-05	3.58E-05	3.80E-05
153	3.61E-05	3.59E-05	3.81E-05
154	3.62E-05	3.59E-05	3.82E-05
155	3.63E-05	3.60E-05	3.83E-05
156	3.64E-05	3.61E-05	3.84E-05
157	3.65E-05	3.62E-05	3.85E-05
158	3.66E-05	3.63E-05	3.86E-05
159	3.67E-05	3.64E-05	3.87E-05
160	3.67E-05	3.65E-05	3.87E-05
161	3.68E-05	3.65E-05	3.88E-05
162	3.69E-05	3.66E-05	3.89E-05
163	3.70E-05	3.67E-05	3.90E-05
164	3.71E-05	3.68E-05	3.91E-05
165	3.72E-05	3.69E-05	3.92E-05
166	3.72E-05	3.70E-05	3.93E-05
167	3.73E-05	3.70E-05	3.94E-05
168	3.74E-05	3.71E-05	3.95E-05
169	3.75E-05	3.72E-05	3.96E-05

170	3.76E-05	3.73E-05	3.96E-05
171	3.77E-05	3.73E-05	3.97E-05
172	3.78E-05	3.74E-05	3.98E-05
173	3.78E-05	3.75E-05	3.99E-05
174	3.79E-05	3.76E-05	4.00E-05
175	3.80E-05	3.77E-05	4.01E-05
176	3.81E-05	3.77E-05	4.02E-05
177	3.82E-05	3.78E-05	4.02E-05
178	3.83E-05	3.79E-05	4.03E-05
179	3.83E-05	3.80E-05	4.04E-05
180	3.84E-05	3.81E-05	4.05E-05
181	3.85E-05	3.81E-05	4.06E-05
182	3.86E-05	3.82E-05	4.07E-05
183	3.87E-05	3.83E-05	4.07E-05
184	3.88E-05	3.84E-05	4.08E-05
185	3.88E-05	3.84E-05	4.09E-05
186	3.89E-05	3.85E-05	4.10E-05
187	3.90E-05	3.86E-05	4.11E-05
188	3.91E-05	3.87E-05	4.12E-05
189	3.92E-05	3.87E-05	4.13E-05
190	3.92E-05	3.88E-05	4.13E-05
191	3.93E-05	3.89E-05	4.14E-05
192	3.94E-05	3.90E-05	4.15E-05
193	3.95E-05	3.90E-05	4.16E-05
194	3.96E-05	3.91E-05	4.17E-05
195	3.96E-05	3.92E-05	4.18E-05
196	3.97E-05	3.93E-05	4.18E-05
197	3.98E-05	3.93E-05	4.19E-05
198	3.99E-05	3.94E-05	4.20E-05
199	4.00E-05	3.95E-05	4.21E-05
200	4.01E-05	3.95E-05	4.22E-05
201	4.01E-05	3.96E-05	4.23E-05
202	4.02E-05	3.97E-05	4.23E-05
203	4.03E-05	3.97E-05	4.24E-05
204	4.04E-05	3.98E-05	4.25E-05
205	4.04E-05	3.99E-05	4.26E-05
206	4.05E-05	3.99E-05	4.27E-05
207	4.06E-05	4.00E-05	4.27E-05
208	4.07E-05	4.01E-05	4.28E-05
209	4.08E-05	4.02E-05	4.29E-05
210	4.08E-05	4.02E-05	4.30E-05
211	4.09E-05	4.03E-05	4.31E-05
212	4.10E-05	4.04E-05	4.32E-05
213	4.11E-05	4.04E-05	4.32E-05

214	4.11E-05	4.05E-05	4.33E-05
215	4.12E-05	4.06E-05	4.34E-05
216	4.13E-05	4.06E-05	4.35E-05
217	4.14E-05	4.07E-05	4.36E-05
218	4.14E-05	4.08E-05	4.36E-05
219	4.15E-05	4.08E-05	4.37E-05
220	4.16E-05	4.09E-05	4.38E-05
221	4.17E-05	4.09E-05	4.39E-05
222	4.17E-05	4.10E-05	4.40E-05
223	4.18E-05	4.11E-05	4.41E-05
224	4.19E-05	4.11E-05	4.41E-05
225	4.20E-05	4.12E-05	4.42E-05
226	4.21E-05	4.12E-05	4.43E-05
227	4.21E-05	4.13E-05	4.44E-05
228	4.22E-05	4.14E-05	4.45E-05
229	4.23E-05	4.14E-05	4.46E-05
230	4.23E-05	4.15E-05	4.46E-05
231	4.24E-05	4.15E-05	4.47E-05
232	4.25E-05	4.16E-05	4.48E-05
233	4.26E-05	4.17E-05	4.49E-05
234	4.26E-05	4.17E-05	4.50E-05
235	4.27E-05	4.18E-05	4.50E-05
236	4.28E-05	4.19E-05	4.51E-05
237	4.28E-05	4.19E-05	4.52E-05
238	4.29E-05	4.20E-05	4.53E-05
239	4.30E-05	4.20E-05	4.54E-05
240	4.31E-05	4.21E-05	4.55E-05
241	4.31E-05	4.22E-05	4.55E-05
242	4.32E-05	4.22E-05	4.56E-05
243	4.33E-05	4.23E-05	4.57E-05
244	4.34E-05	4.23E-05	4.58E-05
245	4.34E-05	4.24E-05	4.58E-05
246	4.35E-05	4.25E-05	4.59E-05
247	4.36E-05	4.25E-05	4.60E-05
248	4.36E-05	4.26E-05	4.61E-05
249	4.37E-05	4.26E-05	4.62E-05
250	4.38E-05	4.27E-05	4.62E-05
251	4.39E-05	4.28E-05	4.63E-05
252	4.40E-05	4.28E-05	4.64E-05
253	4.40E-05	4.29E-05	4.65E-05
254	4.41E-05	4.29E-05	4.66E-05
255	4.41E-05	4.30E-05	4.67E-05
256	4.42E-05	4.31E-05	4.67E-05
257	4.43E-05	4.31E-05	4.68E-05

258	4.44E-05	4.32E-05	4.69E-05
259	4.44E-05	4.32E-05	4.70E-05
260	4.45E-05	4.33E-05	4.70E-05
261	4.46E-05	4.33E-05	4.71E-05
262	4.46E-05	4.34E-05	4.72E-05
263	4.47E-05	4.34E-05	4.73E-05
264	4.48E-05	4.35E-05	4.74E-05
265	4.48E-05	4.36E-05	4.74E-05
266	4.49E-05	4.36E-05	4.75E-05
267	4.50E-05	4.37E-05	4.76E-05
268	4.51E-05	4.37E-05	4.77E-05
269	4.51E-05	4.38E-05	4.78E-05
270	4.52E-05	4.38E-05	4.78E-05
271	4.53E-05	4.39E-05	4.79E-05
272	4.53E-05	4.39E-05	4.80E-05
273	4.54E-05	4.40E-05	4.81E-05
274	4.55E-05	4.41E-05	4.81E-05
275	4.55E-05	4.41E-05	4.82E-05
276	4.56E-05	4.42E-05	4.83E-05
277	4.57E-05	4.42E-05	4.84E-05
278	4.57E-05	4.43E-05	4.85E-05
279	4.58E-05	4.44E-05	4.85E-05
280	4.59E-05	4.44E-05	4.86E-05
281	4.59E-05	4.45E-05	4.87E-05
282	4.60E-05	4.45E-05	4.88E-05
283	4.61E-05	4.46E-05	4.89E-05
284	4.61E-05	4.47E-05	4.89E-05
285	4.62E-05	4.47E-05	4.90E-05
286	4.63E-05	4.48E-05	4.91E-05
287	4.63E-05	4.48E-05	4.91E-05
288	4.64E-05	4.49E-05	4.92E-05
289	4.65E-05	4.50E-05	4.93E-05
290	4.65E-05	4.50E-05	4.94E-05
291	4.66E-05	4.51E-05	4.94E-05
292	4.67E-05	4.52E-05	4.95E-05
293	4.67E-05	4.52E-05	4.96E-05
294	4.68E-05	4.53E-05	4.97E-05
295	4.69E-05	4.53E-05	4.97E-05
296	4.69E-05	4.54E-05	4.98E-05
297	4.70E-05	4.55E-05	4.99E-05
298	4.71E-05	4.55E-05	5.00E-05
299	4.71E-05	4.56E-05	5.00E-05

Table B5: Average CO_2 concentration of five-hour Tablelands experiments with elevated CO_2 concentration and Mg-rich water.

Time (min)	MgOH	MgOH + TCR	MgOH + TWR
0	1.77E-05	1.82E-05	1.80E-05
1	1.79E-05	1.84E-05	1.82E-05
2	1.80E-05	1.85E-05	1.84E-05
3	1.82E-05	1.87E-05	1.85E-05
4	1.83E-05	1.88E-05	1.87E-05
5	1.84E-05	1.89E-05	1.88E-05
6	1.85E-05	1.90E-05	1.89E-05
7	1.86E-05	1.92E-05	1.91E-05
8	1.87E-05	1.93E-05	1.92E-05
9	1.88E-05	1.94E-05	1.93E-05
10	1.89E-05	1.95E-05	1.94E-05
11	1.90E-05	1.96E-05	1.95E-05
12	1.91E-05	1.97E-05	1.96E-05
13	1.92E-05	1.98E-05	1.97E-05
14	1.93E-05	1.99E-05	1.98E-05
15	1.94E-05	2.00E-05	1.99E-05
16	1.95E-05	2.01E-05	2.00E-05
17	1.96E-05	2.02E-05	2.01E-05
18	1.96E-05	2.03E-05	2.02E-05
19	1.97E-05	2.04E-05	2.03E-05
20	1.98E-05	2.05E-05	2.04E-05
21	1.99E-05	2.05E-05	2.05E-05
22	1.99E-05	2.06E-05	2.06E-05
23	2.00E-05	2.07E-05	2.07E-05
24	2.01E-05	2.08E-05	2.08E-05
25	2.02E-05	2.09E-05	2.09E-05
26	2.03E-05	2.10E-05	2.10E-05
27	2.03E-05	2.11E-05	2.10E-05
28	2.04E-05	2.12E-05	2.11E-05
29	2.05E-05	2.12E-05	2.12E-05
30	2.05E-05	2.13E-05	2.13E-05
31	2.06E-05	2.14E-05	2.14E-05
32	2.07E-05	2.15E-05	2.15E-05
33	2.07E-05	2.16E-05	2.15E-05
34	2.08E-05	2.16E-05	2.16E-05
35	2.09E-05	2.17E-05	2.17E-05
36	2.10E-05	2.18E-05	2.18E-05

37	2.10E-05	2.19E-05	2.19E-05
38	2.11E-05	2.20E-05	2.19E-05
39	2.11E-05	2.20E-05	2.20E-05
40	2.12E-05	2.21E-05	2.21E-05
41	2.13E-05	2.22E-05	2.22E-05
42	2.13E-05	2.23E-05	2.23E-05
43	2.14E-05	2.24E-05	2.23E-05
44	2.15E-05	2.24E-05	2.24E-05
45	2.15E-05	2.25E-05	2.25E-05
46	2.16E-05	2.26E-05	2.26E-05
47	2.16E-05	2.27E-05	2.26E-05
48	2.17E-05	2.27E-05	2.27E-05
49	2.18E-05	2.28E-05	2.28E-05
50	2.18E-05	2.29E-05	2.28E-05
51	2.19E-05	2.30E-05	2.29E-05
52	2.19E-05	2.30E-05	2.30E-05
53	2.20E-05	2.31E-05	2.31E-05
54	2.21E-05	2.32E-05	2.31E-05
55	2.21E-05	2.33E-05	2.32E-05
56	2.22E-05	2.33E-05	2.33E-05
57	2.22E-05	2.34E-05	2.33E-05
58	2.23E-05	2.35E-05	2.34E-05
59	2.24E-05	2.36E-05	2.35E-05
60	2.24E-05	2.36E-05	2.36E-05
61	2.25E-05	2.37E-05	2.36E-05
62	2.25E-05	2.38E-05	2.37E-05
63	2.26E-05	2.39E-05	2.38E-05
64	2.26E-05	2.39E-05	2.38E-05
65	2.27E-05	2.40E-05	2.39E-05
66	2.27E-05	2.41E-05	2.40E-05
67	2.28E-05	2.42E-05	2.40E-05
68	2.28E-05	2.42E-05	2.41E-05
69	2.29E-05	2.43E-05	2.42E-05
70	2.30E-05	2.44E-05	2.42E-05
71	2.30E-05	2.44E-05	2.43E-05
72	2.31E-05	2.45E-05	2.44E-05
73	2.31E-05	2.46E-05	2.44E-05
74	2.32E-05	2.46E-05	2.45E-05
75	2.32E-05	2.47E-05	2.46E-05
76	2.33E-05	2.48E-05	2.46E-05
77	2.33E-05	2.48E-05	2.47E-05
78	2.34E-05	2.49E-05	2.48E-05
79	2.34E-05	2.50E-05	2.48E-05
80	2.35E-05	2.50E-05	2.49E-05

81	2.35E-05	2.51E-05	2.49E-05
82	2.36E-05	2.52E-05	2.50E-05
83	2.36E-05	2.53E-05	2.51E-05
84	2.37E-05	2.53E-05	2.51E-05
85	2.37E-05	2.54E-05	2.52E-05
86	2.38E-05	2.54E-05	2.53E-05
87	2.38E-05	2.55E-05	2.53E-05
88	2.39E-05	2.56E-05	2.54E-05
89	2.39E-05	2.56E-05	2.54E-05
90	2.40E-05	2.57E-05	2.55E-05
91	2.40E-05	2.58E-05	2.56E-05
92	2.41E-05	2.58E-05	2.56E-05
93	2.41E-05	2.59E-05	2.57E-05
94	2.42E-05	2.60E-05	2.58E-05
95	2.42E-05	2.60E-05	2.58E-05
96	2.43E-05	2.61E-05	2.59E-05
97	2.43E-05	2.62E-05	2.59E-05
98	2.43E-05	2.62E-05	2.60E-05
99	2.44E-05	2.63E-05	2.61E-05
100	2.44E-05	2.63E-05	2.61E-05
101	2.45E-05	2.64E-05	2.62E-05
102	2.45E-05	2.65E-05	2.62E-05
103	2.46E-05	2.65E-05	2.63E-05
104	2.46E-05	2.66E-05	2.64E-05
105	2.47E-05	2.66E-05	2.64E-05
106	2.47E-05	2.67E-05	2.65E-05
107	2.48E-05	2.68E-05	2.66E-05
108	2.48E-05	2.68E-05	2.66E-05
109	2.49E-05	2.69E-05	2.67E-05
110	2.49E-05	2.70E-05	2.67E-05
111	2.49E-05	2.70E-05	2.68E-05
112	2.50E-05	2.71E-05	2.69E-05
113	2.50E-05	2.71E-05	2.69E-05
114	2.51E-05	2.72E-05	2.70E-05
115	2.51E-05	2.73E-05	2.70E-05
116	2.52E-05	2.73E-05	2.71E-05
117	2.52E-05	2.74E-05	2.72E-05
118	2.52E-05	2.74E-05	2.72E-05
119	2.53E-05	2.75E-05	2.73E-05
120	2.53E-05	2.76E-05	2.73E-05
121	2.54E-05	2.76E-05	2.74E-05
122	2.54E-05	2.77E-05	2.75E-05
123	2.55E-05	2.77E-05	2.75E-05
124	2.55E-05	2.78E-05	2.76E-05

125	2.55E-05	2.79E-05	2.76E-05
126	2.56E-05	2.79E-05	2.77E-05
127	2.56E-05	2.80E-05	2.77E-05
128	2.57E-05	2.80E-05	2.78E-05
129	2.57E-05	2.81E-05	2.79E-05
130	2.57E-05	2.81E-05	2.79E-05
131	2.58E-05	2.82E-05	2.80E-05
132	2.58E-05	2.83E-05	2.80E-05
133	2.59E-05	2.83E-05	2.81E-05
134	2.59E-05	2.84E-05	2.82E-05
135	2.60E-05	2.84E-05	2.82E-05
136	2.60E-05	2.85E-05	2.83E-05
137	2.60E-05	2.85E-05	2.83E-05
138	2.61E-05	2.86E-05	2.84E-05
139	2.61E-05	2.87E-05	2.85E-05
140	2.62E-05	2.87E-05	2.85E-05
141	2.62E-05	2.88E-05	2.86E-05
142	2.62E-05	2.88E-05	2.86E-05
143	2.63E-05	2.89E-05	2.87E-05
144	2.63E-05	2.89E-05	2.87E-05
145	2.64E-05	2.90E-05	2.88E-05
146	2.64E-05	2.90E-05	2.89E-05
147	2.64E-05	2.91E-05	2.89E-05
148	2.65E-05	2.91E-05	2.90E-05
149	2.65E-05	2.92E-05	2.90E-05
150	2.66E-05	2.92E-05	2.91E-05
151	2.66E-05	2.93E-05	2.92E-05
152	2.66E-05	2.93E-05	2.92E-05
153	2.67E-05	2.94E-05	2.93E-05
154	2.67E-05	2.95E-05	2.93E-05
155	2.68E-05	2.95E-05	2.94E-05
156	2.68E-05	2.96E-05	2.94E-05
157	2.68E-05	2.96E-05	2.95E-05
158	2.69E-05	2.97E-05	2.96E-05
159	2.69E-05	2.97E-05	2.96E-05
160	2.70E-05	2.98E-05	2.97E-05
161	2.70E-05	2.98E-05	2.97E-05
162	2.70E-05	2.99E-05	2.98E-05
163	2.71E-05	2.99E-05	2.98E-05
164	2.71E-05	3.00E-05	2.99E-05
165	2.71E-05	3.00E-05	3.00E-05
166	2.72E-05	3.01E-05	3.00E-05
167	2.72E-05	3.01E-05	3.01E-05
168	2.72E-05	3.02E-05	3.01E-05

169	2.73E-05	3.02E-05	3.02E-05
170	2.73E-05	3.03E-05	3.02E-05
171	2.74E-05	3.03E-05	3.03E-05
172	2.74E-05	3.04E-05	3.04E-05
173	2.74E-05	3.04E-05	3.04E-05
174	2.75E-05	3.05E-05	3.05E-05
175	2.75E-05	3.05E-05	3.05E-05
176	2.75E-05	3.06E-05	3.06E-05
177	2.76E-05	3.06E-05	3.06E-05
178	2.76E-05	3.07E-05	3.07E-05
179	2.77E-05	3.07E-05	3.07E-05
180	2.77E-05	3.08E-05	3.08E-05
181	2.77E-05	3.08E-05	3.09E-05
182	2.78E-05	3.09E-05	3.09E-05
183	2.78E-05	3.09E-05	3.10E-05
184	2.78E-05	3.10E-05	3.10E-05
185	2.79E-05	3.10E-05	3.11E-05
186	2.79E-05	3.11E-05	3.11E-05
187	2.79E-05	3.11E-05	3.12E-05
188	2.80E-05	3.12E-05	3.12E-05
189	2.80E-05	3.12E-05	3.13E-05
190	2.80E-05	3.13E-05	3.14E-05
191	2.81E-05	3.13E-05	3.14E-05
192	2.81E-05	3.14E-05	3.15E-05
193	2.81E-05	3.14E-05	3.15E-05
194	2.82E-05	3.14E-05	3.16E-05
195	2.82E-05	3.15E-05	3.16E-05
196	2.83E-05	3.15E-05	3.17E-05
197	2.83E-05	3.16E-05	3.17E-05
198	2.83E-05	3.16E-05	3.18E-05
199	2.84E-05	3.17E-05	3.18E-05
200	2.84E-05	3.17E-05	3.19E-05
201	2.84E-05	3.18E-05	3.19E-05
202	2.85E-05	3.18E-05	3.20E-05
203	2.85E-05	3.19E-05	3.20E-05
204	2.85E-05	3.19E-05	3.21E-05
205	2.86E-05	3.20E-05	3.22E-05
206	2.86E-05	3.20E-05	3.22E-05
207	2.86E-05	3.20E-05	3.23E-05
208	2.87E-05	3.21E-05	3.23E-05
209	2.87E-05	3.21E-05	3.24E-05
210	2.87E-05	3.22E-05	3.24E-05
211	2.88E-05	3.22E-05	3.25E-05
212	2.88E-05	3.23E-05	3.25E-05

213	2.88E-05	3.23E-05	3.26E-05
214	2.89E-05	3.23E-05	3.26E-05
215	2.89E-05	3.24E-05	3.27E-05
216	2.89E-05	3.24E-05	3.27E-05
217	2.90E-05	3.25E-05	3.28E-05
218	2.90E-05	3.25E-05	3.28E-05
219	2.90E-05	3.26E-05	3.29E-05
220	2.91E-05	3.26E-05	3.29E-05
221	2.91E-05	3.26E-05	3.30E-05
222	2.91E-05	3.27E-05	3.30E-05
223	2.92E-05	3.27E-05	3.31E-05
224	2.92E-05	3.28E-05	3.31E-05
225	2.92E-05	3.28E-05	3.32E-05
226	2.93E-05	3.29E-05	3.33E-05
227	2.93E-05	3.29E-05	3.33E-05
228	2.93E-05	3.29E-05	3.34E-05
229	2.94E-05	3.30E-05	3.34E-05
230	2.94E-05	3.30E-05	3.34E-05
231	2.94E-05	3.31E-05	3.35E-05
232	2.95E-05	3.31E-05	3.35E-05
233	2.95E-05	3.32E-05	3.36E-05
234	2.95E-05	3.32E-05	3.37E-05
235	2.96E-05	3.32E-05	3.37E-05
236	2.96E-05	3.33E-05	3.38E-05
237	2.96E-05	3.33E-05	3.38E-05
238	2.97E-05	3.33E-05	3.39E-05
239	2.97E-05	3.34E-05	3.39E-05
240	2.97E-05	3.34E-05	3.39E-05
241	2.98E-05	3.35E-05	3.40E-05
242	2.98E-05	3.35E-05	3.40E-05
243	2.98E-05	3.35E-05	3.41E-05
244	2.98E-05	3.36E-05	3.41E-05
245	2.99E-05	3.36E-05	3.42E-05
246	2.99E-05	3.37E-05	3.42E-05
247	2.99E-05	3.37E-05	3.43E-05
248	3.00E-05	3.37E-05	3.43E-05
249	3.00E-05	3.38E-05	3.44E-05
250	3.00E-05	3.38E-05	3.44E-05
251	3.01E-05	3.38E-05	3.45E-05
252	3.01E-05	3.39E-05	3.45E-05
253	3.01E-05	3.39E-05	3.46E-05
254	3.02E-05	3.40E-05	3.46E-05
255	3.02E-05	3.40E-05	3.47E-05
256	3.02E-05	3.40E-05	3.47E-05

257	3.03E-05	3.41E-05	3.48E-05
258	3.03E-05	3.41E-05	3.48E-05
259	3.03E-05	3.41E-05	3.49E-05
260	3.04E-05	3.42E-05	3.49E-05
261	3.04E-05	3.42E-05	3.49E-05
262	3.04E-05	3.43E-05	3.50E-05
263	3.04E-05	3.43E-05	3.50E-05
264	3.05E-05	3.43E-05	3.51E-05
265	3.05E-05	3.44E-05	3.51E-05
266	3.05E-05	3.44E-05	3.52E-05
267	3.06E-05	3.44E-05	3.52E-05
268	3.06E-05	3.45E-05	3.53E-05
269	3.06E-05	3.45E-05	3.53E-05
270	3.07E-05	3.46E-05	3.54E-05
271	3.07E-05	3.46E-05	3.54E-05
272	3.07E-05	3.46E-05	3.55E-05
273	3.07E-05	3.47E-05	3.55E-05
274	3.08E-05	3.47E-05	3.56E-05
275	3.08E-05	3.47E-05	3.56E-05
276	3.08E-05	3.48E-05	3.57E-05
277	3.09E-05	3.48E-05	3.57E-05
278	3.09E-05	3.48E-05	3.57E-05
279	3.09E-05	3.49E-05	3.58E-05
280	3.10E-05	3.49E-05	3.58E-05
281	3.10E-05	3.50E-05	3.59E-05
282	3.10E-05	3.50E-05	3.59E-05
283	3.10E-05	3.50E-05	3.60E-05
284	3.11E-05	3.51E-05	3.60E-05
285	3.11E-05	3.51E-05	3.60E-05
286	3.11E-05	3.51E-05	3.61E-05
287	3.12E-05	3.52E-05	3.61E-05
288	3.12E-05	3.52E-05	3.62E-05
289	3.12E-05	3.52E-05	3.62E-05
290	3.12E-05	3.53E-05	3.63E-05
291	3.13E-05	3.53E-05	3.63E-05
292	3.13E-05	3.54E-05	3.64E-05
293	3.13E-05	3.54E-05	3.64E-05
294	3.14E-05	3.54E-05	3.65E-05
295	3.14E-05	3.55E-05	3.65E-05
296	3.14E-05	3.55E-05	3.65E-05
297	3.15E-05	3.55E-05	3.66E-05
298	3.15E-05	3.56E-05	3.66E-05
299	3.15E-05	3.56E-05	3.67E-05

Table B6: Average CO_2 concentration of five-hour Tablelands experiments with elevated CO_2 concentration and Ca-rich water.

Time (min)	$NaHCO_3$ +CaOH	$NaHCO_3$ + CaOH + TCR	$NaHCO_3$ + CaOH + TWR
0	1.83E-05	1.75E-05	1.75E-05
1	1.82E-05	1.75E-05	1.74E-05
2	1.81E-05	1.74E-05	1.73E-05
3	1.79E-05	1.73E-05	1.72E-05
4	1.78E-05	1.72E-05	1.71E-05
5	1.77E-05	1.71E-05	1.70E-05
6	1.76E-05	1.70E-05	1.69E-05
7	1.75E-05	1.69E-05	1.68E-05
8	1.74E-05	1.68E-05	1.67E-05
9	1.73E-05	1.67E-05	1.66E-05
10	1.72E-05	1.66E-05	1.65E-05
11	1.71E-05	1.65E-05	1.64E-05
12	1.70E-05	1.64E-05	1.63E-05
13	1.69E-05	1.64E-05	1.63E-05
14	1.68E-05	1.63E-05	1.61E-05
15	1.67E-05	1.62E-05	1.61E-05
16	1.66E-05	1.61E-05	1.60E-05
17	1.65E-05	1.60E-05	1.59E-05
18	1.64E-05	1.59E-05	1.58E-05
19	1.63E-05	1.59E-05	1.57E-05
20	1.62E-05	1.58E-05	1.56E-05
21	1.61E-05	1.57E-05	1.55E-05
22	1.60E-05	1.56E-05	1.54E-05
23	1.60E-05	1.55E-05	1.54E-05
24	1.59E-05	1.55E-05	1.53E-05
25	1.58E-05	1.54E-05	1.52E-05
26	1.57E-05	1.53E-05	1.51E-05
27	1.56E-05	1.52E-05	1.50E-05
28	1.55E-05	1.52E-05	1.50E-05
29	1.54E-05	1.51E-05	1.49E-05
30	1.53E-05	1.50E-05	1.48E-05
31	1.53E-05	1.49E-05	1.47E-05
32	1.52E-05	1.49E-05	1.46E-05
33	1.51E-05	1.48E-05	1.46E-05
34	1.50E-05	1.47E-05	1.45E-05
35	1.49E-05	1.46E-05	1.44E-05
36	1.49E-05	1.46E-05	1.43E-05

37	1.48E-05	1.45E-05	1.43E-05
38	1.47E-05	1.44E-05	1.42E-05
39	1.46E-05	1.44E-05	1.41E-05
40	1.45E-05	1.43E-05	1.40E-05
41	1.45E-05	1.42E-05	1.40E-05
42	1.44E-05	1.42E-05	1.39E-05
43	1.43E-05	1.41E-05	1.38E-05
44	1.42E-05	1.40E-05	1.37E-05
45	1.42E-05	1.40E-05	1.37E-05
46	1.41E-05	1.39E-05	1.36E-05
47	1.40E-05	1.38E-05	1.35E-05
48	1.39E-05	1.38E-05	1.35E-05
49	1.39E-05	1.37E-05	1.34E-05
50	1.38E-05	1.36E-05	1.33E-05
51	1.37E-05	1.36E-05	1.33E-05
52	1.36E-05	1.35E-05	1.32E-05
53	1.36E-05	1.34E-05	1.31E-05
54	1.35E-05	1.34E-05	1.31E-05
55	1.34E-05	1.33E-05	1.30E-05
56	1.34E-05	1.33E-05	1.29E-05
57	1.33E-05	1.32E-05	1.29E-05
58	1.32E-05	1.31E-05	1.28E-05
59	1.32E-05	1.31E-05	1.27E-05
60	1.31E-05	1.30E-05	1.27E-05
61	1.30E-05	1.30E-05	1.26E-05
62	1.30E-05	1.29E-05	1.25E-05
63	1.29E-05	1.28E-05	1.25E-05
64	1.28E-05	1.28E-05	1.24E-05
65	1.28E-05	1.27E-05	1.24E-05
66	1.27E-05	1.27E-05	1.23E-05
67	1.26E-05	1.26E-05	1.22E-05
68	1.26E-05	1.26E-05	1.22E-05
69	1.25E-05	1.25E-05	1.21E-05
70	1.24E-05	1.24E-05	1.21E-05
71	1.24E-05	1.24E-05	1.20E-05
72	1.23E-05	1.23E-05	1.19E-05
73	1.23E-05	1.23E-05	1.19E-05
74	1.22E-05	1.22E-05	1.18E-05
75	1.21E-05	1.22E-05	1.18E-05
76	1.21E-05	1.21E-05	1.17E-05
77	1.20E-05	1.21E-05	1.17E-05
78	1.20E-05	1.20E-05	1.16E-05
79	1.19E-05	1.19E-05	1.15E-05
80	1.18E-05	1.19E-05	1.15E-05

81	1.18E-05	1.19E-05	1.14E-05
82	1.17E-05	1.18E-05	1.14E-05
83	1.17E-05	1.17E-05	1.13E-05
84	1.16E-05	1.17E-05	1.13E-05
85	1.16E-05	1.16E-05	1.12E-05
86	1.15E-05	1.16E-05	1.12E-05
87	1.14E-05	1.15E-05	1.11E-05
88	1.14E-05	1.15E-05	1.11E-05
89	1.13E-05	1.14E-05	1.10E-05
90	1.13E-05	1.14E-05	1.09E-05
91	1.12E-05	1.13E-05	1.09E-05
92	1.12E-05	1.13E-05	1.08E-05
93	1.11E-05	1.12E-05	1.08E-05
94	1.10E-05	1.12E-05	1.07E-05
95	1.10E-05	1.11E-05	1.07E-05
96	1.09E-05	1.11E-05	1.06E-05
97	1.09E-05	1.10E-05	1.06E-05
98	1.08E-05	1.10E-05	1.05E-05
99	1.08E-05	1.09E-05	1.05E-05
100	1.07E-05	1.09E-05	1.04E-05
101	1.07E-05	1.08E-05	1.04E-05
102	1.06E-05	1.08E-05	1.03E-05
103	1.06E-05	1.07E-05	1.03E-05
104	1.05E-05	1.07E-05	1.02E-05
105	1.05E-05	1.07E-05	1.02E-05
106	1.04E-05	1.06E-05	1.01E-05
107	1.03E-05	1.05E-05	1.01E-05
108	1.03E-05	1.05E-05	1.00E-05
109	1.02E-05	1.05E-05	9.99E-06
110	1.02E-05	1.04E-05	9.94E-06
111	1.01E-05	1.04E-05	9.88E-06
112	1.01E-05	1.03E-05	9.84E-06
113	1.00E-05	1.03E-05	9.80E-06
114	9.99E-06	1.02E-05	9.75E-06
115	9.94E-06	1.02E-05	9.70E-06
116	9.89E-06	1.01E-05	9.65E-06
117	9.84E-06	1.01E-05	9.61E-06
118	9.79E-06	1.01E-05	9.57E-06
119	9.74E-06	1.00E-05	9.52E-06
120	9.69E-06	9.96E-06	9.48E-06
121	9.64E-06	9.93E-06	9.43E-06
122	9.59E-06	9.88E-06	9.39E-06
123	9.54E-06	9.84E-06	9.34E-06
124	9.49E-06	9.80E-06	9.30E-06

125	9.45E-06	9.75E-06	9.25E-06
126	9.39E-06	9.71E-06	9.20E-06
127	9.35E-06	9.67E-06	9.16E-06
128	9.30E-06	9.63E-06	9.12E-06
129	9.26E-06	9.58E-06	9.07E-06
130	9.21E-06	9.54E-06	9.03E-06
131	9.17E-06	9.51E-06	8.99E-06
132	9.12E-06	9.46E-06	8.95E-06
133	9.07E-06	9.42E-06	8.90E-06
134	9.03E-06	9.37E-06	8.86E-06
135	8.97E-06	9.33E-06	8.82E-06
136	8.93E-06	9.30E-06	8.77E-06
137	8.89E-06	9.25E-06	8.73E-06
138	8.85E-06	9.22E-06	8.69E-06
139	8.80E-06	9.18E-06	8.65E-06
140	8.75E-06	9.14E-06	8.61E-06
141	8.72E-06	9.10E-06	8.57E-06
142	8.67E-06	9.06E-06	8.53E-06
143	8.62E-06	9.02E-06	8.49E-06
144	8.58E-06	8.98E-06	8.45E-06
145	8.54E-06	8.94E-06	8.41E-06
146	8.49E-06	8.90E-06	8.37E-06
147	8.46E-06	8.86E-06	8.33E-06
148	8.41E-06	8.83E-06	8.29E-06
149	8.37E-06	8.78E-06	8.25E-06
150	8.32E-06	8.75E-06	8.21E-06
151	8.29E-06	8.71E-06	8.17E-06
152	8.24E-06	8.67E-06	8.14E-06
153	8.21E-06	8.64E-06	8.10E-06
154	8.16E-06	8.60E-06	8.06E-06
155	8.12E-06	8.56E-06	8.02E-06
156	8.08E-06	8.52E-06	7.99E-06
157	8.04E-06	8.49E-06	7.95E-06
158	8.00E-06	8.46E-06	7.91E-06
159	7.95E-06	8.42E-06	7.87E-06
160	7.92E-06	8.38E-06	7.84E-06
161	7.88E-06	8.34E-06	7.80E-06
162	7.84E-06	8.31E-06	7.77E-06
163	7.81E-06	8.27E-06	7.73E-06
164	7.77E-06	8.23E-06	7.69E-06
165	7.72E-06	8.20E-06	7.66E-06
166	7.69E-06	8.16E-06	7.62E-06
167	7.65E-06	8.13E-06	7.58E-06
168	7.62E-06	8.10E-06	7.55E-06

169	7.58E-06	8.07E-06	7.52E-06
170	7.54E-06	8.03E-06	7.48E-06
171	7.50E-06	8.00E-06	7.45E-06
172	7.47E-06	7.96E-06	7.41E-06
173	7.43E-06	7.93E-06	7.37E-06
174	7.39E-06	7.89E-06	7.34E-06
175	7.35E-06	7.86E-06	7.31E-06
176	7.32E-06	7.82E-06	7.28E-06
177	7.28E-06	7.79E-06	7.24E-06
178	7.26E-06	7.76E-06	7.22E-06
179	7.21E-06	7.72E-06	7.18E-06
180	7.18E-06	7.69E-06	7.14E-06
181	7.14E-06	7.66E-06	7.11E-06
182	7.11E-06	7.64E-06	7.08E-06
183	7.07E-06	7.60E-06	7.04E-06
184	7.04E-06	7.57E-06	7.01E-06
185	7.01E-06	7.53E-06	6.98E-06
186	6.98E-06	7.50E-06	6.95E-06
187	6.94E-06	7.47E-06	6.92E-06
188	6.91E-06	7.43E-06	6.89E-06
189	6.88E-06	7.41E-06	6.86E-06
190	6.85E-06	7.38E-06	6.83E-06
191	6.81E-06	7.35E-06	6.80E-06
192	6.78E-06	7.31E-06	6.76E-06
193	6.75E-06	7.28E-06	6.73E-06
194	6.71E-06	7.25E-06	6.70E-06
195	6.69E-06	7.22E-06	6.67E-06
196	6.65E-06	7.19E-06	6.64E-06
197	6.62E-06	7.16E-06	6.61E-06
198	6.58E-06	7.14E-06	6.59E-06
199	6.55E-06	7.11E-06	6.56E-06
200	6.53E-06	7.09E-06	6.53E-06
201	6.49E-06	7.05E-06	6.50E-06
202	6.46E-06	7.02E-06	6.47E-06
203	6.43E-06	6.99E-06	6.45E-06
204	6.40E-06	6.96E-06	6.42E-06
205	6.37E-06	6.93E-06	6.38E-06
206	6.35E-06	6.91E-06	6.36E-06
207	6.32E-06	6.87E-06	6.33E-06
208	6.29E-06	6.84E-06	6.29E-06
209	6.26E-06	6.82E-06	6.27E-06
210	6.23E-06	6.79E-06	6.25E-06
211	6.20E-06	6.76E-06	6.22E-06
212	6.17E-06	6.73E-06	6.19E-06

213	6.14E-06	6.71E-06	6.16E-06
214	6.11E-06	6.68E-06	6.14E-06
215	6.08E-06	6.65E-06	6.11E-06
216	6.05E-06	6.63E-06	6.08E-06
217	6.02E-06	6.59E-06	6.06E-06
218	5.99E-06	6.57E-06	6.03E-06
219	5.97E-06	6.55E-06	6.00E-06
220	5.94E-06	6.52E-06	5.98E-06
221	5.91E-06	6.50E-06	5.95E-06
222	5.89E-06	6.46E-06	5.93E-06
223	5.86E-06	6.44E-06	5.91E-06
224	5.84E-06	6.41E-06	5.88E-06
225	5.81E-06	6.39E-06	5.85E-06
226	5.79E-06	6.36E-06	5.82E-06
227	5.76E-06	6.34E-06	5.80E-06
228	5.73E-06	6.31E-06	5.78E-06
229	5.71E-06	6.29E-06	5.75E-06
230	5.68E-06	6.26E-06	5.73E-06
231	5.66E-06	6.24E-06	5.70E-06
232	5.63E-06	6.21E-06	5.68E-06
233	5.61E-06	6.19E-06	5.65E-06
234	5.57E-06	6.17E-06	5.63E-06
235	5.55E-06	6.13E-06	5.61E-06
236	5.53E-06	6.11E-06	5.59E-06
237	5.51E-06	6.09E-06	5.56E-06
238	5.48E-06	6.06E-06	5.54E-06
239	5.45E-06	6.04E-06	5.52E-06
240	5.43E-06	6.02E-06	5.49E-06
241	5.41E-06	5.99E-06	5.47E-06
242	5.38E-06	5.97E-06	5.45E-06
243	5.36E-06	5.95E-06	5.42E-06
244	5.34E-06	5.92E-06	5.40E-06
245	5.32E-06	5.90E-06	5.38E-06
246	5.30E-06	5.87E-06	5.36E-06
247	5.27E-06	5.85E-06	5.33E-06
248	5.25E-06	5.83E-06	5.32E-06
249	5.23E-06	5.81E-06	5.29E-06
250	5.20E-06	5.79E-06	5.27E-06
251	5.18E-06	5.76E-06	5.25E-06
252	5.16E-06	5.74E-06	5.23E-06
253	5.13E-06	5.72E-06	5.20E-06
254	5.11E-06	5.70E-06	5.19E-06
255	5.09E-06	5.67E-06	5.17E-06
256	5.06E-06	5.65E-06	5.13E-06

257	5.05E-06	5.63E-06	5.12E-06
258	5.02E-06	5.61E-06	5.11E-06
259	5.00E-06	5.59E-06	5.08E-06
260	4.98E-06	5.57E-06	5.06E-06
261	4.96E-06	5.55E-06	5.04E-06
262	4.94E-06	5.52E-06	5.01E-06
263	4.92E-06	5.50E-06	5.00E-06
264	4.90E-06	5.48E-06	4.98E-06
265	4.88E-06	5.46E-06	4.96E-06
266	4.86E-06	5.44E-06	4.94E-06
267	4.84E-06	5.42E-06	4.92E-06
268	4.81E-06	5.41E-06	4.90E-06
269	4.79E-06	5.38E-06	4.88E-06
270	4.77E-06	5.36E-06	4.86E-06
271	4.75E-06	5.34E-06	4.84E-06
272	4.73E-06	5.32E-06	4.82E-06
273	4.71E-06	5.31E-06	4.81E-06
274	4.69E-06	5.28E-06	4.78E-06
275	4.68E-06	5.26E-06	4.77E-06
276	4.65E-06	5.24E-06	4.75E-06
277	4.64E-06	5.22E-06	4.73E-06
278	4.62E-06	5.20E-06	4.71E-06
279	4.60E-06	5.19E-06	4.69E-06
280	4.58E-06	5.17E-06	4.67E-06
281	4.56E-06	5.15E-06	4.66E-06
282	4.55E-06	5.13E-06	4.64E-06
283	4.53E-06	5.11E-06	4.62E-06
284	4.51E-06	5.09E-06	4.60E-06
285	4.49E-06	5.07E-06	4.58E-06
286	4.47E-06	5.06E-06	4.57E-06
287	4.45E-06	5.04E-06	4.55E-06
288	4.43E-06	5.01E-06	4.53E-06
289	4.42E-06	5.00E-06	4.51E-06
290	4.39E-06	4.98E-06	4.50E-06
291	4.38E-06	4.96E-06	4.48E-06
292	4.36E-06	4.95E-06	4.46E-06
293	4.34E-06	4.93E-06	4.45E-06
294	4.33E-06	4.91E-06	4.43E-06
295	4.31E-06	4.90E-06	4.41E-06
296	4.29E-06	4.87E-06	4.40E-06
297	4.27E-06	4.86E-06	4.38E-06
298	4.25E-06	4.83E-06	4.36E-06
299	4.24E-06	4.82E-06	4.35E-06

Table B7: Average CO_2 concentration of four-hour White Hills experiments with DI water.

Time (min)	DI (TL 5hr)	DI + SCR	DI + SWR
0	2.03E-05	1.89E-05	1.92E-05
1	2.02E-05	1.88E-05	1.91E-05
2	2.02E-05	1.88E-05	1.91E-05
3	2.02E-05	1.87E-05	1.91E-05
4	2.02E-05	1.87E-05	1.91E-05
5	2.02E-05	1.87E-05	1.91E-05
6	2.02E-05	1.87E-05	1.91E-05
7	2.02E-05	1.86E-05	1.91E-05
8	2.02E-05	1.86E-05	1.91E-05
9	2.02E-05	1.86E-05	1.91E-05
10	2.02E-05	1.86E-05	1.91E-05
11	2.02E-05	1.85E-05	1.91E-05
12	2.02E-05	1.85E-05	1.91E-05
13	2.02E-05	1.85E-05	1.91E-05
14	2.02E-05	1.85E-05	1.91E-05
15	2.02E-05	1.85E-05	1.91E-05
16	2.02E-05	1.84E-05	1.91E-05
17	2.02E-05	1.84E-05	1.91E-05
18	2.02E-05	1.84E-05	1.91E-05
19	2.02E-05	1.84E-05	1.91E-05
20	2.02E-05	1.84E-05	1.91E-05
21	2.02E-05	1.84E-05	1.91E-05
22	2.02E-05	1.83E-05	1.91E-05
23	2.02E-05	1.83E-05	1.91E-05
24	2.02E-05	1.83E-05	1.91E-05
25	2.02E-05	1.83E-05	1.91E-05
26	2.02E-05	1.83E-05	1.91E-05
27	2.02E-05	1.83E-05	1.91E-05
28	2.02E-05	1.82E-05	1.91E-05
29	2.02E-05	1.82E-05	1.91E-05
30	2.02E-05	1.82E-05	1.91E-05
31	2.02E-05	1.82E-05	1.91E-05
32	2.02E-05	1.82E-05	1.91E-05
33	2.02E-05	1.82E-05	1.91E-05
34	2.02E-05	1.81E-05	1.91E-05
35	2.02E-05	1.81E-05	1.91E-05
36	2.02E-05	1.81E-05	1.91E-05
37	2.02E-05	1.81E-05	1.91E-05
38	2.02E-05	1.81E-05	1.91E-05
39	2.02E-05	1.81E-05	1.91E-05

40	2.02E-05	1.81E-05	1.91E-05
41	2.02E-05	1.80E-05	1.91E-05
42	2.02E-05	1.80E-05	1.91E-05
43	2.02E-05	1.80E-05	1.91E-05
44	2.02E-05	1.80E-05	1.91E-05
45	2.02E-05	1.80E-05	1.91E-05
46	2.02E-05	1.80E-05	1.91E-05
47	2.02E-05	1.80E-05	1.91E-05
48	2.02E-05	1.79E-05	1.91E-05
49	2.02E-05	1.79E-05	1.91E-05
50	2.02E-05	1.79E-05	1.91E-05
51	2.02E-05	1.79E-05	1.91E-05
52	2.02E-05	1.79E-05	1.91E-05
53	2.01E-05	1.79E-05	1.91E-05
54	2.02E-05	1.79E-05	1.91E-05
55	2.02E-05	1.79E-05	1.91E-05
56	2.02E-05	1.78E-05	1.91E-05
57	2.02E-05	1.78E-05	1.91E-05
58	2.01E-05	1.78E-05	1.91E-05
59	2.01E-05	1.78E-05	1.91E-05
60	2.01E-05	1.78E-05	1.91E-05
61	2.01E-05	1.78E-05	1.91E-05
62	2.01E-05	1.78E-05	1.91E-05
63	2.01E-05	1.78E-05	1.91E-05
64	2.01E-05	1.77E-05	1.91E-05
65	2.01E-05	1.77E-05	1.91E-05
66	2.01E-05	1.77E-05	1.91E-05
67	2.01E-05	1.77E-05	1.91E-05
68	2.01E-05	1.77E-05	1.91E-05
69	2.01E-05	1.77E-05	1.91E-05
70	2.01E-05	1.77E-05	1.91E-05
71	2.01E-05	1.77E-05	1.91E-05
72	2.01E-05	1.76E-05	1.91E-05
73	2.01E-05	1.76E-05	1.91E-05
74	2.01E-05	1.76E-05	1.91E-05
75	2.01E-05	1.76E-05	1.91E-05
76	2.01E-05	1.76E-05	1.91E-05
77	2.01E-05	1.76E-05	1.91E-05
78	2.01E-05	1.76E-05	1.91E-05
79	2.01E-05	1.76E-05	1.91E-05
80	2.01E-05	1.75E-05	1.91E-05
81	2.01E-05	1.75E-05	1.91E-05
82	2.01E-05	1.75E-05	1.91E-05
83	2.01E-05	1.75E-05	1.91E-05

84	2.01E-05	1.75E-05	1.91E-05
85	2.01E-05	1.75E-05	1.91E-05
86	2.01E-05	1.75E-05	1.91E-05
87	2.01E-05	1.75E-05	1.91E-05
88	2.01E-05	1.74E-05	1.91E-05
89	2.01E-05	1.74E-05	1.91E-05
90	2.01E-05	1.74E-05	1.91E-05
91	2.01E-05	1.74E-05	1.91E-05
92	2.01E-05	1.74E-05	1.91E-05
93	2.01E-05	1.74E-05	1.91E-05
94	2.01E-05	1.74E-05	1.91E-05
95	2.01E-05	1.74E-05	1.91E-05
96	2.01E-05	1.74E-05	1.91E-05
97	2.01E-05	1.73E-05	1.91E-05
98	2.01E-05	1.73E-05	1.91E-05
99	2.01E-05	1.73E-05	1.91E-05
100	2.01E-05	1.73E-05	1.91E-05
101	2.01E-05	1.73E-05	1.91E-05
102	2.01E-05	1.73E-05	1.91E-05
103	2.01E-05	1.73E-05	1.91E-05
104	2.01E-05	1.73E-05	1.91E-05
105	2.01E-05	1.73E-05	1.91E-05
106	2.01E-05	1.73E-05	1.91E-05
107	2.01E-05	1.72E-05	1.91E-05
108	2.01E-05	1.72E-05	1.91E-05
109	2.01E-05	1.72E-05	1.91E-05
110	2.01E-05	1.72E-05	1.90E-05
111	2.01E-05	1.72E-05	1.91E-05
112	2.01E-05	1.72E-05	1.91E-05
113	2.01E-05	1.72E-05	1.91E-05
114	2.01E-05	1.72E-05	1.91E-05
115	2.01E-05	1.71E-05	1.91E-05
116	2.01E-05	1.71E-05	1.90E-05
117	2.01E-05	1.71E-05	1.90E-05
118	2.01E-05	1.71E-05	1.91E-05
119	2.01E-05	1.71E-05	1.90E-05
120	2.01E-05	1.71E-05	1.91E-05
121	2.01E-05	1.71E-05	1.90E-05
122	2.01E-05	1.71E-05	1.90E-05
123	2.00E-05	1.71E-05	1.91E-05
124	2.01E-05	1.71E-05	1.91E-05
125	2.01E-05	1.70E-05	1.91E-05
126	2.00E-05	1.70E-05	1.90E-05
127	2.01E-05	1.70E-05	1.90E-05

128	2.00E-05	1.70E-05	1.90E-05
129	2.01E-05	1.70E-05	1.90E-05
130	2.00E-05	1.70E-05	1.90E-05
131	2.00E-05	1.70E-05	1.90E-05
132	2.00E-05	1.70E-05	1.90E-05
133	2.00E-05	1.69E-05	1.90E-05
134	2.00E-05	1.69E-05	1.91E-05
135	2.00E-05	1.69E-05	1.90E-05
136	2.00E-05	1.69E-05	1.90E-05
137	2.00E-05	1.69E-05	1.90E-05
138	2.00E-05	1.69E-05	1.90E-05
139	2.00E-05	1.69E-05	1.90E-05
140	2.00E-05	1.69E-05	1.90E-05
141	2.00E-05	1.69E-05	1.90E-05
142	2.00E-05	1.68E-05	1.91E-05
143	2.00E-05	1.68E-05	1.90E-05
144	2.00E-05	1.68E-05	1.90E-05
145	2.00E-05	1.68E-05	1.90E-05
146	2.00E-05	1.68E-05	1.90E-05
147	2.00E-05	1.68E-05	1.90E-05
148	2.00E-05	1.68E-05	1.90E-05
149	2.00E-05	1.68E-05	1.90E-05
150	2.00E-05	1.67E-05	1.90E-05
151	2.00E-05	1.67E-05	1.90E-05
152	2.00E-05	1.67E-05	1.90E-05
153	2.00E-05	1.67E-05	1.90E-05
154	2.00E-05	1.67E-05	1.90E-05
155	2.00E-05	1.67E-05	1.90E-05
156	2.00E-05	1.67E-05	1.90E-05
157	2.00E-05	1.67E-05	1.90E-05
158	2.00E-05	1.67E-05	1.90E-05
159	2.00E-05	1.66E-05	1.90E-05
160	2.00E-05	1.66E-05	1.90E-05
161	2.00E-05	1.66E-05	1.90E-05
162	2.00E-05	1.66E-05	1.90E-05
163	2.00E-05	1.66E-05	1.90E-05
164	2.00E-05	1.66E-05	1.90E-05
165	2.00E-05	1.66E-05	1.90E-05
166	2.00E-05	1.66E-05	1.90E-05
167	2.00E-05	1.66E-05	1.90E-05
168	2.00E-05	1.65E-05	1.90E-05
169	2.00E-05	1.65E-05	1.90E-05
170	2.00E-05	1.65E-05	1.90E-05
171	2.00E-05	1.65E-05	1.90E-05

172	2.00E-05	1.65E-05	1.90E-05
173	2.00E-05	1.65E-05	1.90E-05
174	2.00E-05	1.65E-05	1.90E-05
175	2.00E-05	1.65E-05	1.90E-05
176	2.00E-05	1.65E-05	1.90E-05
177	2.00E-05	1.64E-05	1.90E-05
178	2.00E-05	1.64E-05	1.90E-05
179	2.00E-05	1.64E-05	1.90E-05
180	2.00E-05	1.64E-05	1.90E-05
181	2.00E-05	1.64E-05	1.90E-05
182	2.00E-05	1.64E-05	1.90E-05
183	2.00E-05	1.64E-05	1.90E-05
184	2.00E-05	1.64E-05	1.90E-05
185	2.00E-05	1.63E-05	1.90E-05
186	2.00E-05	1.63E-05	1.90E-05
187	2.00E-05	1.63E-05	1.90E-05
188	2.00E-05	1.63E-05	1.90E-05
189	2.00E-05	1.63E-05	1.90E-05
190	2.00E-05	1.63E-05	1.90E-05
191	2.00E-05	1.63E-05	1.90E-05
192	2.00E-05	1.63E-05	1.90E-05
193	2.00E-05	1.63E-05	1.90E-05
194	2.00E-05	1.62E-05	1.90E-05
195	2.00E-05	1.62E-05	1.90E-05
196	2.00E-05	1.62E-05	1.90E-05
197	2.00E-05	1.62E-05	1.90E-05
198	2.00E-05	1.62E-05	1.90E-05
199	2.00E-05	1.62E-05	1.90E-05
200	2.00E-05	1.62E-05	1.90E-05
201	2.00E-05	1.62E-05	1.90E-05
202	2.00E-05	1.62E-05	1.90E-05
203	2.00E-05	1.62E-05	1.90E-05
204	2.00E-05	1.61E-05	1.90E-05
205	2.00E-05	1.61E-05	1.90E-05
206	2.00E-05	1.61E-05	1.90E-05
207	2.00E-05	1.61E-05	1.90E-05
208	2.00E-05	1.61E-05	1.90E-05
209	2.00E-05	1.61E-05	1.90E-05
210	2.00E-05	1.61E-05	1.90E-05
211	2.00E-05	1.61E-05	1.90E-05
212	2.00E-05	1.61E-05	1.90E-05
213	2.00E-05	1.60E-05	1.90E-05
214	2.00E-05	1.60E-05	1.90E-05
215	2.00E-05	1.60E-05	1.90E-05

216	2.00E-05	1.60E-05	1.90E-05
217	2.00E-05	1.60E-05	1.90E-05
218	2.00E-05	1.60E-05	1.90E-05
219	2.00E-05	1.60E-05	1.90E-05
220	2.00E-05	1.60E-05	1.90E-05
221	2.00E-05	1.59E-05	1.90E-05
222	2.00E-05	1.59E-05	1.90E-05
223	2.00E-05	1.59E-05	1.90E-05
224	2.00E-05	1.59E-05	1.90E-05
225	2.00E-05	1.59E-05	1.90E-05
226	2.00E-05	1.59E-05	1.90E-05
227	2.00E-05	1.59E-05	1.90E-05
228	2.00E-05	1.59E-05	1.90E-05
229	2.00E-05	1.59E-05	1.90E-05
230	2.00E-05	1.59E-05	1.90E-05
231	2.00E-05	1.59E-05	1.90E-05
232	2.00E-05	1.58E-05	1.90E-05
233	2.00E-05	1.58E-05	1.90E-05
234	2.00E-05	1.58E-05	1.90E-05
235	2.00E-05	1.58E-05	1.90E-05
236	2.00E-05	1.58E-05	1.90E-05
237	2.00E-05	1.58E-05	1.90E-05
238	2.00E-05	1.58E-05	1.90E-05
239	2.00E-05	1.58E-05	1.90E-05

Table B8: Average CO_2 concentration of four-hour White Hills experiments with Mg-rich water.

Time (min)	MgOH (TL 5hr)	MgOH + SCR	MgOH + SWR
0	1.74E-05	1.83E-05	1.85E-05
1	1.74E-05	1.82E-05	1.84E-05
2	1.74E-05	1.82E-05	1.84E-05
3	1.74E-05	1.81E-05	1.84E-05
4	1.73E-05	1.81E-05	1.84E-05
5	1.73E-05	1.80E-05	1.84E-05
6	1.73E-05	1.80E-05	1.83E-05
7	1.73E-05	1.80E-05	1.83E-05
8	1.72E-05	1.79E-05	1.83E-05
9	1.72E-05	1.79E-05	1.83E-05
10	1.71E-05	1.79E-05	1.83E-05
11	1.71E-05	1.78E-05	1.83E-05
12	1.71E-05	1.78E-05	1.83E-05
13	1.71E-05	1.78E-05	1.83E-05
14	1.70E-05	1.77E-05	1.82E-05
15	1.70E-05	1.77E-05	1.82E-05
16	1.70E-05	1.77E-05	1.82E-05
17	1.69E-05	1.76E-05	1.82E-05
18	1.69E-05	1.76E-05	1.82E-05
19	1.69E-05	1.76E-05	1.82E-05
20	1.69E-05	1.76E-05	1.82E-05
21	1.68E-05	1.75E-05	1.81E-05
22	1.68E-05	1.75E-05	1.81E-05
23	1.68E-05	1.75E-05	1.81E-05
24	1.67E-05	1.74E-05	1.81E-05
25	1.67E-05	1.74E-05	1.81E-05
26	1.67E-05	1.74E-05	1.81E-05
27	1.67E-05	1.74E-05	1.81E-05
28	1.66E-05	1.73E-05	1.81E-05
29	1.66E-05	1.73E-05	1.81E-05
30	1.66E-05	1.73E-05	1.80E-05
31	1.65E-05	1.73E-05	1.80E-05
32	1.65E-05	1.72E-05	1.80E-05
33	1.65E-05	1.72E-05	1.80E-05
34	1.65E-05	1.72E-05	1.80E-05
35	1.64E-05	1.72E-05	1.80E-05
36	1.64E-05	1.71E-05	1.80E-05
37	1.64E-05	1.71E-05	1.79E-05
38	1.64E-05	1.71E-05	1.79E-05

39	1.63E-05	1.71E-05	1.79E-05
40	1.63E-05	1.70E-05	1.79E-05
41	1.63E-05	1.70E-05	1.79E-05
42	1.62E-05	1.70E-05	1.79E-05
43	1.62E-05	1.70E-05	1.79E-05
44	1.62E-05	1.70E-05	1.79E-05
45	1.62E-05	1.69E-05	1.79E-05
46	1.61E-05	1.69E-05	1.78E-05
47	1.61E-05	1.69E-05	1.78E-05
48	1.61E-05	1.69E-05	1.78E-05
49	1.60E-05	1.68E-05	1.78E-05
50	1.60E-05	1.68E-05	1.78E-05
51	1.60E-05	1.68E-05	1.78E-05
52	1.60E-05	1.68E-05	1.78E-05
53	1.59E-05	1.68E-05	1.77E-05
54	1.59E-05	1.67E-05	1.77E-05
55	1.59E-05	1.67E-05	1.77E-05
56	1.59E-05	1.67E-05	1.77E-05
57	1.58E-05	1.67E-05	1.77E-05
58	1.58E-05	1.66E-05	1.77E-05
59	1.58E-05	1.66E-05	1.76E-05
60	1.57E-05	1.66E-05	1.76E-05
61	1.57E-05	1.66E-05	1.76E-05
62	1.57E-05	1.66E-05	1.76E-05
63	1.57E-05	1.65E-05	1.76E-05
64	1.56E-05	1.65E-05	1.76E-05
65	1.56E-05	1.65E-05	1.76E-05
66	1.56E-05	1.65E-05	1.75E-05
67	1.55E-05	1.65E-05	1.75E-05
68	1.55E-05	1.64E-05	1.75E-05
69	1.55E-05	1.64E-05	1.75E-05
70	1.55E-05	1.64E-05	1.75E-05
71	1.54E-05	1.64E-05	1.75E-05
72	1.54E-05	1.63E-05	1.74E-05
73	1.54E-05	1.63E-05	1.74E-05
74	1.53E-05	1.63E-05	1.74E-05
75	1.53E-05	1.63E-05	1.74E-05
76	1.53E-05	1.63E-05	1.74E-05
77	1.53E-05	1.62E-05	1.74E-05
78	1.52E-05	1.62E-05	1.74E-05
79	1.52E-05	1.62E-05	1.73E-05
80	1.52E-05	1.62E-05	1.73E-05
81	1.51E-05	1.62E-05	1.73E-05
82	1.51E-05	1.62E-05	1.73E-05

83	1.51E-05	1.61E-05	1.73E-05
84	1.51E-05	1.61E-05	1.73E-05
85	1.50E-05	1.61E-05	1.72E-05
86	1.50E-05	1.61E-05	1.72E-05
87	1.50E-05	1.61E-05	1.72E-05
88	1.49E-05	1.60E-05	1.72E-05
89	1.49E-05	1.60E-05	1.72E-05
90	1.49E-05	1.60E-05	1.72E-05
91	1.48E-05	1.60E-05	1.71E-05
92	1.48E-05	1.60E-05	1.71E-05
93	1.48E-05	1.59E-05	1.71E-05
94	1.48E-05	1.59E-05	1.71E-05
95	1.47E-05	1.59E-05	1.71E-05
96	1.47E-05	1.59E-05	1.71E-05
97	1.47E-05	1.59E-05	1.71E-05
98	1.46E-05	1.58E-05	1.71E-05
99	1.46E-05	1.58E-05	1.70E-05
100	1.46E-05	1.58E-05	1.70E-05
101	1.46E-05	1.58E-05	1.70E-05
102	1.45E-05	1.58E-05	1.70E-05
103	1.45E-05	1.58E-05	1.70E-05
104	1.45E-05	1.57E-05	1.70E-05
105	1.44E-05	1.57E-05	1.69E-05
106	1.44E-05	1.57E-05	1.69E-05
107	1.44E-05	1.57E-05	1.69E-05
108	1.43E-05	1.56E-05	1.69E-05
109	1.43E-05	1.56E-05	1.69E-05
110	1.43E-05	1.56E-05	1.69E-05
111	1.43E-05	1.56E-05	1.68E-05
112	1.42E-05	1.56E-05	1.68E-05
113	1.42E-05	1.56E-05	1.68E-05
114	1.42E-05	1.55E-05	1.68E-05
115	1.41E-05	1.55E-05	1.68E-05
116	1.41E-05	1.55E-05	1.68E-05
117	1.41E-05	1.55E-05	1.68E-05
118	1.41E-05	1.55E-05	1.67E-05
119	1.40E-05	1.55E-05	1.67E-05
120	1.40E-05	1.54E-05	1.67E-05
121	1.40E-05	1.54E-05	1.67E-05
122	1.39E-05	1.54E-05	1.67E-05
123	1.39E-05	1.54E-05	1.67E-05
124	1.39E-05	1.54E-05	1.66E-05
125	1.39E-05	1.53E-05	1.66E-05
126	1.38E-05	1.53E-05	1.66E-05

127	1.38E-05	1.53E-05	1.66E-05
128	1.38E-05	1.53E-05	1.66E-05
129	1.37E-05	1.53E-05	1.66E-05
130	1.37E-05	1.53E-05	1.65E-05
131	1.37E-05	1.52E-05	1.65E-05
132	1.37E-05	1.52E-05	1.65E-05
133	1.36E-05	1.52E-05	1.65E-05
134	1.36E-05	1.52E-05	1.65E-05
135	1.36E-05	1.52E-05	1.65E-05
136	1.35E-05	1.52E-05	1.65E-05
137	1.35E-05	1.51E-05	1.64E-05
138	1.35E-05	1.51E-05	1.64E-05
139	1.35E-05	1.51E-05	1.64E-05
140	1.34E-05	1.51E-05	1.64E-05
141	1.34E-05	1.51E-05	1.64E-05
142	1.34E-05	1.51E-05	1.64E-05
143	1.33E-05	1.50E-05	1.63E-05
144	1.33E-05	1.50E-05	1.63E-05
145	1.33E-05	1.50E-05	1.63E-05
146	1.33E-05	1.50E-05	1.63E-05
147	1.32E-05	1.50E-05	1.63E-05
148	1.32E-05	1.50E-05	1.63E-05
149	1.32E-05	1.49E-05	1.63E-05
150	1.32E-05	1.49E-05	1.62E-05
151	1.31E-05	1.49E-05	1.62E-05
152	1.31E-05	1.49E-05	1.62E-05
153	1.31E-05	1.49E-05	1.62E-05
154	1.30E-05	1.49E-05	1.62E-05
155	1.30E-05	1.48E-05	1.62E-05
156	1.30E-05	1.48E-05	1.61E-05
157	1.30E-05	1.48E-05	1.61E-05
158	1.29E-05	1.48E-05	1.61E-05
159	1.29E-05	1.48E-05	1.61E-05
160	1.29E-05	1.47E-05	1.61E-05
161	1.29E-05	1.47E-05	1.61E-05
162	1.28E-05	1.47E-05	1.60E-05
163	1.28E-05	1.47E-05	1.60E-05
164	1.28E-05	1.47E-05	1.60E-05
165	1.27E-05	1.47E-05	1.60E-05
166	1.27E-05	1.47E-05	1.60E-05
167	1.27E-05	1.46E-05	1.60E-05
168	1.27E-05	1.46E-05	1.60E-05
169	1.26E-05	1.46E-05	1.59E-05
170	1.26E-05	1.46E-05	1.59E-05

171	1.26E-05	1.46E-05	1.59E-05
172	1.26E-05	1.46E-05	1.59E-05
173	1.25E-05	1.46E-05	1.59E-05
174	1.25E-05	1.45E-05	1.59E-05
175	1.25E-05	1.45E-05	1.59E-05
176	1.25E-05	1.45E-05	1.58E-05
177	1.24E-05	1.45E-05	1.58E-05
178	1.24E-05	1.45E-05	1.58E-05
179	1.24E-05	1.45E-05	1.58E-05
180	1.24E-05	1.44E-05	1.58E-05
181	1.23E-05	1.44E-05	1.58E-05
182	1.23E-05	1.44E-05	1.58E-05
183	1.23E-05	1.44E-05	1.57E-05
184	1.23E-05	1.44E-05	1.57E-05
185	1.22E-05	1.44E-05	1.57E-05
186	1.22E-05	1.43E-05	1.57E-05
187	1.22E-05	1.43E-05	1.57E-05
188	1.22E-05	1.43E-05	1.57E-05
189	1.21E-05	1.43E-05	1.56E-05
190	1.21E-05	1.43E-05	1.56E-05
191	1.21E-05	1.43E-05	1.56E-05
192	1.21E-05	1.42E-05	1.56E-05
193	1.20E-05	1.42E-05	1.56E-05
194	1.20E-05	1.42E-05	1.56E-05
195	1.20E-05	1.42E-05	1.56E-05
196	1.20E-05	1.42E-05	1.55E-05
197	1.19E-05	1.42E-05	1.55E-05
198	1.19E-05	1.41E-05	1.55E-05
199	1.19E-05	1.41E-05	1.55E-05
200	1.19E-05	1.41E-05	1.55E-05
201	1.18E-05	1.41E-05	1.55E-05
202	1.18E-05	1.41E-05	1.54E-05
203	1.18E-05	1.41E-05	1.54E-05
204	1.18E-05	1.41E-05	1.54E-05
205	1.17E-05	1.40E-05	1.54E-05
206	1.17E-05	1.40E-05	1.54E-05
207	1.17E-05	1.40E-05	1.54E-05
208	1.17E-05	1.40E-05	1.54E-05
209	1.16E-05	1.40E-05	1.53E-05
210	1.16E-05	1.40E-05	1.53E-05
211	1.16E-05	1.40E-05	1.53E-05
212	1.16E-05	1.40E-05	1.53E-05
213	1.16E-05	1.39E-05	1.53E-05
214	1.15E-05	1.39E-05	1.53E-05

215	1.15E-05	1.39E-05	1.53E-05
216	1.15E-05	1.39E-05	1.52E-05
217	1.15E-05	1.39E-05	1.52E-05
218	1.14E-05	1.38E-05	1.52E-05
219	1.14E-05	1.38E-05	1.52E-05
220	1.14E-05	1.38E-05	1.52E-05
221	1.14E-05	1.38E-05	1.52E-05
222	1.13E-05	1.38E-05	1.52E-05
223	1.13E-05	1.38E-05	1.51E-05
224	1.13E-05	1.38E-05	1.51E-05
225	1.13E-05	1.38E-05	1.51E-05
226	1.13E-05	1.37E-05	1.51E-05
227	1.12E-05	1.37E-05	1.51E-05
228	1.12E-05	1.37E-05	1.51E-05
229	1.12E-05	1.37E-05	1.51E-05
230	1.12E-05	1.37E-05	1.51E-05
231	1.11E-05	1.37E-05	1.50E-05
232	1.11E-05	1.37E-05	1.50E-05
233	1.11E-05	1.37E-05	1.50E-05
234	1.11E-05	1.36E-05	1.50E-05
235	1.10E-05	1.36E-05	1.50E-05
236	1.10E-05	1.36E-05	1.50E-05
237	1.10E-05	1.36E-05	1.50E-05
238	1.10E-05	1.36E-05	1.50E-05
239	1.09E-05	1.36E-05	1.49E-05

Table B9: Average CO_2 concentration of four-hour White Hills experiments with high and low concentration CaOH water.

Time (min)	CaOHhigh	CaOH	CaOH + SCR	CaOH + SWR
0	1.88E-05	1.82E-05	1.89E-05	1.85E-05
1	1.76E-05	1.78E-05	1.86E-05	1.81E-05
2	1.67E-05	1.75E-05	1.84E-05	1.78E-05
3	1.58E-05	1.73E-05	1.82E-05	1.75E-05
4	1.50E-05	1.71E-05	1.79E-05	1.73E-05
5	1.42E-05	1.68E-05	1.77E-05	1.71E-05
6	1.35E-05	1.66E-05	1.75E-05	1.69E-05
7	1.29E-05	1.64E-05	1.73E-05	1.67E-05
8	1.22E-05	1.62E-05	1.71E-05	1.65E-05
9	1.16E-05	1.61E-05	1.69E-05	1.63E-05
10	1.11E-05	1.59E-05	1.68E-05	1.61E-05
11	1.05E-05	1.57E-05	1.66E-05	1.59E-05
12	1.00E-05	1.55E-05	1.64E-05	1.58E-05
13	9.56E-06	1.54E-05	1.63E-05	1.56E-05
14	9.11E-06	1.52E-05	1.61E-05	1.55E-05
15	8.70E-06	1.51E-05	1.60E-05	1.53E-05
16	8.29E-06	1.49E-05	1.58E-05	1.52E-05
17	7.92E-06	1.48E-05	1.57E-05	1.51E-05
18	7.57E-06	1.46E-05	1.56E-05	1.49E-05
19	7.23E-06	1.45E-05	1.54E-05	1.48E-05
20	6.90E-06	1.44E-05	1.53E-05	1.47E-05
21	6.60E-06	1.42E-05	1.52E-05	1.45E-05
22	6.32E-06	1.41E-05	1.50E-05	1.44E-05
23	6.03E-06	1.40E-05	1.49E-05	1.43E-05
24	5.78E-06	1.39E-05	1.48E-05	1.42E-05
25	5.53E-06	1.37E-05	1.47E-05	1.41E-05
26	5.29E-06	1.36E-05	1.46E-05	1.40E-05
27	5.07E-06	1.35E-05	1.45E-05	1.39E-05
28	4.85E-06	1.34E-05	1.44E-05	1.38E-05
29	4.64E-06	1.33E-05	1.43E-05	1.36E-05
30	4.44E-06	1.32E-05	1.42E-05	1.35E-05
31	4.27E-06	1.31E-05	1.41E-05	1.35E-05
32	4.08E-06	1.30E-05	1.39E-05	1.34E-05
33	3.91E-06	1.29E-05	1.39E-05	1.33E-05
34	3.75E-06	1.28E-05	1.37E-05	1.32E-05
35	3.60E-06	1.27E-05	1.37E-05	1.31E-05
36	3.44E-06	1.26E-05	1.36E-05	1.30E-05
37	3.31E-06	1.25E-05	1.35E-05	1.29E-05

38	3.17E-06	1.24E-05	1.34E-05	1.28E-05
39	3.04E-06	1.23E-05	1.33E-05	1.27E-05
40	2.92E-06	1.22E-05	1.32E-05	1.26E-05
41	2.81E-06	1.21E-05	1.31E-05	1.26E-05
42	2.70E-06	1.20E-05	1.30E-05	1.25E-05
43	2.59E-06	1.20E-05	1.29E-05	1.24E-05
44	2.49E-06	1.19E-05	1.29E-05	1.23E-05
45	2.39E-06	1.18E-05	1.28E-05	1.22E-05
46	2.29E-06	1.17E-05	1.27E-05	1.22E-05
47	2.20E-06	1.16E-05	1.26E-05	1.21E-05
48	2.12E-06	1.15E-05	1.25E-05	1.20E-05
49	2.04E-06	1.15E-05	1.25E-05	1.19E-05
50	1.96E-06	1.14E-05	1.24E-05	1.19E-05
51	1.89E-06	1.13E-05	1.23E-05	1.18E-05
52	1.82E-06	1.12E-05	1.22E-05	1.17E-05
53	1.75E-06	1.12E-05	1.21E-05	1.17E-05
54	1.68E-06	1.11E-05	1.21E-05	1.16E-05
55	1.62E-06	1.10E-05	1.20E-05	1.15E-05
56	1.56E-06	1.09E-05	1.19E-05	1.14E-05
57	1.50E-06	1.09E-05	1.18E-05	1.14E-05
58	1.45E-06	1.08E-05	1.18E-05	1.13E-05
59	1.39E-06	1.07E-05	1.17E-05	1.12E-05
60	1.34E-06	1.06E-05	1.16E-05	1.12E-05
61	1.30E-06	1.06E-05	1.16E-05	1.11E-05
62	1.25E-06	1.05E-05	1.15E-05	1.10E-05
63	1.21E-06	1.04E-05	1.14E-05	1.10E-05
64	1.17E-06	1.04E-05	1.14E-05	1.09E-05
65	1.13E-06	1.03E-05	1.13E-05	1.08E-05
66	1.09E-06	1.02E-05	1.12E-05	1.08E-05
67	1.05E-06	1.02E-05	1.12E-05	1.07E-05
68	1.02E-06	1.01E-05	1.11E-05	1.07E-05
69	9.81E-07	1.00E-05	1.10E-05	1.06E-05
70	9.53E-07	1.00E-05	1.10E-05	1.05E-05
71	9.24E-07	9.92E-06	1.09E-05	1.05E-05
72	8.93E-07	9.87E-06	1.08E-05	1.04E-05
73	8.71E-07	9.81E-06	1.08E-05	1.04E-05
74	8.45E-07	9.75E-06	1.07E-05	1.03E-05
75	8.17E-07	9.68E-06	1.07E-05	1.02E-05
76	7.84E-07	9.62E-06	1.06E-05	1.02E-05
77	7.70E-07	9.55E-06	1.05E-05	1.01E-05
78	7.45E-07	9.50E-06	1.05E-05	1.01E-05
79	7.20E-07	9.45E-06	1.04E-05	1.00E-05
80	7.01E-07	9.38E-06	1.04E-05	9.95E-06
81	6.87E-07	9.34E-06	1.03E-05	9.89E-06

82	6.67E-07	9.27E-06	1.03E-05	9.84E-06
83	6.48E-07	9.21E-06	1.02E-05	9.79E-06
84	6.29E-07	9.17E-06	1.02E-05	9.74E-06
85	6.12E-07	9.10E-06	1.01E-05	9.67E-06
86	5.95E-07	9.05E-06	1.00E-05	9.61E-06
87	5.83E-07	9.00E-06	9.98E-06	9.56E-06
88	5.66E-07	8.94E-06	9.94E-06	9.51E-06
89	5.50E-07	8.89E-06	9.88E-06	9.45E-06
90	5.37E-07	8.84E-06	9.82E-06	9.40E-06
91	5.31E-07	8.79E-06	9.77E-06	9.35E-06
92	5.14E-07	8.73E-06	9.72E-06	9.29E-06
93	5.03E-07	8.68E-06	9.66E-06	9.24E-06
94	4.95E-07	8.63E-06	9.62E-06	9.18E-06
95	4.84E-07	8.58E-06	9.56E-06	9.14E-06
96	4.71E-07	8.53E-06	9.51E-06	9.08E-06
97	4.62E-07	8.48E-06	9.47E-06	9.03E-06
98	4.54E-07	8.43E-06	9.41E-06	8.98E-06
99	4.48E-07	8.38E-06	9.37E-06	8.92E-06
100	4.38E-07	8.33E-06	9.32E-06	8.88E-06
101	4.33E-07	8.27E-06	9.26E-06	8.82E-06
102	4.21E-07	8.23E-06	9.22E-06	8.78E-06
103	4.20E-07	8.19E-06	9.17E-06	8.73E-06
104	4.08E-07	8.14E-06	9.13E-06	8.68E-06
105	4.00E-07	8.10E-06	9.08E-06	8.63E-06
106	3.94E-07	8.04E-06	9.03E-06	8.57E-06
107	3.88E-07	8.00E-06	8.98E-06	8.53E-06
108	3.78E-07	7.96E-06	8.93E-06	8.48E-06
109	3.77E-07	7.91E-06	8.90E-06	8.43E-06
110	3.68E-07	7.86E-06	8.85E-06	8.38E-06
111	3.67E-07	7.82E-06	8.80E-06	8.33E-06
112	3.61E-07	7.77E-06	8.75E-06	8.28E-06
113	3.58E-07	7.73E-06	8.71E-06	8.24E-06
114	3.49E-07	7.69E-06	8.67E-06	8.18E-06
115	3.50E-07	7.64E-06	8.63E-06	8.14E-06
116	3.42E-07	7.59E-06	8.58E-06	8.09E-06
117	3.43E-07	7.55E-06	8.54E-06	8.05E-06
118	3.35E-07	7.51E-06	8.49E-06	8.00E-06
119	3.29E-07	7.46E-06	8.45E-06	7.95E-06
120	3.30E-07	7.43E-06	8.41E-06	7.90E-06
121	3.27E-07	7.38E-06	8.36E-06	7.86E-06
122	3.23E-07	7.34E-06	8.32E-06	7.80E-06
123	3.20E-07	7.30E-06	8.29E-06	7.77E-06
124	3.18E-07	7.26E-06	8.24E-06	7.72E-06
125	3.10E-07	7.22E-06	8.20E-06	7.67E-06

126	3.13E-07	7.18E-06	8.16E-06	7.63E-06
127	3.05E-07	7.13E-06	8.12E-06	7.59E-06
128	3.06E-07	7.09E-06	8.07E-06	7.54E-06
129	3.05E-07	7.05E-06	8.04E-06	7.50E-06
130	3.06E-07	7.01E-06	7.99E-06	7.45E-06
131	2.98E-07	6.97E-06	7.96E-06	7.40E-06
132	2.98E-07	6.93E-06	7.92E-06	7.36E-06
133	2.97E-07	6.90E-06	7.87E-06	7.32E-06
134	2.98E-07	6.86E-06	7.83E-06	7.27E-06
135	2.95E-07	6.82E-06	7.80E-06	7.23E-06
136	2.96E-07	6.78E-06	7.76E-06	7.19E-06
137	2.89E-07	6.74E-06	7.72E-06	7.14E-06
138	2.87E-07	6.71E-06	7.69E-06	7.10E-06
139	2.88E-07	6.66E-06	7.65E-06	7.06E-06
140	2.87E-07	6.63E-06	7.62E-06	7.02E-06
141	2.81E-07	6.59E-06	7.57E-06	6.97E-06
142	2.90E-07	6.55E-06	7.54E-06	6.93E-06
143	2.80E-07	6.52E-06	7.50E-06	6.89E-06
144	2.79E-07	6.48E-06	7.46E-06	6.85E-06
145	2.79E-07	6.44E-06	7.43E-06	6.81E-06
146	2.83E-07	6.41E-06	7.40E-06	6.77E-06
147	2.79E-07	6.38E-06	7.36E-06	6.72E-06
148	2.75E-07	6.34E-06	7.32E-06	6.68E-06
149	2.75E-07	6.31E-06	7.29E-06	6.64E-06
150	2.74E-07	6.26E-06	7.25E-06	6.60E-06
151	2.75E-07	6.23E-06	7.22E-06	6.57E-06
152	2.73E-07	6.19E-06	7.19E-06	6.52E-06
153	2.76E-07	6.16E-06	7.14E-06	6.48E-06
154	2.71E-07	6.13E-06	7.12E-06	6.45E-06
155	2.71E-07	6.10E-06	7.08E-06	6.40E-06
156	2.78E-07	6.06E-06	7.04E-06	6.36E-06
157	2.76E-07	6.02E-06	7.01E-06	6.32E-06
158	2.72E-07	5.99E-06	6.98E-06	6.29E-06
159	2.71E-07	5.96E-06	6.95E-06	6.24E-06
160	2.66E-07	5.92E-06	6.90E-06	6.20E-06
161	2.68E-07	5.89E-06	6.88E-06	6.17E-06
162	2.64E-07	5.86E-06	6.84E-06	6.13E-06
163	2.66E-07	5.83E-06	6.81E-06	6.09E-06
164	2.63E-07	5.79E-06	6.78E-06	6.06E-06
165	2.66E-07	5.77E-06	6.74E-06	6.02E-06
166	2.66E-07	5.73E-06	6.72E-06	5.98E-06
167	2.69E-07	5.70E-06	6.68E-06	5.94E-06
168	2.63E-07	5.67E-06	6.65E-06	5.90E-06
169	2.64E-07	5.64E-06	6.62E-06	5.87E-06

170	2.68E-07	5.61E-06	6.58E-06	5.83E-06
171	2.66E-07	5.58E-06	6.55E-06	5.79E-06
172	2.64E-07	5.55E-06	6.53E-06	5.75E-06
173	2.69E-07	5.51E-06	6.49E-06	5.72E-06
174	2.62E-07	5.49E-06	6.46E-06	5.68E-06
175	2.63E-07	5.44E-06	6.44E-06	5.65E-06
176	2.66E-07	5.42E-06	6.40E-06	5.62E-06
177	2.65E-07	5.39E-06	6.37E-06	5.58E-06
178	2.65E-07	5.36E-06	6.34E-06	5.54E-06
179	2.63E-07	5.33E-06	6.31E-06	5.51E-06
180	2.61E-07	5.31E-06	6.28E-06	5.47E-06
181	2.57E-07	5.27E-06	6.25E-06	5.44E-06
182	2.62E-07	5.25E-06	6.23E-06	5.41E-06
183	2.61E-07	5.21E-06	6.20E-06	5.37E-06
184	2.62E-07	5.19E-06	6.17E-06	5.33E-06
185	2.60E-07	5.16E-06	6.14E-06	5.30E-06
186	2.60E-07	5.13E-06	6.11E-06	5.26E-06
187	2.62E-07	5.10E-06	6.08E-06	5.22E-06
188	2.63E-07	5.07E-06	6.05E-06	5.19E-06
189	2.61E-07	5.05E-06	6.02E-06	5.16E-06
190	2.65E-07	5.02E-06	6.00E-06	5.12E-06
191	2.61E-07	4.99E-06	5.96E-06	5.09E-06
192	2.63E-07	4.97E-06	5.94E-06	5.06E-06
193	2.64E-07	4.94E-06	5.92E-06	5.03E-06
194	2.63E-07	4.91E-06	5.89E-06	4.99E-06
195	2.65E-07	4.89E-06	5.86E-06	4.96E-06
196	2.62E-07	4.86E-06	5.83E-06	4.93E-06
197	2.65E-07	4.83E-06	5.81E-06	4.90E-06
198	2.63E-07	4.80E-06	5.78E-06	4.86E-06
199	2.58E-07	4.78E-06	5.75E-06	4.83E-06
200	2.64E-07	4.75E-06	5.73E-06	4.80E-06
201	2.60E-07	4.72E-06	5.69E-06	4.77E-06
202	2.61E-07	4.69E-06	5.67E-06	4.73E-06
203	2.59E-07	4.67E-06	5.65E-06	4.71E-06
204	2.61E-07	4.64E-06	5.61E-06	4.67E-06
205	2.60E-07	4.62E-06	5.59E-06	4.65E-06
206	2.61E-07	4.59E-06	5.56E-06	4.62E-06
207	2.61E-07	4.57E-06	5.53E-06	4.59E-06
208	2.63E-07	4.54E-06	5.51E-06	4.56E-06
209	2.65E-07	4.51E-06	5.48E-06	4.53E-06
210	2.65E-07	4.49E-06	5.46E-06	4.50E-06
211	2.62E-07	4.46E-06	5.43E-06	4.46E-06
212	2.62E-07	4.45E-06	5.41E-06	4.45E-06
213	2.63E-07	4.41E-06	5.38E-06	4.42E-06

214	2.67E-07	4.39E-06	5.36E-06	4.38E-06
215	2.64E-07	4.37E-06	5.33E-06	4.35E-06
216	2.62E-07	4.34E-06	5.31E-06	4.33E-06
217	2.64E-07	4.32E-06	5.28E-06	4.31E-06
218	2.62E-07	4.30E-06	5.25E-06	4.28E-06
219	2.62E-07	4.28E-06	5.23E-06	4.25E-06
220	2.64E-07	4.25E-06	5.20E-06	4.22E-06
221	2.67E-07	4.22E-06	5.19E-06	4.20E-06
222	2.63E-07	4.20E-06	5.16E-06	4.16E-06
223	2.69E-07	4.18E-06	5.14E-06	4.14E-06
224	2.65E-07	4.15E-06	5.12E-06	4.12E-06
225	2.64E-07	4.14E-06	5.08E-06	4.09E-06
226	2.67E-07	4.11E-06	5.06E-06	4.06E-06
227	2.63E-07	4.09E-06	5.04E-06	4.04E-06
228	2.67E-07	4.06E-06	5.01E-06	4.01E-06
229	2.68E-07	4.04E-06	4.99E-06	3.99E-06
230	2.68E-07	4.02E-06	4.96E-06	3.97E-06
231	2.68E-07	4.00E-06	4.94E-06	3.94E-06
232	2.65E-07	3.98E-06	4.93E-06	3.92E-06
233	2.67E-07	3.95E-06	4.90E-06	3.90E-06
234	2.67E-07	3.93E-06	4.88E-06	3.87E-06
235	2.71E-07	3.92E-06	4.85E-06	3.85E-06
236	2.66E-07	3.89E-06	4.83E-06	3.82E-06
237	2.68E-07	3.87E-06	4.81E-06	3.80E-06
238	2.72E-07	3.85E-06	4.79E-06	3.78E-06
239	2.69E-07	3.82E-06	4.76E-06	3.76E-06

Table B10: Average CO_2 concentration of four-hour White Hills experiments with high and low concentration CaOH water.

Time (min)	NaHCO3 + CaOHhigh (TL 5hrs)	NaHCO3 + CaOH + SCR	NaHCO3 + CaOH + SWR
0	1.83E-05	1.94E-05	1.82E-05
1	1.82E-05	1.94E-05	1.82E-05
2	1.81E-05	1.95E-05	1.90E-05
3	1.79E-05	1.96E-05	1.91E-05
4	1.78E-05	1.97E-05	1.92E-05
5	1.77E-05	1.98E-05	1.93E-05
6	1.76E-05	1.99E-05	1.94E-05
7	1.75E-05	1.99E-05	1.95E-05
8	1.74E-05	2.00E-05	1.96E-05
9	1.73E-05	2.01E-05	1.97E-05
10	1.72E-05	2.02E-05	1.98E-05
11	1.71E-05	2.02E-05	1.99E-05
12	1.70E-05	2.03E-05	2.00E-05
13	1.69E-05	2.04E-05	2.01E-05
14	1.68E-05	2.05E-05	2.02E-05
15	1.67E-05	2.05E-05	2.03E-05
16	1.66E-05	2.06E-05	2.04E-05
17	1.65E-05	2.07E-05	2.04E-05
18	1.64E-05	2.07E-05	2.05E-05
19	1.63E-05	2.08E-05	2.06E-05
20	1.62E-05	2.09E-05	2.07E-05
21	1.61E-05	2.09E-05	2.08E-05
22	1.60E-05	2.10E-05	2.08E-05
23	1.60E-05	2.10E-05	2.09E-05
24	1.59E-05	2.11E-05	2.10E-05
25	1.58E-05	2.12E-05	2.11E-05
26	1.57E-05	2.12E-05	2.11E-05
27	1.56E-05	2.13E-05	2.12E-05
28	1.55E-05	2.13E-05	2.13E-05
29	1.54E-05	2.14E-05	2.14E-05
30	1.53E-05	2.15E-05	2.14E-05
31	1.53E-05	2.15E-05	2.15E-05
32	1.52E-05	2.16E-05	2.16E-05
33	1.51E-05	2.16E-05	2.17E-05
34	1.50E-05	2.17E-05	2.17E-05
35	1.49E-05	2.17E-05	2.18E-05
36	1.49E-05	2.18E-05	2.19E-05

37	1.48E-05	2.19E-05	2.19E-05
38	1.47E-05	2.19E-05	2.20E-05
39	1.46E-05	2.20E-05	2.21E-05
40	1.45E-05	2.20E-05	2.21E-05
41	1.45E-05	2.21E-05	2.22E-05
42	1.44E-05	2.21E-05	2.23E-05
43	1.43E-05	2.22E-05	2.23E-05
44	1.42E-05	2.22E-05	2.24E-05
45	1.42E-05	2.23E-05	2.25E-05
46	1.41E-05	2.23E-05	2.25E-05
47	1.40E-05	2.24E-05	2.26E-05
48	1.39E-05	2.24E-05	2.26E-05
49	1.39E-05	2.25E-05	2.27E-05
50	1.38E-05	2.25E-05	2.28E-05
51	1.37E-05	2.26E-05	2.28E-05
52	1.36E-05	2.26E-05	2.29E-05
53	1.36E-05	2.27E-05	2.30E-05
54	1.35E-05	2.27E-05	2.30E-05
55	1.34E-05	2.28E-05	2.31E-05
56	1.34E-05	2.28E-05	2.31E-05
57	1.33E-05	2.29E-05	2.32E-05
58	1.32E-05	2.29E-05	2.32E-05
59	1.32E-05	2.30E-05	2.33E-05
60	1.31E-05	2.30E-05	2.34E-05
61	1.30E-05	2.31E-05	2.34E-05
62	1.30E-05	2.31E-05	2.35E-05
63	1.29E-05	2.32E-05	2.35E-05
64	1.28E-05	2.32E-05	2.36E-05
65	1.28E-05	2.32E-05	2.36E-05
66	1.27E-05	2.33E-05	2.37E-05
67	1.26E-05	2.33E-05	2.38E-05
68	1.26E-05	2.34E-05	2.38E-05
69	1.25E-05	2.34E-05	2.39E-05
70	1.24E-05	2.35E-05	2.39E-05
71	1.24E-05	2.35E-05	2.40E-05
72	1.23E-05	2.35E-05	2.40E-05
73	1.23E-05	2.36E-05	2.41E-05
74	1.22E-05	2.36E-05	2.41E-05
75	1.21E-05	2.37E-05	2.42E-05
76	1.21E-05	2.37E-05	2.42E-05
77	1.20E-05	2.38E-05	2.43E-05
78	1.20E-05	2.38E-05	2.44E-05
79	1.19E-05	2.39E-05	2.44E-05
80	1.18E-05	2.39E-05	2.45E-05

81	1.18E-05	2.39E-05	2.45E-05
82	1.17E-05	2.40E-05	2.46E-05
83	1.17E-05	2.40E-05	2.46E-05
84	1.16E-05	2.41E-05	2.47E-05
85	1.16E-05	2.41E-05	2.47E-05
86	1.15E-05	2.41E-05	2.48E-05
87	1.14E-05	2.42E-05	2.48E-05
88	1.14E-05	2.42E-05	2.49E-05
89	1.13E-05	2.43E-05	2.49E-05
90	1.13E-05	2.43E-05	2.50E-05
91	1.12E-05	2.43E-05	2.50E-05
92	1.12E-05	2.44E-05	2.51E-05
93	1.11E-05	2.44E-05	2.51E-05
94	1.10E-05	2.45E-05	2.52E-05
95	1.10E-05	2.45E-05	2.52E-05
96	1.09E-05	2.45E-05	2.53E-05
97	1.09E-05	2.46E-05	2.53E-05
98	1.08E-05	2.46E-05	2.54E-05
99	1.08E-05	2.47E-05	2.54E-05
100	1.07E-05	2.47E-05	2.55E-05
101	1.07E-05	2.47E-05	2.55E-05
102	1.06E-05	2.48E-05	2.55E-05
103	1.06E-05	2.48E-05	2.56E-05
104	1.05E-05	2.49E-05	2.56E-05
105	1.05E-05	2.49E-05	2.57E-05
106	1.04E-05	2.49E-05	2.57E-05
107	1.03E-05	2.50E-05	2.58E-05
108	1.03E-05	2.50E-05	2.58E-05
109	1.02E-05	2.50E-05	2.59E-05
110	1.02E-05	2.51E-05	2.59E-05
111	1.01E-05	2.51E-05	2.60E-05
112	1.01E-05	2.52E-05	2.60E-05
113	1.00E-05	2.52E-05	2.61E-05
114	9.99E-06	2.52E-05	2.61E-05
115	9.94E-06	2.53E-05	2.62E-05
116	9.89E-06	2.53E-05	2.62E-05
117	9.84E-06	2.53E-05	2.63E-05
118	9.79E-06	2.54E-05	2.63E-05
119	9.74E-06	2.54E-05	2.63E-05
120	9.69E-06	2.55E-05	2.64E-05
121	9.64E-06	2.55E-05	2.64E-05
122	9.59E-06	2.55E-05	2.65E-05
123	9.54E-06	2.56E-05	2.65E-05
124	9.49E-06	2.56E-05	2.66E-05

125	9.45E-06	2.56E-05	2.66E-05
126	9.39E-06	2.57E-05	2.67E-05
127	9.35E-06	2.57E-05	2.67E-05
128	9.30E-06	2.58E-05	2.68E-05
129	9.26E-06	2.58E-05	2.68E-05
130	9.21E-06	2.58E-05	2.69E-05
131	9.17E-06	2.59E-05	2.69E-05
132	9.12E-06	2.59E-05	2.70E-05
133	9.07E-06	2.59E-05	2.70E-05
134	9.03E-06	2.60E-05	2.70E-05
135	8.97E-06	2.60E-05	2.71E-05
136	8.93E-06	2.60E-05	2.71E-05
137	8.89E-06	2.61E-05	2.72E-05
138	8.85E-06	2.61E-05	2.72E-05
139	8.80E-06	2.62E-05	2.73E-05
140	8.75E-06	2.62E-05	2.73E-05
141	8.72E-06	2.62E-05	2.74E-05
142	8.67E-06	2.63E-05	2.74E-05
143	8.62E-06	2.63E-05	2.75E-05
144	8.58E-06	2.64E-05	2.75E-05
145	8.54E-06	2.64E-05	2.76E-05
146	8.49E-06	2.64E-05	2.76E-05
147	8.46E-06	2.65E-05	2.76E-05
148	8.41E-06	2.65E-05	2.77E-05
149	8.37E-06	2.65E-05	2.77E-05
150	8.32E-06	2.66E-05	2.78E-05
151	8.29E-06	2.66E-05	2.78E-05
152	8.24E-06	2.67E-05	2.79E-05
153	8.21E-06	2.67E-05	2.79E-05
154	8.16E-06	2.67E-05	2.80E-05
155	8.12E-06	2.67E-05	2.80E-05
156	8.08E-06	2.68E-05	2.81E-05
157	8.04E-06	2.68E-05	2.81E-05
158	8.00E-06	2.69E-05	2.82E-05
159	7.95E-06	2.69E-05	2.82E-05
160	7.92E-06	2.69E-05	2.83E-05
161	7.88E-06	2.70E-05	2.83E-05
162	7.84E-06	2.70E-05	2.84E-05
163	7.81E-06	2.70E-05	2.84E-05
164	7.77E-06	2.71E-05	2.85E-05
165	7.72E-06	2.71E-05	2.85E-05
166	7.69E-06	2.72E-05	2.86E-05
167	7.65E-06	2.72E-05	2.86E-05
168	7.62E-06	2.72E-05	2.87E-05

169	7.58E-06	2.73E-05	2.87E-05
170	7.54E-06	2.73E-05	2.88E-05
171	7.50E-06	2.73E-05	2.88E-05
172	7.47E-06	2.74E-05	2.89E-05
173	7.43E-06	2.74E-05	2.89E-05
174	7.39E-06	2.75E-05	2.90E-05
175	7.35E-06	2.75E-05	2.90E-05
176	7.32E-06	2.75E-05	2.91E-05
177	7.28E-06	2.76E-05	2.91E-05
178	7.26E-06	2.76E-05	2.92E-05
179	7.21E-06	2.76E-05	2.92E-05
180	7.18E-06	2.77E-05	2.92E-05
181	7.14E-06	2.77E-05	2.93E-05
182	7.11E-06	2.78E-05	2.94E-05
183	7.07E-06	2.78E-05	2.94E-05
184	7.04E-06	2.78E-05	2.95E-05
185	7.01E-06	2.79E-05	2.95E-05
186	6.98E-06	2.79E-05	2.96E-05
187	6.94E-06	2.79E-05	2.96E-05
188	6.91E-06	2.80E-05	2.96E-05
189	6.88E-06	2.80E-05	2.97E-05
190	6.85E-06	2.80E-05	2.97E-05
191	6.81E-06	2.81E-05	2.98E-05
192	6.78E-06	2.81E-05	2.99E-05
193	6.75E-06	2.82E-05	2.99E-05
194	6.71E-06	2.82E-05	2.99E-05
195	6.69E-06	2.82E-05	3.00E-05
196	6.65E-06	2.83E-05	3.00E-05
197	6.62E-06	2.83E-05	3.01E-05
198	6.58E-06	2.83E-05	3.02E-05
199	6.55E-06	2.84E-05	3.02E-05
200	6.53E-06	2.84E-05	3.02E-05
201	6.49E-06	2.84E-05	3.03E-05
202	6.46E-06	2.85E-05	3.03E-05
203	6.43E-06	2.85E-05	3.04E-05
204	6.40E-06	2.86E-05	3.04E-05
205	6.37E-06	2.86E-05	3.05E-05
206	6.35E-06	2.86E-05	3.05E-05
207	6.32E-06	2.87E-05	3.06E-05
208	6.29E-06	2.87E-05	3.06E-05
209	6.26E-06	2.87E-05	3.07E-05
210	6.23E-06	2.88E-05	3.07E-05
211	6.20E-06	2.88E-05	3.08E-05
212	6.17E-06	2.88E-05	3.08E-05

213	6.14E-06	2.89E-05	3.09E-05
214	6.11E-06	2.89E-05	3.09E-05
215	6.08E-06	2.90E-05	3.10E-05
216	6.05E-06	2.90E-05	3.10E-05
217	6.02E-06	2.90E-05	3.11E-05
218	5.99E-06	2.91E-05	3.11E-05
219	5.97E-06	2.91E-05	3.12E-05
220	5.94E-06	2.91E-05	3.12E-05
221	5.91E-06	2.92E-05	3.13E-05
222	5.89E-06	2.92E-05	3.13E-05
223	5.86E-06	2.92E-05	3.14E-05
224	5.84E-06	2.92E-05	3.14E-05
225	5.81E-06	2.93E-05	3.15E-05
226	5.79E-06	2.93E-05	3.15E-05
227	5.76E-06	2.94E-05	3.16E-05
228	5.73E-06	2.94E-05	3.16E-05
229	5.71E-06	2.94E-05	3.16E-05
230	5.68E-06	2.95E-05	3.17E-05
231	5.66E-06	2.95E-05	3.17E-05
232	5.63E-06	2.96E-05	3.18E-05
233	5.61E-06	2.96E-05	3.19E-05
234	5.57E-06	2.96E-05	3.19E-05
235	5.55E-06	2.96E-05	3.19E-05
236	5.53E-06	2.97E-05	3.20E-05
237	5.51E-06	2.97E-05	3.20E-05
238	5.48E-06	2.97E-05	3.21E-05
239	5.45E-06	2.98E-05	3.21E-05

Table B11: Average CO_2 concentration of four-hour White Hills experiments with elevated CO_2 concentration and Mg-rich water.

Time (min)	NaHCO3 + MgOH (TL 5hrs)	NaHCO3 + MgOH + TCR	NaHCO3 + MgOH + TWR
0	1.77E-05	1.83E-05	1.82E-05
1	1.79E-05	1.83E-05	1.80E-05
2	1.80E-05	1.85E-05	1.82E-05
3	1.82E-05	1.86E-05	1.83E-05
4	1.83E-05	1.87E-05	1.84E-05
5	1.84E-05	1.88E-05	1.85E-05
6	1.85E-05	1.89E-05	1.86E-05
7	1.86E-05	1.90E-05	1.87E-05
8	1.87E-05	1.91E-05	1.88E-05
9	1.88E-05	1.92E-05	1.89E-05
10	1.89E-05	1.93E-05	1.90E-05
11	1.90E-05	1.94E-05	1.90E-05
12	1.91E-05	1.95E-05	1.91E-05
13	1.92E-05	1.96E-05	1.92E-05
14	1.93E-05	1.97E-05	1.93E-05
15	1.94E-05	1.98E-05	1.94E-05
16	1.95E-05	1.98E-05	1.94E-05
17	1.96E-05	1.99E-05	1.95E-05
18	1.96E-05	2.00E-05	1.96E-05
19	1.97E-05	2.01E-05	1.97E-05
20	1.98E-05	2.02E-05	1.97E-05
21	1.99E-05	2.02E-05	1.98E-05
22	1.99E-05	2.03E-05	1.99E-05
23	2.00E-05	2.04E-05	2.00E-05
24	2.01E-05	2.05E-05	2.00E-05
25	2.02E-05	2.05E-05	2.01E-05
26	2.03E-05	2.06E-05	2.01E-05
27	2.03E-05	2.07E-05	2.02E-05
28	2.04E-05	2.08E-05	2.03E-05
29	2.05E-05	2.08E-05	2.03E-05
30	2.05E-05	2.09E-05	2.04E-05
31	2.06E-05	2.10E-05	2.05E-05
32	2.07E-05	2.10E-05	2.05E-05
33	2.07E-05	2.11E-05	2.06E-05
34	2.08E-05	2.12E-05	2.06E-05
35	2.09E-05	2.12E-05	2.07E-05
36	2.10E-05	2.13E-05	2.08E-05

37	2.10E-05	2.14E-05	2.08E-05
38	2.11E-05	2.14E-05	2.09E-05
39	2.11E-05	2.15E-05	2.10E-05
40	2.12E-05	2.16E-05	2.10E-05
41	2.13E-05	2.16E-05	2.11E-05
42	2.13E-05	2.17E-05	2.11E-05
43	2.14E-05	2.17E-05	2.12E-05
44	2.15E-05	2.18E-05	2.13E-05
45	2.15E-05	2.19E-05	2.13E-05
46	2.16E-05	2.19E-05	2.14E-05
47	2.16E-05	2.20E-05	2.14E-05
48	2.17E-05	2.20E-05	2.15E-05
49	2.18E-05	2.21E-05	2.15E-05
50	2.18E-05	2.22E-05	2.16E-05
51	2.19E-05	2.22E-05	2.16E-05
52	2.19E-05	2.23E-05	2.17E-05
53	2.20E-05	2.23E-05	2.18E-05
54	2.21E-05	2.24E-05	2.18E-05
55	2.21E-05	2.24E-05	2.19E-05
56	2.22E-05	2.25E-05	2.19E-05
57	2.22E-05	2.26E-05	2.20E-05
58	2.23E-05	2.26E-05	2.20E-05
59	2.24E-05	2.27E-05	2.21E-05
60	2.24E-05	2.27E-05	2.21E-05
61	2.25E-05	2.28E-05	2.22E-05
62	2.25E-05	2.28E-05	2.22E-05
63	2.26E-05	2.29E-05	2.23E-05
64	2.26E-05	2.30E-05	2.23E-05
65	2.27E-05	2.30E-05	2.24E-05
66	2.27E-05	2.31E-05	2.24E-05
67	2.28E-05	2.31E-05	2.25E-05
68	2.28E-05	2.32E-05	2.25E-05
69	2.29E-05	2.32E-05	2.26E-05
70	2.30E-05	2.33E-05	2.26E-05
71	2.30E-05	2.33E-05	2.27E-05
72	2.31E-05	2.34E-05	2.27E-05
73	2.31E-05	2.34E-05	2.28E-05
74	2.32E-05	2.35E-05	2.28E-05
75	2.32E-05	2.35E-05	2.29E-05
76	2.33E-05	2.36E-05	2.29E-05
77	2.33E-05	2.36E-05	2.30E-05
78	2.34E-05	2.37E-05	2.30E-05
79	2.34E-05	2.37E-05	2.31E-05
80	2.35E-05	2.38E-05	2.31E-05

81	2.35E-05	2.38E-05	2.32E-05
82	2.36E-05	2.39E-05	2.32E-05
83	2.36E-05	2.39E-05	2.33E-05
84	2.37E-05	2.40E-05	2.33E-05
85	2.37E-05	2.40E-05	2.34E-05
86	2.38E-05	2.41E-05	2.34E-05
87	2.38E-05	2.41E-05	2.35E-05
88	2.39E-05	2.42E-05	2.35E-05
89	2.39E-05	2.42E-05	2.36E-05
90	2.40E-05	2.43E-05	2.36E-05
91	2.40E-05	2.43E-05	2.36E-05
92	2.41E-05	2.44E-05	2.37E-05
93	2.41E-05	2.44E-05	2.37E-05
94	2.42E-05	2.45E-05	2.38E-05
95	2.42E-05	2.45E-05	2.38E-05
96	2.43E-05	2.46E-05	2.39E-05
97	2.43E-05	2.46E-05	2.39E-05
98	2.43E-05	2.47E-05	2.40E-05
99	2.44E-05	2.47E-05	2.40E-05
100	2.44E-05	2.47E-05	2.41E-05
101	2.45E-05	2.48E-05	2.41E-05
102	2.45E-05	2.48E-05	2.42E-05
103	2.46E-05	2.49E-05	2.42E-05
104	2.46E-05	2.49E-05	2.42E-05
105	2.47E-05	2.50E-05	2.43E-05
106	2.47E-05	2.50E-05	2.43E-05
107	2.48E-05	2.51E-05	2.44E-05
108	2.48E-05	2.51E-05	2.44E-05
109	2.49E-05	2.52E-05	2.45E-05
110	2.49E-05	2.52E-05	2.45E-05
111	2.49E-05	2.53E-05	2.45E-05
112	2.50E-05	2.53E-05	2.46E-05
113	2.50E-05	2.54E-05	2.46E-05
114	2.51E-05	2.54E-05	2.47E-05
115	2.51E-05	2.54E-05	2.47E-05
116	2.52E-05	2.55E-05	2.48E-05
117	2.52E-05	2.55E-05	2.48E-05
118	2.52E-05	2.56E-05	2.48E-05
119	2.53E-05	2.56E-05	2.49E-05
120	2.53E-05	2.57E-05	2.49E-05
121	2.54E-05	2.57E-05	2.50E-05
122	2.54E-05	2.58E-05	2.50E-05
123	2.55E-05	2.58E-05	2.51E-05
124	2.55E-05	2.59E-05	2.51E-05

125	2.55E-05	2.59E-05	2.51E-05
126	2.56E-05	2.59E-05	2.52E-05
127	2.56E-05	2.60E-05	2.52E-05
128	2.57E-05	2.60E-05	2.53E-05
129	2.57E-05	2.61E-05	2.53E-05
130	2.57E-05	2.61E-05	2.53E-05
131	2.58E-05	2.61E-05	2.54E-05
132	2.58E-05	2.62E-05	2.54E-05
133	2.59E-05	2.62E-05	2.55E-05
134	2.59E-05	2.63E-05	2.55E-05
135	2.60E-05	2.63E-05	2.55E-05
136	2.60E-05	2.64E-05	2.56E-05
137	2.60E-05	2.64E-05	2.56E-05
138	2.61E-05	2.65E-05	2.57E-05
139	2.61E-05	2.65E-05	2.57E-05
140	2.62E-05	2.65E-05	2.57E-05
141	2.62E-05	2.66E-05	2.58E-05
142	2.62E-05	2.66E-05	2.58E-05
143	2.63E-05	2.67E-05	2.59E-05
144	2.63E-05	2.67E-05	2.59E-05
145	2.64E-05	2.68E-05	2.59E-05
146	2.64E-05	2.68E-05	2.60E-05
147	2.64E-05	2.68E-05	2.60E-05
148	2.65E-05	2.69E-05	2.61E-05
149	2.65E-05	2.69E-05	2.61E-05
150	2.66E-05	2.70E-05	2.61E-05
151	2.66E-05	2.70E-05	2.62E-05
152	2.66E-05	2.70E-05	2.62E-05
153	2.67E-05	2.71E-05	2.63E-05
154	2.67E-05	2.71E-05	2.63E-05
155	2.68E-05	2.72E-05	2.63E-05
156	2.68E-05	2.72E-05	2.64E-05
157	2.68E-05	2.73E-05	2.64E-05
158	2.69E-05	2.73E-05	2.65E-05
159	2.69E-05	2.73E-05	2.65E-05
160	2.70E-05	2.74E-05	2.65E-05
161	2.70E-05	2.74E-05	2.66E-05
162	2.70E-05	2.75E-05	2.66E-05
163	2.71E-05	2.75E-05	2.66E-05
164	2.71E-05	2.75E-05	2.67E-05
165	2.71E-05	2.76E-05	2.67E-05
166	2.72E-05	2.76E-05	2.68E-05
167	2.72E-05	2.77E-05	2.68E-05
168	2.72E-05	2.77E-05	2.68E-05

169	2.73E-05	2.77E-05	2.69E-05
170	2.73E-05	2.78E-05	2.69E-05
171	2.74E-05	2.78E-05	2.69E-05
172	2.74E-05	2.79E-05	2.70E-05
173	2.74E-05	2.79E-05	2.70E-05
174	2.75E-05	2.79E-05	2.71E-05
175	2.75E-05	2.80E-05	2.71E-05
176	2.75E-05	2.80E-05	2.72E-05
177	2.76E-05	2.81E-05	2.72E-05
178	2.76E-05	2.81E-05	2.72E-05
179	2.77E-05	2.81E-05	2.72E-05
180	2.77E-05	2.82E-05	2.73E-05
181	2.77E-05	2.82E-05	2.73E-05
182	2.78E-05	2.83E-05	2.74E-05
183	2.78E-05	2.83E-05	2.74E-05
184	2.78E-05	2.84E-05	2.74E-05
185	2.79E-05	2.84E-05	2.75E-05
186	2.79E-05	2.84E-05	2.75E-05
187	2.79E-05	2.85E-05	2.75E-05
188	2.80E-05	2.85E-05	2.76E-05
189	2.80E-05	2.85E-05	2.76E-05
190	2.80E-05	2.86E-05	2.76E-05
191	2.81E-05	2.86E-05	2.77E-05
192	2.81E-05	2.87E-05	2.77E-05
193	2.81E-05	2.87E-05	2.78E-05
194	2.82E-05	2.87E-05	2.78E-05
195	2.82E-05	2.88E-05	2.79E-05
196	2.83E-05	2.88E-05	2.79E-05
197	2.83E-05	2.89E-05	2.79E-05
198	2.83E-05	2.89E-05	2.79E-05
199	2.84E-05	2.89E-05	2.80E-05
200	2.84E-05	2.90E-05	2.80E-05
201	2.84E-05	2.90E-05	2.80E-05
202	2.85E-05	2.91E-05	2.81E-05
203	2.85E-05	2.91E-05	2.81E-05
204	2.85E-05	2.91E-05	2.81E-05
205	2.86E-05	2.92E-05	2.82E-05
206	2.86E-05	2.92E-05	2.82E-05
207	2.86E-05	2.92E-05	2.83E-05
208	2.87E-05	2.93E-05	2.83E-05
209	2.87E-05	2.93E-05	2.83E-05
210	2.87E-05	2.94E-05	2.84E-05
211	2.88E-05	2.94E-05	2.84E-05
212	2.88E-05	2.94E-05	2.85E-05

213	2.88E-05	2.95E-05	2.85E-05
214	2.89E-05	2.95E-05	2.85E-05
215	2.89E-05	2.96E-05	2.86E-05
216	2.89E-05	2.96E-05	2.86E-05
217	2.90E-05	2.96E-05	2.86E-05
218	2.90E-05	2.97E-05	2.87E-05
219	2.90E-05	2.97E-05	2.87E-05
220	2.91E-05	2.98E-05	2.87E-05
221	2.91E-05	2.98E-05	2.88E-05
222	2.91E-05	2.98E-05	2.88E-05
223	2.92E-05	2.99E-05	2.88E-05
224	2.92E-05	2.99E-05	2.89E-05
225	2.92E-05	2.99E-05	2.89E-05
226	2.93E-05	3.00E-05	2.89E-05
227	2.93E-05	3.00E-05	2.90E-05
228	2.93E-05	3.01E-05	2.90E-05
229	2.94E-05	3.01E-05	2.91E-05
230	2.94E-05	3.01E-05	2.91E-05
231	2.94E-05	3.02E-05	2.91E-05
232	2.95E-05	3.02E-05	2.92E-05
233	2.95E-05	3.02E-05	2.92E-05
234	2.95E-05	3.03E-05	2.92E-05
235	2.96E-05	3.03E-05	2.93E-05
236	2.96E-05	3.03E-05	2.93E-05
237	2.96E-05	3.04E-05	2.93E-05
238	2.97E-05	3.04E-05	2.94E-05
239	2.97E-05	3.05E-05	2.94E-05

Table B12: Average CO_2 concentration of four-hour White Hills experiments with elevated CO_2 concentration and DI water.

Time (min)	NaHCO3 + DI (TL 5hrs)	NaHCO3 + DI + SCR	NaHCO3 + DI + SWR
0	1.81E-05	1.88E-05	1.82E-05
1	1.84E-05	1.88E-05	1.83E-05
2	1.86E-05	1.90E-05	1.85E-05
3	1.89E-05	1.91E-05	1.87E-05
4	1.91E-05	1.93E-05	1.89E-05
5	1.93E-05	1.94E-05	1.91E-05
6	1.95E-05	1.95E-05	1.92E-05
7	1.97E-05	1.97E-05	1.94E-05
8	1.99E-05	1.98E-05	1.96E-05
9	2.00E-05	1.99E-05	1.97E-05
10	2.02E-05	2.00E-05	1.99E-05
11	2.04E-05	2.01E-05	2.00E-05
12	2.06E-05	2.02E-05	2.02E-05
13	2.07E-05	2.03E-05	2.03E-05
14	2.09E-05	2.04E-05	2.04E-05
15	2.10E-05	2.06E-05	2.06E-05
16	2.12E-05	2.06E-05	2.07E-05
17	2.14E-05	2.07E-05	2.08E-05
18	2.15E-05	2.08E-05	2.10E-05
19	2.17E-05	2.09E-05	2.11E-05
20	2.18E-05	2.10E-05	2.12E-05
21	2.20E-05	2.11E-05	2.13E-05
22	2.21E-05	2.12E-05	2.14E-05
23	2.22E-05	2.13E-05	2.16E-05
24	2.24E-05	2.14E-05	2.17E-05
25	2.25E-05	2.15E-05	2.18E-05
26	2.27E-05	2.16E-05	2.19E-05
27	2.28E-05	2.17E-05	2.20E-05
28	2.30E-05	2.17E-05	2.21E-05
29	2.31E-05	2.18E-05	2.23E-05
30	2.32E-05	2.19E-05	2.24E-05
31	2.34E-05	2.20E-05	2.25E-05
32	2.35E-05	2.20E-05	2.26E-05
33	2.36E-05	2.21E-05	2.27E-05
34	2.38E-05	2.22E-05	2.28E-05
35	2.39E-05	2.23E-05	2.29E-05
36	2.40E-05	2.24E-05	2.30E-05

37	2.41E-05	2.24E-05	2.31E-05
38	2.43E-05	2.25E-05	2.32E-05
39	2.44E-05	2.26E-05	2.33E-05
40	2.45E-05	2.27E-05	2.34E-05
41	2.47E-05	2.27E-05	2.35E-05
42	2.48E-05	2.28E-05	2.36E-05
43	2.49E-05	2.29E-05	2.37E-05
44	2.50E-05	2.30E-05	2.38E-05
45	2.51E-05	2.30E-05	2.39E-05
46	2.53E-05	2.31E-05	2.40E-05
47	2.54E-05	2.32E-05	2.41E-05
48	2.55E-05	2.32E-05	2.42E-05
49	2.56E-05	2.33E-05	2.43E-05
50	2.58E-05	2.34E-05	2.44E-05
51	2.59E-05	2.35E-05	2.45E-05
52	2.60E-05	2.35E-05	2.46E-05
53	2.61E-05	2.36E-05	2.47E-05
54	2.62E-05	2.37E-05	2.48E-05
55	2.63E-05	2.37E-05	2.49E-05
56	2.65E-05	2.38E-05	2.50E-05
57	2.66E-05	2.39E-05	2.51E-05
58	2.67E-05	2.39E-05	2.52E-05
59	2.68E-05	2.40E-05	2.53E-05
60	2.69E-05	2.41E-05	2.54E-05
61	2.70E-05	2.41E-05	2.55E-05
62	2.71E-05	2.42E-05	2.56E-05
63	2.73E-05	2.43E-05	2.57E-05
64	2.74E-05	2.43E-05	2.58E-05
65	2.75E-05	2.44E-05	2.59E-05
66	2.76E-05	2.45E-05	2.60E-05
67	2.77E-05	2.45E-05	2.60E-05
68	2.78E-05	2.46E-05	2.61E-05
69	2.79E-05	2.47E-05	2.62E-05
70	2.80E-05	2.47E-05	2.63E-05
71	2.81E-05	2.48E-05	2.64E-05
72	2.82E-05	2.49E-05	2.65E-05
73	2.84E-05	2.49E-05	2.66E-05
74	2.85E-05	2.50E-05	2.67E-05
75	2.86E-05	2.51E-05	2.68E-05
76	2.87E-05	2.51E-05	2.69E-05
77	2.88E-05	2.52E-05	2.70E-05
78	2.89E-05	2.52E-05	2.70E-05
79	2.90E-05	2.53E-05	2.71E-05
80	2.91E-05	2.54E-05	2.72E-05

81	2.92E-05	2.54E-05	2.73E-05
82	2.93E-05	2.55E-05	2.74E-05
83	2.94E-05	2.55E-05	2.75E-05
84	2.96E-05	2.56E-05	2.76E-05
85	2.97E-05	2.57E-05	2.76E-05
86	2.97E-05	2.57E-05	2.78E-05
87	2.99E-05	2.58E-05	2.78E-05
88	3.00E-05	2.59E-05	2.79E-05
89	3.01E-05	2.59E-05	2.80E-05
90	3.02E-05	2.60E-05	2.81E-05
91	3.03E-05	2.60E-05	2.82E-05
92	3.04E-05	2.61E-05	2.83E-05
93	3.05E-05	2.62E-05	2.83E-05
94	3.06E-05	2.62E-05	2.84E-05
95	3.07E-05	2.63E-05	2.85E-05
96	3.08E-05	2.63E-05	2.86E-05
97	3.09E-05	2.64E-05	2.87E-05
98	3.10E-05	2.65E-05	2.88E-05
99	3.11E-05	2.65E-05	2.88E-05
100	3.12E-05	2.66E-05	2.89E-05
101	3.13E-05	2.66E-05	2.90E-05
102	3.14E-05	2.67E-05	2.91E-05
103	3.15E-05	2.68E-05	2.92E-05
104	3.16E-05	2.68E-05	2.93E-05
105	3.17E-05	2.69E-05	2.94E-05
106	3.18E-05	2.69E-05	2.94E-05
107	3.19E-05	2.70E-05	2.95E-05
108	3.20E-05	2.70E-05	2.96E-05
109	3.21E-05	2.71E-05	2.97E-05
110	3.22E-05	2.72E-05	2.97E-05
111	3.23E-05	2.72E-05	2.98E-05
112	3.24E-05	2.73E-05	2.99E-05
113	3.25E-05	2.73E-05	3.00E-05
114	3.26E-05	2.74E-05	3.01E-05
115	3.27E-05	2.75E-05	3.02E-05
116	3.28E-05	2.75E-05	3.02E-05
117	3.28E-05	2.76E-05	3.03E-05
118	3.29E-05	2.76E-05	3.04E-05
119	3.30E-05	2.77E-05	3.05E-05
120	3.31E-05	2.77E-05	3.06E-05
121	3.32E-05	2.78E-05	3.06E-05
122	3.33E-05	2.79E-05	3.07E-05
123	3.34E-05	2.79E-05	3.08E-05
124	3.35E-05	2.80E-05	3.09E-05

125	3.36E-05	2.80E-05	3.09E-05
126	3.37E-05	2.81E-05	3.10E-05
127	3.38E-05	2.81E-05	3.11E-05
128	3.39E-05	2.82E-05	3.12E-05
129	3.40E-05	2.83E-05	3.12E-05
130	3.41E-05	2.83E-05	3.13E-05
131	3.41E-05	2.84E-05	3.14E-05
132	3.42E-05	2.84E-05	3.15E-05
133	3.43E-05	2.85E-05	3.16E-05
134	3.44E-05	2.85E-05	3.16E-05
135	3.45E-05	2.86E-05	3.17E-05
136	3.46E-05	2.87E-05	3.18E-05
137	3.47E-05	2.87E-05	3.19E-05
138	3.48E-05	2.88E-05	3.19E-05
139	3.49E-05	2.88E-05	3.20E-05
140	3.50E-05	2.89E-05	3.21E-05
141	3.51E-05	2.89E-05	3.22E-05
142	3.52E-05	2.90E-05	3.22E-05
143	3.52E-05	2.91E-05	3.23E-05
144	3.53E-05	2.91E-05	3.24E-05
145	3.54E-05	2.91E-05	3.25E-05
146	3.55E-05	2.92E-05	3.25E-05
147	3.56E-05	2.93E-05	3.26E-05
148	3.57E-05	2.93E-05	3.27E-05
149	3.58E-05	2.94E-05	3.28E-05
150	3.59E-05	2.94E-05	3.28E-05
151	3.59E-05	2.95E-05	3.29E-05
152	3.60E-05	2.96E-05	3.30E-05
153	3.61E-05	2.96E-05	3.31E-05
154	3.62E-05	2.97E-05	3.31E-05
155	3.63E-05	2.97E-05	3.32E-05
156	3.64E-05	2.98E-05	3.33E-05
157	3.65E-05	2.98E-05	3.34E-05
158	3.66E-05	2.99E-05	3.34E-05
159	3.67E-05	2.99E-05	3.35E-05
160	3.67E-05	3.00E-05	3.36E-05
161	3.68E-05	3.00E-05	3.37E-05
162	3.69E-05	3.01E-05	3.37E-05
163	3.70E-05	3.02E-05	3.38E-05
164	3.71E-05	3.02E-05	3.39E-05
165	3.72E-05	3.03E-05	3.39E-05
166	3.72E-05	3.03E-05	3.40E-05
167	3.73E-05	3.04E-05	3.41E-05
168	3.74E-05	3.04E-05	3.42E-05

169	3.75E-05	3.05E-05	3.42E-05
170	3.76E-05	3.05E-05	3.43E-05
171	3.77E-05	3.06E-05	3.44E-05
172	3.78E-05	3.06E-05	3.44E-05
173	3.78E-05	3.07E-05	3.45E-05
174	3.79E-05	3.07E-05	3.46E-05
175	3.80E-05	3.08E-05	3.46E-05
176	3.81E-05	3.08E-05	3.47E-05
177	3.82E-05	3.09E-05	3.48E-05
178	3.83E-05	3.10E-05	3.49E-05
179	3.83E-05	3.10E-05	3.49E-05
180	3.84E-05	3.11E-05	3.50E-05
181	3.85E-05	3.11E-05	3.51E-05
182	3.86E-05	3.12E-05	3.51E-05
183	3.87E-05	3.12E-05	3.52E-05
184	3.88E-05	3.13E-05	3.53E-05
185	3.88E-05	3.13E-05	3.53E-05
186	3.89E-05	3.14E-05	3.54E-05
187	3.90E-05	3.14E-05	3.55E-05
188	3.91E-05	3.15E-05	3.56E-05
189	3.92E-05	3.15E-05	3.56E-05
190	3.92E-05	3.16E-05	3.57E-05
191	3.93E-05	3.16E-05	3.58E-05
192	3.94E-05	3.17E-05	3.58E-05
193	3.95E-05	3.17E-05	3.59E-05
194	3.96E-05	3.18E-05	3.60E-05
195	3.96E-05	3.18E-05	3.60E-05
196	3.97E-05	3.19E-05	3.61E-05
197	3.98E-05	3.19E-05	3.62E-05
198	3.99E-05	3.20E-05	3.62E-05
199	4.00E-05	3.20E-05	3.63E-05
200	4.01E-05	3.21E-05	3.64E-05
201	4.01E-05	3.21E-05	3.64E-05
202	4.02E-05	3.22E-05	3.65E-05
203	4.03E-05	3.22E-05	3.66E-05
204	4.04E-05	3.23E-05	3.66E-05
205	4.04E-05	3.23E-05	3.67E-05
206	4.05E-05	3.24E-05	3.68E-05
207	4.06E-05	3.24E-05	3.68E-05
208	4.07E-05	3.25E-05	3.69E-05
209	4.08E-05	3.25E-05	3.70E-05
210	4.08E-05	3.26E-05	3.70E-05
211	4.09E-05	3.26E-05	3.71E-05
212	4.10E-05	3.27E-05	3.72E-05

213	4.11E-05	3.27E-05	3.72E-05
214	4.11E-05	3.28E-05	3.73E-05
215	4.12E-05	3.28E-05	3.74E-05
216	4.13E-05	3.29E-05	3.74E-05
217	4.14E-05	3.29E-05	3.75E-05
218	4.14E-05	3.30E-05	3.76E-05
219	4.15E-05	3.30E-05	3.76E-05
220	4.16E-05	3.31E-05	3.77E-05
221	4.17E-05	3.31E-05	3.78E-05
222	4.17E-05	3.32E-05	3.78E-05
223	4.18E-05	3.32E-05	3.79E-05
224	4.19E-05	3.33E-05	3.80E-05
225	4.20E-05	3.33E-05	3.80E-05
226	4.21E-05	3.34E-05	3.81E-05
227	4.21E-05	3.34E-05	3.82E-05
228	4.22E-05	3.35E-05	3.82E-05
229	4.23E-05	3.35E-05	3.83E-05
230	4.23E-05	3.36E-05	3.83E-05
231	4.24E-05	3.36E-05	3.84E-05
232	4.25E-05	3.37E-05	3.85E-05
233	4.26E-05	3.37E-05	3.85E-05
234	4.26E-05	3.38E-05	3.86E-05
235	4.27E-05	3.38E-05	3.87E-05
236	4.28E-05	3.39E-05	3.87E-05
237	4.28E-05	3.39E-05	3.88E-05
238	4.29E-05	3.40E-05	3.89E-05
239	4.30E-05	3.40E-05	3.89E-05

Table B13: Average CO_2 concentration of four-hour Tablelands experiments with low concentration Ca water.

etime	CaOHlow+TCR	CaOHlow+TWR
1	1.93E-05	1.93E-05
2	1.88E-05	1.88E-05
3	1.86E-05	1.85E-05
4	1.83E-05	1.83E-05
5	1.81E-05	1.81E-05
6	1.79E-05	1.78E-05
7	1.77E-05	1.76E-05
8	1.75E-05	1.74E-05
9	1.73E-05	1.72E-05
10	1.71E-05	1.70E-05
11	1.70E-05	1.69E-05
12	1.68E-05	1.67E-05
13	1.66E-05	1.65E-05
14	1.65E-05	1.63E-05
15	1.63E-05	1.62E-05
16	1.62E-05	1.60E-05
17	1.61E-05	1.59E-05
18	1.59E-05	1.57E-05
19	1.58E-05	1.56E-05
20	1.57E-05	1.55E-05
21	1.55E-05	1.53E-05
22	1.54E-05	1.52E-05
23	1.53E-05	1.51E-05
24	1.52E-05	1.49E-05
25	1.51E-05	1.48E-05
26	1.49E-05	1.47E-05
27	1.48E-05	1.46E-05
28	1.47E-05	1.45E-05
29	1.46E-05	1.43E-05
30	1.45E-05	1.42E-05
31	1.44E-05	1.41E-05
32	1.43E-05	1.40E-05
33	1.42E-05	1.39E-05
34	1.41E-05	1.38E-05
35	1.40E-05	1.37E-05
36	1.39E-05	1.36E-05
37	1.38E-05	1.35E-05
38	1.37E-05	1.34E-05

39	1.36E-05	1.33E-05
40	1.36E-05	1.33E-05
41	1.35E-05	1.32E-05
42	1.34E-05	1.31E-05
43	1.33E-05	1.30E-05
44	1.32E-05	1.29E-05
45	1.31E-05	1.28E-05
46	1.31E-05	1.28E-05
47	1.30E-05	1.27E-05
48	1.29E-05	1.26E-05
49	1.28E-05	1.25E-05
50	1.27E-05	1.24E-05
51	1.27E-05	1.24E-05
52	1.26E-05	1.23E-05
53	1.25E-05	1.22E-05
54	1.24E-05	1.21E-05
55	1.24E-05	1.21E-05
56	1.23E-05	1.20E-05
57	1.22E-05	1.19E-05
58	1.22E-05	1.19E-05
59	1.21E-05	1.18E-05
60	1.20E-05	1.17E-05
61	1.19E-05	1.17E-05
62	1.19E-05	1.16E-05
63	1.18E-05	1.15E-05
64	1.17E-05	1.15E-05
65	1.17E-05	1.14E-05
66	1.16E-05	1.13E-05
67	1.15E-05	1.13E-05
68	1.15E-05	1.12E-05
69	1.14E-05	1.12E-05
70	1.14E-05	1.11E-05
71	1.13E-05	1.10E-05
72	1.12E-05	1.10E-05
73	1.12E-05	1.09E-05
74	1.11E-05	1.09E-05
75	1.11E-05	1.08E-05
76	1.10E-05	1.08E-05
77	1.09E-05	1.07E-05
78	1.08E-05	1.07E-05
79	1.08E-05	1.06E-05
80	1.07E-05	1.05E-05
81	1.07E-05	1.05E-05
82	1.06E-05	1.04E-05

83	1.06E-05	1.04E-05
84	1.05E-05	1.03E-05
85	1.04E-05	1.03E-05
86	1.04E-05	1.02E-05
87	1.03E-05	1.02E-05
88	1.03E-05	1.01E-05
89	1.02E-05	1.01E-05
90	1.02E-05	1.00E-05
91	1.01E-05	9.98E-06
92	1.01E-05	9.94E-06
93	1.00E-05	9.89E-06
94	9.96E-06	9.84E-06
95	9.91E-06	9.80E-06
96	9.87E-06	9.75E-06
97	9.81E-06	9.71E-06
98	9.76E-06	9.65E-06
99	9.71E-06	9.61E-06
100	9.66E-06	9.57E-06
101	9.62E-06	9.52E-06
102	9.57E-06	9.48E-06
103	9.52E-06	9.43E-06
104	9.48E-06	9.39E-06
105	9.43E-06	9.35E-06
106	9.38E-06	9.30E-06
107	9.34E-06	9.25E-06
108	9.30E-06	9.21E-06
109	9.25E-06	9.17E-06
110	9.20E-06	9.12E-06
111	9.16E-06	9.08E-06
112	9.12E-06	9.04E-06
113	9.06E-06	9.00E-06
114	9.03E-06	8.96E-06
115	8.99E-06	8.92E-06
116	8.94E-06	8.88E-06
117	8.91E-06	8.84E-06
118	8.86E-06	8.80E-06
119	8.82E-06	8.76E-06
120	8.77E-06	8.71E-06
121	8.74E-06	8.68E-06
122	8.70E-06	8.63E-06
123	8.65E-06	8.60E-06
124	8.61E-06	8.56E-06
125	8.57E-06	8.53E-06
126	8.54E-06	8.48E-06

127	8.50E-06	8.45E-06
128	8.46E-06	8.41E-06
129	8.41E-06	8.37E-06
130	8.38E-06	8.33E-06
131	8.34E-06	8.30E-06
132	8.30E-06	8.26E-06
133	8.26E-06	8.23E-06
134	8.23E-06	8.19E-06
135	8.19E-06	8.15E-06
136	8.15E-06	8.12E-06
137	8.11E-06	8.08E-06
138	8.08E-06	8.04E-06
139	8.04E-06	8.01E-06
140	8.00E-06	7.98E-06
141	7.96E-06	7.94E-06
142	7.93E-06	7.91E-06
143	7.90E-06	7.88E-06
144	7.87E-06	7.83E-06
145	7.83E-06	7.80E-06
146	7.79E-06	7.77E-06
147	7.75E-06	7.73E-06
148	7.72E-06	7.70E-06
149	7.69E-06	7.67E-06
150	7.65E-06	7.64E-06
151	7.61E-06	7.60E-06
152	7.59E-06	7.57E-06
153	7.56E-06	7.54E-06
154	7.52E-06	7.50E-06
155	7.49E-06	7.47E-06
156	7.45E-06	7.44E-06
157	7.42E-06	7.41E-06
158	7.38E-06	7.37E-06
159	7.36E-06	7.33E-06
160	7.33E-06	7.32E-06
161	7.29E-06	7.29E-06
162	7.26E-06	7.25E-06
163	7.23E-06	7.23E-06
164	7.20E-06	7.20E-06
165	7.17E-06	7.16E-06
166	7.14E-06	7.13E-06
167	7.10E-06	7.10E-06
168	7.07E-06	7.07E-06
169	7.05E-06	7.04E-06
170	7.02E-06	7.01E-06

171	6.99E-06	6.98E-06
172	6.95E-06	6.95E-06
173	6.93E-06	6.92E-06
174	6.90E-06	6.89E-06
175	6.87E-06	6.86E-06
176	6.84E-06	6.83E-06
177	6.81E-06	6.81E-06
178	6.78E-06	6.78E-06
179	6.75E-06	6.75E-06
180	6.72E-06	6.73E-06
181	6.70E-06	6.70E-06
182	6.67E-06	6.66E-06
183	6.64E-06	6.64E-06
184	6.61E-06	6.61E-06
185	6.58E-06	6.59E-06
186	6.56E-06	6.57E-06
187	6.53E-06	6.53E-06
188	6.50E-06	6.51E-06
189	6.48E-06	6.48E-06
190	6.45E-06	6.45E-06
191	6.42E-06	6.43E-06
192	6.40E-06	6.40E-06
193	6.37E-06	6.38E-06
194	6.34E-06	6.34E-06
195	6.31E-06	6.33E-06
196	6.29E-06	6.30E-06
197	6.27E-06	6.28E-06
198	6.24E-06	6.25E-06
199	6.22E-06	6.22E-06
200	6.18E-06	6.20E-06
201	6.17E-06	6.18E-06
202	6.14E-06	6.15E-06
203	6.11E-06	6.13E-06
204	6.09E-06	6.11E-06
205	6.06E-06	6.08E-06
206	6.03E-06	6.06E-06
207	6.01E-06	6.03E-06
208	5.99E-06	6.01E-06
209	5.97E-06	5.98E-06
210	5.95E-06	5.96E-06
211	5.92E-06	5.94E-06
212	5.90E-06	5.91E-06
213	5.87E-06	5.89E-06
214	5.85E-06	5.87E-06

215	5.82E-06	5.85E-06
216	5.80E-06	5.83E-06
217	5.78E-06	5.81E-06
218	5.75E-06	5.78E-06
219	5.74E-06	5.76E-06
220	5.71E-06	5.73E-06
221	5.69E-06	5.72E-06
222	5.67E-06	5.69E-06
223	5.65E-06	5.67E-06
224	5.62E-06	5.65E-06
225	5.60E-06	5.62E-06
226	5.58E-06	5.60E-06
227	5.56E-06	5.58E-06
228	5.54E-06	5.56E-06
229	5.52E-06	5.54E-06
230	5.49E-06	5.52E-06
231	5.47E-06	5.50E-06
232	5.45E-06	5.47E-06
233	5.43E-06	5.46E-06
234	5.41E-06	5.44E-06
235	5.39E-06	5.42E-06
236	5.36E-06	5.41E-06
237	5.35E-06	5.38E-06
238	5.33E-06	5.36E-06
239	5.31E-06	5.34E-06
240	5.29E-06	5.32E-06

Appendix C: ICP-MS and ICP-OES data from laboratory experiments

Table C1: Average change in ion concentrations from atmospheric and elevated five-hour Tablelands laboratory sequestration experiments.

Atmospheric CO_2 Tablelands Experiments - Five hours								
	Ca			**Mg**			**Si**	
	Average	**Stdev**		**Average**	**Stdev**		**Average**	**Stdev**
DI + TCR	-1.48E-06	8.88E-05	**DI + TCR**	1.89E-04	9.99E-05	**DI + TCR**	1.42E-05	6.50E-06
DI + TWR	3.45E-06	3.58E-06	**DI + TWR**	1.53E-05	6.18E-06	**DI + TWR**	2.08E-06	8.56E-07
DI + TWR #2	5.84E-06	1.46E-06	**DI + TWR #2**	1.40E-05	2.75E-06	**DI + TWR #2**	2.07E-06	1.07E-06
MgOH	0.00E+00	0.00E+00	**MgOH**	1.21E-04	1.86E-05	**MgOH**	2.52E-06	3.45E-07
MgOH + TCR	2.48E-05	2.15E-05	**MgOH + TCR**	1.92E-04	7.41E-05	**MgOH + TCR**	9.72E-06	1.93E-06
MgOH + TWR	0.00E+00	0.00E+00	**MgOH + TWR**	1.46E-04	4.88E-05	**MgOH + TWR**	3.26E-06	3.70E-07
CaOH	-6.35E-03	5.50E-03	**CaOH**	-2.09E-05	1.04E-04	**CaOH**	-2.13E-06	4.81E-06
CaOH + TCR	-5.07E-03	2.84E-04	**CaOH + TCR**	4.11E-05	7.97E-05	**CaOH + TCR**	1.27E-05	1.47E-05
CaOH + TWR	-1.09E-03	7.57E-04	**CaOH + TWR**	1.22E-05	2.40E-05	**CaOH + TWR**	6.21E-06	1.66E-06
Elevated CO_2 Tablelands Experiments - Five hours								
	Ca			**Mg**			**Si**	
	Average	**Stdev**		**Average**	**Stdev**		**Average**	**Stdev**
NaHCO3	9.85E-07	1.00E-06	**NaHCO3**	2.15E-06	4.61E-06	**NaHCO3**	6.26E-06	1.04E-06
NaHCO3 + TCR	0.00E+00	0.00E+00	**NaHCO3 + TCR**	2.89E-04	7.49E-05	**NaHCO3 + TCR**	6.55E-05	3.20E-05
NaHCO3 + TWR	0.00E+00	0.00E+00	**NaHCO3 + TWR**	2.32E-05	3.13E-06	**NaHCO3 + TWR**	3.86E-06	1.46E-06
NaHCO3 + MgOH	4.56E-07	1.53E-06	**NaHCO3 + MgOH**	5.12E-04	2.04E-04	**NaHCO3 + MgOH**	2.60E-06	1.43E-06
NaHCO3 + MgOH + TCR	7.68E-06	2.85E-06	**NaHCO3 + MgOH + TCR**	3.11E-04	6.43E-05	**NaHCO3 + MgOH + TCR**	6.02E-05	2.71E-05
NaHCO3 + MgOH + TWR	2.69E-06	1.77E-06	**NaHCO3 + MgOH + TWR**	5.49E-04	2.57E-04	**NaHCO3 + MgOH + TWR**	5.46E-06	7.10E-07
NaHCO3 + CaOH	3.72E-06	9.04E-06	**NaHCO3 + CaOH**	4.93E-05	8.04E-06	**NaHCO3 + CaOH**	2.76E-06	2.75E-06
NaHCO3 + CaOH + TCR	-1.42E-06	2.15E-06	**NaHCO3 + CaOH + TCR**	1.31E-04	1.96E-05	**NaHCO3 + CaOH + TCR**	5.59E-05	1.03E-05
NaHCO3 + CaOH + TWR	-2.68E-06	2.10E-06	**NaHCO3 + CaOH + TWR**	3.30E-05	8.83E-06	**NaHCO3 + CaOH + TWR**	1.78E-06	9.17E-07

Table C2: Average change in ion concentrations from atmospheric and elevated four-hour White Hills laboratory sequestration experiments.

Atmospheric CO_2 White Hills Experiments - Four hours								
	Ca			Mg			Si	
	Average	Stdev		Average	Stdev		Average	Stdev
DI + SCR	2.88E-05	8.51E-06	**DI + SCR**	1.02E-04	3.35E-05	**DI + SCR**	4.26E-05	1.35E-05
DI + SWR	-1.73E-05	3.15E-05	**DI + SWR**	3.29E-06	2.70E-06	**DI + SWR**	3.09E-06	4.11E-07
MgOH	0.00E+00	0.00E+00	**MgOH**	1.21E-04	1.86E-05	**MgOH**	2.52E-06	3.45E-07
MgOH + SCR	2.20E-05	3.42E-06	**MgOH + SCR**	6.88E-05	1.25E-05	**MgOH + SCR**	3.15E-05	7.00E-06
MgOH + SWR	-1.82E-05	2.25E-06	**MgOH + SWR**	5.68E-05	1.89E-05	**MgOH + SWR**	4.98E-06	1.42E-06
CaOH	-4.99E-05	5.56E-04	**CaOH**	0.00E+00	0.00E+00	**CaOH**	5.58E-06	2.02E-06
CaOHlow	-2.20E-04	4.58E-05	**CaOHlow**	-2.88E-06	6.06E-06	**CaOHlow**	6.41E-06	1.98E-06
CaOHlow + SCR	-4.47E-04	2.51E-04	**CaOHlow + SCR**	9.74E-06	1.66E-06	**CaOHlow + SCR**	4.76E-05	8.22E-07
CaOHlow + SWR	-2.36E-04	3.37E-05	**CaOHlow + SWR**	1.10E-06	1.56E-06	**CaOHlow + SWR**	8.43E-06	2.53E-06
Elevated CO_2 White Hills Experiments - Four hours								
NaHCO3 (TL 5hrs)	9.85E-07	1.00E-06	**NaHCO3 (TL 5hrs)**	2.15E-06	4.61E-06	**NaHCO3 (TL 5hrs)**	6.26E-06	1.04E-06
NaHCO3 + SCR	9.48E-06	1.46E-05	**NaHCO3 + SCR**	1.74E-04	2.16E-05	**NaHCO3 + SCR**	4.01E-05	4.94E-06
NaHCO3 + SWR	2.41E-06	1.42E-06	**NaHCO3 + SWR**	9.46E-06	6.47E-06	**NaHCO3 + SWR**	1.90E-06	1.79E-06
NaHCO3 + MgOH (TL 5hrs)	4.56E-07	1.53E-06	**NaHCO3 + MgOH (TL 5hrs)**	5.12E-04	2.04E-04	**NaHCO3 + MgOH (TL 5hrs)**	2.60E-06	1.43E-06
NaHCO3 + MgOH + SCR	1.75E-05	1.50E-06	**NaHCO3 + MgOH + SCR**	1.87E-04	1.42E-05	**NaHCO3 + MgOH + SCR**	5.06E-05	4.32E-06
NaHCO3 + MgOH + SWR	2.25E-06	1.09E-06	**NaHCO3 + MgOH + SWR**	2.05E-04	9.26E-05	**NaHCO3 + MgOH + SWR**	0.00E+00	0.00E+00
NaHCO3 + CaOHhigh (TL 5hrs)	3.72E-06	9.04E-06	**NaHCO3 + CaOHhigh (TL 5hrs)**	4.93E-05	8.04E-06	**NaHCO3 + CaOHhigh (TL 5hrs)**	2.76E-06	2.75E-06
NaHCO3 + CaOH + SCR	3.41E-06	1.77E-06	**NaHCO3 + CaOH + SCR**	1.61E-04	3.97E-05	**NaHCO3 + CaOH + SCR**	5.03E-05	1.07E-05
NaHCO3 + CaOH + SWR	-1.42E-05	9.51E-06	**NaHCO3 + CaOH + SWR**	7.95E-06	4.98E-06	**NaHCO3 + CaOH + SWR**	1.19E-06	2.06E-06

Table C3: Average change in ion concentrations from atmospheric four-hour Tablelands laboratory sequestration experiments.

Atmospheric CO_2 Tablelands Experiments - Four hours								
	Ca			Mg			Si	
	Average	Stdev		Average	Stdev		Average	Stdev
CaOH	-2.20E-04	4.58E-05	**CaOH**	-2.88E-06	6.06E-06	**CaOH**	6.41E-06	1.98E-06
CaOHlow+TCR	-9.73E-01	3.11E-02	**CaOHlow+TCR**	1.39E-02	3.08E-03	**CaOHlow+TCR**	2.42E-02	1.60E-03
CaOHlow+TWR	-3.34E-01	4.03E-02	**CaOHlow+TWR**	4.86E-04	4.86E-04	**CaOHlow+TWR**	3.46E-03	4.29E-04

Appendix D: TIC data from laboratory experiments

Table D1: Average change in TIC concentrations from laboratory sequestration experiments.

Atmospheric CO_2 - Tablelands, Five Hours

Experiment	Average Change (mol)	Stdev (mol
DI + TCR	1.91E-04	3.87E-05
DI + TWR	2.40E-05	1.31E-05
DI + TWR 2	1.89E-05	6.81E-06
MgOH	1.27E-04	1.23E-04
MgOH + TCR	2.62E-04	2.27E-05
MgOH + TWR	9.56E-05	1.58E-05
CaOHhigh	4.22E-06	1.22E-05
CaOHhigh + TCR	-2.77E-06	2.91E-06
CaOHhigh + TWR	8.76E-06	2.09E-05

Elevated CO_2 - Tablelands, Five Hours

Experiment	Average Change (mol)	Stdev (mol
DI	-1.52E-03	1.84E-03
DI + TCR	-1.61E-04	1.82E-03
DI + TWR	-9.82E-04	5.82E-04
MgOH	-3.39E-04	4.25E-04
MgOH + TCR	-8.38E-04	6.05E-04
MgOH + TWR	2.54E-03	2.93E-03
CaOHhigh	-1.24E-03	8.84E-04
CaOHhigh + TCR	1.99E-03	2.65E-04
CaOHhigh + TWR	-2.21E-03	2.92E-04

Atmospheric CO_2 - White Hills, Four Hours

Experiment	Average Change (mol)	Stdev (mol)
DI+SCR	1.89E-04	3.15E-05
DI+SWR	-2.76E-06	4.83E-06
MgOH	-3.39E-04	4.25E-04
MgOH+SCR	1.58E-04	1.03E-05
MgOH+SWR	5.04E-05	2.18E-05
CaOHhigh	0.00E+00	0.00E+00
CaOH	-1.40E-05	2.20E-06
CaOH+SCR	-1.54E-05	3.63E-06
CaOH+SWR	-1.85E-05	9.68E-06

Elevated CO_2 - White Hills, Four Hours

Experiment	Average Change (mol)	Stdev (mol)
NaHCO3 (TL 5hrs)	-1.52E-03	1.84E-03
NaHCO3+SCR	-2.97E-04	2.93E-04
NaHCO3+SWR	-1.94E-04	1.65E-04
NaHCO3 + MgOH (TL 5hrs)	-3.39E-04	4.25E-04
NaHCO3+MgOH+SCR	-4.87E-04	1.79E-04
NaHCO3+MgOH+SWR	-3.96E-04	2.21E-04
NaHCO3 + CaOHhigh (TL 5hrs)	-1.24E-03	8.84E-04
NaHCO3+CaOH+SCR	1.08E-04	2.38E-04
NaHCO3+CaOH+SWR	-3.54E-04	1.66E-04

Atmospheric - Tablelands, Four Hours

Experiment	Average Change (mol)	Stdev (mol)
CaOHlow+TCR	-3.15E-06	5.22E-07
CaOHlow+TWR	-5.48E-06	5.27E-06

Appendix E: pH measurements from laboratory experiments

Table E1: Average change in pH measurements from laboratory sequestration experiments.

Atmospheric CO_2 - Tablelands, Five hours

Experiment	Average change	Stdev.
DI + TCR	-3.18	0.47
DI + TWR #1	-0.60	0.61
DI + TWR #2	-0.79	0.47
MgOH	-0.14	0.04
MgOH + TCR	-0.36	0.09
MgOH + TWR	-0.29	0.26
CaOHhigh	0.06	0.16
CaOHhigh + TCR	-0.59	0.58
CaOHhigh + TWR	0.10	0.14

Elevated CO_2 - Tablelands, Five hours

Experiment	Average change	Stdev
DI	-0.09	0.14
DI + TCR	0.17	0.27
DI + TWR	0.05	0.05
MgOH	0.05	0.04
MgOH + TCR	-0.04	0.10
MgOH + TWR	0.02	0.02
CaOHhigh	0.07	0.05
CaOHhigh + TCR	-0.21	0.28
CaOHhigh + TWR	-0.01	0.07

Atmospheric CO_2 - White Hills, Four hours

Experiment	Average Change	Stdev
DI	-0.09	0.37
DI+SCR	2.85	0.62
DI+SWR	-0.09	1.58
MgOH	-0.14	0.04
MgOH+SCR	-0.05	0.06
MgOH+SWR	0.26	0.04
CaOH	-0.18	0.15
CaOHhigh	0.01	0.01
CaOH+SCR	-0.23	0.05
CaOH+SWR	-0.10	0.03

Elevated CO_2 - White Hills, Four hours

Experiment	Average Change	Stdev
DI	-0.09	0.14
DI+SCR	0.25	0.04
DI+SWR	0.06	0.06
MgOH	0.05	0.04
MgOH+SCR	0.15	0.13
MgOH+SWR	0.25	0.14
CaOH	0.07	0.05
CaOH+SCR	0.11	0.01
CaOH+SWR	0.05	0.03

Atmospheric CO_2 - Tablelands, Four hours

Experiment	Average	Stdev
CaOH	-0.18	0.15
CaOH+TCR	-0.36	0.12
CaOH+TWR	-0.31	0.13

Appendix F: Conductivity measurements from laboratory experiments

Table F1: Average change in pH measurements from laboratory sequestration experiments.

Atmospheric CO_2 - Tablelands, Five hours

	Average Change	Stdev
DI	0.00E+00	0.00E+00
DI+TCR	4.62E-02	7.19E-03
DI+TWR1	8.68E-04	2.09E-02
DI+TWR2	3.83E-02	7.75E-02
MgOH	1.41E-03	6.51E-03
MgOH+TCR	-1.63E-02	5.74E-02
MgOH+TWR	1.07E-03	1.53E-02
CaOHhigh	-1.62E-01	8.39E-02
CaOHhigh+TCR	-1.13E+00	2.21E-01
CaOHhigh+TWR	-2.44E-01	1.85E-01

Elevated CO_2 - Tablelands, Five hours

Elevated CO2	Average Change	Stdev
DI	-1.47E-02	3.40E-02
DI+TCR	4.33E-02	1.33E-02
DI+TWR	3.17E-02	3.45E-02
MgOH	3.73E-02	2.87E-02
MgOH+TCR	3.33E-03	4.27E-02
MgOH+TWR	3.83E-02	3.40E-02
CaOHhigh	7.00E-03	1.49E-02
CaOHhigh+TCR	-3.77E-02	8.45E-02
CaOHhigh+TWR	1.67E-02	8.25E-02

Atmospheric CO_2 - White Hills, Four hours

	Average Change	Stdev
DI	-1.08E-04	7.58E-04
DI+SCR	4.20E-02	1.20E-02
DI+SWR	1.52E-04	4.87E-03
MgOH	1.41E-03	6.51E-03
MgOH+SCR	2.19E-02	4.47E-03
MgOH+SWR	2.14E-02	6.33E-03
CaOHlow	-2.99E-02	1.17E-02
CaOHhigh	-1.25E-04	1.17E-05
CaOH+SCR	-2.54E-01	1.44E-02
CaOH+SWR	-8.62E-02	2.26E-02

Elevated CO_2 - White Hills, Four hours

Elevated CO2	Average Change	Stdev
DI (TL 5 hrs)	-1.47E-02	3.40E-02
DI+SCR	-3.70E-02	1.04E-01
DI+SWR	4.33E-03	1.42E-02
MgOH (TL 5hrs)	3.73E-02	2.87E-02
MgOH+SCR	3.60E-02	1.39E-02
MgOH+SWR	5.33E-02	9.29E-03
CaOHhigh (TL 5hrs)	7.00E-03	1.49E-02
CaOH+SCR	2.97E-02	1.00E-02
CaOH+SWR	1.67E-03	1.50E-02

Atmospheric CO_2 - Tablelands, Four hours

CaOH	-2.99E+01	1.17E+01
CaOH+TCR	-2.96E+02	2.01E+01
CaOH+TWR	-1.41E+02	1.12E+02